Steven D. Bass

The Spin Structure of the Proton

World Scientific

The Spin Structure of the Proton

This page intentionally left blank

The Spin Structure of the Proton

STEVEN D. BASS
Innsbruck University, Austria

World Scientific
NEW JERSEY • LONDON • SINGAPORE • BEIJING • SHANGHAI • HONG KONG • TAIPEI • CHENNAI

Published by

World Scientific Publishing Co. Pte. Ltd.
5 Toh Tuck Link, Singapore 596224
USA office: 27 Warren Street, Suite 401-402, Hackensack, NJ 07601
UK office: 57 Shelton Street, Covent Garden, London WC2H 9HE

British Library Cataloguing-in-Publication Data
A catalogue record for this book is available from the British Library.

THE SPIN STRUCTURE OF THE PROTON

ISBN-13 978-981-270-946-2
ISBN-10 981-270-946-0
ISBN-13 978-981-270-947-9 (pbk)
ISBN-10 981-270-947-9 (pbk)

Printed in Singapore.

To Céline

This page intentionally left blank

PREFACE

The Spin Structure of the Proton is one of the most challenging open puzzles in Quantum Chromodynamics. Key particle physics experiments in deep inelastic scattering suggest that just $\sim 30\%$ of the spin of the proton is carried by the intrinsic spin of its quark constituents – considerably less than the prediction of relativistic constituent quark models ($\sim 60\%$). This discovery has challenged our understanding about the internal structure of the proton and inspired vast experimental and theoretical activity to understand the role of spin in the proton's internal structure: about 1000 theoretical papers and a new programme of dedicated experiments at CERN and DESY in Europe, and BNL, JLab and SLAC in the United States.

Until recently, the main experimental activity has focussed on fully inclusive measurements of the proton's g_1 spin structure function with longitudinally polarized targets. New experiments are underway to measure the separate flavour- and spin-dependent parton distributions for the proton's valence quark, sea quark and gluonic constituents, and to investigate the spin structure of transversely polarized protons. The important questions are: How is the spin of the proton built up out from the intrinsic spin and orbital angular momentum of its quark and gluonic constituents? What happens to spin and orbital angular momentum in the transition from current quarks to constituent quarks in low-energy QCD? Does the proton spin puzzle involve the suppression of the valence quark spin contribution or do the sea quarks and gluons conspire to reduce the total quark spin content in the proton? Here we give an overview of the present status of our understanding: *How does the proton spin?*

Steven D. Bass

This page intentionally left blank

CONTENTS

PREFACE vii

1. INTRODUCTION 1

   1.1 Spin and the proton spin problem 3
   1.2 Outline 9

2. SPIN EXPERIMENTS AND DATA 11

   2.1 Introduction 11
   2.2 Scaling and polarized deep inelastic scattering 14
   2.3 The QCD parton model 15
   2.4 Spin experiments 19
   2.5 Spin data 23
   2.6 Regge theory and the small x behaviour of spin structure functions 26

3. DISPERSION RELATIONS AND SPIN SUM RULES 31

   3.1 Spin amplitudes 31
   3.2 Light cone dominance and the operator product expansion 36
   3.3 The QCD parton model 39
   3.4 Parton distributions and light-cone correlation functions 43
   3.5 Renormalization group and QCD evolution 45
   3.6 Polarized partons and high-energy proton-proton collisions 47

4. g_1 SPIN SUM RULES 51

   4.1 The first moment of g_1 51
   4.2 SU(3) breaking 56
   4.3 νp elastic scattering 58
   4.4 The Burkhardt-Cottingham sum rule 62
   4.5 The Gerasimov-Drell-Hearn sum rule 64
   4.6 The transition region 67

5. FIXED POLES 69
5.1 Adler sum rule . . . 70
5.2 Schwinger term sum rule . . . 70
5.3 Burkhardt-Cottingham sum rule . . . 71
5.4 g_1 spin sum rules . . . 72

6. THE AXIAL ANOMALY, GLUON TOPOLOGY AND $g_A^{(0)}$ 73
6.1 The axial anomaly . . . 73
6.2 The anomaly and the first moment of g_1 . . . 75
6.3 Gluon topology and $g_A^{(0)}$ . . . 76
6.4 Instantons and $U_A(1)$ symmetry . . . 79
6.5 Photon gluon fusion . . . 82

7. CHIRAL SYMMETRY AND AXIAL U(1) DYNAMICS 89
7.1 Chiral symmetry and the spin structure of the proton . . . 89
7.2 QCD considerations . . . 90
7.3 The low-energy effective Lagrangian . . . 94
7.4 OZI violation and the η'–nucleon interaction . . . 96
7.5 Proton-proton collisions . . . 98
7.6 Light mass "exotic" resonances . . . 99
7.7 η bound states in nuclei . . . 101

8. QCD INSPIRED MODELS OF THE PROTON SPIN PROBLEM 107
8.1 Constituent quarks and $g_A^{(k)}$ . . . 107
8.2 Possible explanations of the proton spin problem . . . 109

9. THE SPIN-FLAVOUR STRUCTURE OF THE PROTON 117
9.1 The valence region and large x . . . 117
9.2 The isovector part of g_1 . . . 121

10. QCD FITS TO g_1 DATA 125
10.1 Regge theory and perturbative evolution at small x . . . 130

11. POLARIZED QUARK DISTRIBUTIONS 137
11.1 Semi-inclusive polarized deep inelastic scattering . . . 138
11.2 Weak boson production . . . 145
11.3 Inclusive spin-dependent structure functions . . . 146

12. POLARIZED GLUE $\Delta g(x, Q^2)$ 149
12.1 Polarized lepto-production . . . 149
12.2 RHIC data . . . 152

13. TRANSVERSITY 157

14. DEEPLY VIRTUAL COMPTON SCATTERING AND EXCLUSIVE PROCESSES 165

15. POLARIZED PHOTON STRUCTURE FUNCTIONS 173

15.1 A sum-rule for g_1^γ 175
15.2 Twist expansion for g_1^γ when $Q^2 \to \infty$ 176
15.2.1 Leading twist 2 177
15.2.2 Higher twists 179
15.3 $g_1^\gamma(x, Q^2)$ in QCD: The leading order Witten analysis 179

16. CONCLUSIONS AND OPEN QUESTIONS: HOW DOES THE PROTON SPIN? 185

BIBLIOGRAPHY 189

This page intentionally left blank

Chapter 1

INTRODUCTION

Protons behave like quantum spinning-tops with spin $\frac{1}{2}$ in units of Planck's constant $\hbar$. This spin is responsible for many fundamental properties of nature including the proton's magnetic moment, the different phases of matter in low temperature physics, the properties of neutron stars and the stability of the known Universe.

One of the main questions in particle and nuclear physics the last 20 years has been: How is the proton's spin built up from its quark and gluon constituents? It is nearly 20 years since the European Muon Collaboration (EMC) published their polarized deep inelastic measurement of the proton's g_1 spin dependent structure function and the flavour-singlet axial-charge $g_A^{(0)}|_{\rm pDIS}$ [Ashman *et al.* (1988)]. Their results suggested that the quarks' intrinsic spin contributes little of the proton's spin. Relativistic constituent quark models of the proton generally predict that about 60% of the proton's spin should be carried by the spin of its three valence quarks with the rest carried by orbital angular momentum. The most accurate polarization experiments have taught us that the contribution from the spin or helicity of the quarks inside is small, only about 30%, challenging our understanding about the structure of the proton. The challenge to understand the spin structure of the proton has inspired a vast programme of theoretical activity and new experiments at CERN, DESY, JLab, RHIC and SLAC to map out the individual quark and gluon angular momentum contributions to the proton's spin. These experiments are yielding exciting results. *Where are we today? What happens to spin in the transition between current and constituent quarks in low-energy quantum chromodynamics (QCD)?*

The story of the proton's spin dates from the discovery by Dennison (1927) that the proton is a fermion of spin $\frac{1}{2}$. Six years later [Estermann and Stern (1933)] measured the proton's anomalous magnetic moment, $\kappa_p = 1.79$ Bohr magnetons, revealing that the proton is not pointlike and has internal structure. The challenge to understand the structure of the proton had begun!

We now understand the proton as a bound state of three confined valence quarks (spin $\frac{1}{2}$ fermions) interacting through the exchange of spin-one gluons, with the gauge group being colour SU(3) – QCD (quantum chromodynamics, the theory of quarks and gluons). The proton is special because of confinement, dynamical

chiral symmetry breaking and the very strong colour gauge fields at large distances [Thomas and Weise (2001)]. In high-momentum processes the coupling constant or interaction strength for quark-gluon and gluon-gluon interactions is small because of asymptotic freedom. The coupling increases with decreasing momentum or resolution. It becomes so strong that the quarks and gluons are always bound inside nuclear particles like the proton: they are never observed by themselves as free particles. (The restoring confinement force is 10 tonnes regardless of separation.) In low-energy processes the proton behaves like a system of three massive constituent-quark quasi-particles interacting self-consistently with a cloud of virtual pions (light-mass spin-zero particles made out of a quark and an antiquark) and condensates generated through spontaneous breaking of the chiral symmetry between left and right handed quarks. When probed at high resolution the proton looks like three valence "current" quarks plus a sea of quark-antiquark pairs and gluons. The current quarks probed in high-resolution processes are almost massless whereas the constituent quark quasi-particles of low-energy QCD each have a mass about one third of the mass of the proton.

Our present knowledge about the spin structure of the proton at the quark level comes from polarized deep inelastic scattering experiments (pDIS) which use high-energy polarized electrons or muons to probe the structure of a polarized proton and new experiments in semi-inclusive polarized deep inelastic scattering, polarized proton-proton collisions and polarized photoproduction experiments. The spin experiments at CERN, DESY, JLab and SLAC involve firing high-energy charged leptons (electrons or muons) at a polarized proton target. The electron exchanges a deeply-virtual spin-one photon which makes a high resolution probe of the quark-gluon structure of the target. The photon can be absorbed by a spin $\frac{1}{2}$ quark polarized in the opposite direction to the photon but not by one polarized in the same direction as the photon (quarks have no spin $\frac{3}{2}$ state). This allows us to extract information about the spin of the quarks when one controls the polarization of both the beam and the proton target. The RHIC spin experiments involve high-energy polarized proton-proton collisions.

The present excitement and global programme in high-energy spin physics was inspired by an intriguing discovery in polarized deep inelastic scattering. Following pioneering experiments at SLAC [Alguard *et al.* (1976, 1978); Baum *et al.* (1983)], recent experiments in fully inclusive polarized deep inelastic scattering have extended measurements of the nucleon's g_1 spin dependent structure function (the inclusive form-factor measured in these experiments) over a broad kinematic region where one is sensitive to scattering on the *valence* quarks *plus* the quark-antiquark *sea* fluctuations – see e.g. Windmolders (1999). These experiments have been interpreted to imply that quarks and anti-quarks carry just a small fraction of the proton's spin ($\sim 30\%$) – about half the prediction of relativistic constituent quark models ($\sim 60\%$). This result has inspired vast experimental and theoretical activity to understand the spin structure of the proton. Before embarking on a detailed

study of the spin structure of the proton it is essential to understand why the small value of this "quark spin content" measured in polarized deep inelastic scattering caused such excitement and why it has so much challenged our understanding of the structure of the proton.

Many elements of subatomic physics and quantum field theory are important in our understanding of the proton spin problem. These include:

- the dispersion relations for polarized photon-nucleon scattering,
- Regge theory and the high-energy behaviour of scattering amplitudes,
- the renormalization of the operators which enter the light-cone operator product expansion description of high energy polarized deep inelastic scattering,
- perturbative QCD: the physics of large transverse momentum plus parton model factorization,
- the non-perturbative and non-local topological properties of gluon gauge fields in QCD and the chiral structure of the QCD θ vacuum,
- the role of gluon dynamics in dynamical chiral symmetry breaking (the large mass of the η and η' mesons and the absence of a flavour-singlet pseudoscalar Goldstone boson in spontaneous chiral symmetry breaking).

In this book we review our present understanding of the proton spin problem and the physics of the new and ongoing programme aimed at resolving the spin-flavour structure of the nucleon.

1.1 Spin and the proton spin problem

Spin is the characteristic property of a particle besides its mass and gauge charges. The two invariants of the Poincare group are

$$\begin{aligned} \mathcal{P}_\mu \mathcal{P}^\mu &= M^2 \\ \mathcal{W}_\mu \mathcal{W}^\mu &= -M^2 s(s+1). \end{aligned} \tag{1.1}$$

Here $\mathcal{P}$ and $\mathcal{W}$ denote the momentum and Pauli-Lubanski spin vectors respectively, M is the particle mass and s denotes its spin. The spin of a particle, whether elementary or composite, determines its equation of motion and its statistics properties. The discovery of spin and its properties are reviewed in Tomonaga (1997) and Martin (2002). Spin $\frac{1}{2}$ particles are governed by the Dirac equation and Fermi-Dirac statistics whereas spin 0 and spin 1 particles are governed by the Klein-Gordon equation and Bose-Einstein statistics.

The proton's spin vector s_μ is measured through the forward matrix element of the axial-vector current

$$2Ms_\mu = \langle p, s| \ \overline{\psi}\gamma_\mu\gamma_5\psi \ |p, s\rangle \tag{1.2}$$

where ψ denotes the proton field operator and M is the proton mass. The quark axial charges

$$2Ms_\mu\Delta q = \langle p,s|\ \overline{q}\gamma_\mu\gamma_5 q\ |p,s\rangle \tag{1.3}$$

then measure information about the quark "spin content" of the proton. (Here q denotes the quark field operator.) The flavour dependent axial charges Δu, Δd and Δs can be written as linear combinations of the isovector, SU(3) octet and flavour-singlet axial charges

$$\begin{aligned} g_A^{(3)} &= \Delta u - \Delta d \\ g_A^{(8)} &= \Delta u + \Delta d - 2\Delta s \\ g_A^{(0)} &= \Delta u + \Delta d + \Delta s. \end{aligned} \tag{1.4}$$

In semi-classical quark models Δq is interpreted as the amount of spin carried by quarks and antiquarks of flavour q.

In polarized deep inelastic scattering experiments one measures the nucleon's g_1 spin structure function as a function of the Bjorken variable x, the fraction of the proton's momentum which carried by quark, antiquark and gluon partons in incoherent photon-parton scattering with the proton boosted to an infinite momentum frame.

Spin sum-rules relate the measured g_1 spin structure function to the quark spin content of the proton. These sum-rules are derived starting from the dispersion relation for polarized photon-nucleon scattering and, for deep inelastic scattering, the light-cone operator product expansion. One finds that the first moment of the g_1 structure function is related to the scale-invariant axial charges of the target nucleon by

$$\begin{aligned} \int_0^1 dx\ g_1^p(x,Q^2) = &\left(\frac{1}{12}g_A^{(3)} + \frac{1}{36}g_A^{(8)}\right)\Big\{1 + \sum_{\ell\geq 1} c_{\mathrm{NS}\ell}\,\alpha_s^\ell(Q)\Big\} \\ &+\frac{1}{9}g_A^{(0)}|_{\mathrm{inv}}\Big\{1 + \sum_{\ell\geq 1} c_{\mathrm{S}\ell}\,\alpha_s^\ell(Q)\Big\} + \mathcal{O}(\frac{1}{Q^2}) - \ \beta_1(Q^2)\frac{Q^2}{4M^2}. \end{aligned} \tag{1.5}$$

Here $g_A^{(3)}$, $g_A^{(8)}$ and $g_A^{(0)}|_{\mathrm{inv}}$ are the isovector, SU(3) octet and scale-invariant flavour-singlet axial charges respectively. The flavour non-singlet $c_{\mathrm{NS}\ell}$ and singlet $c_{\mathrm{S}\ell}$ Wilson coefficients are calculable in ℓ-loop perturbative QCD [Larin *et al.* (1997)]. The term $\beta_1(Q^2)\frac{Q^2}{4M^2}$ represents a possible subtraction constant from the circle at infinity when one closes the contour in the complex plane in the dispersion relation where $\beta_1 \sim 1/Q^2$ for $Q^2 \to \infty$ for a leading-twist subtraction [Bass (2005)]. If finite, it affects just the first moment sum-rule. The first moment of g_1 plus the subtraction constant, if finite, is equal to the axial-charge contribution. The subtraction constant corresponds to a real term in the spin-dependent part of the forward Compton amplitude.

If one assumes no twist-two subtraction constant ($\beta_1(Q^2) = O(1/Q^4)$) then the axial charge contributions saturate the first moment at leading twist. The isovector axial-charge is measured independently in neutron beta-decays ($g_A^{(3)} = 1.2695 \pm 0.0029$ [Particle Data Group (2004)]) and the octet axial charge is extracted from hyperon beta-decays ($g_A^{(8)} = 0.58 \pm 0.03$). From the first moment of g_1, polarized deep inelastic scattering experiments have been interpreted to imply a small value for the flavour-singlet axial-charge:

$$g_A^{(0)}\big|_{\rm pDIS} \sim 0.15 - 0.35 \tag{1.6}$$

– considerably less than the value of $g_A^{(8)}$. In the naive parton model $g_A^{(0)}|_{\rm pDIS}$ is interpreted as the fraction of the proton's spin which is carried by the intrinsic spin of its quark and anti-quark constituents. When combined with the octet axial charge this value corresponds to a negative strange-quark polarization $\Delta s = \frac{1}{3}(g_A^{(0)}|_{\rm pDIS} - g_A^{(8)})$:

$$\Delta s \sim -0.10 \pm 0.04 \tag{1.7}$$

– that is, polarized in the opposite direction to the spin of the proton. Relativistic quark models generally predict values $g_A^{(0)} \sim 0.6$ with little polarized strangeness in the nucleon.

The small value of $g_A^{(0)}|_{\rm pDIS}$ suggests the following two questions. *What dynamics suppresses the singlet axial-charge extracted from polarized deep inelastic scattering relative to the OZI prediction $g_A^{(0)} = g_A^{(8)} \sim 0.6$?* Strange quarks or some dynamics related to singlet gluon related dynamics must be at work. *How is the proton's spin built up from the spin and orbital angular momentum of its constituents? – viz.* one would like to understand the decomposition of the sum-rule for the longitudinal spin structure of the nucleon

$$\frac{1}{2} = \frac{1}{2}\sum_q \Delta q + \Delta g + L_q + L_g \tag{1.8}$$

where L_q and L_g denote the orbital momentum contributions.

The Goldberger-Treiman relation relates the isovector axial charge $g_A^{(3)}$ to the product of the pion decay constant f_π and the pion-nucleon coupling constant $g_{\pi NN}$, viz.

$$2Mg_A^{(3)} = f_\pi g_{\pi NN} \tag{1.9}$$

through spontaneously broken chiral symmetry [Adler and Dashen (1968)]. The Goldberger-Treiman relation leads immediately to the result that the spin structure of the proton is related to the dynamics of chiral symmetry breaking.

What happens to gluonic degrees of freedom? The axial anomaly, a fundamental property of quantum field theory, tells us that the axial-vector current which measures the quark "spin content" of the proton cannot be treated independently of the gluon fields that the quarks live in and that the quark "spin content" is linked to the physics of dynamical axial U(1) symmetry breaking in the flavour-singlet

channel. For each flavour q the gauge invariantly renormalized axial-vector current satisfies the anomalous divergence equation [Adler (1969); Bell and Jackiw (1969)]

$$\partial^\mu \left(\overline{q}\gamma_\mu\gamma_5 q\right) = 2m\overline{q}i\gamma_5 q + \frac{\alpha_s}{4\pi}G_{\mu\nu}\tilde{G}^{\mu\nu}. \tag{1.10}$$

Here m denotes the quark mass and $\frac{\alpha_s}{4\pi}G_{\mu\nu}\tilde{G}^{\mu\nu}$ is the topological charge density. The anomaly is important in the flavour-singlet channel and intrinsic to $g_A^{(0)}$. It cancels in the non-singlet axial-vector currents which define $g_A^{(3)}$ and $g_A^{(8)}$. In the QCD parton model the anomaly corresponds to physics at the maximum transverse momentum squared [Carlitz *et al.* (1988)]. The anomaly contribution also involves non-local structure associated with gluon field topology – see Jaffe and Manohar (1990) and Bass (1998, 2003b). In dynamical axial U(1) symmetry breaking the anomaly and gluon topology are associated with the large masses of the η and η' mesons.

What values should we expect for the Δq? First, consider the static quark model. The simple SU(6) proton wavefunction

$$\begin{aligned}|p\uparrow\rangle = \frac{1}{\sqrt{2}}|u\uparrow(ud)_{S=0}\rangle + \frac{1}{\sqrt{18}}|u\uparrow(ud)_{S=1}\rangle - \frac{1}{3}|u\downarrow(ud)_{S=1}\rangle \\ -\frac{1}{3}|d\uparrow(uu)_{S=1}\rangle + \frac{\sqrt{2}}{3}|d\downarrow(uu)_{S=1}\rangle\end{aligned} \tag{1.11}$$

yields the values $g_A^{(3)} = \frac{5}{3}$ and $g_A^{(8)} = g_A^{(0)} = 1$.

In relativistic quark models one has to take into account the four-component Dirac spinor $\psi = \frac{N}{\sqrt{4\pi}}\binom{f}{i\sigma.\hat{r}g}$ where N is a normalization factor. The lower component of the Dirac spinor is p-wave with intrinsic spin primarily pointing in the opposite direction to the spin of the nucleon. Relativistic effects renormalize the axial charges obtained from SU(6) by the factor $N^2\int drr^2(f^2 - \frac{1}{3}g^2) \sim 0.6$ with a net transfer of angular momentum from intrinsic spin to orbital angular momentum – see e.g. Jaffe and Manohar (1990). $g_A^{(3)} \simeq 1.25$ (in agreement with experiment) and $g_A^{(0)} = g_A^{(8)} \simeq 0.6$. The model prediction $g_A^{(8)} \simeq 0.6$ agrees with the value extracted from hyperon beta-decays [$g_A^{(8)} = 0.58 \pm 0.03$ [Close and Roberts (1993)]] whereas the relativistic quark model prediction for $g_A^{(0)}$ exceeds the measured value of $g_A^{(0)}|_{\rm pDIS}$ by a factor of 2.

The overall picture of the spin structure of the proton that has emerged from a combination of experiment and theoretical QCD studies can be summarized in the following key observations:

First, the isovector Bjorken (1966, 1970) spin sum-rule relating the first moment of the isovector combination $g_1^{(p-n)} = g_1^p - g_1^n$ to the nucleon's isovector axial-charge $g_A^{(3)}$ has been successfully tested to better than 10% accuracy. Further, in the measured "small x" region $0.02 < x < 0.1$ the isovector spin structure exhibits a valence like rising behaviour $\sim x^{-0.5}$ in an x range where one would, a priori, not necessarily expect quark model results to apply. Constituent quark

model predictions work remarkably well for the isovector part of the nucleon's g_1 spin structure function at deep inelastic Q^2 [Bass (1999)].

Second, there has been considerable theoretical effort to understand the flavour-singlet axial-charge in QCD and the small value of $g_A^{(0)}|_{\rm pDIS}$. QCD theoretical analysis leads to the formula

$$g_A^{(0)} = \left(\sum_q \Delta q - 3\frac{\alpha_s}{2\pi}\Delta g \right)_{\rm partons} + \mathcal{C}_\infty. \tag{1.12}$$

Here $\Delta g_{\rm partons}$ is the amount of spin carried by polarized gluon partons in the polarized proton and $\Delta q_{\rm partons}$ measures the spin carried by quarks and antiquarks carrying "soft" transverse momentum $k_t^2 \sim P^2, m^2$ where P is a typical gluon virtuality and m is the light quark mass [Efremov and Teryaev (1988); Altarelli and Ross (1988)]. Since $\Delta g \sim 1/\alpha_s$ under QCD evolution, the polarized gluon term $[-\frac{\alpha_s}{2\pi}\Delta g]$ in Eq. (1.12) scales as $Q^2 \to \infty$ [Efremov and Teryaev (1988); Altarelli and Ross (1988)]. The polarized gluon term is associated with events in polarized deep inelastic scattering where the hard photon strikes a quark or antiquark generated from photon-gluon fusion and carrying $k_t^2 \sim Q^2$ [Carlitz *et al.* (1988)]. $\mathcal{C}_\infty$ denotes a potential non-perturbative gluon topological contribution [Bass (1998)] which is associated with the possible subtraction constant in the dispersion relation for g_1 [Bass (2005)]. It affects only the first moment and has support only at Bjorken x equal to zero so that it cannot be directly measured in polarized deep inelastic scattering.

The topological term $\mathcal{C}_\infty$ may be identified with a leading twist "subtraction at infinity" in the dispersion relation for g_1. It probes the role of gluon topology in dynamical axial U(1) symmetry breaking in the transition from current to constituent quarks in low energy QCD. If $\mathcal{C}_\infty$ is finite it would mean that $\lim_{\epsilon\to 0}\int_\epsilon^1 dx g_1$ will measure the difference of the singlet axial-charge and the subtraction constant; that is polarized deep inelastic scattering measures the combination $g_A^{(0)}|_{\rm pDIS} = g_A^{(0)} - C_\infty$. The deep inelastic measurement of $g_A^{(0)}$, Eq. (1.6), is not necessarily inconsistent with the constituent quark model prediction 0.6 *if* a substantial fraction of the spin of the constituent quark is associated with gluon topology in the transition from constituent to current quarks (measured in polarized deep inelastic scattering).

Possible explanations for the small value of $g_A^{(0)}$ extracted from the polarized deep inelastic experiments include screening from positive gluon polarization, negative strangeness polarization in the nucleon, a subtraction at infinity in the dispersion relation for g_1 associated with non-perturbative gluon topology, and connections to axial U(1) dynamics.

Why is the measured quark spin contribution so small compared to quark model predictions? Is the "missing spin" a valence quark or a sea effect? Are the quark-antiquark sea excitations polarized in the opposite direction to the proton's spin (thus cancelling some of the spin)? The spin of the gluons which bind the proton can screen the spin of the quarks measured in high-energy experiments through

Eq. (1.12). (Here $\alpha_s \sim 0.3$ is the QCD coupling at the scale of the present experiments and Δg is the gluon polarization). How large is the gluon polarization? The QCD vacuum is a quantum superposition of an infinite number of states characterized by non-local topological properties of QCD and non-trivial spin structure. When one puts a valence quark in this vacuum as a "source", the spin of the constituent quark can become delocalized so that the total spin becomes a property of the proton rather than the sum over localized current quark contributions probed in high energy experiments. How big is this effect?

A direct measurement of the strange-quark axial-charge, independent of the analysis of polarized deep inelastic scattering data and any possible "subtraction at infinity" correction, could be made using neutrino proton elastic scattering through the axial coupling of the Z^0 gauge boson. Comparing the values of Δs extracted from high-energy polarized deep inelastic scattering and low-energy neutrino-proton elastic scattering will provide vital information about the QCD structure of the proton.

On the theoretical side, when assessing models which attempt to explain the proton's spin structure it is important to look at the transverse momentum dependence of the proposed dynamics plus the model predictions for the shape of the spin structure functions as a function of Bjorken x in addition to the first moment and the nucleon's axial charges $g_A^{(3)}$, $g_A^{(8)}$ and $g_A^{(0)}$.

There is presently a vigorous programme to disentange the different contributions. Key experiments involve semi-inclusive polarized deep inelastic scattering (COMPASS and HERMES) and polarized proton-proton collisions at the world's first polarized proton-proton collider RHIC (PHENIX and STAR), and future polarized electron-proton collider studies. Experiments at Jefferson Laboratory are probing the spin properties of valence quarks in kinematics where they are sensitive to the confinement process.

Measurements by the COMPASS Collaboration at CERN and PHENIX and STAR experiments at RHIC suggest that the gluon polarization is much too small to resolve the difference between the quark model prediction $\sim 60\%$ for the quark spin contribution and the measured value $\sim 30\%$ through the anomaly mechanism although it may still make an important contribution to the net spin of the proton [Bass and Aidala (2006); Mallot (2006)]. The COMPASS and RHIC experiments use different processes to access the gluon polarization. The COMPASS measurements are extracted from the production of charm-particles and charged-particles with large transverse-momentum in polarized muon-nucleon collisions. The RHIC measurements are extracted from high-energy particle production in polarized proton-proton collisions. Measurements of the sea polarization by the HERMES experiment (DESY) suggest that this is also small, too small to resolve the spin puzzle and that the 30% quark spin contribution is approximately saturated by valence quark contributions [Airapetian *et al.* (2004)]. Independent measurements of the valence and sea quark contributions are being made by COMPASS.

Further interesting information about the structure of the proton are coming from the study of "transversity" spin distributions [Barone *et al.* (2002)]. Working in an infinite momentum frame, these observables measure the distribution of spin polarized transverse to the momentum of the proton in a transversely polarized proton. Since rotations and Euclidean boosts commute and a series of boosts can convert a longitudinally polarized nucleon into a transversely polarized nucleon at infinite momentum, it follows that the difference between the transversity and helicity distributions reflects the relativistic character of quark motion in the nucleon. Furthermore, the transversity spin distribution of the nucleon is charge-parity odd ($C = -1$) and therefore valence like (gluons decouple from its QCD evolution equation in contrast to the evolution equation for flavour-singlet quark distribution appearing in g_1) making a comparison of the different spin dependent distributions most interesting. Studies of transversity sensitive observables in lepton nucleon and polarized proton-proton scattering are being performed by the HERMES [Airapetian *et al.* (2005b)], COMPASS [Ageev *et al.* (2007)] and RHIC [Adams *et al.* (2004)] experiments.

One would also like to measure the parton orbital angular momentum contributions to the proton's spin. Exclusive measurements of deeply virtual Compton scattering and single meson production at large Q^2 offer a possible route to the quark and gluon angular momentum contributions through the physics and formalism of generalized parton distributions [Ji (1998); Goeke *et al.* (2001); Diehl (2003)]. A vigorous programme to study these reactions is being designed and investigated at several major world laboratories.

Spin measurements have a bright future, continue to surprise and to challenge our understanding about the structure of the proton and fundamental aspects of quark dynamics. Much exciting progress has been made. The next years promise to be equally exciting.

1.2 Outline

The book is organized as follows. In the first part (Chapters 2-8) we review the present status of the proton spin problem focussing on the present experimental situation for tests of polarized deep inelastic spin sum-rules and the theoretical understanding of $g_A^{(0)}$. In the second part (Chapters 9-15) we give an overview of the present global programme aimed at disentangling the spin-flavour structure of the proton and the exciting prospects for the new generation of experiments aimed at resolving the proton's internal spin structure. In Chapters 2-4 we give an overview of the derivation of the spin sum-rules for polarized photon-nucleon scattering, detailing the assumptions that are made at each step. Here we explain how these sum rules could be affected by potential subtraction constants (subtractions at infinity) in the dispersion relations for the spin dependent part of the forward Compton amplitude. We next give a brief review of the partonic (Chapter 3) and possible fixed

pole (Chapter 5) contributions to deep inelastic scattering. Fixed poles are well known to play a vital role in the Adler sum-rule for W-boson nucleon scattering [Adler (1966)] and the Schwinger term sum-rule for the longitudinal structure function measured in unpolarized deep inelastic ep scattering [Broadhurst *et al.* (1973)]. We explain how fixed poles could, in principle, affect the sum-rules for the first moments of the g_1 and g_2 spin structure functions. For example, a subtraction constant correction to the Ellis-Jaffe sum rule for the first moment of the nucleon's g_1 spin dependent structure function would follow if there is a constant real term in the spin dependent part of the deeply virtual forward Compton scattering amplitude. Chapter 6 discusses the QCD axial anomaly and its possible role in understanding the first moment of g_1. The relationship between the spin structure of the proton and chiral symmetry is outlined in Chapter 7. This first part of the paper concludes with an overview in Chapter 8 of the different possible explanations of the small value of $g_A^{(0)}$ that have been proposed in the literature, how they relate to QCD, and possible future experimental tests which could help clarrify the key issues. We next focus on the new programme to disentangle the proton's spin-flavour structure and the Bjorken x dependence of the separate valence, sea and gluonic contributions (Chapters 9-12), the theory and experimental investigation of transversity observables (Chapter 13), quark orbital angular momentum and exclusive reactions (Chapter 14) and the g_1 spin structure function of the polarized photon (Chapter 15). A summary of key issues and challenging questions for the next generation of experiments is given in Chapter 16.

Complementary review articles on the spin structure of the proton, each with a different emphasis, are given in Anselmino *et al.* (1995), Cheng (1996), Shore (1998b), Lampe and Reya (2000), Fillipone and Ji (2001), Jaffe (2001), Barone *et al.* (2002), Stoesslein (2002), Bass (2005) and Bass and Aidala (2006).

Chapter 2

SPIN EXPERIMENTS AND DATA

2.1 Introduction

Our present knowledge about the high-energy spin structure of the nucleon comes from polarized deep inelastic scattering experiments at CERN, DESY, JLab and SLAC, and high-energy polarized proton-proton collisions at RHIC.

We first consider polarized deep inelastic scattering. (Polarized proton-proton collisions are described in Section 2.4 below.) Polarized deep inelastic experiments involve scattering a high-energy charged lepton beam from a nucleon target at large momentum transfer squared. The lepton beam (electrons at DESY, JLab and SLAC and muons at CERN) is longitudinally polarized. The nucleon target may be either longitudinally or transversely polarized.

Consider polarized ep scattering. We work in one photon exchange approximation – Fig. 2.1. Whilst the lepton photon vertex is described by perturbative QED, the internal QCD structure of the proton means that the photon proton interaction is described in terms of various structure functions (form-factors). Polarized

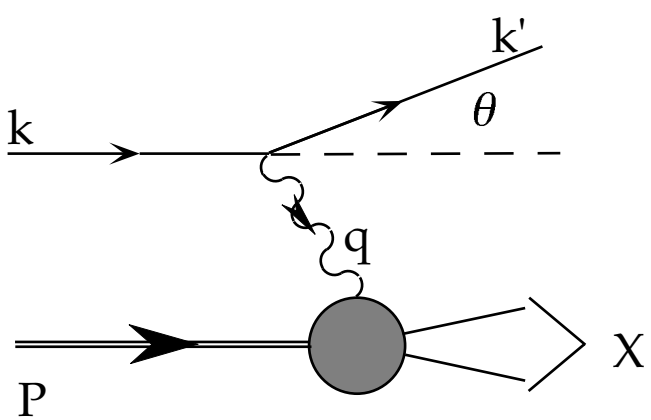

Fig. 2.1 Deep inelastic lepton-nucleon scattering mediated by virtual photon exchange.

deep inelastic scattering experiments have so far all been performed using a fixed target. We specialise to the target rest frame and let E and $k^\mu = (E;\vec{k})$ denote the energy and momentum of the incident electron with mass m which is scattered through an angle θ to emerge in the final state with energy E' and momentum $k^{'\mu} = (E';\vec{k}')$. The exchanged photon carrying momentum $q_\mu = k_\mu - k'_\mu$ scatters from a polarized proton with momentum p_μ, mass M and spin s_μ.

The photon-nucleon scattering is characterised by the two invariants $Q^2 = -q^2$ and $\nu = p.q/M$, where $\nu = (E - E')$ in the target rest frame. The Bjorken variable x is defined by the ratio $x = Q^2/2M\nu$.

For inclusive scattering the final state hadrons X are not separated, – that is, we sum over all accessible hadronic final states and scattered lepton spins and measure the inclusive cross-section. For semi-inclusive deep inelastic scattering processes we tag on a particular final state hadron carrying a significant fraction of the energy of the incident photon or with high transverse momentum. These final state hadrons carry memory of the struck quark and tell us about the distribution of quarks, antiquarks and gluons carrying different momenta and spin in the nucleon. We discuss these processes in detail in Chapters 11 and 12.

The differential cross section for the one photon exchange process for inclusive lepton nucleon scattering is given by

$$\frac{d^2\sigma}{d\Omega dE'} = \frac{\alpha^2}{Q^4}\frac{E'}{E}L_{\mu\nu}W^{\mu\nu} \tag{2.1}$$

Here α is the fine structure constant; $L_{\mu\nu}$ and $W_{\mu\nu}$ describe the muon and hadronic vertices respectively. Since the electron is pointlike we can write an exact expression for $L_{\mu\nu}$ using the Feynman rules:

$$\begin{aligned}\frac{1}{2}\,L_{\mu\nu} &= \mathrm{Tr}\,\{\overline{u}_k\gamma_\mu u_{k'}\}\,\{\overline{u}_{k'}\gamma_\nu u_k\} \\ &= \quad k_\mu k'_\nu + k'_\mu k_\nu - g_{\mu\nu}(k.k' - m^2) + i\epsilon_{\mu\nu\alpha\beta}k^\alpha q^\beta \end{aligned}\tag{2.2}$$

Since the proton is a complex bound state governed by non-perturbative confinement dynamics and not an elementary state one cannot write down an exact expression for $W^{\mu\nu}$ in contrast to the situation where, for example, we scatter from a lepton target. Form-factors or structure functions in the hadron tensor $W_{\mu\nu}$ parametrise the information about the target. The general structure of the hadron tensor for photon-nucleon scattering is determined by symmetry arguments: covariance, even parity and current conservation ($q^\mu W_{\mu\nu} = q^\nu W_{\mu\nu} = 0$). The spin independent and spin dependent components of $W_{\mu\nu}$ are

$$W^S_{\mu\nu} = -W_1(g_{\mu\nu} + \frac{q_\mu q_\nu}{Q^2}) + \frac{1}{M^2}W_2(p_\mu + \frac{p.q}{Q^2}q_\mu)(p_\nu + \frac{p.q}{Q^2}q_\nu) \tag{2.3}$$

and

$$W^A_{\mu\nu} = \frac{i}{M^2}\epsilon_{\mu\nu\lambda\sigma}q^\lambda\left[s^\sigma(G_1 + \frac{\nu}{M}G_2) - \frac{1}{M^2}s.qp^\sigma G_2\right] \tag{2.4}$$

respectively. The structure functions contain all of the target dependent information in the inclusive scattering process.

Using the expressions for $L_{\mu\nu}$ and $W_{\mu\nu}$ in Eqs. (2.2)-(2.4) we can readily obtain the cross-sections for inclusive photon-nucleon and lepton-nucleon scattering. We take standard photon polarization vectors ϵ_μ satisfying $\epsilon.q = 0$, with $\epsilon_T^2 = -1$ for transverse polarization and $\epsilon_0^2 = 1$ for longitudinal polarization. The proton spin vector is defined as

$$s_\mu = \left(\frac{\mathrm{p}.\xi}{M}, \xi + \frac{(\mathrm{p}.\xi)\mathrm{p}}{M(E+M)}\right) \tag{2.5}$$

where ξ is the unit vector along the direction of the polarization in the nucleon rest frame. The proton spin vector satisfies $s^2 = -1$ and $s.p = 0$.

The cross sections for the absorption of a transversely polarized photon with spin polarized parallel $\sigma_{\frac{3}{2}}$ and anti-parallel $\sigma_{\frac{1}{2}}$ to the spin of a longitudinally polarized target nucleon are

$$\begin{aligned}
\sigma_{\frac{3}{2}} &= \frac{4\pi^2\alpha}{\sqrt{\nu^2+Q^2}}\left[W_1 - \frac{\nu}{M^2}G_1 + \frac{Q^2}{M^3}G_2\right] \\
\sigma_{\frac{1}{2}} &= \frac{4\pi^2\alpha}{\sqrt{\nu^2+Q^2}}\left[W_1 + \frac{\nu}{M^2}G_1 - \frac{Q^2}{M^3}G_2\right],
\end{aligned} \tag{2.6}$$

where we use usual conventions for the virtual photon flux factor [Roberts (1990)]: $\texttt{flux} = \sqrt{\nu^2+Q^2}$. The spin dependent and spin independent parts of the inclusive

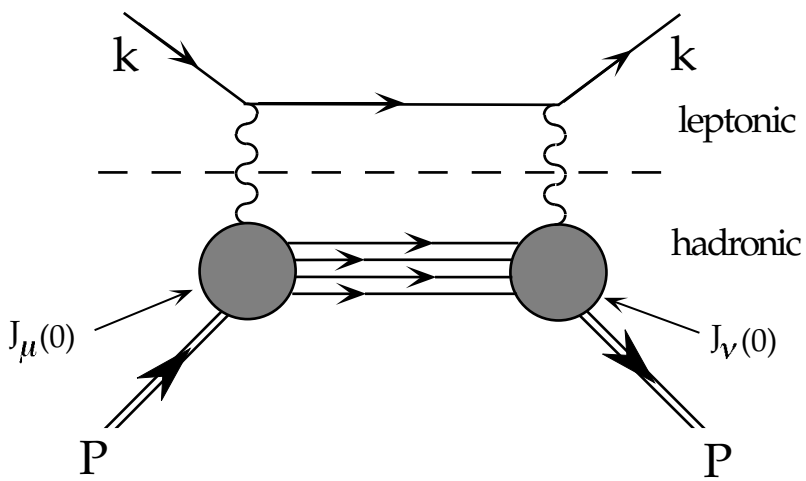

Fig. 2.2 The squared amplitude $\mathcal{A}$ for electron-hadron scattering can be separated into a leptonic tensor $L_{\mu\nu}$ and a hadronic tensor $W_{\mu\nu}$.

photon-nucleon cross section are

$$\sigma_{\frac{1}{2}} - \sigma_{\frac{3}{2}} = \frac{8\pi^2\alpha}{\sqrt{\nu^2+Q^2}}\left[\frac{\nu}{M^2}G_1 - \frac{Q^2}{M^3}G_2\right] \tag{2.7}$$

and

$$\sigma_{\frac{1}{2}} + \sigma_{\frac{3}{2}} = \frac{8\pi^2\alpha}{\sqrt{\nu^2+Q^2}}W_1. \tag{2.8}$$

The G_2 spin structure function decouples from polarized photoproduction. For real photons ($Q^2 = 0$) one finds the equation $\sigma_{\frac{1}{2}} - \sigma_{\frac{3}{2}} = \frac{8\pi^2\alpha}{M^2}G_1$. The cross section for the absorption of a longitudinally polarized photon is

$$\sigma_0 = \frac{4\pi^2\alpha}{\sqrt{\nu^2+Q^2}}W_L = \frac{4\pi^2\alpha}{\sqrt{\nu^2+Q^2}}\left[\left\{1+\frac{\nu^2}{Q^2}\right\}W_2 - W_1\right]. \tag{2.9}$$

The W_2 structure function is measured in unpolarized lepton nucleon scattering through the absorption of transversely and longitudinally polarized photons.

The final state hadrons in the photon-nucleon scattering process have invariant mass squared (centre of mass energy squared)

$$W^2 = (p+q)^2 = M^2 + 2p.q - Q^2 = M^2 + Q^2\left(\frac{1-x}{x}\right) \geq M^2 \tag{2.10}$$

It follows that $0 \leq x \leq 1$ where $x = 1$ corresponds to elastic scattering $W^2 = M^2$ and $Q^2 = 0$ to photoproduction. (The case $x \leq 0$ corresponds to the process $p \to \gamma^* X$.)

2.2 Scaling and polarized deep inelastic scattering

In high Q^2 deep inelastic scattering the structure functions exhibit approximate scaling. One finds

$$\begin{aligned} M\ W_1(\nu, Q^2) &\to F_1(x, Q^2) \\ \nu\ W_2(\nu, Q^2) &\to F_2(x, Q^2) \\ \frac{\nu}{M}\ G_1(\nu, Q^2) &\to g_1(x, Q^2) \\ \frac{\nu^2}{M^2}\ G_2(\nu, Q^2) &\to g_2(x, Q^2). \end{aligned} \tag{2.11}$$

The structure functions F_1, F_2, g_1 and g_2 are to a very good approximation independent of Q^2 and depend *only* on x. (The small Q^2 dependence which is present in these structure functions is logarithmic and determined by perturbative QCD evolution.)

The relation between deep inelastic lepton nucleon cross-sections and the virtual-photon nucleon cross-sections is discussed and derived in Roberts (1990) and Windmolders (2002). We work in the target rest frame using the kinetic variables defined above and let $\uparrow\downarrow$ denote the longitudinal polarization of the electron

beam. For a longitudinally polarized proton target (with spin denoted $\Uparrow\Downarrow$) the unpolarized and polarized differential cross-sections are

$$\left(\frac{d^2\sigma\uparrow\Uparrow}{d\Omega dE'}+\frac{d^2\sigma\uparrow\Downarrow}{d\Omega dE'}\right)=\frac{\alpha^2}{4E^2\sin^4\frac{\theta}{2}}\left[2\sin^2\frac{\theta}{2}\ F_1(x,Q^2)\ +\ \frac{M}{\nu}\cos^2\frac{\theta}{2}\ F_2(x,Q^2)\right] \tag{2.12}$$

and

$$\left(\frac{d^2\sigma\uparrow\Uparrow}{d\Omega dE'}-\frac{d^2\sigma\uparrow\Downarrow}{d\Omega dE'}\right)=\frac{4\alpha^2}{M\nu}\frac{E'}{Q^2E}\left[(E+E'\cos\theta)\ g_1(x,Q^2)-2xM\ g_2(x,Q^2)\right] \tag{2.13}$$

For a target polarized transverse to the electron beam the spin dependent part of the differential cross-section is

$$\left(\frac{d^2\sigma\uparrow\Rightarrow}{d\Omega dE'}-\frac{d^2\sigma\uparrow\Leftarrow}{d\Omega dE'}\right)=\frac{4\alpha^2}{M\nu}\frac{E'^2}{Q^2E}\sin\theta\left[\ g_1(x,Q^2)+\frac{2E}{\nu}\ g_2(x,Q^2)\right] \tag{2.14}$$

In unpolarized scattering, where we average over the target polarization, the antisymmetric part of $W_{\mu\nu}$ vanishes and we measure the form factors $F_1(x,Q^2)$ and $F_2(x,Q^2)$. The two form factors $g_1(x,Q^2)$ and $g_2(x,Q^2)$ contribute to the cross section in the product of $W^A_{\mu\nu}$ and the antisymmetric part of $L_{\mu\nu}$. They can be measured only with a polarized nucleon target and a polarized lepton (electron or muon) beam.

Substituting (2.11) in the cross-section formulae (2.12) and (2.13) for the longitudinally polarized target one finds that the g_2 contribution to the differential cross section and the longitudinal spin asymmetry is suppressed relative to the g_1 contribution by the kinematic factor $\frac{M}{E}\sim 0$, *viz.*

$$\mathcal{A}_1=\frac{\sigma_{\frac{1}{2}}-\sigma_{\frac{3}{2}}}{\sigma_{\frac{1}{2}}+\sigma_{\frac{3}{2}}}=\frac{M\nu G_1-Q^2G_2}{M^3W_1}=\frac{g_1-\gamma^2\ g_2}{F_1}\rightarrow\frac{g_1}{F_1} \tag{2.15}$$

where

$$\gamma=2Mx/\sqrt{Q^2}=\sqrt{Q^2}/\nu \tag{2.16}$$

For a transverse polarized target this kinematic suppression factor for g_2 is missing meaning that transverse polarization is vital to measure g_2. We refer to Roberts (1990) and Windmolders (2002) for the procedure how the spin dependent structure functions are extracted from the spin asymmetries measured in polarized deep inelastic scattering.

2.3 The QCD parton model

Deep inelastic scattering involves working in the Bjorken limit: Q^2 and ν both $\rightarrow\infty$ with the Bjorken variable $x=Q^2/2p.q$ held fixed. One should be out of the resonance region $W^2\gg M^2$ so that W^2 does not coincide with the mass squared

of one of the excited nucleon resonances. We are free to choose the z axis in our target rest frame so that $q^\mu = (q^0; 0_t, q^3)$. Since $-q^2 = Q^2$ we may write

$$q^\mu = \left(q^0; 0_t, q^0\sqrt{1 + \frac{Q^2}{q_0^2}}\right) \tag{2.17}$$

whereby $q_+ = \frac{1}{\sqrt{2}}(q_0 + q_3) =$ finite and $q_- = \frac{1}{\sqrt{2}}(q_0 - q_3) \to \infty$ in the deep inelastic (Bjorken) limit. The Bjorken variable becomes

$$x = -q_+/p_+ \tag{2.18}$$

In the kinematic region of deep inelastic scattering the structure functions behave as functions of x alone. The Q^2 dependence becomes almost trivial and is observed only as a slow logarithmic variation $\sim \ln Q^2$. This scaling property inspired Feynman to deduce the parton model of the nucleon. The deep inelastic cross-section is, in first approximation, the incoherent sum over elastic lepton quark-parton scattering.

In the (pre-QCD) parton model the deep inelastic structure functions F_1 and F_2 are written as

$$F_1(x) = \frac{1}{2x}F_2(x) = \frac{1}{2}\sum_q e_q^2\{q + \bar{q}\}(x) \tag{2.19}$$

and the polarized structure function g_1 is

$$g_1(x) = \frac{1}{2}\sum_q e_q^2 \Delta q(x). \tag{2.20}$$

Here e_q denotes the electric charge of the struck quark and

$$\begin{aligned} \{q + \bar{q}\}(x) &= (q^\uparrow + \overline{q}^\uparrow)(x) + (q^\downarrow + \overline{q}^\downarrow)(x) \\ \Delta q(x) &= (q^\uparrow + \overline{q}^\uparrow)(x) - (q^\downarrow + \overline{q}^\downarrow)(x) \end{aligned} \tag{2.21}$$

denote the spin-independent (unpolarized) and spin-dependent quark parton distributions which measure the distribution of quark momentum and spin in the proton. For example, $\overline{q}^\uparrow(x)$ is interpreted as the probability to find an anti-quark of flavour q with plus component of momentum xp_+ (p_+ is the plus component of the target proton's momentum) and spin polarized in the same direction as the spin of the target proton.

The spin asymmetry $\mathcal{A}_1$ can be understood as follows. A quark having its spin projection along the reference axis (+OZ) can absorb a virtual photon which has its spin projection along (−OZ) and flip its spin, while no absorption can occur when the two spins in the initial state are oriented in the same direction. The absorption cross section for virtual photons with spin projection opposite to the nucleon spin, $\sigma_{1/2}$, will be proportional to $q^\uparrow(x)$ while the absorption cross section for virtual

photons with spin parallel to the nucleon spin, $\sigma_{3/2}$, will be proportional to $q^{\downarrow}(x)$. One then obtains Eq. (2.15), *viz.*

$$\mathcal{A}_1 = \frac{\sigma_{1/2} - \sigma_{3/2}}{\sigma_{1/2} + \sigma_{3/2}} \cong \frac{\sum e_i^2 (q_i^{\uparrow}(x) + \bar{q}_i^{\uparrow}(x) - q_i^{\downarrow}(x)) - \bar{q}_i^{\downarrow}(x))}{\sum e_i^2 (q_i^{\uparrow}(x) + \bar{q}_i^{\uparrow}(x) + q_i^{\downarrow}(x)) + \bar{q}_i^{\downarrow}(x))} \tag{2.22}$$

When we integrate out the momentum fraction x the first moments of the unpolarized parton distributions measure the number of valence quarks in the proton:

$$\begin{aligned} \int_0^1 dx(u - \bar{u})(x) &= 2 \\ \int_0^1 dx(d - \bar{d})(x) &= 1 \\ \int_0^1 dx(s - \bar{s})(x) &= 0 \end{aligned} \tag{2.23}$$

for the up, down and strange quarks respectively. The quantity

$$\Delta q = \int_0^1 dx \ \Delta q(x) \tag{2.24}$$

is interpreted as the fraction of the proton's spin which is carried by quarks (and anti-quarks) of flavour q – hence the parton model interpretation of $g_A^{(0)}$ as the total fraction of the proton's spin carried by up, down and strange quarks. In QCD the flavour-singlet combination of these quark parton distributions mixes with the spin independent and spin dependent gluon distributions respectively under Q^2 evolution.

The second spin structure function g_2 has a non-trivial parton interpretation [Jaffe (1990)] and vanishes without the effect of quark transverse momentum – see e.g. Roberts (1990).

The logarithmic $\sim \ln Q^2$ scaling violations observed in deep inelastic structure functions are associated with QCD and asymptotic freedom. These scaling violations are shown in Fig. 2.4 for the unpolarized structure function F_2 and Fig. 2.8 for the spin dependent structure function g_1. The QCD quark-gluon and gluon-gluon coupling is scale dependent and runs with the momentum transfer Q^2. In leading order perturbation theory

$$\alpha_s(Q^2) = \frac{4\pi}{\beta_0 \ln(Q^2/\Lambda^2)} \tag{2.25}$$

Here $\beta_0 = 11 - \frac{2}{3}f$ where f is the number of active flavours and $\Lambda \approx 200$ MeV is the QCD scale. The running coupling goes logarithmically to zero at infinite Q^2 and becomes large in the infra-red, leading to confinement and dynamical chiral symmetry breaking. This running of α_s is shown in Fig. 2.3 for a recent compilation of measurements [Bethke (2002)].

The scale dependence shows excellent agreement with the predictions of perturbative QCD over a wide energy range. When translated into measurements of

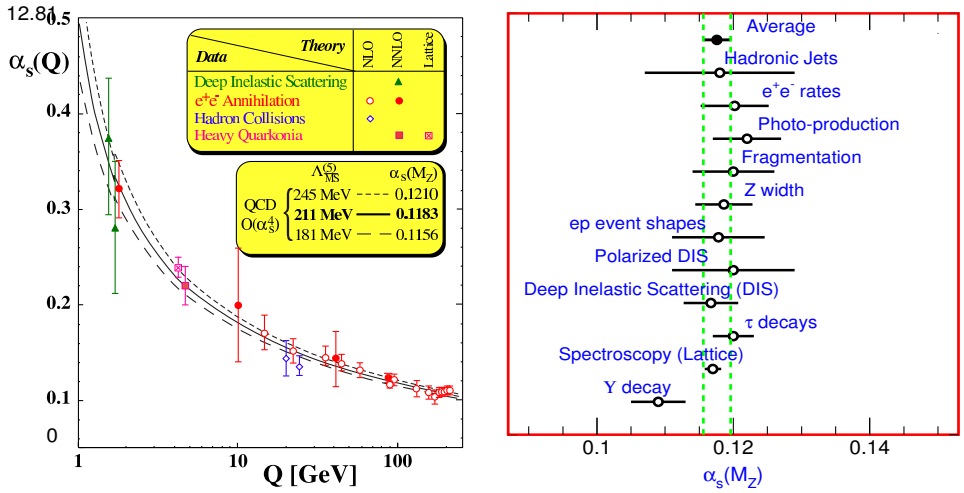

Fig. 2.3 Compilation of α_s values from different measurements from Bethke (2002).

$\alpha_s(M_z)$, the separate measurements are consistent with each other and each overlap with the world average value $\alpha_s(M_z) = 0.1183 \pm 0.0027$.

The finite QCD coupling means that we have to consider the effects of gluon radiation and (renormalization group) mixing of the flavour-singlet quark distribution with the polarized gluon distribution of the proton. The parton model description of polarized deep inelastic scattering involves writing the deep inelastic structure functions as the sum over the convolution of "soft" quark and gluon parton distributions with "hard" photon-parton scattering coefficients. For the F_2 unpolarized structure function

$$
\begin{aligned}
F_2\ (x,Q^2) \ &= 2x\int_x^1 \frac{dz}{z}\Bigg\{\frac{1}{12}(u+\bar{u}-d-\bar{d})(z,Q^2)) \\
&\quad + \frac{1}{36}(u+\bar{u}+d+\bar{d}-2(s+\bar{s}))(z,Q^2)\Bigg\}E^q_{ns}(\frac{x}{z},\alpha_s) \\
&\quad + \frac{2}{9}x\Bigg\{\int_x^1 \frac{dz}{z}(u+\bar{u}+d+\bar{d}+s+\bar{s})(z,Q^2)E^q_s(\frac{x}{z},\alpha_s) \\
&\quad + f\int_x^1 \frac{dz}{z}g(z,Q^2)E^g(\frac{x}{z},\alpha_s)\Bigg\}
\end{aligned}
\tag{2.26}
$$

For the g_1 spin structure function

$$\begin{aligned} & g_1\ (x,Q^2) \\ & = \int_x^1 \frac{dz}{z}\left\{ \frac{1}{12}(\Delta u - \Delta d)(z,Q^2) + \frac{1}{36}(\Delta u + \Delta d - 2\Delta s)(z,Q^2) \right\} C_{ns}^q(\frac{x}{z},\alpha_s) \\ & \quad + \frac{1}{9}\left\{ \int_x^1 \frac{dz}{z}(\Delta u + \Delta d + \Delta s)(z,Q^2) C_s^q(\frac{x}{z},\alpha_s) + f\int_x^1 \frac{dz}{z}\Delta g(z,Q^2) C^g(\frac{x}{z},\alpha_s) \right\}. \end{aligned} \tag{2.27}$$

In these equations $q(x)$ and $g(x)$ denote the unpolarized quark and gluon parton distributions and $\Delta q(x)$ and $\Delta g(x)$ denote the polarized quark and gluon parton distributions ($q = u, d, s$); $E^q(z)$ and $E^g(z)$ and $C^q(z)$ and $C^g(z)$ denote the corresponding hard scattering coefficients, and f is the number of quark flavours liberated into the final state ($f = 3$ below the charm production threshold). The parton distributions contain all the target dependent information and describe a flux of quark and gluon partons into the (target independent) interaction between the hard photon and the parton which is described by the coefficients and which is calculable using perturbative QCD – essentially the cross-sections for hard-photon parton scattering. The perturbative coefficients are independent of infra-red mass singularities in the photon-parton collision which are absorbed into the soft parton distributions (and softened by confinement related physics).

The logarithmic $\ln Q^2$ dependence of the polarized and unpolarized parton distributions is determined by the DGLAP equations (Dokshitzer, Gribov, Lipatov, Altarelli, Parisi). We describe this evolution in Chapters 3 and 10 below. One prediction of QCD evolution is that in the asymptotic limit $Q^2 \to \infty$ the fraction of momentum carried by quarks and gluons should go to [Gross and Wilczek (1974)]

$$\begin{aligned} \langle x(q+\overline{q})(x)\rangle &\to \frac{3f}{(16+3f)} \\ \langle xg(x)\rangle &\to \frac{16}{(16+3f)} \end{aligned} \tag{2.28}$$

Experimentally, each term is observed to be about 50% at typical deep inelastic values of Q^2.

In Figures 2.4 and 2.5 we show the world data set on the unpolarized structure function F_2 and a recent fit to the unpolarized quark and gluon parton distributions. Note the large sea and gluon distributions at small Bjorken x. The valence quarks all but saturate the structure function for x greater than about 0.2.

2.4 Spin experiments

Deep inelastic measurements of g_1 have been performed in experiments at CERN, DESY, JLab and SLAC.

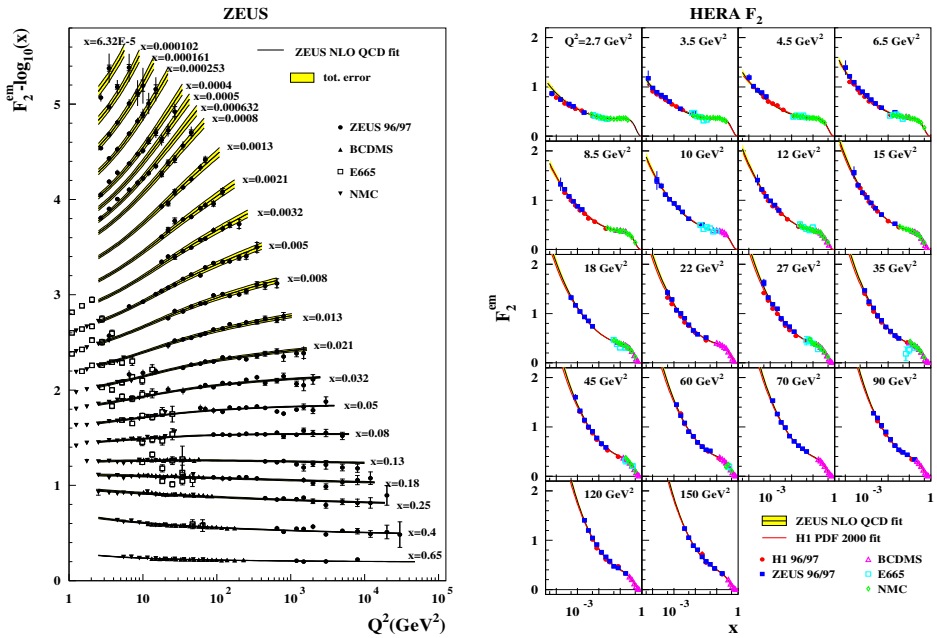

Fig. 2.4 The plot on the left shows the world data on F_2 as a function of Q^2 for fixed values of x. On the right we show the converse: F_2 as a function of x for fixed values of Q^2. From Chekanov *et al.* (2003a).

The first polarized deep inelastic scattering experiments were performed by the SLAC-Yale Collaboration [Baum *et al.* (1983)] in the early 1980's using an electron beam and proton target and measured g_1 down to $x = 0.1$. These measurements were consistent with the naive parton model view that $\sim 60\%$ of the nucleon spin is carried by its quark parton constituents. The EMC (European Muon Collaboration) experiment [Ashman *et al.* (1988, 1989)] at CERN used a muon beam and extended the inclusive measurements down to $x = 0.01$. The EMC data led to the spin puzzle, hinting that the contribution of the quarks to the spin of the proton is small. These findings triggered a whole program of polarized deep inelastic fixed target experiments, with electron beams at SLAC [Abe *et al.* (1997); Anthony *et al.* (1999, 2000)], a muon beam at CERN (the SMC or Spin Muon Collaboration) [Adeva *et al.* (1998a); Adeva *et al.* (1999)] and the electron ring of the HERA collider on an internal target (HERMES) [Ackerstaff *et al.* (1997); Airapetian *et al.* (1998, 2007)] at DESY. The lowest values in x for a Q^2 around

1 GeV^2 which could be achieved in these experiments amounts to approximately 10^{-3} in SMC, due to the high energy of the muon beam.

These experiments confirmed the spin puzzle with much increased precision and launched a series of new measurements, such as semi-inclusive ones to disentangle the separate spin contributions carried by the valence and sea quarks and polarized gluons. A new fixed target experiment COMPASS [Abbon *et al.* (2007)] has been assembled in the last years using the muon beam at CERN, with its main mission to make a direct measurement of gluon polarization Δg in the region $x \sim 0.1$. The present COMPASS programme involves a substantial increase (factor of 5) in the luminosity compared to the SMC with an integrated luminosity during the years 2002-04 of about 2 fb^{-1}. The COMPASS and HERMES experiments are also making semi-inclusive measurements of valence and sea quark polarization and gluon polarization in the nucleon.

The CERN muon beams experiments have the highest energy (100-200 GeV) but much lower beam intensity (10^7 muons per second for the SMC, compared to 10^{12} electrons per second at SLAC). Due to the limited intensity, muon experiments

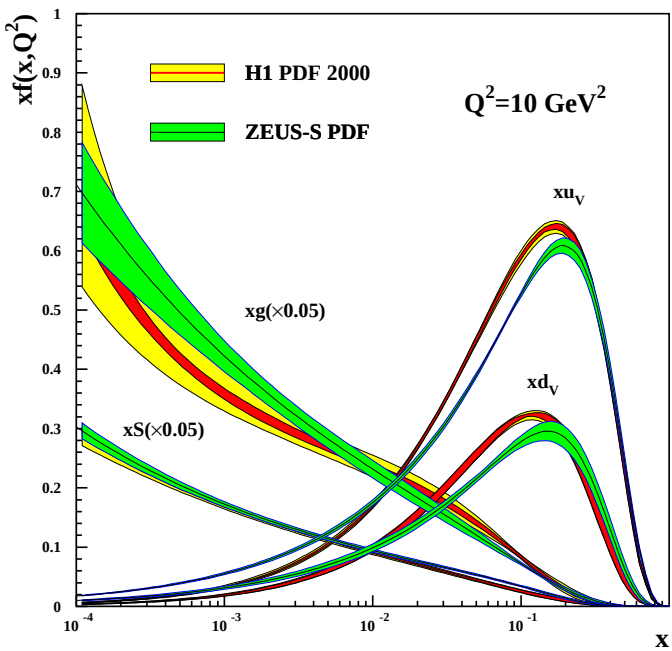

Fig. 2.5 The valence (up and down) quark, sea quark and gluon distributions plotted as a function of x for fixed $Q^2 = 10$ GeV^2. Note that the sea and glue distributions are scaled down by a factor of 1/20. From Chekanov *et al.* (2003a).

need large polarized targets. The polarized electron beam experiments were run at Jefferson Lab with continuous electron beams (in the energy range of 2-6 GeV), SLAC (10-50 GeV) and HERMES at DESY (27 GeV). These experiments also use high intensity beams and consequently need only relatively small targets to reach a high statistical accuracy. They invert very frequently either the beam polarization (Jefferson Lab and SLAC) or the target polarization (DESY) and are therefore not very sensitive to systematic effects due to changes in detector acceptance. Their kinematic range has however been limited due to the relatively low incident beam energy. At CERN the incident muons are obtained from two-body decays of pions and kaons, and are naturally polarized due to the non-conservation of parity in the weak decay.

In parallel to developments in polarized deep inelastic scattering it was realised that polarized proton-proton collisions could also give valuable information on polarized glue in the proton, and the Relativistic Heavy Ion Collider, RHIC, was "upgraded" during its construction phase to include the option of polarized proton-proton scattering [Bunce *et al.* (2000)]. The programme relies on the QCD factorization theorem (see Chapter 3) so that measurements of high-energy and high-momentum pion and photon production in polarized proton-proton collisions tell us about the distribution of polarized quarks and gluons in the proton. Future experiments plan to use W-boson production in a Drell-Yan like experiment to extract information about valence and sea quark polarization. Polarization of the proton beam is technically more involved than for the electron beam, since protons do not polarize naturally in a storage ring, at least not within any useful time span. Hence beams from a source of polarized protons have to be accelerated through the whole chain, keeping the polarization during the process. Special magnets called Siberian Snakes allow the protons to pass depolarizing resonances during the acceleration and correct for depolarizing distortions during the storage of the beam. Thus polarized proton-proton collisions with a centre of mass system (CMS) energy in the range of 50-500 GeV could be provided at RHIC, with an integrated luminosity of 320 pb^{-1} at 200 GeV and 800 pb^{-1} at 500 GeV. There are two major experiments pursuing this programme: PHENIX and STAR which measure both longitudinal and transverse spin asymmetries, and also two smaller spin experiments: BRAHMS which measures transverse spin asymmetries and pp2pp which measures spin dependence in small-angle elastic scattering. The present status at the time of writing is that 60% average beam polarization and average luminosity $\mathcal{L} = 2 \times 10^{31}$ cm$^{-2}s^{-1}$ were achieved in 2006 at $\sqrt{s} = 200$ GeV.

The figure of merit for the comparison of experiments performed with different beams or different targets is given by

$$(P_b \; P_T \; f)^2 \; N_{tot}. \tag{2.29}$$

Here P_b is the polarization of the beam, P_T is the polarization of the target, f is the dilution factor (the fraction of scattered events that result from the polarized atoms of interest) and N_{tot} is the number of interactions. Examples of the large

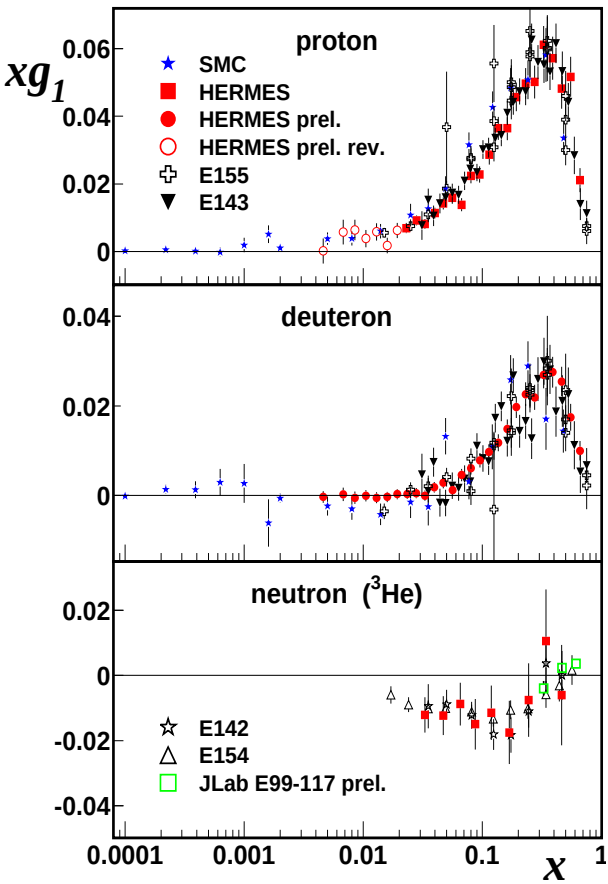

Fig. 2.6 The world data on xg_1 with data points shown at the Q^2 they were measured at. Figure courtesy of U. Stoesslein.

range of experimental parameters for the measurements include variations in the beam polarization of $40-80\%$, in the target polarization of $30-90\%$ and in the correction for dilution of the experimental asymmetry due to unpolarized material of $0.1-1$.

2.5 Spin data

An overview of the world data on the nucleon's g_1 spin structure function (pre-COMPASS) is shown in Figure 2.6 (which shows xg_1) and Figure 2.7 (which shows g_1). Recent precise COMPASS data for the deuteron spin structure function g_1^d is

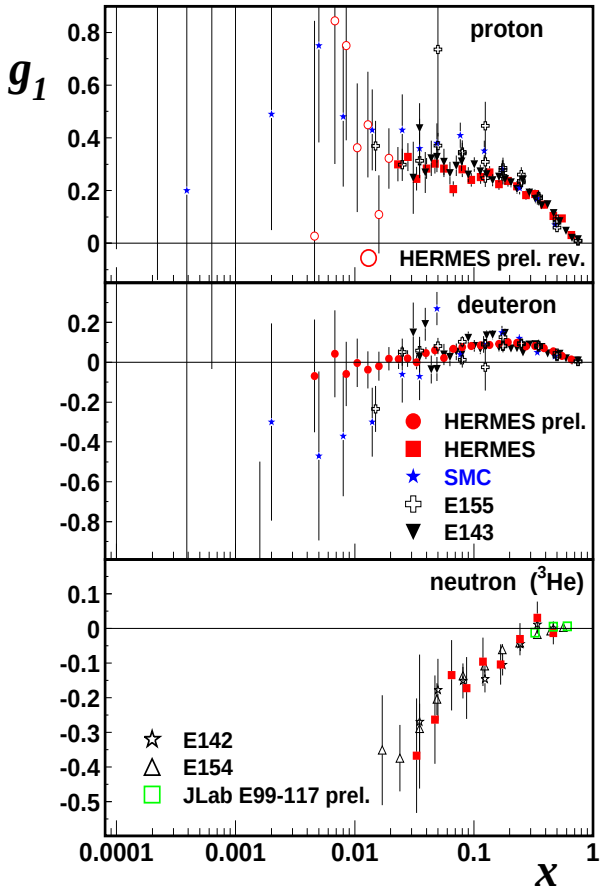

Fig. 2.7 The world data on g_1 with data points shown at the Q^2 they were measured at. Figure courtesy of U. Stoesslein.

shown in Fig. 2.9. There is a general consistency between all data sets. The largest range is provided by the SMC and COMPASS experiments [Adeva *et al.* (1998a); Adeva *et al.* (1999)], namely $0.00006 < x < 0.8$ and $0.02 < Q^2 < 100$ GeV^2. These experiments use proton and deuteron targets with 100-200 GeV muon beams. The final results from SMC are given in [Adeva *et al.* (1998a)]. The deuteron data from COMPASS are shown separately in Fig. 2.9 [Alexakhin *et al.* (2007a)] and reveal the remarkable feature that g_1^d is consistent with zero in the small x region between 0.004 and 0.02. The low x data from SMC [Adeva *et al.* (1999)] are at a Q^2 well below 1 GeV^2, and the asymmetries are found to be compatible with zero. The most precise data comes from the electron scattering experiments at SLAC (E154

on the neutron [Abe *et al.* (1997)] and E155 on the proton [Anthony *et al.* (1999, 2000)]), JLab [Zheng *et al.* (2004a,b)] (on the neutron) and HERMES at DESY [Airapetian *et al.* (1998); Ackerstaff *et al.* (1997)] (on the proton and neutron), with JLab focussed on the large x region.

The recipes for extracting the neutron's spin structure function from experiments using a deuteron or ^{3}He target are discussed in Piller and Weise (2000) and Thomas (2002). Corrections should be made to allow for the D-state component of the deuteron or ^{3}He wavefunctions. The deuteron spin projection +1 is primarily a neutron or a proton in an S-state each with spin $\frac{1}{2}$ but there is also a small probability $\sim 5\%$ to find them in a relative D-state, in which case the spins can be up or down. One also has to correct for Fermi motion, binding and the fact that the nucleons can be slightly off mass-shell. The best estimates are that for $x < 0.8$

$$g_1^n(x,Q^2) = \frac{2g_1^d(x,Q^2)}{(1-1.5\omega_D)} - g_1^p(x,Q^2) \tag{2.30}$$

where $\omega_D \sim 5\%$ is the D-state probability of the deuteron [Lacombe *et al.* (1981)]. For polarized ^{3}He the largest component of the nuclear wavefunction consists of two protons with spins opposite, so that the nuclear spin is carried entirely by the neutron. Fermi motion and binding corrections are larger than for the deuteron and one must again correct for the D-state component of the ^{3}He wavefunction. One finds

$$g_1^n(x,Q^2) = \frac{1}{\rho_n}(g_1^{^3He} - 2\rho_p g_1^p) \ , \tag{2.31}$$

where $\rho_n = (86 \pm 2)\%$ and $\rho_p = (-2.8 \pm 0.4)\%$ [Ciofi degli Atti *et al.* (1993)].

Note the large isovector component in the data at small x (between 0.01 and 0.1) which considerably exceeds the isoscalar component in the measured kinematics. This result is in stark contrast to the situation in the unpolarized structure function F_2 where the small x region is dominated by isoscalar pomeron exchange.

The structure function data at different values of x (Figs. 2.6 and 2.7) are measured at different Q^2 values in the experiments, *viz.* $x_{\rm expt.} = x(Q^2)$. For the ratios g_1/F_1 there is no experimental evidence of Q^2 dependence in any given x bin. The E155 Collaboration at SLAC found the following good phenomenological fit to their final data set with $Q^2 > 1{\rm GeV}^2$ and energy of the hadronic final state $W > 2$GeV [Anthony *et al.* (2000)]:

$$\begin{aligned}\frac{g_1^p}{F_1^p} &= x^{0.700}(0.817 + 1.014x - 1.489x^2) \times (1 + \frac{c^p}{Q^2}) \\ \frac{g_1^n}{F_1^n} &= x^{-0.335}(-0.013 - 0.330x + 0.761x^2) \times (1 + \frac{c^n}{Q^2}).\end{aligned} \tag{2.32}$$

The coefficients $c^p = -0.04 \pm 0.06$ and $c^n = 0.13 \pm 0.45$ describing the Q^2 dependence are found to be small and consistent with zero. The Q^2 dependence of the g_1 spin structure function is shown in Fig. 2.8. It is useful to compare data at the same Q^2,

e.g. for the comparison of experimental data with the predictions of deep inelastic sum-rules. To this end, the measured x points are shifted to the same value of Q^2 using either the (approximate) Q^2 independence of the asymmetry or performing next-to-leading-order (NLO) QCD motivated fits [Gehrmann and Stirling (1996); Altarelli *et al.* (1997); Adeva *et al.* (1998b); Anthony *et al.* (2000); Goto *et al.* (2000); Glück *et al.* (2001); Blümlein and Böttcher (2002); Leader *et al.* (2002); Hirai *et al.* (2004, 2006a,b); Airapetian *et al.* (2007); Alexakhin *et al.* (2007a)] to the measured data and evolving the measured data points all to the same value of Q^2.

In the experiments the different data points are measured at different values of Q^2, *viz.* $x_{\text{expt.}}(Q^2)$. Next-to-leading order (NLO) QCD motivated fits taking into account the scaling violations associated with perturbative QCD are frequently used to evolve all the data points to the same Q^2.

2.6 Regge theory and the small x behaviour of spin structure functions

The small x or high energy behaviour of spin structure functions is an important issue both for the extrapolation of data needed to test spin sum rules for the first moment of g_1 and also in its own right.

Regge theory makes predictions for the high-energy asymptotic behaviour of the structure functions:

$$\begin{aligned} W_1 &\sim \nu^{\alpha} \\ W_2 &\sim \nu^{\alpha-2} \\ G_1 &\sim \nu^{\alpha-1} \\ G_2 &\sim \nu^{\alpha-1}. \end{aligned} \tag{2.33}$$

Here α denotes the (effective) intercept for the leading Regge exchange contributions. The Regge predictions for the leading exchanges include $\alpha = 1.08$ for the pomeron contributions to W_1 and W_2, and $\alpha \simeq 0.5$ for the ρ and ω exchange contributions to the spin independent structure functions.

We refer to Landshoff (1994) and Kuti (1995) for an introduction to Regge theory and its phenomenology. The basic idea is that the exchange of ladder diagrams generates singularities $\alpha(t) = \alpha_0 + \alpha' t$ in the complex angular momentum plane and that these singularities generate the leading high energy behaviour of scattering amplitudes. High energy scattering amplitudes are predicted to behave as $\sim s^{\alpha(t)}$. The linear slope reflects the QCD string associated with scalar confinement. For angular momentum J, $\alpha = J$ corresponds to a hadron state with mass $m^2 = t$. The inclusive cross-section for deep inelastic scattering is related through the optical theorem to the imaginary part of the forward Compton amplitude leading to Eq. (2.33).

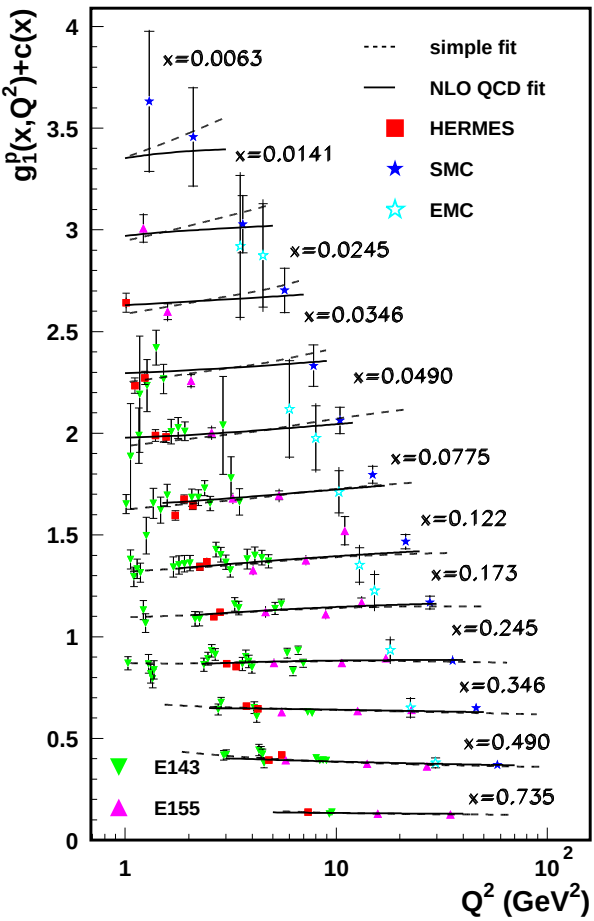

Fig. 2.8 Q^2 dependence of g_1^p for $Q^2 > 1\text{GeV}^2$ together with a simple fit according to Anthony *et al.* (2000) and a NLO perturbative QCD fit from Stoesslein (2002).

For G_1 the leading gluonic exchange behaves as $\{\ln\nu\}/\nu$ [Close and Roberts (1994); Bass and Landshoff (1994)]. In the isovector and isoscalar channels there are also isovector a_1 and isoscalar f_1 Regge exchanges plus contributions from the pomeron-a_1 and pomeron-f_1 cuts [Heimann (1973)]. If one makes the usual assumption that the a_1 and f_1 Regge trajectories are straight lines parallel to the (ρ,ω) trajectories then one finds $\alpha_{a_1} \simeq \alpha_{f_1} \simeq -0.4$, within the phenomenological range $-0.5 \leq \alpha_{a_1} \leq 0$ discussed in Ellis and Karliner (1988). Taking the masses of the $a_1(1260)$ and $a_3(2070)$ states plus the $a_1(1640)$ and $a_3(2310)$ states from the Particle Data Group (2004) yields two parallel a_1 trajectories with slope

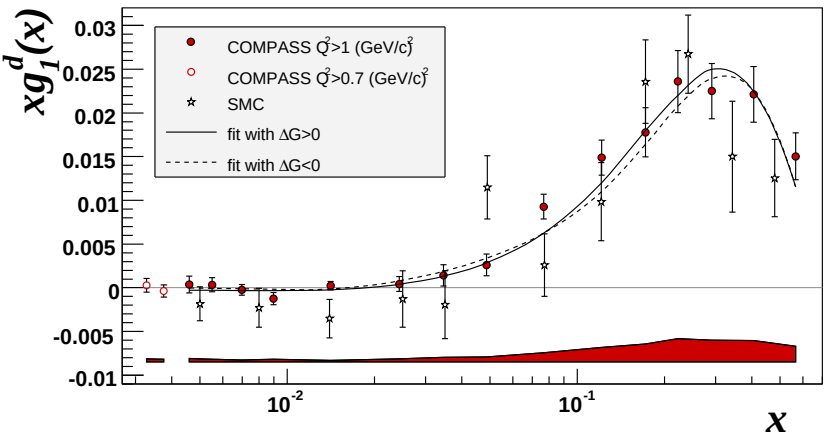

Fig. 2.9 Recent data on g_1^d from COMPASS [Alexakhin *et al.* (2007a)].

$\sim 0.75\text{GeV}^{-2}$ and a leading trajectory with slightly lower intercept: $\alpha_{a_1} \simeq -0.18$.

For this value of the a_1 intercept the effective intercepts corresponding to the soft-pomeron a_1 cut and the hard-pomeron a_1 cut are $\simeq -0.1$ and $\simeq +0.25$ respectively *if* one takes the soft and hard pomerons as two distinct exchanges [Cudell *et al.* (1999)]. In the framework of the Donnachie-Landshoff-Nachtmann model of soft pomeron physics [Landshoff and Nachtmann (1987); Donnachie and Landshoff (1988)] the logarithm in the $\frac{\ln \nu}{\nu}$ contribution comes from the region of internal momentum where two non-perturbative gluons are radiated collinear with the proton [Bass and Landshoff (1994)].

For G_2 one expects contributions from possible multi-pomeron (three or more) cuts ($\sim (\ln \nu)^{-5}$) and Regge-pomeron cuts ($\sim \nu^{\alpha_i(0)-1}/\ln \nu$) with $\alpha_i(0) < 1$ (since the pomeron does not couple to A_1 or A_2 as a single gluonic exchange) – see Ioffe *et al.* (1984).

In terms of the scaling structure functions of deep inelastic scattering the relations (2.33) become

$$\begin{aligned} F_1 &\sim \frac{1}{x}^{\alpha} \\ F_2 &\sim \frac{1}{x}^{\alpha-1} \\ g_1 &\sim \frac{1}{x}^{\alpha} \\ g_2 &\sim \frac{1}{x}^{\alpha+1} \quad . \end{aligned} \tag{2.34}$$

For deep inelastic values of Q^2 there is some debate about the application of Regge arguments. In the conventional approach the effective intercepts for small x, or high ν, physics tend to increase with increasing Q^2 through perturbative QCD evolution

which acts to shift the weight of the structure functions to smaller x. The polarized isovector combination $g_1^p - g_1^n$ is observed to rise in the small x data from SLAC and SMC like $\sim x^{-0.5}$ although it should be noted that, in the measured x range, this exponent could be softened through multiplication by a $(1-x)^n$ factor – for example associated with perturbative QCD counting rules at large x (x close to one). For example, the exponent $x^{-0.5}$ could be modified to about $x^{-0.25}$ through multiplication by a factor $(1-x)^6$. In an alternative approach Cudell *et al.* (1999) have argued that the Regge intercepts should be independent of Q^2 and that the "hard pomeron" revealed in unpolarized deep inelastic scattering at HERA is a distinct exchange independent of the soft pomeron which should also be present in low Q^2 photoproduction data.

Detailed investigation of spin dependent Regge theory and the low x behaviour of spin structure functions could be performed using a future polarized ep collider or with low x and low Q^2 proton target measurements at COMPASS, where measurements could be obtained through a broad range of Q^2 from photoproduction through the "transition region" to polarized deep inelastic scattering. These measurements would provide a baseline for investigations of perturbative QCD motivated small x behaviour in g_1. Open questions include: Does the rise in $g_1^p - g_1^n$ at small Bjorken x persist to small values of Q^2? How does this rise develop as a function of Q^2? Further possible exchange contributions in the flavour-singlet sector associated with polarized glue could also be looked for. For example, colour coherence predicts that the ratio of polarized to unpolarized gluon distributions $\Delta g(x)/g(x) \propto x$ as $x \to 0$ [Brodsky *et al.* (1995)] suggesting that, perhaps, there is a spin analogue of the hard pomeron with intercept about 0.45 corresponding to the polarized gluon distribution.

The s and t dependence of spin dependent Regge theory is being investigated by the pp2pp experiment [Bültmann *et al.* (2003)] at RHIC which is studying polarized proton-proton elastic scattering. at centre of mass energies $50 < \sqrt{s} < 500$GeV and four momentum transfer $0.0004 < |t| < 1.3\text{GeV}^2$. The emphasis so far has been on transverse polarization measurements. For $\sqrt{s} = 200$GeV and $0.01 < t < 0.03$ GeV^2 pp2pp found that the difference between the total cross sections for transversely polarized protons is $\Delta\sigma_T = -0.19 \pm 0.53$mb [Bültmann *et al.* (2007)]. Future measurements of the longitudinal spin dependent total cross-section are expected, extending previous measurements by the FNAL Collaboration E581/E704 which found $\Delta\sigma_L = -42 \pm 48(\text{stat.}) \pm 53(\text{syst.})\mu$b in the collision of 200 GeV polarized protons on a polarized proton target [Grosnick *et al.* (1997)].

This page intentionally left blank

Chapter 3

DISPERSION RELATIONS AND SPIN SUM RULES

3.1 Spin amplitudes

In photon-nucleon scattering the spin dependent structure functions g_1 and g_2 are defined through the imaginary part of the forward Compton scattering amplitude. Consider the amplitude for forward scattering of a photon carrying momentum q_μ ($q^2 = -Q^2 \leq 0$) from a polarized nucleon with momentum p_μ, mass M and spin s_μ. Let $J_\mu(z)$ denote the electromagnetic current in QCD. The forward Compton amplitude

$$T_{\mu\nu}(q,p) = i \int d^4z \; e^{iq.z} \langle p,s| \; T(J_\mu(z) J_\nu(0)) \; |p,s\rangle \tag{3.1}$$

is given by the sum of spin independent (symmetric in μ and ν) and spin dependent (antisymmetric in μ and ν) contributions, *viz.*

$$\begin{aligned} T^S_{\mu\nu} &= \frac{1}{2}(T_{\mu\nu} + T_{\nu\mu}) \\ &= -T_1(g_{\mu\nu} + \frac{q_\mu q_\nu}{Q^2}) + \frac{1}{M^2} T_2(p_\mu + \frac{p.q}{Q^2} q_\mu)(p_\nu + \frac{p.q}{Q^2} q_\nu) \end{aligned} \tag{3.2}$$

and

$$\begin{aligned} T^A_{\mu\nu} &= \frac{1}{2}(T_{\mu\nu} - T_{\nu\mu}) \\ &= \frac{i}{M^2} \epsilon_{\mu\nu\lambda\sigma} q^\lambda \left[s^\sigma (A_1 + \frac{\nu}{M} A_2) - \frac{1}{M^2} s.q p^\sigma A_2 \right]. \end{aligned} \tag{3.3}$$

Here $\nu = p.q/M$ and $\epsilon_{0123} = +1$; the proton spin vector is normalized to $s^2 = -1$. The form-factors T_1, T_2, A_1 and A_2 are functions of ν and Q^2.

The hadron tensor for inclusive photon nucleon scattering which contains the spin dependent structure functions is obtained from the imaginary part of $T_{\mu\nu}$

$$W_{\mu\nu} = \frac{1}{\pi} \mathrm{Im} T_{\mu\nu} = \frac{1}{2\pi} \int d^4z \; e^{iq.z} \langle p,s| \; [J_\mu(z), J_\nu(0)] \; |p,s\rangle. \tag{3.4}$$

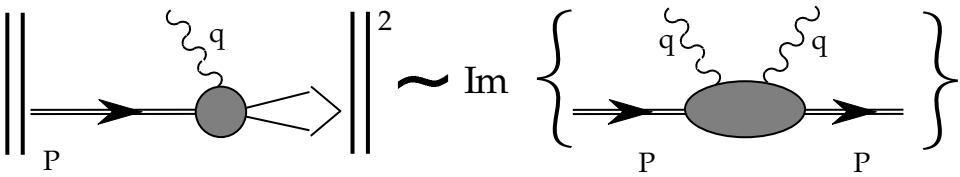

Fig. 3.1 The optical theorem relates the hadronic structure tensor $W_{\mu\nu}$ to the imaginary part of the forward virtual Compton scattering amplitude.

Here the connected matrix element is understood (indicating that the photon interacts with the target and not the vacuum).

To see this, the general expression for the hadronic tensor $W_{\mu\nu}$ is given by

$$W_{\mu\nu} = \frac{1}{2\pi}(2\pi)^4\delta(p+q-p_X)\sum_X \langle p,s|J_\mu(0)|X\rangle\langle X|J_\nu(0)|p,s\rangle \tag{3.5}$$

where we sum over all accessible final hadronic states $|X\rangle$. Translational invariance means that the choice of origin in $J_\mu(0)$ is arbitrary. The energy momentum conserving delta function can be absorbed into the proton matrix elements. We take out the complete set set of hadronic states and obtain

$$\begin{aligned} W_{\mu\nu} &= \frac{1}{2\pi}\int d^4z\ e^{iq.z}\langle p,s|J_\mu(z)J_\nu(0)|p,s\rangle \\ &= \frac{1}{2\pi}\int d^4z\ e^{iq.z}\langle p,s|[J_\mu(z),J_\nu(0)]|p,s\rangle \end{aligned} \tag{3.6}$$

where the second step follows from energy momentum conservation. The extra term in the commutator corresponds to an unphysical $\delta(p-q+p_X)$ term (or $W^2 \leq M^2$) and therefore vanishes.

Sum rules for the (spin) structure functions measured in deep inelastic scattering are derived using dispersion relations and the operator product expansion. For fixed Q^2 the forward Compton scattering amplitude $T_{\mu\nu}(\nu,Q^2)$ is analytic in the photon energy ν except for branch cuts along the positive real axis for $|\nu| \geq Q^2/2M$. Crossing symmetry implies that

$$\begin{aligned} A_1^*(Q^2,-\nu) &= A_1(Q^2,\nu) \\ A_2^*(Q^2,-\nu) &= -A_2(Q^2,\nu). \end{aligned} \tag{3.7}$$

The spin structure functions in the imaginary parts of A_1 and A_2 satisfy the crossing relations

$$\begin{aligned} G_1(Q^2,-\nu) &= -G_1(Q^2,\nu) \\ G_2(Q^2,-\nu) &= +G_2(Q^2,\nu). \end{aligned} \tag{3.8}$$

For g_1 and g_2 these relations become

$$\begin{aligned} g_1(x,Q^2) &= +g_1(-x,Q^2) \\ g_2(x,Q^2) &= +g_2(-x,Q^2). \end{aligned} \tag{3.9}$$

We use Cauchy's integral theorem and the crossing relations to derive dispersion relations for A_1 and A_2. We refer to Bjorken and Drell (1965) for a primer on dispersion relations.

Cauchy's integral formula says that

$$f(z) = \frac{1}{2\pi i}\oint_C d\omega\ \frac{f(\omega)}{\omega - z} \tag{3.10}$$

where $f(z)$ is a function which is analytic inside a contour C. For the spin dispersion relations we shall consider the cases $f = A_1(Q^2,\nu)$ and $f = A_2(Q^2,\nu)$. If we let z approach real values ω from the upper half plane then we find

$$\begin{aligned} f(\omega) &= \lim_{\epsilon\to 0^+} f(\omega + i\epsilon) \\ &= \frac{1}{2\pi i}\mathcal{P}\int_{-\infty}^{+\infty} d\omega' \frac{f(\omega')}{\omega' - \omega} + \frac{1}{2}f(\omega) + \frac{1}{2}\mathcal{C}_\infty \end{aligned} \tag{3.11}$$

where the complex quantity $\mathcal{C}_\infty = C_\infty + iC'_\infty$ represents any contribution from the infinite circle at infinity when we close the contour in the complex plane. The real and imaginary parts of (3.11) are

$$\begin{aligned} \mathrm{Re}f(\omega) &= \frac{1}{\pi}\mathcal{P}\int_{-\infty}^{+\infty} d\omega' \frac{\mathrm{Im}f(\omega')}{\omega' - \omega} + C_\infty \\ \mathrm{Im}f(\omega) &= -\frac{1}{\pi}\mathcal{P}\int_{-\infty}^{+\infty} d\omega' \frac{\mathrm{Re}f(\omega')}{\omega' - \omega} + C'_\infty \end{aligned} \tag{3.12}$$

The first equation in (3.12) is the real part of the equation

$$\begin{aligned} f(\omega) &= \lim_{\epsilon\to 0^+} f(\omega + i\epsilon) \\ &= \lim_{\epsilon\to 0^+} \frac{1}{\pi}\int_{-\infty}^{+\infty} d\omega' \frac{\mathrm{Im}f(\omega')}{\omega' - \omega - i\epsilon} + C_\infty \end{aligned} \tag{3.13}$$

and is the more generally useful form of a dispersion relation.

Assuming that the asymptotic behaviour of the spin structure functions G_1 and G_2 yield convergent integrals we are tempted to write the two unsubtracted dispersion relations:

$$\begin{aligned} A_1(Q^2,\nu) &= \frac{2}{\pi}\int_{Q^2/2M}^{\infty} \frac{\nu' d\nu'}{\nu'^2 - \nu^2}\ \mathrm{Im}A_1(Q^2,\nu') \\ A_2(Q^2,\nu) &= \frac{2}{\pi}\nu\int_{Q^2/2M}^{\infty} \frac{d\nu'}{\nu'^2 - \nu^2}\ \mathrm{Im}A_2(Q^2,\nu'). \end{aligned} \tag{3.14}$$

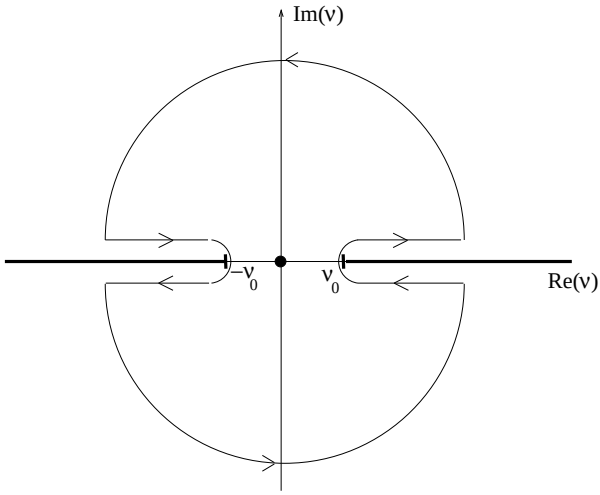

Fig. 3.2 The contour C for the dispersion integral Eq. (3.14). The forward Compton amplitude $T_{\mu\nu}$ has branch cuts along the real ω axis for $\omega \leq -1$ and $\omega \geq 1$. The hadronic tensor $W_{\mu\nu} = \frac{1}{\pi}\mathrm{Im}\ T_{\mu\nu}$ is calculated by performing a Cauchy integration along the contour C around the cuts.

These expressions can be rewritten as dispersion relations involving g_1 and g_2. We define:

$$\begin{aligned} \alpha_1(\omega, Q^2) &= \frac{\nu}{M}\ A_1 \\ \alpha_2(\omega, Q^2) &= \frac{\nu^2}{M^2}\ A_2. \end{aligned} \tag{3.15}$$

Then, the formulae in (3.14) become

$$\begin{aligned} \alpha_1(\omega, Q^2) &= 2\omega \int_1^\infty \frac{d\omega'}{\omega'^2 - \omega^2}\ g_1(\omega', Q^2) \\ \alpha_2(\omega, Q^2) &= 2\omega^3 \int_1^\infty \frac{d\omega'}{\omega'^2(\omega'^2 - \omega^2)}\ g_2(\omega', Q^2) \end{aligned} \tag{3.16}$$

where $\omega = \frac{1}{x} = \frac{2M\nu}{Q^2}$.

In general there are two alternatives to an unsubtracted dispersion relation.

(1) First, if the high energy behaviour of G_1 and/or G_2 (at some fixed Q^2) produced a divergent integral, then the dispersion relation would require a subtraction. Regge predictions for the high energy behaviour of G_1 and G_2 – see Eq. (2.33) – each lead to convergent integrals so this scenario is not expected to occur, even after including the possible effects of QCD evolution.

(2) Second, even if the integral in the unsubtracted relation converges, there is still the potential for a "subtraction at infinity". This scenario would occur if

the real part of A_1 and/or A_2 does not vanish sufficiently fast enough when $\nu \to \infty$ so that we pick up a finite contribution from the contour (or "circle at infinity"). In the context of Regge theory such subtractions can arise from fixed poles (with $J = \alpha(t) = 0$ in A_2 or $J = \alpha(t) = 1$ in A_1 for all t) in the real part of the forward Compton amplitude. We shall discuss these fixed poles and potential subtractions in Chapter 5.

In the presence of a potential "subtraction at infinity" the dispersion relations (3.14) are modified to:

$$\begin{aligned} A_1(Q^2,\nu) &= \mathcal{P}_1(\nu,Q^2) + \frac{2}{\pi}\int_{Q^2/2M}^{\infty} \frac{\nu' d\nu'}{\nu'^2-\nu^2}\ \mathrm{Im}A_1(q^2,\nu') \\ A_2(Q^2,\nu) &= \mathcal{P}_2(\nu,Q^2) + \frac{2}{\pi}\nu\int_{Q^2/2M}^{\infty} \frac{d\nu'}{\nu'^2-\nu^2}\ \mathrm{Im}A_2(q^2,\nu'). \end{aligned} \tag{3.17}$$

Here $\mathcal{P}_1(\nu,Q^2)$ and $\mathcal{P}_2(\nu,Q^2)$ denote the subtraction constants. Factoring out the ν dependence of these subtraction constants, we define two ν independent quantities $\beta_1(Q^2)$ and $\beta_2(Q^2)$:

$$\begin{aligned} \mathcal{P}_1(\nu,Q^2) &= \beta_1(Q^2) \\ \mathcal{P}_2(\nu,Q^2) &= \beta_2(Q^2)\frac{M}{\nu}. \end{aligned} \tag{3.18}$$

The crossing relations (3.7) for A_1 and A_2 are observed by the functions $\mathcal{P}_i$. Scaling requires that $\beta_1(Q^2)$ and $\beta_2(Q^2)$ (if finite) must be nonpolynomial in Q^2 – see Chapter 5. The equations (3.17) can be rewritten:

$$\begin{aligned} \alpha_1(\omega,Q^2) &= \frac{Q^2}{2M^2}\ \beta_1(Q^2)\ \omega + 2\omega\int_1^{\infty} \frac{d\omega'}{\omega'^2-\omega^2}\ g_1(\omega',Q^2) \\ \alpha_2(\omega,Q^2) &= \frac{Q^2}{2M^2}\ \beta_2(Q^2)\ \omega + 2\omega^3\int_1^{\infty} \frac{d\omega'}{\omega'^2(\omega'^2-\omega^2)}\ g_2(\omega',Q^2). \end{aligned} \tag{3.19}$$

Next, the fact that both α_1 and α_2 are analytic for $|\omega| \le 1$ allows us to make the Taylor series expansions (about $\omega = 0$)

$$\begin{aligned} \alpha_1(x,Q^2) &= \frac{Q^2}{2M^2}\ \beta_1(Q^2)\ \frac{1}{x} \\ &\quad + \frac{2}{x}\sum_{n=0,2,4,..}\left(\frac{1}{x^n}\right)\int_0^1 dy\ y^n g_1(y,Q^2) \\ \alpha_2(x,Q^2) &= \frac{Q^2}{2M^2}\ \beta_2(Q^2)\ \frac{1}{x} \\ &\quad + \frac{2}{x^3}\sum_{n=0,2,4,..}\left(\frac{1}{x^n}\right)\int_0^1 dy\ y^{n+2} g_2(y,Q^2) \end{aligned} \tag{3.20}$$

with $x = \frac{1}{\omega}$. Note that the power series in $\omega = 1/x$ converges only for $|\omega| < 1$. Since energy-momentum conservation fixes $0 \leq x \leq 1$ (or $\omega \geq 1$) it follows that $\alpha_1(x)$ and $\alpha_2(x)$ are unphysical exactly where they converge.

These equations form the basis for the spin sum rules for polarized photon nucleon scattering. We next outline the derivation of the Bjorken (1966, 1970) and Ellis and Jaffe (1974) sum rules for the isovector and flavour-singlet parts of g_1 in polarized deep inelastic scattering, the Burkhardt-Cottingham sum rule for G_2 [Burkhardt and Cottingham (1970)], and the Gerasimov-Drell-Hearn sum rule for polarized photoproduction [Gerasimov (1965); Drell and Hearn (1966)]. Each of these spin sum rules assumes no subtraction at infinity.

Sum rules for polarized deep inelastic scattering are derived by combining the dispersion relation expressions (3.20) with the light cone operator production expansion. When $Q^2 \to \infty$ the leading contribution to the spin dependent part of the forward Compton amplitude comes from the nucleon matrix elements of a tower of gauge invariant local operators multiplied by Wilson coefficients, *viz.*

$$T^A_{\mu\nu} = i\epsilon_{\mu\nu\lambda\sigma}q^\lambda \sum_{n=0,2,4,..} \left(-\frac{2}{q^2}\right)^{n+1} q^{\mu_1}q^{\mu_2}...q^{\mu_n} \sum_{i=q,g} \Theta^{(i)}_{\sigma\{\mu_1...\mu_n\}} E^i_n(\frac{Q^2}{\mu^2}, \alpha_s) \tag{3.21}$$

where

$$\Theta^{(q)}_{\sigma\{\mu_1...\mu_n\}} \equiv i^n \bar{\psi}\gamma_\sigma\gamma_5 D_{\{\mu_1}...D_{\mu_n\}}\psi - \text{traces} \tag{3.22}$$

and

$$\Theta^{(g)}_{\sigma\{\mu_1...\mu_n\}} \equiv i^{n-1}\epsilon_{\alpha\beta\gamma\sigma}G^{\beta\gamma}D_{\{\mu_1}...D_{\mu_{n-1}}G^\alpha{}_{\mu_n\}} - \text{traces} \tag{3.23}$$

are twist-two local operators. Here $D_\mu = \partial_\mu + igA_\mu$ is the gauge covariant derivative and the sum over even values of n in Eq. (3.21) reflects the crossing symmetry properties of $T_{\mu\nu}$. The functions $E^q_n(\frac{Q^2}{\mu^2}, \alpha_s)$ and $E^g_n(\frac{Q^2}{\mu^2}, \alpha_s)$ are the respective Wilson coefficients. (Note that, for simplicity, in this discussion we consider the case of a single quark flavour with unit charge and zero quark mass. The results quoted in Section 3.3 below include the extra steps of using the full electromagnetic current in QCD.)

3.2 Light cone dominance and the operator product expansion

To understand the operator product expansion, consider the product of two currents $J_\mu(z)$ and $J_\nu(0)$. This product has to be treated carefully in quantum field theory because of potential singular behaviour in the short distance limit $z_\mu \to 0$ and the light-cone limit $z^2 \to 0$. The light-cone limit is important for deep inelastic scattering.

The Riemann Lebesgue Theorem tells us that the integral in the the definition of $T_{\mu\nu}$ and $W_{\mu\nu}$ in Eqs. (3.1) and (3.4) receives a finite contribution only when there is small oscillation in the exponential (*viz.* $q.z \sim 1$). Choose a frame where $q^\mu = (q^0; 0_T, q^3)$ so that $q_+ = \frac{1}{\sqrt{2}}(q_0 + q_3) =$ finite and $q_- = \frac{1}{\sqrt{2}}(q_0 - q_3) \to \infty$ in the Bjorken limit. The dominant (finite) contribution to $T_{\mu\nu}$ and $W_{\mu\nu}$ then comes from

$$q.z = q_+ z_- + q_- z_+ - z_T.q_T \sim 1 \tag{3.24}$$

or $z_- \sim \frac{1}{q_+}$ and $z_+ \sim \frac{1}{q_-} \to 0$; $q_T = 0$ in our frame of reference. Since $q_+ = -p_+ x$ (see Eq. (2.18)) it follows that z_- need not be small, particularly at small x.

Causality tells us that

$$[J_\mu(z), J_\nu(0)] = 0 \quad \text{with } z^2 < 0 \tag{3.25}$$

That is, we get a non-zero contribution to the hadronic cross section only when

$$z^2 = 2z_+ z_- - z_T^2 \sim \frac{2}{q_- q_+} - z_T^2 \sim \frac{4}{q^2} - z_T^2 \geq 0 \tag{3.26}$$

or when $z_T^2 \to 0$. Thus, $z^2 \to 0$ in the Bjorken limit and deep inelastic scattering is said to probe QCD physics "on the light cone".

The singular operator product is treated systematically using Wilson's operator product expansions. There is a well defined expansion of the current operator product in each of the short distance and light cone limits. We focus on the light cone expansion relevant to deep inelastic scattering. On the light cone it may be shown that the product of two electromagnetic currents is equal to an infinite sum over gauge invariant, local, composite renormalized operators – each of which is multiplied by a coefficient function of z^2, which may be singular is at $z^2 = 0$. The idea is that we probe the quark and gluonic structure of the proton at large Q^2 and receive contributions from the proton matrix elements of all the quark and gluonic operators with the right quantum numbers.

The strength of the singularity in the coefficient functions is determined by power counting arguments. The renormalized current operators $J_\mu(z)$ have canonical dimension +3. We let $d_{Op}(n)$ denote the dimension of an operator $Op(n)$ on the right hand side of the operator product expansion which is accompanied by n factors of z_μ. Dimensional consistency requires that the corresponding Wilson coefficient behaves as $\sim (z^2)^{(-6+d_{Op}(n)-n)/2}$ for $z^2 \to 0$. The strongest singularity occurs when $\tau = d_{Op}(n) - n$ is a minimum. We call τ the twist of the operator and n is its spin. Deep inelastic scattering is dominated by the operators with lowest twist (=2) in the operator product expansion. The Wilson coefficients $E_n^i(\frac{Q^2}{\mu^2}, \alpha_s)$ in the operator product expansion formula Eq. (3.21) are then the Fourier transforms of these light-cone coefficients in z.

The operator product expansion is an equation relating operators and does not depend on the states that we choose to evaluate the operator matrix elements between. This means that the Wilson coefficients are target independent and may

be evaluated using perturbative QCD. The calculation goes as follows. We consider deep inelastic scattering from an idealized free quark or gluon target and evaluate $T_{\mu\nu}$ for each target up to some fixed order in the QCD coupling constant α_s. The next step is to evaluate the quark and gluon matrix elements of the operators appearing on the right hand side of the operator product expansion. The coefficients may be read off by comparing the two results at a given order in α_s. The non-singlet quark operators do not mix with any gluonic operators under renormalization. Glue is flavour-singlet and decouples from non-singlet isovector and SU(3) octet contributions. The leading quark and gluon coefficients start at $E_n^q = 1 + O(\alpha_s)$ and $E_n^g = O(\alpha_s)$.

The operators in Eq. (3.21) may each be written as the sum of a totally symmetric operator and an operator with mixed symmetry

$$\Theta_{\sigma\{\mu_1\ldots\mu_n\}} = \Theta_{\{\sigma\mu_1\ldots\mu_n\}} + \Theta_{[\sigma,\{\mu_1]\ldots\mu_n\}}. \tag{3.27}$$

These operators have the matrix elements:

$$\begin{aligned}
&\langle p,s|\Theta_{\{\sigma\mu_1\ldots\mu_n\}}|p,s\rangle \\
&\qquad = \{s_\sigma p_{\mu_1}\ldots p_{\mu_n} + s_{\mu_1}p_\sigma p_{\mu_2}\ldots p_{\mu_n} + \ldots\}\frac{a_n}{n+1} \\
&\langle p,s|\Theta_{[\{\sigma\mu_1]\ldots\mu_n\}}|p,s\rangle \\
&\qquad = \{(s_\sigma p_{\mu_1} - s_{\mu_1}p_\sigma)p_{\mu_2}\ldots p_{\mu_n} + (s_\sigma p_{\mu_2} - s_{\mu_2}p_\sigma)p_{\mu_1}\ldots p_{\mu_n} + \ldots\}\frac{d_n}{n+1}.
\end{aligned} \tag{3.28}$$

Now define $\tilde{a}_n = a_n^{(q)}E_{1n}^q + a_n^{(g)}E_{1n}^g$ and $\tilde{d}_n = d_n^{(q)}E_{2n}^q + d_n^{(g)}E_{2n}^g$ where E_{1n}^i and E_{2n}^i are the Wilson coefficients for a_n^i and d_n^i respectively. Combining equations (3.21) and (3.28) one obtains the following equations for α_1 and α_2:

$$\begin{aligned}
\alpha_1(x,Q^2) + \alpha_2(x,Q^2) &= \sum_{n=0,2,4,\ldots} \frac{\tilde{a}_n + n\tilde{d}_n}{n+1}\frac{1}{x^{n+1}} \\
\alpha_2(x,Q^2) &= \sum_{n=2,4,\ldots} \frac{n(\tilde{d}_n - \tilde{a}_n)}{n+1}\frac{1}{x^{n+1}}.
\end{aligned} \tag{3.29}$$

These equations are compared with the Taylor series expansions (3.20), whence we obtain the moment sum rules for g_1 and g_2:

$$\int_0^1 dx x^n g_1 = \frac{1}{2}\tilde{a}_n \;-\; \delta_{n0}\;\frac{1}{2}\frac{Q^2}{2M^2}\beta_1(Q^2) \tag{3.30}$$

for $n = 0, 2, 4, \ldots$ and

$$\int_0^1 dx x^n g_2 = \frac{1}{2}\frac{n}{n+1}(\tilde{d}_n - \tilde{a}_n) \tag{3.31}$$

for $n = 2, 4, 6, \ldots$

The higher moments determine the behaviour of the structure functions near $x = 1$ whilst the first moment tells us about the small x region.

Note:

(1) The first moment of g_1 is given by the nucleon matrix element of the axial vector current $\bar{\psi}\gamma_\sigma\gamma_5\psi$. There is no twist-two, spin-one, gauge-invariant, local gluon operator to contribute to the first moment of g_1 [Jaffe and Manohar (1990)].
(2) The potential subtraction term $\frac{Q^2}{2M^2}\beta_1(Q^2)$ in the dispersion relation in (3.20) multiplies a $\frac{1}{x}$ term in the series expansion on the left hand side, and thus provides a potential correction factor to sum rules for the first moment of g_1. It follows that the first moment of g_1 measured in polarized deep inelastic scattering measures the nucleon matrix element of the axial vector current up to this potential "subtraction at infinity" term, which corresponds to the residue of any $J = 1$ fixed pole with nonpolynomial residue contribution to the real part of A_1.
(3) There is no $\frac{1}{x}$ term in the operator product expansion formula (3.29) for $\alpha_2(x, Q^2)$. This is matched by the lack of any $\frac{1}{x}$ term in the unsubtracted version of the dispersion relation (3.20). The operator product expansion provides no information about the first moment of g_2 without additional assumptions concerning analytic continuation and the $x \sim 0$ behaviour of g_2 [Jaffe (1990)]. We shall return to this discussion in the context of the Burkhardt-Cottingham sum rule for g_2 in Section 4.4 below.

If there are finite subtraction constant corrections to one (or more) spin sum rules, one can include the correction by re-interpreting the relevant structure function as a distribution with the subtraction constant included as twice the coefficient of a $\delta(x)$ term [Broadhurst *et al.* (1973)].

3.3 The QCD parton model

There is a close connection between the operator product expansion description of deep inelastic scattering and the QCD parton model.

We now return to g_1 in the scaling regime of polarized deep inelastic scattering. As noted in Chapter 2, in the (pre-QCD) parton model g_1 is written as

$$g_1(x) = \frac{1}{2}\sum_q e_q^2 \Delta q(x) \tag{3.32}$$

where e_q denotes the quark charge and $\Delta q(x)$ is the polarized quark distribution.

In QCD we have to consider the effects of gluon radiation and (renormalization group) mixing of the flavour-singlet quark distribution with the polarized gluon distribution of the proton. The parton model description of polarized deep inelastic scattering involves writing the deep inelastic structure functions as the sum over the convolution of "soft" quark and gluon parton distributions with "hard" photon-

parton scattering coefficients:

$$\begin{aligned} & g_1(x,Q^2) \\ & = \int_x^1 \frac{dz}{z}\left\{\frac{1}{12}(\Delta u - \Delta d)(z,Q^2) + \frac{1}{36}(\Delta u + \Delta d - 2\Delta s)(z,Q^2)\right\} C_{ns}^q(\frac{x}{z},\alpha_s) \\ & \quad + \frac{1}{9}\left\{\int_x^1 \frac{dz}{z}(\Delta u + \Delta d + \Delta s)(z,Q^2) C_s^q(\frac{x}{z},\alpha_s)\right. \\ & \qquad \left. + f\int_x^1 \frac{dz}{z}\Delta g(z,Q^2) C^g(\frac{x}{z},\alpha_s)\right\}. \end{aligned} \tag{3.33}$$

Here $\Delta q(x,Q^2)$ and $\Delta g(x,Q^2)$ denote the polarized quark and gluon parton distributions, $C^q(z,\alpha_s)$ and $C^g(z,\alpha_s)$ denote the corresponding hard scattering coefficients, and f is the number of quark flavours liberated into the final state ($f = 3$ below the charm production threshold). The parton distributions contain all the target dependent information and describe a flux of quark and gluon partons into the (target independent) interaction between the hard photon and the parton which is described by the coefficients and which is calculable using perturbative QCD. The perturbative coefficients are independent of infra-red mass singularities in the photon-parton collision which are absorbed into the soft parton distributions (and softened by confinement related physics). When we take even moments of the g_1 spin structure function we project out the product of operator matrix elements and coefficients in the operator product expansion:

$$\begin{aligned} & \int_0^1 dx x^n g_1(x,Q^2) \\ & = \int_0^1 dx x^n \left\{\frac{1}{12}(\Delta u - \Delta d) + \frac{1}{36}(\Delta u + \Delta d - 2\Delta s)\right\}(x,Q^2) \int_0^1 dz z^n C_{ns}^q(z,\alpha_s) \\ & \quad + \frac{1}{9}\int_0^1 dx x^n (\Delta u + \Delta d + \Delta s)(x,Q^2) \int_0^1 dz z^n C_s^q(z,\alpha_s) \\ & \quad + \frac{f}{9}\int_0^1 dx x^n \Delta g(x,Q^2) \int_0^1 dz z^n C^g(z,\alpha_s) \end{aligned} \tag{3.34}$$

where

$$\begin{aligned} \int_0^1 dx\ x^n \Delta q(x) &= a_n^{(q)} - \delta_{n0}\ \frac{1}{2}\frac{Q^2}{2M^2}\beta_1(Q^2) \\ \int_0^1 dx\ x^n\ \Delta g(x) &= a_n^{(g)} \\ \int_0^1 dx\ x^n\ C^q(x) &= E_{1n}^q \\ \int_0^1 dx\ x^n\ C^g(x) &= E_{1n}^g \end{aligned} \tag{3.35}$$

for $n = 0, 2, 4, ...$ The Q^2 scale dependence in Eqs. (3.33)-(3.35) is induced by the finite and running value of α_s – see Eq. (2.25).

To understand the principle behind factorization, first consider deep inelastic scattering from a massless quark or gluon parton with virtuality $P^2 = -p^2$. If we work at $O(\alpha_s)$ the cross-section for this process contains a term $\sim \alpha_s \ln Q^2/P^2$ which diverges when the virtuality of the parton goes to zero. The divergence is known as a mass singularity and is associated with the infrared part of phase space where a (massless) parton splits collinearly into two (massless) partons. To resolve this, we write

$$\begin{aligned} 1 + \alpha_s \ln \frac{Q^2}{P^2} &= 1 + \alpha_s \ln \frac{Q^2}{\lambda^2} + \alpha_s \ln \frac{\lambda^2}{P^2} \\ &= (1 + \alpha_s \ln \frac{Q^2}{\lambda^2}) \; (1 + \alpha_s \ln \frac{\lambda^2}{P^2}) \; + \; O(\alpha_s^2) \end{aligned} \tag{3.36}$$

Here λ^2 is called the factorization scale, which separates the cross-section into a product of long and short distance contributions. The hard term $(1 + \alpha_s \ln Q^2/\lambda^2)$ is free of any mass singularity. The long distance effects, including the mass singularity, are factored into the quark and gluon parton distributions of the proton wavefunction.

The separation of g_1 into "hard" and "soft" is not unique and depends on the choice of "factorization scheme". For example, one might use a kinematic cut-off on the partons' transverse momentum squared ($k_t^2 > \lambda^2$) to define the factorization scheme and thus separate the hard and soft parts of the phase space for the photon-parton collision. The cut-off λ^2 is called the factorization scale. The coefficients have the perturbative expansion $C^q = \delta(1-x) + \frac{\alpha_s}{2\pi} f^q(x, Q^2/\lambda^2)$ and $C^g = \frac{\alpha_s}{2\pi} f^g(x, Q^2/\lambda^2)$ where the strongest singularities in the functions f^q and f^g as $x \to 1$ are $\ln(1-x)/(1-x)_+$ and $\ln(1-x)$ respectively where the regularized function $1/(1-z)_+$ is defined by

$$\int_0^1 dz \; \frac{f(z)}{(1-z)_+} \equiv \int_0^1 dz \; \frac{f(z) - f(1)}{(1-z)} \tag{3.37}$$

– see e.g. Lampe and Reya (2000). The deep inelastic structure functions are dependent on Q^2 and independent of the factorization scale λ^2 and the "scheme" used to separate the γ^*-parton cross-section into "hard" and "soft" contributions. Examples of different "schemes" one might use include using modified minimal subtraction ($\overline{\rm MS}$) ['t Hooft and Veltman (1972); Bodwin and Qiu (1990)] to regulate the mass singularities which arise in scattering from massless partons, and cut-offs on other kinematic variables such as the invariant mass squared or the virtuality of the struck quark. Other schemes which have been widely used in the literature and analysis of polarized deep inelastic scattering data are the "AB" [Ball *et al.* (1996)] and "CI" (chiral invariant) [Cheng (1996)] or "JET" [Leader *et al.* (1998)] schemes. We illustrate factorization scheme dependence and the use of these schemes in the analysis of g_1 data in Chapter 10 below.

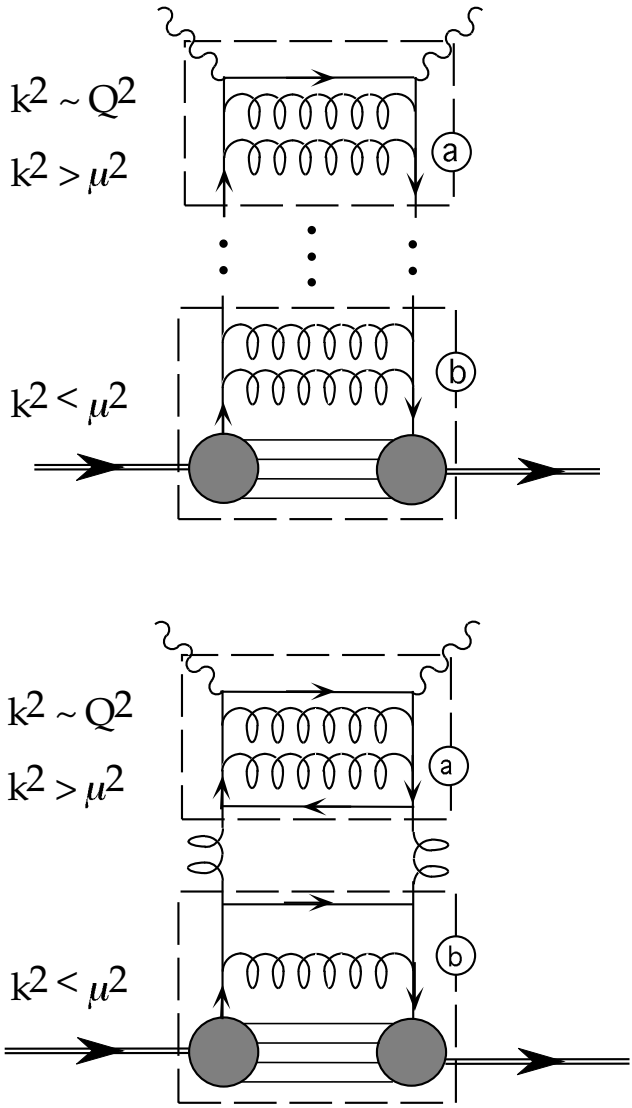

Fig. 3.3 The operator product expansion and QCD factorization at work: the $\gamma^* p$ cross-section separates into "hard" coefficients characterized by $k^2 > \mu^2$ and "soft" quark and gluon parton distributions characterized by $k^2 < \mu^2$ where μ is the factorization scale. The parton distributions contain all of the information about the target proton.

If the same "scheme" is applied consistently to all hard processes then the factorization theorem asserts that the parton distributions that one extracts from experiments should be process independent [Collins (1993a)]. In other words, the same polarized quark and gluon distributions should be obtained from future experiments involving polarized hard QCD processes in polarized proton-proton collisions (e.g. at RHIC) and polarized deep inelastic scattering experiments. The factorization theorem for unpolarized hard processes has been successfully tested in a large number of experiments involving different reactions at various laboratories. Tests of the polarized version await future independent measurements of the polarized gluon and sea-quark distributions from a variety of different hard scattering processes with polarized beams. This programme has been initiated with independent measurements of quark and gluon polarization at COMPASS and RHIC using totally different experimental conditions: polarized deep inelastic scattering and high energy polarized proton-proton collisions.

3.4 Parton distributions and light-cone correlation functions

The (spin-dependent) parton distributions may also be defined via the operator product expansion. For g_1 this means that the odd moments of the polarized quark and gluon distributions project out the target matrix elements of the renormalized, spin-odd, composite operators which appear in the operator product expansion, *viz.*

$$\begin{aligned} &2Ms_+(p_+)^{2n}\int_0^1 dx\ x^{2n}\Delta q(x,\mu^2) \\ &\quad = \langle p,s|\left[\overline{q}(0)\gamma_+\gamma_5(iD_+)^{2n}q(0)\right]_{\mu^2}|p,s\rangle \end{aligned} \tag{3.38}$$

$$\begin{aligned} &2Ms_+(p_+)^{2n}\int_0^1 dx\ x^{2n}\Delta g(x,\mu^2) \\ &\quad = \langle p,s|\left[\mathrm{Tr}\ G_{+\alpha}(0)(iD_+)^{2n-1}\tilde{G}^{\alpha}{}_{+}(0)\right]_{\mu^2}|p,s\rangle, \qquad (n\geq 1). \end{aligned} \tag{3.39}$$

The association of $\Delta q(x,\mu^2)$ with quarks and $\Delta g(x,\mu^2)$ with gluons follows when we evaluate the target matrix elements in Eqs. (3.38) and (3.39) in the light-cone gauge, where $D_+ \to \partial_+$ and the explicit dependence of D_+ on the gluon field drops out. The operator product expansion involves writing the product of electromagnetic currents $J_\mu(z)J_\nu(0)$ in Eq. (3.1) as the expansion over gauge invariantly renormalized, local, composite quark and gluonic operators at lightlike separation $z^2 \to 0$ – the realm of deep inelastic scattering [Muta (1998)]. The subscript μ^2 on the operators in

Eqs. (3.38)-(3.39) emphasises the dependence on the renormalization scale.[1]

Mathematically, the relation between the parton distributions and the operator product expansion is given in terms of light-cone correlation functions of point split operator matrix elements along the light-cone. Define

$$\psi^{\pm} = P^{\pm}\psi \tag{3.40}$$

where

$$P^{\pm} = \frac{1}{2}(1 \pm \alpha_3) = \frac{1}{2}\gamma^{\pm}\gamma^{\mp}. \tag{3.41}$$

The polarized quark and antiquark distributions are given by

$$\begin{aligned}
\Delta\psi(x) &= \frac{1}{2\sqrt{2}\pi}\int d\xi^- e^{-ixM\xi^-/\sqrt{2}} \\
&\quad \langle p,s|(\psi^{+R})^\dagger(\xi^-)\psi^{+R}(0) - (\psi^{+L})^\dagger(\xi^-)\psi^{+L}(0)|p,s\rangle, \\
\Delta\bar{\psi}(x) &= \frac{1}{2\sqrt{2}\pi}\int d\xi^- e^{-ixM\xi^-/\sqrt{2}} \\
&\quad \langle p,s|\psi^{+L}(\xi^-)(\psi^{+L})^\dagger(0) - \psi^{+R}(\xi^-)(\psi^{+R})^\dagger(0)|p,s\rangle.
\end{aligned} \tag{3.42}$$

In this notation $\Delta q = \Delta\psi + \Delta\bar{\psi}$. The non-local operator in the correlation function is rendered gauge invariant through a path ordered exponential

$$\mathrm{P}e^{i\int_0^{z_-} dy_- A_+} \tag{3.43}$$

which simplifies to unity in the light-cone gauge $A_+ = 0$. Taking the moments of these distributions reproduces the results of the operator product expansion in Eq. (3.30). The Mellin theorem [Courant and Hilbert (1953)] tells us that the parton distribitions defined in this way are unique up to the choice of renormalization scheme.[2]

The light-cone correlation function for the polarized gluon distribution is

$$\begin{aligned}
x\Delta g(x) &= \frac{i}{2\sqrt{2}M\pi}\int d\xi^- \; e^{-ix\xi^- M/\sqrt{2}} \\
&\quad \langle p,s|G_{+\nu}(\xi^-)\tilde{G}^{\nu}{}_{+}(0) - G_{+\nu}(0)\tilde{G}^{\nu}{}_{+}(\xi^-)|p,s\rangle.
\end{aligned} \tag{3.45}$$

[1] Note that the parton distributions defined through the operator product expansion include the effect of renormalization effects such as the axial anomaly (and the trace anomaly for the spin-independent distributions which appear in F_1 and F_2) in addition to absorbing the mass singularities in photon-parton scattering.

[2] Some care has to be taken regarding renormalization of the light-cone correlation functions. The bare correlation function from which we project out moments as local operators is ultraviolet divergent. Llewellyn Smith (1988) proposed a solution of this problem by defining the renormalized light cone correlation function as a series expansion in the proton matrix elements of gauge invariant local operators. For the polarized quark distribution this becomes:

$$\langle\overline{\psi}(z_-)\gamma_+\gamma_5\psi(0)\rangle = \sum_n \frac{(-z_-)^n}{n!}\langle[\overline{\psi}\gamma_+\gamma_5(D_+)^n\psi](0)\rangle. \tag{3.44}$$

In the light-cone gauge ($A_+ = 0$) one finds $G_a^{+\nu} = \partial^+ A_a^\nu - \partial^\nu A_a^+ = \partial^+ A_a^\nu$ so that

$$G^{+\nu}\tilde{G}_\nu{}^+ = G_R^+ G_{-L} - G_L^+ G_{-R} = G_R^+ G^{+R} - G_L^+ G^{+L}. \tag{3.46}$$

Thus $\Delta g(x)$ measures the distribution of gluon polarization in the nucleon. One can evaluate the first moment of $\Delta g(x)$ from its light-cone correlation function. One first assumes that

$$\lim_{x\to 0^+} x\Delta g(x) = 0. \tag{3.47}$$

In $A_+ = 0$ gauge the first moment becomes

$$\int_0^1 dx \Delta g(x) = \frac{1}{\sqrt{2}M}\left[\langle A^\nu(\xi^-)\tilde{G}_\nu{}^+(0)\rangle|_{\xi^-\to\infty} - \langle A^\nu(0)\tilde{G}_\nu{}^+(0)\rangle\right] \tag{3.48}$$

– that is, the sum of the forward matrix element of the gluonic Chern Simons current K_+ plus a surface term [Manohar (1990)] which may or may not vanish in QCD.

3.5 Renormalization group and QCD evolution

Deep inelastic scattering and the operator product expansion involve three momentum scales: the virtuality Q^2 of the exchanged photon, the factorization scale and a "renormalization scale" μ^2 which enters because the composite operators which on the right hand side of the operator product expansion need to be renormalized. The factorization and renormalization scales enter as part of the calculation procedure and are independent of the physical kinematic variables. When we calculate the matrix elements of the quark and gluon operators in perturbative QCD there are divergences associated with the loop integrals which have to be subtracted out. In the case of the operator matrix elements these divergences cannot all be absorbed into the usual vertex and wavefunction renormalization constants. There are extra divergences which are intrinsic to the operator itself. The renormalization procedure introduces a new momentum scale μ^2 into the calculation. While the theoretical procedure introduces this renormalization scale in the calculation of a physical process like deep inelastic scattering, it is clear that the physical cross section is independent of μ^2. Any observable is independent of how a theorist might choose to calculate it! Therefore, it is common to take $\mu^2 = Q^2$. The renormalization scale independence of cross-sections leads to the idea of the renormalization group equations.

Let us consider a renormalized operator Ω_R, which is constructed from a bare operator Ω. We first consider the case where Ω_R is multiplicatively renormalized and does not mix with any other operators under renormalization. This example applies to the flavour non-singlet operators in the operator product expansion. We write $\Omega_R = Z_\Omega^{-1}\Omega$. Here Z_Ω is the renormalization constant for Ω. The divergences associated with the composite operator are isolated using some ultraviolet

regularization and subtracted at a renormalization scale μ^2. The bare operator Ω is independent of μ^2. One finds the differential equation

$$\frac{d}{d\ \ln\mu^2}\Omega = \left(\frac{d}{d\ \ln\mu^2}Z_\Omega\right)\Omega_R + Z_\Omega\left(\frac{d}{d\ \ln\mu^2}\Omega_R\right) = 0 \tag{3.49}$$

which we may rewrite as

$$\left(\frac{d}{d\ \ln\mu^2} + \gamma_\Omega\right)\Omega_R = 0 \tag{3.50}$$

Here

$$\gamma_\Omega = \frac{1}{Z_\Omega}\frac{d}{d\ \ln\mu^2}Z_\Omega \tag{3.51}$$

is called the anomalous dimension of the operator Ω. Suppose that Ω_R occurs on the right hand side of the operator product expansion, *viz.* $J_\mu(z)J_\nu(0) \sim \Omega_R(0)E(z^2)$. The renormalization group equation for the two electromagnetic current Greens function is

$$\left(\frac{d}{d\ \ln\mu^2} + 2\gamma_j\right)\ \langle p,s|J_\mu(z)J_\nu(0)|p,s\rangle = 0 \tag{3.52}$$

where γ_j is the anomalous dimension of the electromagnetic current. For conserved currents like the vector current one finds $\gamma_j = 0$. The scale dependence of Ω_R is

$$\left(\frac{d}{d\ \ln\mu^2} + \gamma_\Omega\right)\langle p,s|\Omega_R|p,s\rangle = 0 \tag{3.53}$$

We apply the operator product expansion and subtract this equation to find

$$\left(\frac{d}{d\ln\mu^2} - \gamma_\Omega\right)\ E_\Omega\left(\frac{Q^2}{\mu^2},\alpha_s(\mu^2)\right) = 0 \tag{3.54}$$

This equation may be written as

$$\left(\frac{d}{dg} - \frac{\gamma_\Omega}{\beta(g)}\right)\ E_\Omega(\frac{Q^2}{\mu^2},\alpha_s(\mu^2)) = 0 \tag{3.55}$$

where $\alpha_s = g^2/4\pi$ and

$$\beta(g) = \frac{\partial}{\partial\ln\mu^2}\ g \tag{3.56}$$

is the QCD beta function. We call Eq. (3.55) the renormalization group equation. It has the solution

$$E_\Omega\left(\frac{Q^2}{\mu^2},\alpha_s(\mu^2)\right) = \exp\left\{\int_{g(\mu_0^2)}^{g(\mu^2)} dg\ \frac{-\gamma_\Omega(g)}{\beta(g)}\right\}E_\Omega(\frac{Q^2}{\mu_0^2},\alpha_s(\mu_0^2)) \tag{3.57}$$

which may be solved perturbatively. Let

$$\begin{aligned}\beta(g) &= -\beta_0 g^3 - \beta_1 g^5 + O(g^7)\\ \gamma_\Omega(g) &= \gamma_0 g^2 + \gamma_1 g^4 + O(g^6)\\ E_\Omega(1,g) &= E_{\Omega,0} + E_{\Omega,1}g^2 + O(g^4)\end{aligned} \tag{3.58}$$

Substituting into Eq. (3.57), we find that the coefficients evolve with Q^2 as

$$E_\Omega(\frac{Q^2}{\mu^2}, g(\mu^2)) = \left[\frac{g(Q^2)}{g(\mu^2)}\right]^{\frac{\gamma_0}{\beta_0}} E_{\Omega,0} \tag{3.59}$$

at leading order.

The renormalization group equation is slightly more complicated in the singlet case due to operator mixing. The anomalous dimensions for each moment γ_Ω now form a 2×2 matrix and one finds

$$\begin{pmatrix} E^q \\ E^g \end{pmatrix}(\frac{Q^2}{\mu^2}, \alpha_s(\mu^2)) = T \exp \int_{g(Q^2)}^{g(\mu^2)} dg \begin{bmatrix} \gamma_{qq}^q & \gamma_{gg}^q \\ \gamma_{qq}^g & \gamma_{gg}^g \end{bmatrix}(g) \begin{pmatrix} E^q \\ E^g \end{pmatrix}(1, \alpha_s(Q^2)) \tag{3.60}$$

The scale dependence in deep inelastic scattering is summarized in the DGLAP (Dokshitzer, Gribov, Lipatov, Altarelli, Parisi) equations. The anomalous dimensions of the operators in the operator product expansion correspond to the Mellin transform of the DGLAP splitting functions P_{ij}: $\int_0^1 \, dx \; P_{ij}(x) = \gamma_{jj}^i$. These splitting functions have the nice physical interpretation that they are the probability of finding a parton i in a parton j at a scale Q^2. The physical picture behind this renormalization group evolution is that the virtuality Q^2 of the probe sets a resolution scale for the partons, so that a change in Q^2 corresponds to a change in the state of the probed partons: increasing Q^2 is like using a microscope to probe deeper and deeper insider the proton. The Q^2 dependence of the spin-dependent parton distributions is then given by the DGLAP equations

$$\begin{aligned} \frac{d}{dt}\Delta\Sigma(x,t) &= \frac{\alpha_s(t)}{2\pi}\left\{\int_x^1 \frac{dy}{y}\Delta P_{qq}(\frac{x}{y})\Delta\Sigma(y,t) + 2f\int_x^1 \frac{dy}{y}\Delta P_{qg}(\frac{x}{y})\Delta g(y,t)\right\} \\ \frac{d}{dt}\Delta g(x,t) &= \frac{\alpha_s(t)}{2\pi}\left\{\int_x^1 \frac{dy}{y}\Delta P_{gq}(\frac{x}{y})\Delta\Sigma(y,t) + \int_x^1 \frac{dy}{y}\Delta P_{gg}(\frac{x}{y})\Delta g(y,t) \right\} \end{aligned} \tag{3.61}$$

where $\Sigma(x,t) = \sum_q \Delta q(x,t)$ and $t = \ln Q^2$ [Altarelli and Parisi (1977)]. The non-singlet term evolves as

$$\frac{d}{dt}\Delta q_3(x,t) = \frac{\alpha_s(t)}{2\pi}\int_x^1 \frac{dy}{y}\Delta P_{qq}\left(\frac{x}{y}\right)\Delta q_3(y,t) \tag{3.62}$$

where $\Delta q_3(x,t) = \Delta u(x,t) - \Delta d(x,t)$.

We explore the application of this DGLAP formalism to polarized deep inelastic scattering in Chapter 10.

3.6 Polarized partons and high-energy proton-proton collisions

The parton model factorization arguments can be extended to include fragmentation processes, for example the production of a pion with large transverse momentum p_t in high-energy proton-proton or lepton-proton collisions. Consider the RHIC

process of high p_t pion production, $pp \to \pi X$, shown in Fig. 3.4. One defines the fragmentation function $D_f^\pi(z, \mu^2)$ as the probability density for a parton f to produce a pion in the final state with momentum fraction z of the parton f through hadronization. In the QCD parton model the cross section for this process is given by the formula

$$\frac{d\sigma^{pp\to\pi X}}{d\mathcal{P}} = \sum_{f_1,f_2,f} \int dx_1 dx_2 dz f_1^p(x_1,\mu^2) f_2^p(x_2,\mu^2) \times \frac{d\hat{\sigma}^{f_1 f_2 \to f X'}}{d\mathcal{P}}(x_1\, p_1, x_2\, p_2, p_\pi/z, \mu) D_f^\pi(z,\mu^2) \tag{3.63}$$

Here p_1 and p_2 are the momenta of the incident protons and $\mathcal{P}$ stands for any appropriate set of the kinematic variables of the reaction. The $f_i^p(x,\mu^2)$ are the quark and gluon parton distributions of the incident protons. The $\hat{\sigma}^{f_1 f_2 \to f X'}$ are the underlying hard-scattering cross sections for initial partons f_1 and f_2 producing a final-state parton f plus unobserved X'.

An example of the power of this factorization programme is shown in Fig. 3.5 for pion production in unpolarized proton-proton collisions at RHIC. The prediction using parton distributions and fragmentation functions extracted from previous measurements in unpolarized scattering processes is in very good agreement with the data over the full range of RHIC kinematics.

The parton model description is readily extended to spin dependent processes. The fragmentation function for a parton to produce a pion should not depend on the spin of the parton because the pion has spin zero. The formula (3.63) generalises

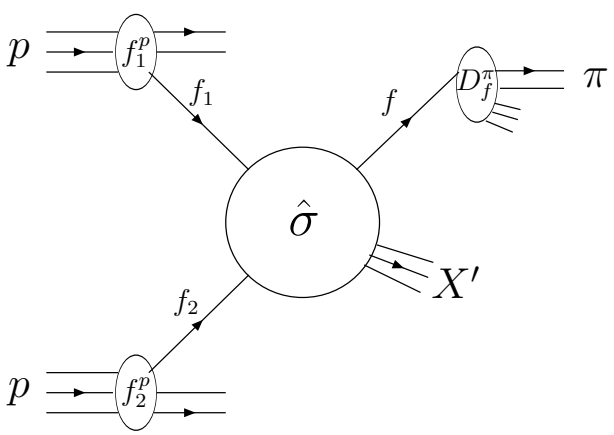

Fig. 3.4 Production of a large-p_t pion in a high-energy proton-proton collision.

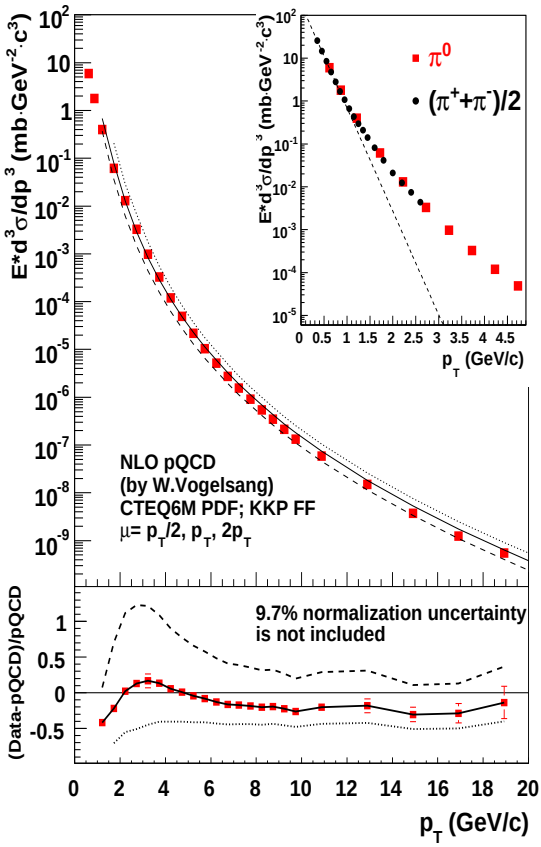

Fig. 3.5 Perturbative QCD factorization at work. The figure shows the invariant differential cross section for inclusive π^0 production in unpolarized proton-proton collisions together with the prediction of NLO perturbative QCD calculations using parton distributions and fragmentation functions extracted from other hard processes. There is excellent agreement with RHIC data [Adare *et al.* (2007)].

to

$$\begin{aligned}\frac{d\Delta\sigma^{pp\to\pi X}}{d\mathcal{P}} &\equiv \frac{1}{4}\left[\frac{d\sigma^{pp\to\pi X}_{++}}{d\mathcal{P}} - \frac{d\sigma^{pp\to\pi X}_{+-}}{d\mathcal{P}} - \frac{d\sigma^{pp\to\pi X}_{-+}}{d\mathcal{P}} + \frac{d\sigma^{pp\to\pi X}_{--}}{d\mathcal{P}}\right] \\ &= \sum_{f_1,f_2,f}\int dx_1 dx_2 dz\ \Delta f_1^p(x_1,\mu^2)\ \Delta f_2^p(x_2,\mu^2) \\ &\quad\times\frac{d\Delta\hat{\sigma}^{f_1 f_2\to f X'}}{d\mathcal{P}}(x_1,p_1,x_2,p_2,p_\pi/z,\mu)\ D_f^\pi(z,\mu^2)\ , \end{aligned} \tag{3.64}$$

where

$$\frac{d\Delta\hat{\sigma}^{f_1 f_2 \to f X'}}{d\mathcal{P}} \equiv \frac{1}{4}\left[\frac{d\hat{\sigma}_{++}^{f_1 f_2 \to f X'}}{d\mathcal{P}} - \frac{d\hat{\sigma}_{+-}^{f_1 f_2 \to f X'}}{d\mathcal{P}} - \frac{d\hat{\sigma}_{-+}^{f_1 f_2 \to f X'}}{d\mathcal{P}} + \frac{d\hat{\sigma}_{--}^{f_1 f_2 \to f X'}}{d\mathcal{P}}\right]. \tag{3.65}$$

Here the subscripts + and − denote the helicities of the incoming particles. The spin dependent cross section $d\Delta\sigma^{pp\to\pi X}/d\mathcal{P}$ depends only on the spin dependent parton distributions, the hard scattering coefficients calculable using perturbative QCD and the pion fragmentation functions D_f^π.

Chapter 4

g_1 SPIN SUM RULES

4.1 The first moment of g_1

We now focus on the proton spin puzzle.

The value of $g_A^{(0)}$ extracted from polarized deep inelastic scattering is obtained as follows. One includes the sum over quark charges squared in $W_{\mu\nu}$ and assumes no twist-two subtraction constant ($\beta_1(Q^2) = O(1/Q^4)$). The first moment of the structure function g_1 is then related to the scale-invariant axial charges of the target nucleon by:

$$\int_0^1 dx\ g_1^p(x,Q^2) = \left(\frac{1}{12}g_A^{(3)} + \frac{1}{36}g_A^{(8)}\right)\Big\{1 + \sum_{\ell\geq 1} c_{\mathrm{NS}\ell}\,\alpha_s^\ell(Q)\Big\} + \frac{1}{9}g_A^{(0)}|_{\mathrm{inv}}\Big\{1 + \sum_{\ell\geq 1} c_{\mathrm{S}\ell}\,\alpha_s^\ell(Q)\Big\} + \mathcal{O}(\frac{1}{Q^2}) - \ \beta_1(Q^2)\frac{Q^2}{4M^2}. \tag{4.1}$$

Here $g_A^{(3)}$, $g_A^{(8)}$ and $g_A^{(0)}|_{\mathrm{inv}}$ are the isotriplet, SU(3) octet and scale-invariant flavour-singlet axial charges respectively. The flavour non-singlet $c_{\mathrm{NS}\ell}$ and singlet $c_{\mathrm{S}\ell}$ Wilson coefficients are calculable in ℓ-loop perturbative QCD [Larin *et al.* (1997)]. One then assumes no twist-two subtraction constant ($\beta_1(Q^2) = O(1/Q^4)$) so that the axial charge contributions saturate the first moment at leading twist.

The first moment of g_1 is constrained by low energy weak interactions. For proton states $|p,s\rangle$ with momentum p_μ and spin s_μ

$$\begin{aligned} 2Ms_\mu\ g_A^{(3)} &= \langle p,s|\left(\bar{u}\gamma_\mu\gamma_5 u - \bar{d}\gamma_\mu\gamma_5 d\right)|p,s\rangle \\ 2Ms_\mu\ g_A^{(8)} &= \langle p,s|\left(\bar{u}\gamma_\mu\gamma_5 u + \bar{d}\gamma_\mu\gamma_5 d - 2\bar{s}\gamma_\mu\gamma_5 s\right)|p,s\rangle. \end{aligned} \tag{4.2}$$

Here $g_A^{(3)} = 1.2695 \pm 0.0029$ is the isotriplet axial charge measured in neutron beta-decay; $g_A^{(8)} = 0.58 \pm 0.03$ is the octet charge measured in hyperon beta decays (and SU(3)) [Close and Roberts (1993)].

The non-singlet axial charges are scale invariant. This follows because the non-singlet axial vector currents are soft operators: they are conserved in the limit

of massless quarks. This means that they are not renormalized and have vanishing anomalous dimension [Itzykson and Zuber (1980)]. The singlet axial vector current is not conserved due to the axial anomaly

$$\partial^\mu \left(\overline{q}\gamma_\mu\gamma_5 q\right) = 2m\overline{q}i\gamma_5 q + \frac{\alpha_s}{4\pi}G_{\mu\nu}\tilde{G}^{\mu\nu}. \tag{4.3}$$

The scale-invariant flavour-singlet axial charge $g_A^{(0)}|_{\rm inv}$ is defined by

$$2Ms_\mu g_A^{(0)}|_{\rm inv} = \langle p,s|\ E(\alpha_s)J_{\mu 5}^{GI}\ |p,s\rangle \tag{4.4}$$

where

$$J_{\mu 5}^{GI} = \left(\bar{u}\gamma_\mu\gamma_5 u + \bar{d}\gamma_\mu\gamma_5 d + \bar{s}\gamma_\mu\gamma_5 s\right)_{GI} \tag{4.5}$$

is the gauge-invariantly renormalized singlet axial-vector operator and

$$E(\alpha_s) = \exp\int_0^{\alpha_s} d\tilde{\alpha}_s\,\gamma(\tilde{\alpha}_s)/\beta(\tilde{\alpha}_s) \tag{4.6}$$

is a renormalization group factor which corrects for the (two loop) non-zero anomalous dimension $\gamma(\alpha_s)$ [Kodaira (1980)] of $J_{\mu 5}^{GI}$ and which goes to one in the limit $Q^2 \to \infty$; $\beta(\alpha_s)$ is the QCD beta function. We are free to choose the QCD coupling $\alpha_s(\mu)$ at either a hard or a soft scale μ. The singlet axial charge $g_A^{(0)}|_{\rm inv}$ is independent of the renormalization scale μ and corresponds to the three flavour $g_A^{(0)}(Q^2)$ evaluated in the limit $Q^2 \to \infty$.

How big is $E(\alpha_s)$?

The perturbative QCD expansion of $E(\alpha_s)$ is

$$\begin{aligned} E(\alpha_s) = \Bigg[1 &- \frac{24f}{33-2f}\frac{\alpha_s}{4\pi} \\ &+ \frac{1}{2}\left(\frac{\alpha_s}{4\pi}\right)^2 \frac{f}{33-2f}\left(\frac{16f}{3} - 472 + 72\frac{102-\frac{14f}{3}}{33-2f}\right) + ...\Bigg] \end{aligned} \tag{4.7}$$

where f is the number of flavours. To $\mathcal{O}(\alpha_s^2)$ the perturbative expansion (4.7) remains close to one – even for large values of α_s. If we take $\alpha_s \sim 0.6$ as typical of the infra-red then

$$E(\alpha_s) \simeq 1 - 0.13 - 0.03 + ... = 0.84 + ... \tag{4.8}$$

Here -0.13 and -0.03 are the $\mathcal{O}(\alpha_s)$ and $\mathcal{O}(\alpha_s^2)$ corrections respectively.

In terms of the flavour dependent axial-charges

$$2Ms_\mu \Delta q = \langle p,s|\overline{q}\gamma_\mu\gamma_5 q|p,s\rangle \tag{4.9}$$

the isovector, octet and singlet axial charges are:

$$\begin{aligned} g_A^{(3)} &= \Delta u - \Delta d \\ g_A^{(8)} &= \Delta u + \Delta d - 2\Delta s \\ g_A^{(0)} \equiv g_A^{(0)}|_{\rm inv}/E(\alpha_s) &= \Delta u + \Delta d + \Delta s. \end{aligned} \tag{4.10}$$

The perturbative QCD coefficients in Eq. (4.1) have been calculated to $O(\alpha_s^3)$ precision [Larin *et al.* (1997)]. For three flavours they evaluate as:

$$\begin{aligned}
&\Big\{1+\sum_{\ell\geq 1} c_{\mathrm{NS}\ell}\,\alpha_s^\ell(Q)\Big\} \\
&\quad = \left[1-(\frac{\alpha_s}{\pi})-3.58333(\frac{\alpha_s}{\pi})^2-20.21527(\frac{\alpha_s}{\pi})^3+...\right] \\
&\Big\{1+\sum_{\ell\geq 1} c_{\mathrm{S}\ell}\,\alpha_s^\ell(Q)\Big\} \\
&\quad = \left[1-0.33333(\frac{\alpha_s}{\pi})-0.54959(\frac{\alpha_s}{\pi})^2-4.44725(\frac{\alpha_s}{\pi})^3+...\right].
\end{aligned} \tag{4.11}$$

In the isovector channel the Bjorken sum rule [Bjorken (1966, 1970)]

$$\begin{aligned}
I_{Bj} &= \int_0^1 dx\left(g_1^p-g_1^n\right) \\
&= \frac{g_A^{(3)}}{6}\left[1-\frac{\alpha_s}{\pi}-3.583\left(\frac{\alpha_s}{\pi}\right)^2-20.215\left(\frac{\alpha_s}{\pi}\right)^3+...\right]
\end{aligned} \tag{4.12}$$

has been confirmed in polarized deep inelastic scattering experiments at the level of 10% (where the perturbative QCD coefficient expansion is truncated at $O(\alpha_s^3)$). The E155 Collaboration at SLAC found $\int_0^1 dx(g_1^p-g_1^n) = 0.176\pm 0.003\pm 0.007$ using a next-to-leading order QCD motivated fit to evolve g_1 data from the E154 and E155 experiments to $Q^2=5$ GeV^2 – in good agreement with the theoretical prediction 0.182 ± 0.005 from the Bjorken sum-rule [Anthony *et al.* (2000)]. Using a similar procedure the SMC experiment obtained $\int_0^1 dx(g_1^p-g_1^n) = 0.174^{+0.024}_{-0.012}$, also at 5 GeV^2 [Adeva *et al.* (1998b)] and also in agreement with the theoretical prediction.

The evolution of the Bjorken integral [Abe *et al.* (1997)] $\int_{x_{\min}}^1 dx(g_1^p-g_1^n)$ as a function of x_{min} is shown for the SLAC data (E143 and E154) in Fig. 4.1. Note that about 50% of the sum-rule comes from x values below about 0.12 and that about 10-20% comes from values of x less than about 0.01. Likewise, Fig. 4.2 shows the convergence of the proton, neutron, singlet deuteron and non-singlet isovector (NS) g_1 first moment integrals from HERMES [Airapetian *et al.* (2007)]. One again sees that about half of the Bjorken integral comes from x less than 0.12. The singlet deuteron integral converges much faster and is all but saturated by contributions from x bigger than 0.05. This is consistent with the recent COMPASS measurements of g_1^d at small x, where the singlet structure function is consistent with zero for $0.004<x<0.02$, as shown in Fig. 2.9 [Alexakhin *et al.* (2007a)].

Substituting the values of $g_A^{(3)}$ and $g_A^{(8)}$ from beta-decays (and assuming no subtraction constant correction) in the first moment equation (4.1) polarized deep inelastic data implies

$$g_A^{(0)}|_{\mathrm{pDIS}} = 0.15-0.35 \tag{4.13}$$

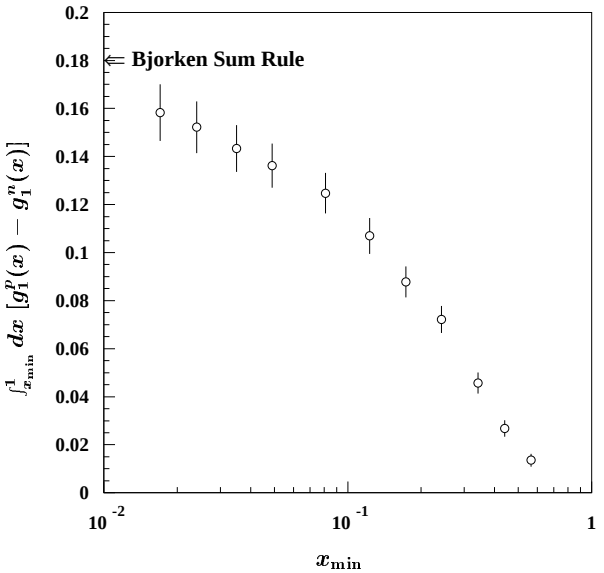

Fig. 4.1 Difference between the measured proton (SLAC E-143) and neutron (SLAC E-154) integrals calculated from a minimum x value, $x_{\rm min}$ up to x of 1. The value is compared to the theoretical prediction from the Bjorken sum rule which makes a prediction over the full x range. For the prediction, the Bjorken sum rule is evaluated up to third order in α_s[Larin *et al.* (1997)] and at $Q^2 = 5$ GeV^2. Error bars on the data are dominated by systematic uncertainties and are highly correlated point-to-point. Figure from Abe *et al.* (1997).

for the flavour singlet (Ellis-Jaffe) moment corresponding to the polarized strangeness $\Delta s = -0.10 \pm 0.04$ quoted in Chapter 1. The measured value of $g_A^{(0)}|_{\rm pDIS}$ compares with the value 0.6 predicted by relativistic quark models and is less than 50% of the value one would expect if strangeness were not important (*viz.* the Ellis-Jaffe sum rule hypothesis $g_A^{(0)} = g_A^{(8)}$) and the value predicted by relativistic quark models without additional gluonic input.

The small x extrapolation of g_1 data is the largest source of experimental error on measurements of the nucleon's axial charges from deep inelastic scattering. The first polarized deep inelastic experiments [Ashman *et al.* (1988, 1989)] used a simple Regge motivated extrapolation $\{g_1 \sim \texttt{constant}\}$ to evaluate the first moment sum-rules. More recent measurements quoted in the literature frequently use the technique of performing next-to-leading-order QCD motivated fits to the g_1 data, evolving the data points all to the same value of Q^2 and then extrapolating these fits to $x = 0$. These NLO QCD fits take into account the scaling violations associated with perturbative QCD. In the most recent fits reported from COMPASS and HERMES to their deuteron target data, COMPASS evolve the data to a common value $Q^2 = 3$ GeV^2 and HERMES to $Q^2 = 5$ GeV^2. The values reported are

$$g_A^{(0)}|_{\rm pDIS} = 0.35 \pm 0.03({\rm stat.}) \pm 0.05({\rm syst.}) \tag{4.14}$$

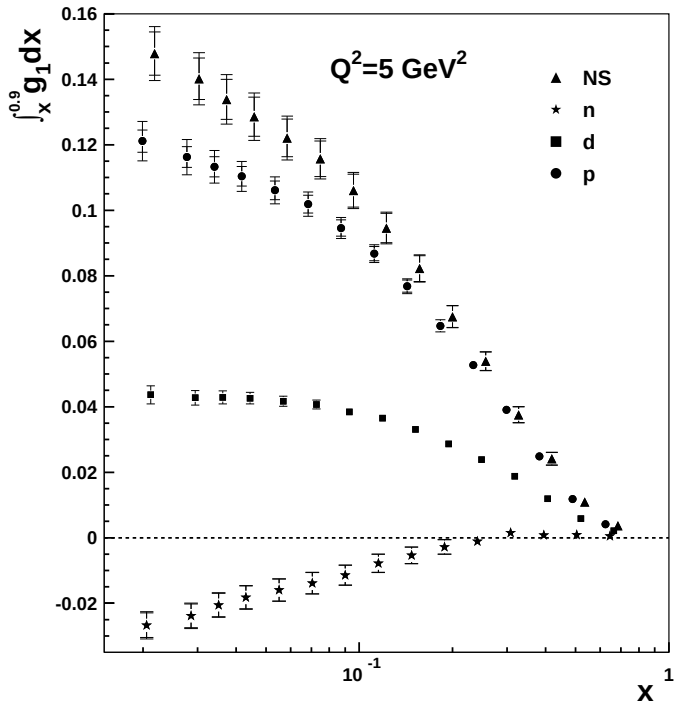

Fig. 4.2 Convergence of the first moment integrals for the proton, neutron, deuteron and isovector (NS) g_1 combination in HERMES data. Figure from Airapetian *et al.* (2007).

from COMPASS and

$$g_A^{(0)}|_{\rm pDIS} = 0.330 \pm 0.011({\rm th.}) \pm 0.025({\rm exp.}) \pm 0.028({\rm evol.}) \tag{4.15}$$

from HERMES. The COMPASS result corresponds to

$$g_A^{(0)}|_{{\rm pDIS},{\rm Q}^2\to\infty} = 0.33 \pm 0.03({\rm stat.}) \pm 0.05({\rm syst.}) \tag{4.16}$$

and polarized strangeness

$$\Delta s_{Q^2\to\infty} = \frac{1}{3}(g_A^{(0)}|_{{\rm pDIS},{\rm Q}^2\to\infty} - g_A^{(8)}) = -0.08 \pm 0.01({\rm stat.}) \pm 0.02({\rm syst.}) \tag{4.17}$$

In a fit to the world g_1 data, COMPASS found that for $Q^2 = 3$ GeV^2

$$g_A^{(0)}|_{\rm pDIS} = 0.30 \pm 0.01({\rm stat.}) \pm 0.02({\rm evol.}) \tag{4.18}$$

Note that polarized deep inelastic scattering experiments measure g_1 between some small but finite value $x_{\rm min}$ and an upper value $x_{\rm max}$ which is close to one. As we decrease $x_{\rm min} \to 0$ we measure the first moment

$$\Gamma \equiv \lim_{x_{\rm min}\to 0} \int_{x_{\rm min}}^1 dx\ g_1(x, Q^2). \tag{4.19}$$

Polarized deep inelastic experiments cannot, even in principle, measure at $x = 0$ with finite Q^2. They miss any possible $\delta(x)$ terms which might exist in g_1 at large

Q^2. That is, they miss any potential (leading twist) fixed pole correction to the deep inelastic spin sum rules.

Measurements of g_1 could be extended to smaller x with a future polarized ep collider. The low x behaviour of g_1 is itself an interesting topic. Small x measurements, besides reducing the error on the first moment (and gluon polarization, Δg, in the proton – see Chapter 10), would provide valuable information about Regge and QCD dynamics at low x where the shape of g_1 is particularly sensitive to the different theoretical inputs discussed in the literature: e.g. $(\alpha_s \ln^2 \frac{1}{x})^k$ resummation and DGLAP evolution [Kwiecinski and Ziaja (1999)], possible Q^2 independent Regge intercepts [Cudell *et al.* (1999)], and the non-perturbative "confinement physics" to hard (perturbative QCD) scale transition. Does the colour glass condensate of small x physics [Iancu *et al.* (2002)] carry net spin polarization? We refer to Ziaja (2003) for a recent discussion of perturbative QCD predictions for the small x behaviour of g_1 in deep inelastic scattering. In the conventional picture based on QCD evolution and no separate hard pomeron trajectory much larger changes in the effective intercepts which describe the shape of the structure functions at small Bjorken x are expected in g_1 than in the unpolarized structure function F_2 so far studied at HERA as one increases Q^2 through the transition region from photoproduction to deep inelastic values of Q^2 [Bass and De Roeck (2001)]. Alternatively, are the Regge intercepts which govern small x physics Q^2 independent, in which case one would see g_1^{p-n} rising like $x^{-\alpha}$ where α is between about 0.2 and 0.5 also at small Q^2. It will be fascinating to study this physics in future experiments, perhaps using a future polarized ep collider or through low x and low Q^2 measurements with COMPASS.

4.2 SU(3) breaking

The extraction of $g_A^{(0)}|_{\rm pDIS}$ from polarized deep inelastic scattering data used SU(3) and hyperon β-decays. We briefly review this physics. Flavour SU(3) symmetry suggests that hyperon β-decays should be describable in terms of two symmetry parameters F and D. The SU(3) baryon-meson coupling part of the effective Lagrangian for low-energy QCD is written to $O(p)$ in the meson momentum as

$$\begin{aligned}\mathcal{L}_{\rm mB} = {} & {\rm Tr}\ \overline{B}(i\gamma_\mu D^\mu - M_0)B \\ & + F\ {\rm Tr}\Big(\overline{B}\gamma_\mu\gamma_5[a^\mu, B]_-\Big) + D\ {\rm Tr}\Big(\overline{B}\gamma_\mu\gamma_5\{a^\mu, B\}_+\Big)\end{aligned} \tag{4.20}$$

Here

$$B = \begin{pmatrix} \frac{1}{\sqrt{2}}\Sigma^0 + \frac{1}{\sqrt{6}}\Lambda & \Sigma^+ & p \\ \Sigma^- & -\frac{1}{\sqrt{2}}\Sigma^0 + \frac{1}{\sqrt{6}}\Lambda & n \\ \Xi^- & \Xi^0 & -\frac{2}{\sqrt{6}}\Lambda \end{pmatrix} \tag{4.21}$$

denotes the baryon octet and M_0 denotes the baryon mass in the chiral limit; D_μ is the chiral covariant derivative (which is defined in Eq. (7.33) in Chapter 7) and

$$a_\mu = -\frac{1}{2F_\pi}\partial_\mu\phi + ... \tag{4.22}$$

is the axial-vector current operator expressed in terms of the octet ϕ of would-be Goldstone bosons associated with spontaneous chiral $SU(3)_L \otimes SU(3)_R$ breaking

$$\phi = \sum \pi_a \lambda_a = \sqrt{2}\begin{pmatrix} \frac{1}{\sqrt{2}}\pi^0 + \frac{1}{\sqrt{6}}\eta_8 & \pi^+ & K^+ \\ \pi^- & -\frac{1}{\sqrt{2}}\pi^0 + \frac{1}{\sqrt{6}}\eta_8 & K^0 \\ K^- & \bar{K}^0 & -\frac{2}{\sqrt{6}}\eta_8 \end{pmatrix} \tag{4.23}$$

In Eq. (4.20) F and D denote the two types of axial coupling allowed in SU(3) and F_π is the pion decay constant.

In the language of SU(3) and the Lagrangian (4.20) one finds $g_A^{(3)} = F + D$ and $g_A^{(8)} = 3F - D$. The quoted value for $g_A^{(8)} = 0.58 \pm 0.03$ was obtained from a best fit to the Λp, $\Xi\Lambda$ and Σn hyperon decays which yielded

$$\begin{aligned} F &= 0.459 \pm 0.008 \\ D &= 0.798 \pm 0.008 \\ F/D &= 0.575 \pm 0.016 \end{aligned} \tag{4.24}$$

with a $\chi^2 = 1.55$ for one degree of freedom and the combination $g_A^{(3)} = F + D = 1.257$ constrained to the value measured in neutron β-decays [Close and Roberts (1993)]. The assumption of good SU(3) used to get $g_A^{(8)}$ here is supported by recent NA-48 Collaboration measurements at CERN [Batley *et al.* (2007)] and KTeV measurements at Fermilab [Alavi-Harati *et al.* (2001)] of the Ξ^0 β-decay $\Xi^0 \to \Sigma^+ e\bar{\nu}$. This decay is very interesting because it is the direct analogue of neutron β-decay under an exchange between the down quark and the strange quark. If the flavor SU(3) symmetry is manifest, the combination $g_A^{(3)} = g_A/g_V$ should be identical to that extracted from neutron β-decays. In other words, this particular decay is highly sensitive to the $SU(3)$ breaking. The results are $1.32^{+0.21}_{-0.17\text{stat.}} \pm 0.05_{\text{syst.}}$ from KTeV and 1.20 ± 0.05 from NA-48, in very good agreement with the value extracted from neutron beta-decays. Further, a recent NLO analysis of inclusive and semi-inclusive polarized deep inelastic data which allows $g_A^{(8)}$ to float in a QCD motivated fit reproduces the SU(3) value $g_A^{(8)} = 0.58$ up to 8% error [de Florian *et al.* (2005)].

In a more conservative discussion Leader and Stamenov (2003) consider a scenario where the experimental uncertainties on the hyperon β-decay measurements correspond to a maximum of 20% violation of SU(3) corresponding to a value of $g_A^{(8)}$ in the range

$$0.47 \leq g_A^{(8)} \leq 0.70 \tag{4.25}$$

If we go to the limit $Q^2 \to \infty$ then the axial-charge combination that we extract from polarized deep inelastic scattering is

$$g_A^{(8)} + 4g_A^{(0)} = 1.90 \pm 0.12 \tag{4.26}$$

If there were zero polarized strangeness in the nucleon ($\Delta s = 0$), then the polarized deep inelastic measurements would correspond to

$$g_A^{(8)} \sim g_A^{(0)} \sim 0.38 \pm 0.03 \tag{4.27}$$

– much below the 0.6 value predicted by relativistic quark models and well outside the range quoted in Eq. (4.25).

4.3 νp elastic scattering

Neutrino proton elastic scattering measures the proton's weak axial charge $g_A^{(Z)}$ through elastic Z^0 exchange. Because of anomaly cancellation in the Standard Model the weak neutral current couples to the combination $u - d + c - s + t - b$, *viz.*

$$J_{\mu 5}^Z \;=\; \frac{1}{2}\Big\{ \sum_{q=u,c,t} - \sum_{q=d,s,b} \Big\}\, \bar{q}\gamma_\mu\gamma_5 q. \tag{4.28}$$

It measures the combination

$$2g_A^{(Z)} = \big(\Delta u - \Delta d - \Delta s\big) + \big(\Delta c - \Delta b + \Delta t\big). \tag{4.29}$$

Heavy quark renormalization group arguments can be used to calculate the heavy t, b and c quark contributions to $g_A^{(Z)}$ both at leading-order [Collins *et al.* (1978); Kaplan and Manohar (1988); Chetyrkin and Kühn (1993)] and at next-to-leading-order (NLO) [Bass *et al.* (2002)]. Working to NLO it is necessary to introduce "matching functions" to maintain renormalization group invariance through-out [Bass *et al.* (2003, 2006)]. The result is

$$2g_A^{(Z)} = \big(\Delta u - \Delta d - \Delta s\big)_{\rm inv} \,+\, \mathcal{H}\big(\Delta u + \Delta d + \Delta s\big)_{\rm inv} \;+\; O(m_{t,b,c}^{-1}) \tag{4.30}$$

where $\mathcal{H}$ is a polynomial in the running couplings $\widetilde{\alpha}_h$,

$$\begin{aligned}\mathcal{H} = \frac{6}{23\pi}\big(\widetilde{\alpha}_b - \widetilde{\alpha}_t\big)\Big\{1 + \frac{125663}{82800\pi}\widetilde{\alpha}_b + \frac{6167}{3312\pi}\widetilde{\alpha}_t - \frac{22}{75\pi}\widetilde{\alpha}_c\Big\} \\ -\frac{6}{27\pi}\widetilde{\alpha}_c - \frac{181}{648\pi^2}\widetilde{\alpha}_c^2 + O\big(\widetilde{\alpha}_{t,b,c}^3\big).\end{aligned} \tag{4.31}$$

Here $(\Delta q)_{\rm inv}$ denotes the scale-invariant version of Δq which are obtained from linear combinations of $g_A^{(3)}$, $g_A^{(8)}$ and $g_A^{(0)}$ and $\widetilde{\alpha}_h$ denotes Witten's renormalization-group-invariant running couplings for heavy quark physics [Witten (1976)]. Taking $\widetilde{\alpha}_t = 0.1$, $\widetilde{\alpha}_b = 0.2$ and $\widetilde{\alpha}_c = 0.35$ in (4.31), one finds a small heavy-quark correction

factor $\mathcal{H} = -0.02$, with leading-order terms dominant. The factor $\left(\widetilde{\alpha}_b - \widetilde{\alpha}_t\right)$ ensures that all contributions from b and t quarks cancel for $m_t = m_b$ (as they should).

Modulo the small heavy-quark corrections quoted above, a precision measurement of $g_A^{(Z)}$, together with $g_A^{(3)}$ and $g_A^{(8)}$, would provide a weak interaction determination of $(\Delta s)_{\rm inv}$, complementary to the deep inelastic measurement of "Δs" in Eq. (4.17). The singlet axial charge in principle measurable in νp elastic scattering is independent of any assumptions about the presence or absence of a subtraction at infinity correction to the deep inelastic first moment of g_1, the $x \sim 0$ behaviour of g_1 or SU(3) flavour breaking. Modulo any "subtraction at infinity" correction to the first moment of g_1, one obtains a rigorous sum-rule relating deep inelastic scattering in the Bjorken region of high-energy and high-momentum-transfer to three independent, low-energy measurements in weak interaction physics: the neutron and hyperon beta decays plus νp elastic scattering.

A precision measurement of the Z^0 axial coupling to the proton is therefore of very high priority. Ideas are being discussed for a dedicated experiment [Tayloe (2002); Pate (2007)]. Key issues are the ability to measure close to the elastic point and a very low duty factor ($\sim 10^{-5}$) neutrino beam to control backgrounds, e.g. from cosmic rays. The neutral-current axial-charge $g_A^{(Z)}$ could also be measured through parity violation in light atoms [Fortson and Lewis (1984); Missimer and Simons (1985); Campbell *et al.* (1989); Khriplovich (1991); Bruss *et al.* (1998, 1999); Alberico *et al.* (2002)].

The experiment E734 at BNL made the first attempt to measure Δs in νp and $\overline{\nu} p$ elastic scattering [Ahrens *et al.* (1987)]. This experiment extracted differential cross-sctions $d\sigma/dQ^2$ in the range $0.4 < Q^2 < 1.1{\rm GeV}^2$. Extrapolating the axial form factor

$$(1 - \Delta s|_{\rm inv}/g_A^{(3)})/(1 + Q^2/M_A^2)^2 \tag{4.32}$$

to the elastic limit one obtains the value for Δs [Kaplan and Manohar (1988)]: $\Delta s = -0.15 \pm 0.09$ taking the mass parameter in the dipole form factor to be $M_A = 1.032 \pm 0.036{\rm GeV}$. However, the data is also consistent with $\Delta s = 0$ if one takes the mass parameter to be $M_A = 1.06 \pm 0.05{\rm GeV}$ which is consistent with the world average and therefore equally valid as a solution. That is, there is a strong correlation between the value of Δs and the dipole mass parameter M_A used in the analysis which prevents an unambiguous extraction of Δs from the E734 data [Garvey *et al.* (1993)]. The analysis of the E734 data also suffered from lack of knowledge about the strange-quark vector form-factors which enter because of the V-A coupling of the exchanged Z^0. A new dedicated precision experiment is required.

To understand the issues involved, recall the currents involved in the coupling of the Z^0 boson to the nucleon. In addition to the axial vector current in Eq. (4.28) there is also the vector current contribution

$$V_\mu^Z = \frac{1}{2}\left(1 - \frac{8}{3}\sin^2\theta_W\right)\bar{u}\gamma_\mu u - \frac{1}{2}\left(1 - \frac{4}{3}\sin^2\theta_W\right)\left(\bar{d}\gamma_\mu d + \bar{s}\gamma_\mu s\right) \tag{4.33}$$

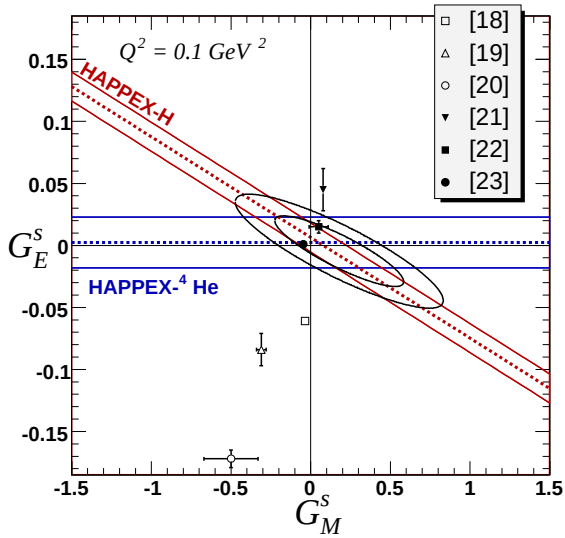

Fig. 4.3 The contours display the 68% and 95% confidence intervals for the joint determination of G_M^s and G_E^s at $Q^2 = 0.1$ GeV^2 plus the results of several theoretical predictions, from Young *et al.* (2006); Acha *et al.* (2007). The theoretical predictions include a lattice calculation denoted by [23] and chiral quark soliton model calculation denoted by [21].

In elastic scattering from the nucleon the information that we can obtain can be summarized as a number of form-factors. These are related to the matrix elements of the vector and axial-vector currents as

$$\langle p', s|V_\mu^Z(0)|p, s\rangle = \bar{u}(p', s)\left[F_1^Z(Q^2)\gamma_\mu + iF_2^Z(Q^2)\frac{\sigma_{\mu\nu}}{2M}q^\nu\right]u(p, s) \tag{4.34}$$

and

$$\langle p', s|J_{\mu 5}^Z(0)|p, s\rangle = \bar{u}(p', s)\left[G_A^Z(Q^2)\gamma_\mu\gamma_5 + i\frac{G_P^Z(Q^2)}{2M}q_\mu\gamma_5\right]u(p, s) \tag{4.35}$$

where $Q^2 = -q^2$ and $q = p' - p$ is the momentum of the Z^0 boson. Each of the vector form-factors can be expressed as a linear combination of flavour triplet, octet and singlet combinations

$$F_i^Z(Q^2) = (1 - 2\sin^2\theta_W)\left[F_i^3(Q^2) + \frac{1}{3}F_i^8(Q^2)\right] - \frac{1}{3}F_i^0(Q^2) \tag{4.36}$$

That is, they involve contributions from up, down and strange quark matrix elements.

A strong effort has been made to measure the strange quark contribution to the elastic form factors of the proton, in particular the electric and magnetic vector form-factors. These experiments [Mueller *et al.* (1997); Hasty *et al.* (2000); Spayde *et al.* (2004); Ito *et al.* (2004); Aniol *et al.* (2004); Maas *et al.* (2004, 2005); Armstrong *et al.* (2005); Aniol *et al.* (2006); Acha *et al.* (2007)] exploit an

interference between the γ-exchange and Z-exchange amplitudes in order to measure weak elastic form factors $G_E^{Z,p}$ and $G_M^{Z,p}$ which are the weak-interaction analogs of the more traditional electromagnetic elastic form factors $G_E^{\gamma,p}$ and $G_M^{\gamma,p}$ for which copious experimental data are available. The interference term is observable as a parity-violating asymmetry in elastic $\vec{e}p$ scattering, with the electron longitudinally polarized. By combining the electromagnetic form factors of the proton and neutron with the weak form factors of the proton, one may separate the up, down, and strange quark contributions. For example, the electric form factors may be written as follows:

$$
\begin{aligned}
G_E^{\gamma,p} &= \frac{2}{3}G_E^u - \frac{1}{3}G_E^d - \frac{1}{3}G_E^s \\
G_E^{\gamma,n} &= \frac{2}{3}G_E^d - \frac{1}{3}G_E^u - \frac{1}{3}G_E^s \\
G_E^{Z,p} &= \left(1 - \frac{8}{3}\sin^2\theta_W\right)G_E^u + \left(-1 + \frac{4}{3}\sin^2\theta_W\right)G_E^d + \left(-1 + \frac{4}{3}\sin^2\theta_W\right)G_E^s.
\end{aligned}
$$

For $Q^2 = 0$ the electric form-factors G_E^q reduce to the number of valence quarks of flavour q, the magnetic form-factors G_M^q reduce to the contribution to the proton's magentic moment from quarks and the axial-form factor $G_A^Z(0) = g_A^{(Z)}$.

The recent parity-violating ep forward-scattering elastic asymmetry data from Jefferson Lab (HAPPEX and G0), when combined with the νp elastic cross section data from Brookhaven (E734), permit an extraction of the strangeness contribution to the vector and axial nucleon form factors for momentum transfers in the range $0.45 < Q^2 < 1.0$ GeV^2. Further recent determinations of the strange vector form factors at $Q^2 = 0.1$ GeV^2 have been performed by the SAMPLE, HAPPEX, PVA4 and G0 experiments.

Information about the strange form factors of the nucleon from ν-nucleon or ν-nucleus scattering is best extracted from measurements of the ratios these cross-sections. This limits some of the experimental uncertainties plus (for ν-nucleus scattering) some of the model dependence of the calculated cross sections. Consider the neutrino-antineutrino asymmetry combination

$$
\mathcal{A}(Q^2) = \frac{\left(\frac{d\sigma}{dQ^2}\right)_\nu^{NC} - \left(\frac{d\sigma}{dQ^2}\right)_{\overline{\nu}}^{NC}}{\left(\frac{d\sigma}{dQ^2}\right)_\nu^{CC} - \left(\frac{d\sigma}{dQ^2}\right)_{\overline{\nu}}^{CC}} \tag{4.37}
$$

For elastic scattering this becomes

$$
\mathcal{A}_{p(n)} = \frac{1}{4}\left(\pm 1 - \frac{G_A^s}{G_A}\right)\left(\pm 1 - 2\sin^2\theta_W \frac{{G_M}^{p(n)}}{G_M^3} - \frac{1}{2}\frac{G_M^s}{G_M^3}\right). \tag{4.38}
$$

The strange axial and vector form-factors enter through the ratios G_A^s/G_A and G_M^s/G_M^3. Combining future νp elastic measurements with with the strangeness magnetic moment extracted from experiments at Bates, JLab and MAMI would

allow one to extract the strangeness polarization Δs. For proposed new experiments [Tayloe (2002); Pate (2007)] the plan is to measure the ratio of the neutral-current to the charged-current νN and $\bar{\nu} N$ processes: $R_{NC/CC} = \sigma(\nu p \to \nu p)/\sigma(\nu n \to \mu^- p)$ and $\bar{R}_{NC/CC} = \sigma(\bar{\nu} p \to \bar{\nu} p)/\sigma(\bar{\nu} p \to \mu^+ n)$. When combined with the world's data on forward-scattering parity-violating ep data the aim is to produce a dense set of data points for G_A^s in the range $0.25 < Q^2 < 0.75$ GeV^2 with an uncertainty at each point of about ± 0.02. The result would be to push the range of Q^2 to much lower values, to greatly increase the precision of the νp elastic data and to extract a quality measurement of the strangeness contribution to the nucleon spin, Δs. Nuclear targets (e.g. C or Ar) are to be used in these neutrino experiments, and so a deep understanding of the nuclear physics, particularly in regard to final state effects, is needed before the potential of these precision experiments can be fully realized. A number of theoretical efforts have been made which suggest that the planned measurements of $R_{NC/CC}$ and $\bar{R}_{NC/CC}$ will be relatively insensitive to nuclear physics effects and final state interactions – see Pate (2007) and references therein.

4.4 The Burkhardt-Cottingham sum rule

The Burkhardt-Cottingham sum rule [Burkhardt and Cottingham (1970)] reads:

$$\int_{Q^2/2M}^{\infty} d\nu G_2(Q^2, \nu) = \frac{2M^3}{Q^2} \int_0^1 dx g_2 = 0, \qquad \forall Q^2. \tag{4.39}$$

For deep inelastic scattering, this sum rule is derived by assuming that the moment formula (3.31) can be analytically continued to $n = 0$. In general, the Burkhardt-Cottingham sum rule is derived by assuming no $\alpha \geq 0$ singularity in G_2 (or, equivalently, no $\frac{1}{x}$ or more singular small behaviour in g_2) and no "subtraction at infinity" (from an $\alpha = J = 0$ fixed pole in the real part of G_2) [Jaffe (1990)]. The most precise measurements of g_2 to date in polarized deep inelastic scattering come from the SLAC E-155 and E-143 experiments, which report $\int_{0.02}^{0.8} dx\ g_2^p = -0.042 \pm 0.008$ for the proton and $\int_{0.02}^{0.8} dx\ g_2^d = -0.006 \pm 0.011$ for the deuteron at $Q^2 = 5$ GeV^2 [Anthony *et al.* (2003)]. New, even more accurate, measurements of g_2 (for the neutron using a ^{3}He target) from Jefferson Laboratory [Amarian *et al.* (2004)] for Q^2 between 0.1 and 0.9 GeV^2 are consistent with the sum rule. Further measurements to test the Burkhardt-Cottingham sum rule would be most valuable, particularly given the SLAC proton result quoted above.

The formula (3.31) indicates that g_2 can be written as the sum

$$g_2 = g_2^{\mathrm{WW}}(x) + \overline{g}_2(x) \tag{4.40}$$

of a twist-two term [Wandzura and Wilczek (1977)], denoted g_2^{WW}

$$g_2^{\mathrm{WW}} = -g_1(x) + \int_x^1 \frac{dy}{y} g_1(y) \tag{4.41}$$

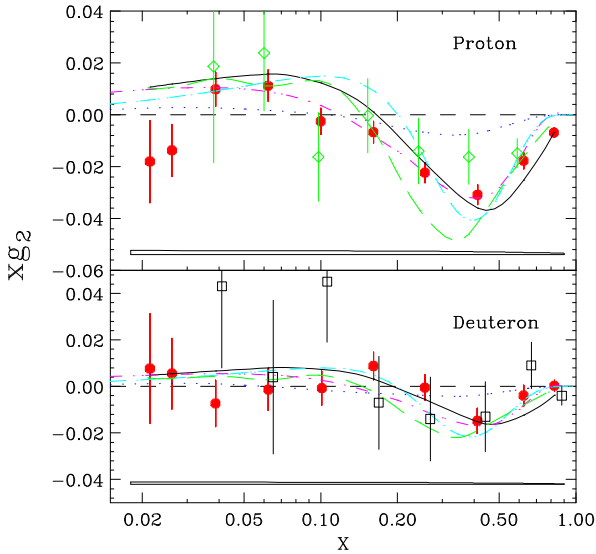

Fig. 4.4 The Q^2 averaged measured of xg_2 (SLAC data) compared with the twist-two Wandzura-Wilczek contribution g_2^{WW} term (solid line) and several quark model calculations. Figure from Anthony *et al.* (2003).

and a second contribution $\bar{g}_2$ which is the sum of a higher-twist (twist 3) contribution $\xi(x, Q^2)$ and a "transversity" term $h_1(x, Q^2)$ which is suppressed by the ratio of the quark to target nucleon masses and therefore negligible for light u and d quarks

$$\overline{g}_2(x, Q^2) = -\int_x^1 \frac{dy}{y}\frac{\partial}{\partial y}\left(\frac{m_q}{M}h_1(y, Q^2) + \xi(y, Q^2)\right) \tag{4.42}$$

– see Cortes *et al.* (1992). The first moment of the twist 2 contribution $g_2^{\rm WW}$ vanishes through integrating the convolution formula (4.41). If one drops the transversity contribution from the formalism (being proportional to the light quark mass), one obtains the equation

$$\tilde{d}_2(Q^2) = 3\int_0^1 dx x^2\left[g_2(x, Q^2) - g_2^{\rm WW}(x, Q^2)\right] \tag{4.43}$$

for the leading twist 3 matrix element in Eq. (3.31).

Higher-twist observables are interesting because they represent the quark and gluon correlations in the nucleon which cannot otherwise be studied. The quantity $\tilde{d}_2(Q^2)$ is given by the matrix element of a twist-three operator

$$\langle PS|\frac{1}{4}\bar{\psi}g\tilde{F}^{\sigma(\mu}\gamma^{\nu)}\psi|PS\rangle = 2d_2 S^{[\sigma}P^{(\mu]}P^{\nu)} \ , \tag{4.44}$$

where $\tilde{F}^{\mu\nu} = (1/2)\epsilon^{\mu\nu\alpha\beta}F_{\alpha\beta}$, and the different brackets – $(\cdots)$ and $[\cdots]$ – denote symmetrisation and antisymmetrisation of indices, respectively.

The values extracted from dedicated SLAC measurements are $d_2^p = 0.0032 \pm 0.0017$ for the proton and $d_2^n = 0.0079 \pm 0.0048$ for the neutron – that is, consistent with zero (no twist-3) at two standard deviations [Anthony *et al.* (2003)]. These twist 3 matrix elements are related in part to the response of the collective colour electric and magnetic fields to the spin of the nucleon. Recent analyses attempt to extract the twist-four corrections to g_1. The results and the gluon field polarizabilities are small and consistent with zero [Deur *et al.* (2004)].

4.5 The Gerasimov-Drell-Hearn sum rule

The Gerasimov-Drell-Hearn (GDH) sum-rule [Gerasimov (1965); Drell and Hearn (1966)] for spin dependent photoproduction relates the difference of the two cross-sections for the absorption of a real photon with spin polarized anti-parallel, $\sigma_{\frac{1}{2}}$, and parallel, $\sigma_{\frac{3}{2}}$, to the target spin to the square of the anomalous magnetic moment of the target. The GDH sum rule reads

$$\int_{\text{threshold}}^{\infty} \frac{d\nu}{\nu}(\sigma_{\frac{1}{2}} - \sigma_{\frac{3}{2}}) = \frac{8\pi^2\alpha}{M^2}\int_{\text{threshold}}^{\infty}\frac{d\nu}{\nu}G_1$$
$$= -\frac{2\pi^2\alpha}{M^2}\kappa^2 = \begin{cases} -204.5\ \mu\text{b} & p \\ -232.8\ \mu\text{b} & n \end{cases}, \qquad (4.45)$$

where κ is the anomalous magnetic moment. The sum rule follows from the very general principles of causality, unitarity, Lorentz and electromagnetic gauge invariance and one assumption: that the g_1 spin structure function satisfies an unsubtracted dispersion relation. Modulo the no-subtraction hypothesis, the Gerasimov-Drell-Hearn sum-rule is valid for a target of arbitrary spin S, whether elementary or composite [Brodsky and Primack (1969)] – for reviews, see Bass (1997) and Drechsel and Tiator (2004).

The GDH sum-rule is derived by setting $\nu = 0$ in the dispersion relation for A_1, Eq. (3.17). For small photon energy $\nu \to 0$

$$A_1(0,\nu) = -\frac{1}{2}\kappa^2 + \tilde{\gamma}\nu^2 + O(\nu^4). \qquad (4.46)$$

Here $\gamma_N = \frac{\alpha}{M^2}\tilde{\gamma}$ is the spin polarizability which measures the stiffness of the nucleon spin against electromagnetic induced deformations relative to the axis defined by the nucleon's spin. This low-energy theorem follows from Lorentz invariance and electromagnetic gauge invariance (plus the existence of a finite mass gap between the ground state and continuum contributions to forward Compton scattering) [Brodsky and Primack (1969); Low (1954); Gell-Mann and Goldberger (1954)].

The integral in Eq. (4.45) converges for each of the leading Regge contributions (discussed in Section 2.6). If the sum rule were observed to fail (with a finite integral) the interpretation would be a "subtraction at infinity" induced by a $J = 1$ fixed pole in the real part of the spin amplitude A_1 [Abarbanel and Goldberger (1968)].

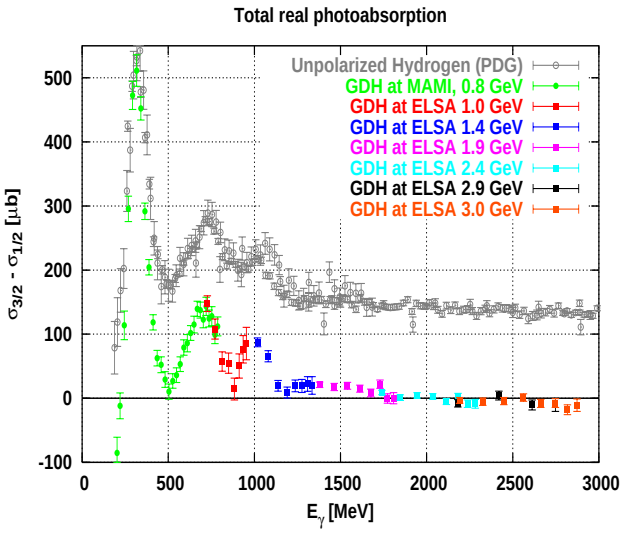

Fig. 4.5 The spin dependent photoproduction cross-section for the proton target (ELSA and MAMI data). Figure courtesy of K. Helbing.

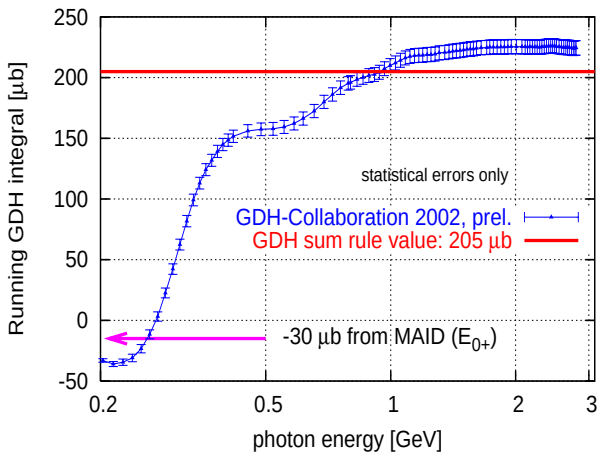

Fig. 4.6 Running GDH integral for the proton (ELSA and MAMI). Figure courtesy of K. Helbing.

Present experiments at ELSA and MAMI are aimed at measuring the GDH integrand through the range of incident photon energies $E_\gamma = 0.14$ - 0.8 GeV (MAMI) [Ahrens *et al.* (2000, 2001, 2002)] and 0.7 - 3.1 GeV (ELSA) [Dutz *et al.* (2003, 2005)]. The inclusive cross-section for the proton target $\sigma_{\frac{3}{2}} - \sigma_{\frac{1}{2}}$ is shown in Fig. 4.5. The presently analysed GDH integral on the proton is shown in Fig. 4.6 and is dominated by the Δ resonance contribution. (The contribution to the sum-rule from the unmeasured region close to threshold is estimated from the MAID model [Drechsel *et al.* (2003)].) The combined data from the ELSA-MAMI experiments suggest that

the contribution to the GDH integral for a proton target from energies $\nu < 3$ GeV exceeds the total sum rule prediction (-204.5μb) by about 5-10% [Helbing (2002)]. Phenomenological estimates suggest that about $+25 \pm 10\mu$b of the sum rule may reside at higher energies [Bass and Brisudova (1999); Bianchi and Thomas (1999)] and that this high energy contribution is predominantly in the isovector channel. (It should be noted, however, that any 10% fixed pole correction would be competitive with this high energy contribution within the errors.) Further measurements, including at higher energy, would be valuable. First neutron data has been obtained from ELSA using a deuteron target [Dutz *et al.* (2005)]. The result is a contribution to the neutron GDH integral of $33.9 \pm 5.5(\text{stat.}) \pm 4.5(\text{syst.})\mu$b from the measured energy range from 815 to 1825 MeV. It is interesting to note that, just like the measured g_1 at deep inelastic Q^2, the high-energy part of the spin dependent cross-section $\sigma_{\frac{1}{2}} - \sigma_{\frac{3}{2}}$ at $Q^2 = 0$ seems to be largely isovector prompting the question whether there is some physics conspiracy to suppress the singlet term. It should be noted however that perturbative QCD motivated fits to g_1 data with a positive polarized gluon distribution (and no node in it) predict that g_1 should develop a strong negative contribution at $x < 0.0001$ at deep inelastic Q^2 – see e.g. De Roeck *et al.* (1999) and references therein. However, one should note that there is no evidence for any such trend in the COMPASS measurements of g_1^d for $0.004 < x < 0.02$ shown in Fig. 2.9.

In addition to the GDH sum-rule, one also finds a second sum-rule for the nucleon's spin polarizability. This spin polarizability sum-rule is derived by taking the second derivative of $A_1(Q^2, \nu)$ in the dispersion relation (3.17) and evaluating the resulting expression at $\nu = 0$, *viz.* $\frac{\partial^2}{\partial \nu^2} A_1(Q^2, \nu)|_{\nu=0}$. One finds

$$\int_0^\infty \frac{d\nu'}{\nu'^3} \left(\sigma_{\frac{1}{2}} - \sigma_{\frac{3}{2}} \right)(\nu') = 4\pi^2 \, \gamma_N. \tag{4.47}$$

In comparison with the GDH sum-rule the relevant information is now concentrated more on the low energy side because of the $1/\nu'^3$ weighting factor under the integral. Main contributions come from the $\Delta(1232)$ resonance and the low energy pion photoproduction continuum described by the electric dipole amplitude E_{0+}. The value extracted from MAMI data [Drechsel *et al.* (2003)]

$$\gamma_p = (-1.01 \pm 0.13) \times 10^{-4} \text{ fm}^4 \tag{4.48}$$

is within the range of predictions of chiral perturbation theory.

Further experiments to test the GDH sum-rule and to measure the $\sigma_{\frac{1}{2}} - \sigma_{\frac{3}{2}}$ at and close to $Q^2 = 0$ are being carried out at Jefferson Laboratory, GRAAL at Grenoble, LEGS at BNL, and SPRING-8 in Japan.

We note two interesting properties of the GDH sum rule.

First, we write the anomalous magnetic moment κ as the sum of its isovector κ_V and isoscalar κ_S contributions, *viz.* $\kappa_N = \kappa_S + \tau_3 \kappa_V$. One then obtains the

isospin dependent expressions:

$$\begin{aligned}(\text{GDH})_{I=0} &= (\text{GDH})_{VV} + (\text{GDH})_{SS} = -\frac{2\pi^2\alpha}{m^2}(\kappa_V^2 + \kappa_S^2)\\ (\text{GDH})_{I=1} &= (\text{GDH})_{VS} = -\frac{2\pi^2\alpha}{m^2}2\kappa_V\kappa_S.\end{aligned} \tag{4.49}$$

The physical values of the proton and nucleon anomalous magnetic moments $\kappa_p = 1.79$ and $\kappa_n = -1.91$ correspond to $\kappa_S = -0.06$ and $\kappa_V = +1.85$. Since $\kappa_S/\kappa_V \simeq -\frac{1}{30}$, it follows that $(\text{GDH})_{SS}$ is negligible compared to $(\text{GDH})_{VV}$. That is, to good approximation, the isoscalar sum-rule $(\text{GDH})_{I=0}$ measures the isovector anomalous magnetic moment κ_V. Given this isoscalar measurement, the isovector sum-rule $(\text{GDH})_{I=1}$ then measures the isoscalar anomalous magnetic moment κ_S.

Second, the anomalous magnetic moment is measured in the matrix element of the vector current. Furry's theorem tells us that the real-photon GDH integral for a gluon or a photon target vanishes. Indeed, this is the reason that the first moment of the g_1 spin structure function for a real polarized photon target vanishes to all orders and at every twist: $\int_0^1 dx\ g_1^\gamma(x, Q^2)$ independent of the virtuality Q^2 of the second photon that it is probed with [Bass *et al.* (1998)]. Assuming correction to the GDH sum rule, this result implies that the two non-perturbative gluon exchange contribution to $\sigma_{\frac{1}{2}} - \sigma_{\frac{3}{2}}$ which behaves as $\ln\nu/\nu$ in the high energy Regge limit has a node at some value $\nu = \nu_0$ so that it does not contribute to the GDH integral. There is no axial anomaly contribution to the anomalous magnetic moment and hence no axial anomaly contribution to the GDH sum-rule.

4.6 The transition region

Several experiments have explored the transition region between polarized photoproduction (the physics of the GDH sum-rule) and polarized deep inelastic scattering (the physics of the Bjorken sum-rule and $g_A^{(0)}$ through the Ellis-Jaffe moment).

The Q^2 dependent quantity [Anselmino *et al.* (1989)]

$$\begin{aligned}\Gamma(Q^2) \equiv I(Q^2) &= \int_{\frac{Q^2}{2M}}^\infty \frac{d\nu}{\nu} G_1(\nu, Q^2)\\ &= \frac{2M^2}{Q^2}\int_0^1 dx g_1(x, Q^2)\end{aligned} \tag{4.50}$$

interpolates between the two limits with $I(0) = -\frac{1}{4}\kappa_N^2$ implied by the GDH sum rule. Measurements of $\int_0^1 dx g_1^p = \frac{Q^2}{2M^2} I(Q^2)$ are shown in Fig. 4.7. Note the negative slope predicted at $Q^2 = 0$ by the GDH sum rule and the sign change around $Q^2 \sim 0.3$ GeV^2. The shape of the curve is driven predominantly by the role of the Δ resonance and the $1/Q^2$ pole in Eq. (4.50). Figure 4.7 shows also the predictions of various models [Soffer and Teryaev (1993); Burkert and Ioffe (1994)] which try to

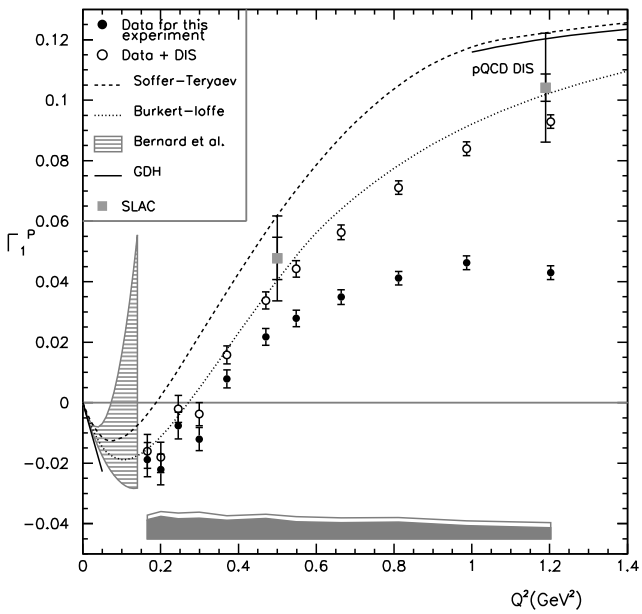

Fig. 4.7 Data from JLab (CLAS) and SLAC on the low Q^2 behaviour of $\int_0^1 dx g_1^p$ compared to various theoretical models interpolating the scaling and photoproduction limits [Fatemi *et al.* (2003)].

describe the intermediate Q^2 range through a combination of resonance physics and vector-meson dominance at low Q^2 and scaling parton physics at DIS Q^2. Chiral perturbation theory [Bernard *et al.* (2003)] may describe the behaviour of this "generalized GDH integral" close to threshold – see the shaded band in Fig. 4.7.

In the model of Ioffe and collaborators [Anselmino *et al.* (1989); Burkert and Ioffe (1994)] the integral at low to intermediate Q^2 for the inelastic part of $(\sigma_A - \sigma_P)$ is given as the sum of a contribution from resonance production, denoted $I^{\rm res}(Q^2)$, which has a strong Q^2 dependence for small Q^2 and then drops rapidly with Q^2, and a non-resonant vector-meson dominance contribution which they took as the sum of a monopole and a dipole term, *viz.*

$$I(Q^2) = I^{\rm res}(Q^2) + 2M^2\Gamma^{\rm as}\left(\frac{1}{Q^2+\mu^2} - \frac{C\mu^2}{(Q^2+\mu^2)^2}\right). \tag{4.51}$$

Here $\Gamma^{\rm as}$ is taken as

$$\Gamma^{\rm as} = \int_0^1 dx g_1(x,\infty) \tag{4.52}$$

and

$$C = 1 + \frac{1}{2}\,\frac{\mu^2}{M^2}\,\frac{1}{\Gamma^{\rm as}}\,\left(\frac{1}{4}\kappa^2 + I^{\rm res}(0)\right). \tag{4.53}$$

The mass parameter μ is identified with rho meson mass, $\mu^2 \simeq m_\rho^2$.

Chapter 5

FIXED POLES

We saw in Chapter 3 that the first moment of g_1 is given by the matrix elements of the proton's axial charges up to a possible "subtraction at infinity" in the dispersion relation for g_1. The contribution to the dispersion relation from integrating along the real axis is the parton model contribution. The contribution from the circle at infinity, if finite, is associated with what was is known in Regge phenomenology as a $J = 1$ fixed pole. We next give a brief overview of these fixed poles: what they are and how they can contribute to sum rules for deep inelastic structure functions.

Fixed poles are exchanges in Regge phenomenology with no t dependence: the trajectories are described by $J = \alpha(t) = 0$ or 1 for all t [Abarbanel *et al.* (1967); Brodsky *et al.* (1972); Landshoff and Polkinghorne (1972)]. For example, for fixed Q^2 a $t-$independent real constant term in the spin amplitude A_1 would correspond to a $J = 1$ fixed pole. Fixed poles are excluded in hadron-hadron scattering by unitarity but are not excluded from Compton amplitudes (or parton distribution functions) because these are calculated only to lowest order in the current-hadron coupling. Indeed, there are two famous examples where fixed poles are required: (by current algebra) in the Adler sum rule for W-boson nucleon scattering, and to reproduce the Schwinger term sum rule for the longitudinal structure function measured in unpolarized deep inelastic ep scattering. We review the derivation of these fixed pole contributions, and then discuss potential fixed pole corrections to the Burkhardt-Cottingham, g_1 and Gerasimov-Drell-Hearn sum-rules.

Fixed poles in the real part of the forward Compton amplitude have the potential to induce "subtraction at infinity" corrections to sum rules for photon nucleon (or lepton nucleon) scattering. For example, a ν independent term in the real part of A_1 would induce a subtraction constant correction to the spin sum rule for the first moment of g_1. Bjorken scaling at large Q^2 constrains the Q^2 dependence of the residue of any fixed pole in the real of the forward Compton amplitude (e.g. $\beta_1(Q^2)$ and $\beta_2(Q^2)$ in the dispersion relations (3.20)). To be consistent with scaling these residues must decay as or faster than $1/Q^2$ as $Q^2 \to \infty$. That is, they must be nonpolynomial in Q^2.

5.1 Adler sum rule

The first example we consider is the Adler sum rule for W-boson nucleon scattering [Adler (1966)]:

$$\int_{Q^2/2M}^{+\infty} d\nu \left[W_2^{\bar{\nu}p}(\nu, Q^2) - W_2^{\nu p}(\nu, Q^2) \right] = \int_0^1 \frac{dx}{x} \left[F_2^{\bar{\nu}p}(x, Q^2) - F_2^{\nu p}(x, Q^2) \right]$$
$$= \begin{array}{ll} 4 - 2\cos^2\theta_c & \text{(BCT)} \\ 2 & \text{(ACT).} \end{array} \tag{5.1}$$

Here θ_c is the Cabibbo angle, and BCT and ACT refer to below and above the charm production threshold.

The Adler sum rule is derived from current algebra. The right hand side of the sum rule is the coefficient of a $J = 1$ fixed pole term

$$\frac{i}{\pi} f_{abc}\ F_c \left[(p_\mu q_\nu + q_\mu p_\nu) - M\nu g_{\mu\nu} \right] / Q^2 \tag{5.2}$$

in the imaginary part of the forward Compton amplitude for W-boson nucleon scattering [Heimann *et al.* (1972)]. This fixed pole term is required by the commutation relations between the charge raising and lowering weak currents

$$q_\mu T_{ab}^{\mu\nu} = -\frac{1}{\pi} \int d^4x\ e^{iq.x}\ \langle p, s | \left[J_a^0(x), J_b^\nu(0) \right] | p, s \rangle \delta(x^0)$$
$$= -\frac{i}{\pi} f_{abc} \langle ps | J_c^\nu(0) | ps \rangle. \tag{5.3}$$

Here F_c is a generalized form factor at zero momentum transfer:

$$\langle p, s | J_c^\nu(0) | p, s \rangle \equiv p^\nu F_c. \tag{5.4}$$

The fixed pole term appears in lowest order perturbation theory, and is not renormalized because it is a consequence of the charge algebra. The Adler sum rule is protected against radiative QCD corrections

5.2 Schwinger term sum rule

Our second example is the Schwinger term sum rule [Broadhurst *et al.* (1973)] which relates the logarithmic integral in ω (or Bjorken x) of the longitudinal structure function $F_L(\omega, Q^2)$ ($F_L = \frac{1}{2}\omega F_2 - F_1$) measured in unpolarized deep inelastic scattering to the target matrix element of the operator Schwinger term $\mathcal{S}$ defined through the equal-time commutator of the electromagnetic charge and current densities

$$\langle p, s | \left[J_0(\vec{y}, 0), J_i(0) \right] | p, s \rangle = i\ \partial_i\ \delta^3(\vec{y})\ \mathcal{S}. \tag{5.5}$$

The Schwinger term sum rule reads

$$\mathcal{S} = \lim_{Q^2 \to \infty} \left[4 \int_1^\infty \frac{d\omega}{\omega} \tilde{F}_L(\omega, Q^2) - 4 \sum_{\alpha > 0} \gamma(\alpha, Q^2)/\alpha - C(q^2) \right]. \tag{5.6}$$

Here $C(Q^2)$ is the nonpolynomial residue of any $J = 0$ fixed pole contribution in the real part of T_2 and

$$\tilde{F}_L(\omega, Q^2) = F_L(\omega, Q^2) - \sum_{\alpha \geq 0} \gamma(\alpha, Q^2)\omega^\alpha \tag{5.7}$$

represents F_L with the leading ($\alpha > 0$) Regge behaviour subtracted. The integral in Eq. (5.6) is convergent because $\tilde{F}_L(\omega, Q^2)$ is defined with all Regge contributions with effective intercept greater than or equal to zero removed from $F_L(Q^2, \omega)$. The Schwinger term $\mathcal{S}$ vanishes in vector gauge theories like QCD.

Since $F_L(\omega, Q^2)$ is positive definite, it follows that QCD possesses the required non-vanishing $J = 0$ fixed pole in the real part of T_2.

The Schwinger term sum rule and the presence of the required $J = 0$ fixed pole have been checked in ϕ^3 theory and in perturbative QCD where the fixed pole appears at $O(\alpha_s)$ [Broadhurst *et al.* (1973)].

5.3 Burkhardt-Cottingham sum rule

The third example, and the first in connection with spin, is the Burkhardt-Cottingham sum rule for the first moment of g_2 [Burkhardt and Cottingham (1970)]:

$$\int_{Q^2/2M}^{\infty} d\nu \; G_2(Q^2, \nu) = \frac{2M^3}{Q^2} \int_0^1 dx g_2 = 0\,. \tag{5.8}$$

Suppose that future experiments find that the sum rule is violated and that the integral is finite. The conclusion [Jaffe (1990)] would be a $J = 0$ fixed pole with nonpolynomial residue in the real part of A_2. To see this work at fixed Q^2 and assume that all Regge-like singularities contributing to $A_2(\nu, Q^2)$ have intercept less than zero so that

$$A_2(\nu, Q^2) \sim \nu^{-1-\epsilon} \tag{5.9}$$

as $\nu \to \infty$ for some $\epsilon > 0$. Then the large ν behaviour of A_2 is obtained by taking $\nu \to \infty$ under the ν' integral giving

$$A_2(Q^2, \nu) \sim -\frac{2}{\pi\nu} \int_{Q^2/2M}^{\infty} d\nu' \; \mathrm{Im}A_2(Q^2, \nu') \tag{5.10}$$

which contradicts the assumed behaviour unless the integral vanishes; hence the sum rule. *If* there is an $\alpha(0) = 0$ fixed pole in the real part of A_2 the fixed pole will not contribute to $\mathrm{Im}A_2$ and therefore not spoil the convergence of the integral.

One finds

$$\beta_2(Q^2) \sim -\frac{2}{\pi M} \int_{Q^2/2M}^{\infty} d\nu' \; \mathrm{Im}A_2(Q^2, \nu') \tag{5.11}$$

for the residue of any $J = 0$ fixed pole coupling to $A_2(Q^2, \nu)$.

5.4 g_1 spin sum rules

Scaling requires that any fixed pole correction to the Ellis-Jaffe g_1 sum rule must have nonpolynomial residue. Through Eq. (3.20), the fixed pole coefficient $\beta_1(Q^2)$ must decay as or faster than $O(1/Q^2)$ as $Q^2 \to \infty$. The coefficient is further constrained by the requirement that G_1 contains no kinematic singularities (for example at $Q^2 = 0$). In Chapter 6 we will identify a potential leading-twist topological $x = 0$ contribution to the first moment of g_1 through analysis of the axial anomaly contribution to $g_A^{(0)}$. This zero-mode topological contribution (if finite) generates a leading twist fixed pole correction to the flavour-singlet part of $\int_0^1 dx g_1$. *If* present, this fixed pole will also violate the Gerasimov-Drell-Hearn sum rule (since the two sum rules are derived from A_1) *unless* the underlying dynamics suppress the fixed pole's residue at $Q^2 = 0$. The possibility of a fixed pole correction to g_1 spin sum-rules was raised in pre-QCD work as early as Abarbanel and Goldberger (1968) and Heimann (1973).

Note that any fixed pole correction to the Gerasimov-Drell-Hearn sum rule is most probably a non-perturbative effect. The sum rule (3.20) has been verified to $O(\alpha^2)$ for all $2 \to 2$ processes $\gamma a \to bc$ where a is either a real lepton, quark, gluon or elementary Higgs target [Altarelli *et al.* (1972); Brodsky and Schmidt (1995)], and for electrons in QED to $O(\alpha^3)$ [Dicus and Vega (2001)].

One could test for a fixed pole correction to the Ellis-Jaffe moment through a precision measurement of the flavour singlet axial charge from an independent process where one is not sensitive to theoretical assumptions about the presence or absence of a $J = 1$ fixed pole in A_1. Here the natural choice is elastic neutrino proton scattering where the parity violating part of the cross-section includes a direct weak interaction measurement of the scale invariant flavour-singlet axial charge $g_A^{(0)}|_{\rm inv}$.

A further test could come from a precision measurement of the Q^2 dependence of the polarized gluon distribution at next-to-next-to-leading order accuracy where one becomes sensitive to any possible leading-twist subtraction constant – see below Eq. (6.41).

The subtraction constant fixed pole correction hypothesis could also, in principle, be tested through measurement of the real part of the spin dependent part of the forward deeply virtual Compton amplitude. While this measurement may seem extremely difficult at the present time one should not forget that Bjorken believed when writing his original Bjorken sum rule paper that the sum rule would never be tested!

Chapter 6

THE AXIAL ANOMALY, GLUON TOPOLOGY AND $g_A^{(0)}$

We have seen in Chapter 3 that the first moment of g_1 projects out the nucleon matrix elements of the axial-vector currents and that, in the singlet channel, there is no gauge-invariant twist-two spin-one local gluonic operator which might contribute to $\int_0^1 dx g_1$. However, the flavour-singlet current $J_{\mu 5}^{GI}$ is sensitive to gluonic degrees of freedom through a QCD effect called the axial anomaly. The anomaly induces both perturbative and non-perturbative QCD effects in $g_A^{(0)}$.

6.1 The axial anomaly

In QCD one has to consider the effects of renormalization. The flavour singlet axial vector current $J_{\mu 5}^{GI}$ in Eq. (4.5) satisfies the anomalous divergence equation [Adler (1969); Bell and Jackiw (1969); Crewther (1979); Shore (1998a)]

$$\partial^\mu J_{\mu 5}^{GI} = 2f\partial^\mu K_\mu + \sum_{i=1}^{f} 2im_i\bar{q}_i\gamma_5 q_i \tag{6.1}$$

where

$$K_\mu = \frac{g^2}{32\pi^2}\epsilon_{\mu\nu\rho\sigma}\left[A_a^\nu\left(\partial^\rho A_a^\sigma - \frac{1}{3}gf_{abc}A_b^\rho A_c^\sigma\right)\right] \tag{6.2}$$

is the gluonic Chern-Simons current and the number of light flavours f is 3. Here A_a^μ is the gluon field and $\partial^\mu K_\mu = \frac{g^2}{32\pi^2}G_{\mu\nu}\tilde{G}^{\mu\nu}$ is the topological charge density. Eq. (6.1) allows us to define a partially conserved current

$$J_{\mu 5}^{GI} = J_{\mu 5}^{\rm con} + 2fK_\mu \tag{6.3}$$

viz. $\partial^\mu J_{\mu 5}^{\rm con} = \sum_{i=1}^{f} 2im_i\bar{q}_i\gamma_5 q_i$.

The anomaly is the physical manifestation of a clash of classical symmetries under renormalization. When one renormalizes the flavour-singlet axial-vector current operator the triangle diagram with one axial-vector current vertex and two vector current vertices is important. One can choose an ultraviolet regularization which preserves current conservation (gauge-invariance) at the gluon vector-current vertices *or* one can preserve the partially conserved axial-vector current relation at

the $\gamma_\mu\gamma_5$ vertex but not both. Gauge invariance must win because it is dynamical and is required for renormalization leading to the anomaly on the right hand side of Eq. (6.1).

When we make a gauge transformation U the gluon field transforms as

$$A_\mu \to UA_\mu U^{-1} + \frac{i}{g}(\partial_\mu U)U^{-1} \tag{6.4}$$

and the operator K_μ transforms as

$$\begin{aligned} K_\mu \to K_\mu &+ i\frac{g}{8\pi^2}\epsilon_{\mu\nu\alpha\beta}\partial^\nu\left(U^\dagger\partial^\alpha U A^\beta\right) \\ &+ \frac{1}{24\pi^2}\epsilon_{\mu\nu\alpha\beta}\left[(U^\dagger\partial^\nu U)(U^\dagger\partial^\alpha U)(U^\dagger\partial^\beta U)\right]. \end{aligned} \tag{6.5}$$

(Partially) conserved currents are not renormalized. It follows that $J^{\rm con}_{\mu5}$ is renormalization scale invariant and the scale dependence of $J^{GI}_{\mu5}$ associated with the factor $E(\alpha_s)$ is carried by K_μ. This is summarized in the equations:

$$\begin{aligned} J^{GI}_{\mu5} &= Z_5\ J^{GI}_{\mu5}\Big|_{\rm bare} \\ K_\mu &= K_\mu|_{\rm bare}\ +\ \frac{1}{2f}(Z_5-1)J_{\mu5}\Big|_{\rm bare} \\ J^{\rm con}_{\mu5} &= J^{\rm con}_{\mu5}\Big|_{\rm bare} \end{aligned} \tag{6.6}$$

where Z_5 denotes the renormalization factor for $J^{GI}_{\mu5}$. Gauge transformations shuffle a scale invariant operator quantity between the two operators $J^{\rm con}_{\mu5}$ and K_μ whilst keeping $J^{GI}_{\mu5}$ invariant.

The nucleon matrix element of $J^{GI}_{\mu5}$ is

$$\langle p,s|J^{GI}_{5\mu}|p',s'\rangle = 2M\left[\tilde{s}_\mu G_A(l^2) + l_\mu l.\tilde{s} G_P(l^2)\right] \tag{6.7}$$

where $l_\mu = (p'-p)_\mu$ and $\tilde{s}_\mu = \overline{u}_{(p,s)}\gamma_\mu\gamma_5 u_{(p',s')}/2M$. The current $J^{GI}_{5\mu}$ does not couple to a massless Goldstone boson – the lightest mass isosinglet 0^- bosons are the η with mass 547.75 MeV and the η' with mass 958 MeV. It follows that $G_A(l^2)$ and $G_P(l^2)$ contain no massless pole terms. The forward matrix element of $J^{GI}_{5\mu}$ is well defined and

$$g^{(0)}_A|_{\rm inv} = E(\alpha_s)G_A(0). \tag{6.8}$$

We would like to isolate the gluonic contribution to $G_A(0)$ associated with K_μ and thus write $g^{(0)}_A$ as the sum of (measurable) "quark" and "gluonic" contributions. Here one has to be careful because of the gauge dependence of the operator K_μ. To understand the gluonic contributions to $g^{(0)}_A$ it is helpful to go back to the deep inelastic cross-section in Chapter 2.

6.2 The anomaly and the first moment of g_1

We specialise to the target rest frame and let E denote the energy of the incident charged lepton which is scattered through an angle θ to emerge in the final state with energy E'. Let $\uparrow\downarrow$ denote the longitudinal polarization of the beam and $\Uparrow\Downarrow$ denote a longitudinally polarized proton target. The spin dependent part of the differential cross-sections is

$$\left(\frac{d^2\sigma\ \uparrow\Downarrow}{d\Omega dE'} - \frac{d^2\sigma\ \uparrow\Uparrow}{d\Omega dE'}\right)$$

$$= \frac{4\alpha^2 E^{'}}{Q^2 EM\nu}\left[(E + E^{'}\cos\theta)\ g_1(x,Q^2) - 2xM\ g_2(x,Q^2)\right] \tag{6.9}$$

$$\tag{6.10}$$

which is obtained from the product of the lepton and hadron tensors

$$\frac{d^2\sigma}{d\Omega dE'} = \frac{\alpha^2}{Q^4}\frac{E'}{E}\ L^A_{\mu\nu}\ W^{\mu\nu}_A. \tag{6.11}$$

Here the lepton tensor

$$L^A_{\mu\nu} = 2i\epsilon_{\mu\nu\alpha\beta}k^\alpha q^\beta \tag{6.12}$$

describes the lepton-photon vertex and the hadronic tensor

$$\frac{1}{M}W^{\mu\nu}_A = i\epsilon^{\mu\nu\rho\sigma}q_\rho\Bigg(s_\sigma\frac{1}{p.q}g_1(x,Q^2) + [p.qs_\sigma - s.qp_\sigma]\frac{1}{M^2 p.q}g_2(x,Q^2)\Bigg) \tag{6.13}$$

describes the photon-nucleon interaction.

Deep inelastic scattering involves the Bjorken limit: $Q^2 = -q^2$ and $p.q = M\nu$ both $\to\infty$ with $x = \frac{Q^2}{2M\nu}$ held fixed. In terms of light-cone coordinates this corresponds to taking $q_- \to \infty$ with $q_+ = -xp_+$ held finite. The leading term in $W^{\mu\nu}_A$ is obtained by taking the Lorentz index of s_σ as $\sigma = +$. (Other terms are suppressed by powers of $\frac{1}{q_-}$.)

If we wish to understand the first moment of g_1 in terms of the matrix elements of anomalous currents ($J^{\rm con}_{\mu 5}$ and K_μ), then we have to understand the forward matrix element of K_+ and its contribution to $G_A(0)$.

Here we are fortunate in that the parton model is formulated in the light-cone gauge ($A_+ = 0$) where the forward matrix elements of K_+ are invariant. In the light-cone gauge the non-abelian three-gluon part of K_+ vanishes. The forward matrix elements of K_+ are then invariant under all residual gauge degrees of freedom. Furthermore, in this gauge, K_+ measures the gluonic "spin" content of the polarized target [Jaffe (1996); Manohar (1990)] – strictly speaking, up to the

non-perturbative surface term we find from integrating the light-cone correlation function, Eq. (3.48). One finds

$$G_A^{(\mathrm{A}_+=0)}(0) = \sum_q \Delta q_{\mathrm{con}} - f\frac{\alpha_s}{2\pi}\Delta g \tag{6.14}$$

where Δq_{con} is measured by the partially conserved current J^{con}_{+5} and $-\frac{\alpha_s}{2\pi}\Delta g$ is measured by K_+. Positive gluon polarization tends to reduce the value of $g_A^{(0)}$ and offers a possible source for OZI violation in $g_A^{(0)}|_{\mathrm{inv}}$. The connection between this more formal derivation and the QCD parton model will be explored in Section 6.5 below. In perturbative QCD Δq_{con} is identified with $\Delta q_{\mathrm{partons}}$ and Δg is identified with $\Delta g_{\mathrm{partons}}$ – see Section 6.5 below and Altarelli and Ross (1988), Carlitz *et al.* (1988), Efremov and Teryaev (1988) and Bass *et al.* (1991).

6.3 Gluon topology and $g_A^{(0)}$

If we were to work only in the light-cone gauge we might think that we have a complete parton model description of the first moment of g_1. However, one is free to work in any gauge including a covariant gauge where the forward matrix elements of K_+ are not necessarily invariant under the residual gauge degrees of freedom [Jaffe and Manohar (1990)]. Understanding the interplay between spin and gauge invariance leads to rich and interesting physics possibilities.

We illustrate this by an example in covariant gauge.

The matrix elements of K_μ need to be specified with respect to a specific gauge. In a covariant gauge we can write

$$\langle p,s|K_\mu|p',s'\rangle = 2M\left[\tilde{s}_\mu K_A(l^2) + l_\mu l.\tilde{s} K_P(l^2)\right] \tag{6.15}$$

where K_P contains a massless Kogut-Susskind pole [Kogut and Susskind (1974)]. This massless pole is an essential ingredient in the solution of the axial U(1) problem [Crewther (1979)] (the absence of any near massless Goldstone boson in the singlet channel associated with spontaneous axial U(1) symmetry breaking) and cancels with a corresponding massless pole term in $(G_P - K_P)$. The Kogut Susskind pole is associated with the (unphysical) massless boson that one expects to couple to $J^{\mathrm{con}}_{\mu 5}$ in the chiral limit and which is not seen in the physical spectrum.

We next define gauge-invariant form-factors $\chi^g(l^2)$ for the topological charge density and $\chi^q(l^2)$ for the quark chiralities in the divergence of $J_{\mu 5}$:

$$\begin{aligned} 2M\ l.\tilde{s}\ \chi^g(l^2) &= \langle p,s|\frac{g^2}{32\pi^2}G_{\mu\nu}\tilde{G}^{\mu\nu}|p',s'\rangle \\ 2M\ l.\tilde{s}\ \chi^q(l^2) &= \langle p,s|\sum_{i=1}^{f} 2im_i\bar{q}_i\gamma_5 q_i|p',s'\rangle. \end{aligned} \tag{6.16}$$

Working in a covariant gauge, we find

$$\chi^g(l^2) = K_A(l^2) + l^2 K_P(l^2) \tag{6.17}$$

by contracting Eq. (6.15) with l^μ. (Also, note the general gauge invariant formula $g_A^{(0)} = \chi^q(0) + f\chi^g(0)$.)

When we make a gauge transformation any change $\delta_{\rm gt}$ in $K_A(0)$ is compensated by a corresponding change in the residue of the Kogut-Susskind pole in K_P, *viz.*

$$\delta_{\rm gt}[K_A(0)] + \lim_{l^2\to 0} \delta_{\rm gt}[l^2 K_P(l^2)] = 0. \tag{6.18}$$

As emphasised above, the Kogut-Susskind pole corresponds to the Goldstone boson associated with spontaneously broken $U_A(1)$ symmetry [Crewther (1979)]. There is no Kogut-Susskind pole in perturbative QCD. It follows that the quantity which is shuffled between the $J^{\rm con}_{+5}$ and K_+ contributions to $g_A^{(0)}$ is strictly non-perturbative; it vanishes in perturbative QCD and is not present in the QCD parton model.

The QCD vacuum is understood to be a Bloch superposition of states characterised by different topological winding number [Callan *et al.* (1976); Jackiw and Rebbi (1976)]

$$|{\rm vac}, \theta\rangle = \sum_n e^{in\theta}\ |n\rangle \tag{6.19}$$

where the QCD θ angle is zero (experimentally less than 10^{-10}) – see e.g. Quinn (2004).

One can show [Jaffe and Manohar (1990)] that the forward matrix elements of K_μ are invariant under "small" gauge transformations (which are topologically deformable to the identity) but not invariant under "large" gauge transformations which change the topological winding number. Perturbative QCD involves only "small" gauge transformations; "large" gauge transformations involve strictly non-perturbative physics. The second term on the right hand side of Eq. (6.5) is a total derivative; its matrix elements vanish in the forward direction. The third term on the right hand side of Eq. (6.5) is associated with the gluon topology [Cronström and Mickelsson (1983)].

The topological winding number is determined by the gluonic boundary conditions at "infinity", *viz.*

$$\int d\sigma_\mu K^\mu = n \tag{6.20}$$

where n is an integer and σ_μ is a large surface with boundary which is spacelike with respect to the positions z_k of any operators or fields in the physical problem [Crewther (1979)]. It is insensitive to local deformations of the gluon field $A_\mu(z)$ or of the gauge transformation $U(z)$. When we take the Fourier transform to momentum space the topological structure induces a light-cone zero-mode which can contribute to g_1 only at $x = 0$. Hence, we are led to consider the possibility that there may be a term in g_1 which is proportional to $\delta(x)$ [Bass (1998)].

It remains an open question whether the net non-perturbative quantity which is shuffled between $K_A(0)$ and $(G_A - K_A)(0)$ under "large" gauge transformations is finite or not. If it is finite and, therefore, physical, then, when we choose $A_+ = 0$,

this non-perturbative quantity must be contained in some combination of the $\Delta q_{\rm con}$ and Δg in Eq. (6.14).

Previously, in Chapters 3 and 5, we found that a $J = 1$ fixed pole in the real part of A_1 in the forward Compton amplitude could also induce a "$\delta(x)$ correction" to the sum rule for the first moment of g_1 through a subtraction at infinity in the dispersion relation (3.19). Both the topological $x = 0$ term and the subtraction constant $\frac{Q^2}{2M^2}\beta_1(Q^2)$ (if finite) give real coefficients of $\frac{1}{x}$ terms in Eq. (3.20). It seems reasonable therefore to conjecture that the physics of gluon topology may induce a $J = 1$ fixed pole correction to the Ellis-Jaffe sum rule. Whether this correction is finite or not is an issue for future experiments.

Instantons provide an example how to generate topological $x = 0$ polarization [Bass (1998)]. Quarks instanton interactions flip chirality, thus connecting left and right handed quarks. To understand this process and its phenomenology, we first need a rigorous definition of the chirality that gets flipped in this process.

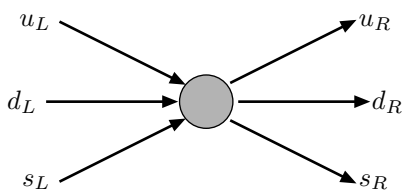

The axial anomaly presents us with three candidate currents we might try to use to define the quark spin content: $J^{GI}_{\mu 5}$, the renormalization scale invariant $E(\alpha_s)J^{GI}_{\mu 5}$ and $J^{\rm con}_{\mu 5}$. One might also consider using the chiralities $\chi^{(q)}$ from Eq. (6.16). We next explain how each current yields gauge invariant possible definitions.

First, note that if we try to define intrinsic spin operators

$$S_k = \int d^3x \ (\overline{q}\gamma_k\gamma_5 q) \qquad k = 1, 2, 3 \tag{6.21}$$

using the axial vector current operators, then we find that the operators constructed using the gauge invariantly renormalized current $J_{\mu 5}$ cannot satisfy the (spin) commutation relations of SU(2) $[S_i, S_j](\mu^2) = i\epsilon_{ijk}S_k(\mu^2)$ at more than one scale μ^2 because of the anomalous dimension and the renormalization group factor associated with $E(\alpha_s)$ and the axial anomaly [Bass and Thomas (1993b)]. The most natural scale to normalize the axial vector current operators to satisfy SU(2) is, perhaps, $\mu \to \infty$ – that is, using the scale invariant current $\{E(\alpha_s)J^{GI}_{\mu 5}\}$. Then we find $[S_i, S_j](\mu^2) = i\epsilon_{ijk}E(\alpha_s)S_k(\mu^2)$ if we use the gauge invariant current renormalized at another scale. One might argue that gluon spin is renormalization scale dependent – see Eq. (6.40) – so not worry too much about this issue but there are further points to consider.

Next choose the $A_0 = 0$ gauge and define two operator charges:

$$X(t) = \int d^3z \; J_{05}^{GI}(z)$$
$$Q_5 = \int d^3z \; J_{05}^{\rm con}(z). \tag{6.22}$$

Because partially conserved currents are not renormalized it follows that Q_5 is a time independent operator. The charge $X(t)$ is manifestly gauge invariant whereas Q_5 is invariant only under "small" gauge transformations; the charge Q_5 transforms as

$$Q_5 \to Q_5 - 2f \; n \tag{6.23}$$

where n is the winding number associated with the gauge transformation U. Although Q_5 is gauge dependent we can define a gauge invariant chirality q_5 for a given operator $\mathcal{O}$ through the gauge-invariant eigenvalues of the equal-time commutator

$$[\; Q_5 \;,\; \mathcal{O} \;]_- = -q_5 \; \mathcal{O}. \tag{6.24}$$

The gauge invariance of q_5 follows since this commutator appears in gauge invariant Ward Identities [Crewther (1979)] despite the gauge dependence of Q_5. The time derivative of spatial components of the gluon field have zero chiralty q_5

$$[\; Q_5 \;,\; \partial_0 A_i \;]_- \;=\; 0 \tag{6.25}$$

but non-zero X charge

$$\lim_{t' \to t} \Big[\; X(t') \;,\; \partial_0 A_i(\vec{x}, t) \; \Big]_- \;=\; \frac{ifg^2}{4\pi^2} \tilde{G}_{0i} \;+\; O(g^4 \ln|t' - t|). \tag{6.26}$$

The analogous situation in QED is discussed in Adler and Boulware (1969), Jackiw and Johnson (1969) and Adler (1970). Eq. (6.25) follows from the non-renormalization of the conserved current $J_{\mu 5}^{\rm con}$. Eq. (6.26) follows from the implicit A_μ dependence of the (anomalous) gauge invariant current $J_{\mu 5}^{GI}$. The higher-order terms $g^4 \ln|t' - t|$ are caused by wavefunction renormalization of $J_{\mu 5}^{GI}$ [Crewther (1979)].

6.4 Instantons and $U_A(1)$ symmetry

To help understand topological $x = 0$ polarization, it is interesting to consider the relation between instanton tunneling processes and the realization of axial U(1) symmetry breaking in QCD.

For integer values of the topological winding number n, the states $|n\rangle$ contain nf quark-antiquark pairs with non-zero Q_5 chirality

$$\sum_l \chi_l = -2\xi_{\rm R} f n \tag{6.27}$$

where f is the number of light-quark flavours. Relative to the $|n=0\rangle$ state, the $|n=+1\rangle$ state carries topological winding number +1 and f quark-antiquark pairs with Q_5 chirality equal to $-2f\xi_{\rm R}$. The factor $\xi_{\rm R}$ is equal to +1 if the $U_A(1)$ symmetry of QCD is associated with $J^{\rm con}_{\mu 5}$ and equal to -1 if the $U_A(1)$ symmetry is associated with $J^{GI}_{\mu 5}$ – see below.

There are two schools of thought [Crewther (1979); 't Hooft (1986)] about how instantons break $U_A(1)$ symmetry. Both of these schools start from 't Hooft's observation ['t Hooft (1976a,b)] that the flavour determinant

$$\langle \det \left[\overline{\rm q}_{\rm L}{}^i {\rm q}_{\rm R}{}^j({\rm z}) \right] \rangle_{\rm inst.} \neq 0 \tag{6.28}$$

in the presence of a vacuum tunneling process between states with different topological winding number. (We denote the tunneling process by the subscript "inst.". It is not specified at this stage whether "inst." denotes an instanton or an anti-instanton.)

Whether instantons spontaneously or explicitly break axial U(1) symmetry depends on the role of zero modes in the quark instanton interaction and how one should include non local structure in the local anomalous Ward identity. Topological $x=0$ polarization is natural in theories of spontaneous axial U(1) symmetry breaking by instantons [Crewther (1979)] where any instanton induced suppression of $g_A^{(0)}|_{\rm pDIS}$ is compensated by a shift of flavour-singlet axial charge from quarks carrying finite momentum to a zero mode ($x=0$). It is not generated by mechanisms ['t Hooft (1986)] of explicit U(1) symmetry breaking by instantons. Experimental evidence for or against a "subtraction at infinity" correction to the Ellis-Jaffe sum rule would provide valuable information about gluon topology and vital clues to the nature of dynamical axial U(1) symmetry breaking in QCD.

(1) **Explicit $U_A(1)$ symmetry breaking**

In this scenario ['t Hooft (1976a,b, 1986)] the $U_A(1)$ symmetry of QCD is associated with the current $J^{GI}_{\mu 5}$ and the topological charge density is treated like a mass term in the divergence of $J^{GI}_{\mu 5}$. The quark chiralities which appear in the flavour determinant (6.28) are associated with $X(t)$ so that the net axial charge $g_A^{(0)}$ is not conserved ($\Delta X \neq 0$) and the net Q_5 chirality is conserved ($\Delta Q_5 = 0$) in quark instanton scattering processes.

In QCD with f light flavoured quarks the (anti-)instanton "vertex" involves a total of $2f$ light quarks and antiquarks. Consider a flavour-singlet combination of f right-handed ($Q_5 = +1$) quarks incident on an anti-instanton. The final state for this process consists of a flavour-singlet combination of f left-handed ($Q_5 = -1$) quarks; $+2f$ units of Q_5 chirality are taken away by an effective "schizon" ['t Hooft (1986)] which carries zero energy and zero momentum. The "schizon" is introduced to ensure Q_5 conservation. Energy and momentum are conserved between the in-state and out-state quarks in the quark-instanton scattering process. The non-conservation of $g_A^{(0)}$ is ensured by a term coupled

to K_μ with equal magnitude and opposite sign to the "schizon" term which also carries zero energy and zero momentum. This gluonic term describes the change in the topological winding number which is induced by the tunneling process. The anti-instanton changes the net $U_A(1)$ chirality by an amount ($\Delta X = -2f$).

(2) **Spontaneous $U_A(1)$ symmetry breaking**
In this scenario the $U_A(1)$ symmetry of QCD is associated with the partially-conserved axial-vector current $J_{\mu 5}^{\rm con}$. Here, the quark chiralities which appear in the flavour determinant (6.28) are identified with Q_5. With this identification, the net axial charge $g_A^{(0)}$ is conserved ($\Delta X = 0$) and the net Q_5 chirality is not conserved ($\Delta Q_5 \neq 0$) in quark instanton scattering processes. This result is the opposite to what happens in the explicit symmetry breaking scenario. When f right-handed quarks scatter on an instanton[1] the final state involves f left-handed quarks. There is no "schizon" and the instanton induces a change in the net Q_5 chirality $\Delta Q_5 = -2f$. The conservation of $g_A^{(0)}$ is ensured by the gluonic term coupled to K_μ which measures the change in the topological winding number and which carries zero energy and zero momentum. The charge Q_5 is time independent for massless quarks (where $J_{\mu 5}^{\rm con}$ is conserved). Since $\Delta Q_5 \neq 0$ in quark instanton scattering processes we find that the $U_A(1)$ symmetry is spontaneously broken by instantons. The Goldstone boson is manifest [Crewther (1979)] as the massless Kogut-Susskind pole which couples to $J_{\mu 5}^{\rm con}$ and K_μ but not to $J_{\mu 5}^{GI}$.

In both the explicit and spontaneous symmetry breaking scenarios we may consider multiple scattering of the incident quark first from an instanton and then from an anti-instanton. Let this process recur a large number of times. When we time-average over a large number of such interactions, then the time averaged expectation value of the chirality Q_5 carried by the incident quark is reduced from the naive value $+1$ that it would take in the absence of vacuum tunneling processes. Indeed, in one flavour QCD the time averaged value of Q_5 tends to zero at large times [Forte and Shuryak (1991)].

In the spontaneous $U_A(1)$ symmetry breaking scenario [Crewther (1979)] any instanton induced suppression of the flavour-singlet axial charge which is measured in polarized deep inelastic scattering is compensated by a net transfer of axial charge or "spin" from partons carrying finite momentum fraction x to the flavour-singlet topological term at $x = 0$. It induces a flavour-singlet $\delta(x)$ term in g_1 which is not present in the explicit $U_A(1)$ symmetry breaking scenario.

The net topological term is gauge invariant. In the $A_0 = 0$ gauge the $x = 0$ polarisation is "gluonic" and is measured by $\int d^3z K_0$. In the light-cone gauge this polarisation may be re-distributed between the "quark" and "gluonic" terms measured by $J_{+5}^{\rm con}$ and K_+ respectively.

[1] cf. an anti-instanton in the explicit $U_A(1)$ symmetry breaking scenario.

One argument for the spontaneous symmetry breaking scenario comes from looking at renormalization scale dependence if we seek to extend this discussion to higher-orders in the QCD coupling α_s. For the instanton tunneling process

$$\Delta X = \Delta Q_5 + 2fn \tag{6.29}$$

where n is the winding number associated with the instanton, the winding number is an integer and is therefore renormalization scale independent. The term ΔQ_5 is renormalization scale invariant because it corresponds to the partially conserved axial-current. On the other hand, the X charge is associated with the multiplicatively renormalized gauge-invariant axial-current and carries the 2-loop anomalous dimension associated with $E(\alpha_s)$. It is scale dependent. One cannot equate a scale dependent quantity to a scale invariant one.

This formalism generalizes readily to the definition of baryon number in the presence of electroweak gauge fields. The vector baryon number current is sensitive to the axial anomaly through the parity violating electroweak interactions. If one requires that baryon number is renormalization group invariant and that the time derivative of the spatial components of the W boson field have zero baryon number, then one is led to using the conserved vector current analogy of q_5 to define the baryon number. Sphaleron induced electroweak baryogenesis in the early Universe [Rubakov and Shaposhnikov (1996); Kuzmin *et al.* (1985)] is then accompanied by the formation of a "topological condensate" [Bass (2004)] which (probably) survives in the Universe we live in today.

Lastly, we comment on the use of the chiralities χ^q and the quantity χ^g to define the "quark spin" and "gluon spin" content of the proton. This suggestion starts from the decomposition

$$g_A^{(0)} = \chi^q(0) + 3\chi^g(0) \tag{6.30}$$

but is less optimal because the separate "quark" and "gluonic" pieces is very much infra-red sensitive and strongly dependent of the ratios of the light quark masses m_u/m_d [Cheng and Li (1989); Veneziano (1989)] – see also Gross *et al.* (1979) and Ioffe (1979). Indeed, for the polarized real photon structure function g_1^γ the quantity $\chi^g_{\texttt{photon}} \sim 30$ at realistic deep inelastic values of Q^2 [Bass (1992)] !

6.5 Photon gluon fusion

We next consider the role of the axial anomaly in the QCD parton model and its relation to semi-inclusive measurements of jets and high k_t hadrons in polarized deep inelastic scattering.

Consider the polarized photon-gluon fusion process $\gamma^* g \to q\bar{q}$. We evaluate the g_1 spin structure function for this process as a function of the transverse momentum squared of the struck quark, k_t^2, with respect to the photon-gluon direction. We use q and p to denote the photon and gluon momenta and use the cut-off $k_t^2 \geq \lambda^2$

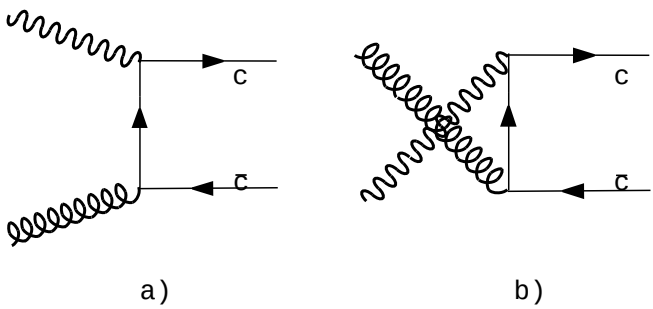

Fig. 6.1 Feynman diagrams for charm production via photon-gluon fusion.

to separate the total phase space into "hard" ($k_t^2 \geq \lambda^2$) and "soft" ($k_t^2 < \lambda^2$) contributions. One finds

$$g_1^{(\gamma^* g)}|_{\rm hard} = -\frac{\alpha_s}{2\pi}\frac{\sqrt{1-\frac{4(m^2+\lambda^2)}{s}}}{1-\frac{4x^2P^2}{Q^2}}\Bigg[(2x-1)(1-\frac{2xP^2}{Q^2}) \Bigg\{1-\frac{1}{\sqrt{1-\frac{4(m^2+\lambda^2)}{s}}\sqrt{1-\frac{4x^2P^2}{Q^2}}}\ln\Bigg(\frac{1+\sqrt{1-\frac{4x^2P^2}{Q^2}}\sqrt{1-\frac{4(m^2+\lambda^2)}{s}}}{1-\sqrt{1-\frac{4x^2P^2}{Q^2}}\sqrt{1-\frac{4(m^2+\lambda^2)}{s}}}\Bigg)\Bigg\} +(x-1+\frac{xP^2}{Q^2})\frac{\Big(2m^2(1-\frac{4x^2P^2}{Q^2})-P^2x(2x-1)(1-\frac{2xP^2}{Q^2})\Big)}{(m^2+\lambda^2)(1-\frac{4x^2P^2}{Q^2})-P^2x(x-1+\frac{xP^2}{Q^2})}\Bigg] \tag{6.31}$$

for each flavour of quark liberated into the final state [Bass *et al.* (1998)]. Here m is the quark mass, $Q^2 = -q^2$ is the virtuality of the hard photon, $P^2 = -p^2$ is the virtuality of the gluon target, x is the Bjorken variable ($x = \frac{Q^2}{2p.q}$) and s is the centre of mass energy squared, $s = (p+q)^2 = Q^2\big(\frac{1-x}{x}\big) - P^2$, for the photon-gluon collision.

When $Q^2 \to \infty$ the expression for $g_1^{(\gamma^* g)}|_{\rm hard}$ simplifies to the leading twist (=2) contribution:

$$g_1^{(\gamma^* g)}|_{\rm hard} = \frac{\alpha_s}{2\pi}\Bigg[(2x-1)\Bigg\{\ln\frac{1-x}{x} - 1 + \ln\frac{Q^2}{x(1-x)P^2+(m^2+\lambda^2)}\Bigg\} +(1-x)\frac{2m^2-P^2x(2x-1)}{m^2+\lambda^2-P^2x(x-1)}\Bigg] \tag{6.32}$$

Here we take λ to be independent of x. Note that for finite quark masses, phase space limits Bjorken x to $x_{max} = Q^2/(Q^2+P^2+4(m^2+\lambda^2))$ and protects $g_1^{(\gamma^* g)}|_{\rm hard}$

from reaching the $\ln(1-x)$ singularity in Eq. (6.32). For this photon-gluon fusion process, the first moment of the "hard" contribution is:

$$\int_0^1 dx\; g_1^{(\gamma^* g)}|_{\rm hard}$$
$$= -\frac{\alpha_s}{2\pi}\left[1+\frac{2m^2}{P^2}\frac{1}{\sqrt{1+\frac{4(m^2+\lambda^2)}{P^2}}}\ln\left(\frac{\sqrt{1+\frac{4(m^2+\lambda^2)}{P^2}}-1}{\sqrt{1+\frac{4(m^2+\lambda^2)}{P^2}}+1}\right)\right]. \tag{6.33}$$

The "soft" contribution to the first moment of g_1 is then obtained by subtracting Eq. (6.33) from the inclusive first moment (obtained by setting $\lambda = 0$), *viz.*

$$g_1^{(\gamma^* g)}|_{\rm soft} = g_1^{(\gamma^* g)}|_{\rm full} - g_1^{(\gamma^* g)}|_{\rm hard} \tag{6.34}$$

For fixed gluon virtuality P^2 the photon-gluon fusion process induces two distinct contributions to the first moment of g_1. Consider the leading twist contribution, Eq. (6.33). The first term, $-\frac{\alpha_s}{2\pi}$, in Eq. (6.33) is mass-independent and comes from the region of phase space where the struck quark carries large transverse momentum squared $k_t^2 \sim Q^2$. It measures a contact photon-gluon interaction and is associated with the axial anomaly though the K_+ Chern-Simons current contribution to $J_{\mu 5}^{GI}$ [Carlitz *et al.* (1988); Bass *et al.* (1991)]. The second mass-dependent term comes from the region of phase-space where the struck quark carries transverse momentum $k_t^2 \sim m^2, P^2$. This positive mass dependent term is proportional to the mass squared of the struck quark. The mass-dependent in Eq. (6.33) can safely be neglected for light-quark flavor (up and down) production. It is very important for strangeness and charm production [Bass *et al.* (1999)]. For vanishing cut-off ($\lambda^2 = 0$) this term vanishes in the limit $m^2 \ll P^2$ and tends to $+\frac{\alpha_s}{2\pi}$ when $m^2 \gg P^2$ (so that the first moment of $g_1^{(\gamma^* g)}$ vanishes in this limit). The vanishing of $\int_0^1 dx g_1^{(\gamma^* g)}$ in the limit $m^2 \ll P^2$ to leading order in $\alpha_s(Q^2)$ follows from an application [Bass *et al.* (1998)] of the fundamental GDH sum-rule.

The cut-off λ^2 in Eqs. (6.31) and (6.32) may, in general, be a function of x:

$$\lambda^2 = \lambda_0^2 f_0(x) + P^2 f_1(x) + m^2 f_2(x). \tag{6.35}$$

Examples include the virtuality of the struck quark

$$m^2 - k^2 = P^2 x + \frac{k_t^2 + m^2}{(1-x)} > \lambda_0^2 = \text{constant}(x) \tag{6.36}$$

or the invariant mass squared of the quark-antiquark pair produced in the photon-gluon collision

$$\mathcal{M}_{q\overline{q}}^2 = \frac{k_t^2 + m^2}{x(1-x)} + P^2 = (m^2 - k^2)/x \geq \lambda_0^2 = \text{constant}(x). \tag{6.37}$$

These different choices of infrared cut-offs correspond to different jet definitions and different factorization schemes for photon-gluon fusion in the QCD parton model – see Bass *et al.* (1991, 1998); Mankiewicz (1991) and Manohar (1991).

If we evaluate the first moment of $g_1^{(\gamma^* g)}$ using the cut-off on the quarks' virtuality, then we find "half of the anomaly" in the gluon coefficient through the mixing of transverse and longitudinal momentum components. The anomaly coefficient for the first moment is recovered with the invariant mass squared cut-off through a sensitive cancellation of large and small x contributions [Bass *et al.* (1991)]. If we set λ^2 to zero, including the maximum phase space, then we obtain the full box graph contribution to $g_1^{(\gamma^* g)}$. If we take λ^2 to be finite and independent of x, then the crossing symmetry of $g_1^{(\gamma^* g)}$ under the exchange of $(p \leftrightarrow q)$ is realised separately in each of the "hard" and "soft" parts of $g_1^{(\gamma^* g)}$ which corresponds to phase space with $(k_T^2 > \lambda^2)$ and $(k_T^2 < \lambda^2)$ respectively. Substituting Eqs. (6.36) and (6.37) into Eq. (6.31) we find that the "hard" and "soft" contributions to $g_1^{(\gamma^* g)}$ do not separately satisfy the $(p \leftrightarrow q)$ symmetry of $g_1^{(\gamma^* g)}(x, Q^2)$ if use an x dependent cut-off to define the "hard" part of the total phase space. The reason for this is that the transverse momentum is defined perpendicular to the plane spanned by p_μ and q_μ in momentum space. The x dependent cut-offs mix the transverse and longitudinal components of momentum. They induce a violation of crossing symmetry in $g_1^{(\gamma^* g)}|_{\rm hard}(x, Q^2)$ under $(p \leftrightarrow q)$. Among the possible kinematic cut-offs, the x independent cut-off on the transverse momentum squared preserves the crossing symmetry of $g_1^{(\gamma^* g)}$ under $(p \leftrightarrow q)$ in both the hard gluonic coefficient $C^g = g_1^{(\gamma^* g)}|_{\rm hard}(x, Q^2)$ and the soft polarized quark distribution of the gluon $\Delta q^{(g)} = g_1^{(\gamma^* g)}|_{\rm soft}(x, Q^2)$.

We noted above that when one applies the operator product expansion the first term in Eq. (6.33) corresponds to the gluon matrix element of the anomalous gluonic current K_+. This operator product expansion analysis can be generalized to the higher moments of $g_1^{(\gamma^* g)}$. The anomalous contribution to the higher moments is controlled by choosing the correct prescription for γ_5. One finds that the axial anomaly contribution to the *shape* of g_1 at finite x is given by the convolution of the polarized gluon distribution $\Delta g(x, Q^2)$ with the hard coefficient

$$\tilde{C}^{(g)}|_{\rm anom} = -\frac{\alpha_s}{\pi}(1 - x) \tag{6.38}$$

[Bass (1992a); Cheng (1996)]. This anomaly contribution is a small x effect in g_1; it is essentially negligible for x less than 0.05. The hard coefficient $\tilde{C}^{(g)}|_{\rm anom}$ is normally included as a term in the gluonic Wilson coefficent C^g – see Chapter 10. It is associated with two-quark jet events carrying $k_t^2 \sim Q^2$ in the final state.

Eq. (6.33) leads to the well known formula quoted in Chapter 1

$$g_A^{(0)} = \left(\sum_q \Delta q - 3\frac{\alpha_s}{2\pi}\Delta g \right)_{\rm partons} + \mathcal{C}_\infty. \tag{6.39}$$

Here Δg is the amount of spin carried by polarized gluon partons in the polarized proton and $\Delta q_{\rm partons}$ measures the spin carried by quarks and antiquarks carrying "soft" transverse momentum $k_t^2 \sim m^2, P^2$. Note that the mass independent contact

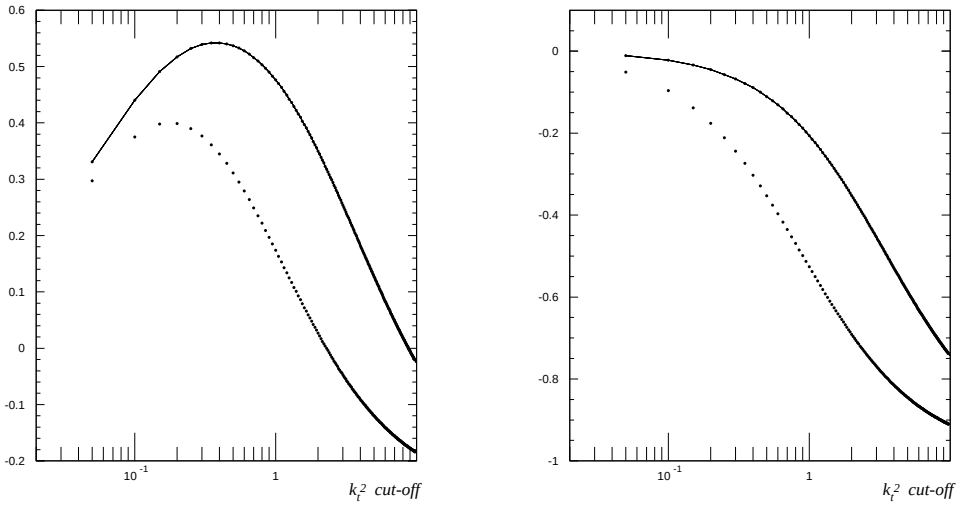

Fig. 6.2 $\int_0^1 dx\ g_1^{(\gamma^* g)}|_{\rm soft}$ for polarized strangeness production (left) and light-flavor (u or d) production (right) with $k_t^2 < \lambda^2$ in units of $\frac{\alpha_s}{2\pi}$ [Bass (2003a)]. Here $Q^2 = 2.5$ GeV^2 (dotted line) and 10 GeV^2 (solid line).

interaction in Eq. (6.33) is flavour independent. The mass dependent term associated with low k_t breaks flavour SU(3) in the perturbative sea. The third term $\mathcal{C}_\infty = \frac{1}{2}\lim_{Q^2\to\infty}\frac{Q^2}{2M^2}\beta_1(Q^2)$ describes any fixed pole "subtraction at infinity" correction to $g_A^{(0)}$.

Equations (6.6) yield the renormalization group equation

$$\left\{\frac{\alpha_s}{2\pi}\Delta g\right\}_{Q^2} = \left\{\frac{\alpha_s}{2\pi}\Delta g\right\}_{\infty} + \frac{1}{3}\left\{1/E(\alpha_s) - 1\right\} g_A^{(0)}\Big|_{\rm inv}. \tag{6.40}$$

It follows that the polarized gluon term satisfies

$$\alpha_s \Delta g \sim \texttt{constant}, \quad Q^2 \to \infty. \tag{6.41}$$

This key result, first noted in the context of the QCD parton model by Altarelli and Ross (1988) and Efremov and Teryaev (1988) means that the polarized gluon contribution makes a scaling contribution to the first moment of g_1 at next-to-leading order. (In higher orders the Q^2 evolution of Δg depends on the value of $g_A^{(0)}|_{\rm inv}$ suggesting one, in principle, method to search for any finite $\mathcal{C}_\infty$.) The growth in the gluon polarization $\Delta g \sim 1/\alpha_s$ at large Q^2 is compensated by growth with opposite sign in the gluon orbital angular momentum.

The transverse momentum dependence of the gluonic and sea quark partonic contributions to $g_A^{(0)}$ suggests the interpretation of measurements of quark sea polarization will depend on the large k_t acceptance of the apparatus. Let $g_1^{(\gamma^* g)}|_{\rm soft}(\lambda)$

denote the contribution to $g_1^{(\gamma^* g)}$ for photon-gluon fusion where the hard photon scatters on the struck quark or antiquark carrying transverse momentum $k_t^2 < \lambda^2$. Fig. 6.2 shows the first moment of $g_1^{(\gamma^* g)}|_{\rm soft}$ for the strange and light (up and down) flavour production respectively as a function of the transverse momentum cut-off λ^2. Here we set $Q^2 = 2.5$ GeV^2 (corresponding to the HERMES experiment) and 10 GeV^2 (COMPASS and SMC). Following Carlitz *et al.* (1988), we take $P^2 \sim \Lambda^2_{\rm qcd}$ and set $P^2 = 0.1$ GeV^2. Observe the small value for the light-quark sea polarization at low transverse momentum and the positive value for the integrated strange sea polarization at low k_t^2: $k_t < 1.5$ GeV at the HERMES $Q^2 = 2.5$ GeV^2.

This page intentionally left blank

Chapter 7

CHIRAL SYMMETRY AND AXIAL U(1) DYNAMICS

The physics of the flavour-singlet axial-vector current which is central to the proton spin problem also plays a vital role in the physics of the η and η' mesons. Naively, one expects a nonet of would-be pseudoscalar Goldstone bosons associated with spontaneously broken chiral symmetry. The light-mass pion and kaon fit well in this picture but the isosinglet η and η' states are too heavy to fit. This is the famous $U_A(1)$ problem: the masses of the η and η' mesons are much greater than the values they would have if these mesons were pure Goldstone bosons associated with spontaneously broken chiral symmetry [Weinberg (1975)]. This extra mass is induced by non-perturbative gluon dynamics and the axial anomaly in the singlet axial-vector current ['t Hooft (1976a,b); Crewther (1979); Veneziano (1979); Witten (1979)]. The flavour-singlet generalization of the Goldberger-Treiman relation relates the flavour-singlet axial-charge $g_A^{(0)}$ to the η'-nucleon coupling constant $g_{\eta' NN}$ – thus connecting the proton spin structure with the role of gluonic degrees of freedom in dynamical axial U(1) symmetry breaking.

7.1 Chiral symmetry and the spin structure of the proton

The isovector Goldberger-Treiman relation [Adler and Dashen (1968)]

$$2Mg_A^{(3)} \simeq f_\pi g_{\pi NN} \tag{7.1}$$

relates $g_A^{(3)}$ and therefore $(\Delta u - \Delta d)$ to the product of the pion decay constant f_π and the pion-nucleon coupling constant $g_{\pi NN}$. This result is non-trivial. It means that the spin structure of the nucleon measured in high-energy, high Q^2 polarized deep inelastic scattering is intimately related to spontaneous chiral symmetry breaking and low-energy pion physics. The Bjorken sum rule can also be written

$$\int_0^1 dx(g_1^p - g_1^n) = \frac{1}{6}\{f_\pi g_{\pi NN}/2M\}\Big\{1 + \sum_{\ell \geq 1} c_{\mathrm{NS}\ell}\, \alpha_s^\ell(Q)\Big\} \tag{7.2}$$

(modulo small chiral corrections $\sim$ 5% coming the finite light quark and pion masses).

7.2 QCD considerations

In classical field theory Noether's theorem tells us that there is a conserved current associated with each global symmetry of the Lagrangian. The QCD Lagrangian

$$\mathcal{L}_{QCD} = \sum_q \bar{q}_L \left(i\hat{D} - g\hat{A} \right) q_L + \bar{q}_R \left(i\hat{D} - g\hat{A} \right) q_R - \sum_q m_q \left(\bar{q}_L q_R + \bar{q}_R q_L \right) - \frac{1}{2} G_{\mu\nu} G^{\mu\nu} \tag{7.3}$$

exhibits chiral symmetry for massless quarks: when the quark mass term is turned off the left- and right-handed quark fields do not couple in the Lagrangian and transform independently under chiral rotations.

Chiral $SU(2)_L \otimes SU(2)_R$

$$\begin{pmatrix} u_L \\ d_L \end{pmatrix} \mapsto e^{i\frac{1}{2}\vec{\alpha}.\vec{\tau}\gamma_5} \begin{pmatrix} u_L \\ d_L \end{pmatrix} \quad , \quad \begin{pmatrix} u_R \\ d_R \end{pmatrix} \mapsto e^{i\frac{1}{2}\vec{\beta}.\vec{\tau}\gamma_5} \begin{pmatrix} u_R \\ d_R \end{pmatrix} \tag{7.4}$$

is associated with the isotriplet axial-vector current $J^{(3)}_{\mu 5}$

$$J^{(3)}_{\mu 5} = \left[\bar{u}\gamma_\mu\gamma_5 u - \bar{d}\gamma_\mu\gamma_5 d \right] \tag{7.5}$$

which is partially conserved

$$\partial^\mu J^{(3)}_{\mu 5} = 2m_u \bar{u} i\gamma_5 u - 2m_d \bar{d} i\gamma_5 d \tag{7.6}$$

The absence of parity doublets in the hadron spectrum tells us that the near-chiral symmetry for light u and d quarks is spontaneously broken.

The light-mass pion is identified as the corresponding Goldstone boson and the current $J^{(3)}_{\mu 5}$ is associated with the pion through PCAC (the partially conserved axial current) [Adler and Dashen (1968)]

$$\langle \text{vac} | J^{(3)}_{\mu 5}(z) | \pi(q) \rangle = -i f_\pi q_\mu e^{-iq.z} \tag{7.7}$$

Taking the divergence equation

$$\langle \text{vac} | \partial^\mu J^{(3)}_{\mu 5}(z) | \pi(q) \rangle = -f_\pi m_\pi^2 e^{-iq.z} \tag{7.8}$$

the pion mass-squared vanishes in the chiral limit as $m_\pi^2 \sim m_q$. This is the starting point for chiral perturbation theory.

The Goldberger-Treiman relation is derived as follows. First, the nucleon matrix element of $J^{(3)}_{\mu 5}$ is

$$\langle p, s | J^{(3)}_{\mu 5} | p', s' \rangle = 2M \left[\tilde{s}_\mu G_A(l^2) + l_\mu l.\tilde{s} G_P(l^2) \right] \tag{7.9}$$

where $l_\mu = (p' - p)_\mu$ and $\tilde{s}_\mu = \overline{u}_{(p,s)} \gamma_\mu \gamma_5 u_{(p',s')} / 2M$. Since the pion has a small mass, $J^{(3)}_{\mu 5}$ does not couple to a massless boson and $G_A(l^2)$ and $G_P(l^2)$ contain no massless pole terms. The forward matrix element of $J^{(3)}_{\mu 5}$ is well-defined and

$$g_A^{(3)} = G_A(0). \tag{7.10}$$

We take the divergence of $J^{(3)}_{\mu 5}$, contract the formula (7.9) with l^μ and define the form-factor $\chi^{(3)}(l^2)$

$$2M\ l.\tilde{s}\ \chi^{(3)}(l^2) = \langle p,s|2im_u\bar{u}_i\gamma_5 u_i - 2im_d\bar{d}_i\gamma_5 d|p',s'\rangle. \tag{7.11}$$

Thus

$$\chi^{(3)}(l^2) = G_A(l^2) + l^2 G_P(l^2). \tag{7.12}$$

The form-factor $\chi^{(3)}(l^2)$ is analytic in the l^2 plane, apart from a cut along the real axis from $9m_\pi^2$ to ∞ and the pion pole at $l^2 = m_\pi^2$. If we assume an unsubtracted dispersion relation in l^2, we can write

$$\chi^{(3)}(l^2) = \frac{f_\pi g_{\pi NN}}{m_\pi^2 - l^2} + \frac{1}{\pi}\int_{9m_\pi^2}^{\infty} d(m^2)\frac{\rho(m^2)}{m^2 - l^2} \tag{7.13}$$

If we suppose that $\chi^{(3)}(l^2)$ is dominated by the pion pole term in the dispersion integral (this is plausible because the beginning of the cut is nine times as far from $l^2 = 0$ as is the pion pole), we get

$$2Mg_A^{(3)} \simeq f_\pi g_{\pi NN} \tag{7.14}$$

which is the Goldberger-Treiman relation.

Isoscalar extensions of the Goldberger-Treiman relation are quite subtle because of the axial U(1) problem whereby gluonic degrees of freedom mix with the flavour-singlet Goldstone state to increase the masses of the η and η' mesons. Spontaneous chiral symmetry breaking is associated with a non-vanishing chiral condensate

$$\langle\ \text{vac}\ |\ \bar{q}q\ |\ \text{vac}\ \rangle < 0. \tag{7.15}$$

where $q = u, d, s$. One expects a nonet of would-be Goldstone bosons: the physical pions and kaons plus also octet and singlet states. The non-vanishing chiral condensate also spontaneously breaks the axial U(1) symmetry so, naively, in the two-flavour theory one expects an isosinglet pseudoscalar degenerate with the pion. The lightest mass isosinglet is the η meson, which has a mass of 547.75 MeV. In the singlet channel the axial anomaly and non-perturbative gluon topology induce a substantial gluonic mass term for the singlet boson.

The puzzle deepens when one considers SU(3). Spontaneous chiral symmetry breaking suggests an octet of would-be Goldstone bosons: the octet associated with chiral $SU(3)_L \otimes SU(3)_R$ plus a singlet boson associated with axial U(1) – each with mass squared $m^2_{\text{Goldstone}} \sim m_q$. The physical η and η' masses are about 300-400 MeV too big to fit in this picture. One needs extra mass in the singlet channel associated with non-perturbative topological gluon configurations and the QCD axial anomaly. The strange quark mass induces considerable η-η' mixing. For free mesons the η-η' mass matrix (at leading order in the chiral expansion) is

$$M^2 = \begin{pmatrix} \frac{4}{3}m_{\text{K}}^2 - \frac{1}{3}m_\pi^2 & -\frac{2}{3}\sqrt{2}(m_{\text{K}}^2 - m_\pi^2) \\ -\frac{2}{3}\sqrt{2}(m_{\text{K}}^2 - m_\pi^2) & [\frac{2}{3}m_{\text{K}}^2 + \frac{1}{3}m_\pi^2 + \tilde{m}_{\eta_0}^2] \end{pmatrix}. \tag{7.16}$$

Here $\tilde{m}^2_{\eta_0}$ is the gluonic mass term which has a rigorous interpretation through the Witten-Veneziano mass formula [Witten (1979); Veneziano (1979); Di Vecchia and Veneziano (1980)] and which is associated with non-perturbative gluon topology, related perhaps to confinement [Kogut and Susskind (1974)] or instantons ['t Hooft (1976a,b)]. The Witten-Veneziano mass formula relates the gluonic mass term for the singlet boson to the topological susceptibility of pure Yang-Mills (glue with no quarks)

$$\tilde{m}^2_{\eta_0} = -\frac{6}{f^2_\pi}\chi(0) \tag{7.17}$$

where $\chi(k^2) = \int d^4z\ i\ e^{ik.z}\ \langle \mathrm{vac}|\ T\ Q(z)Q(0)\ |\mathrm{vac}\rangle\big|_{\mathrm{YM}}$ and $Q(z)$ denotes the topological charge density. Without this singlet gluonic mass term the η meson would be approximately degenerate with the pion and the η' meson would have a mass $\sim \sqrt{2m^2_K - m^2_\pi}$ after we take into account mixing between the octet and singlet bosons induced by the strange quark mass. The masses of the physical η and η' mesons are found by diagonalizing this matrix, *viz.*

$$\begin{aligned} |\eta\rangle &= \cos\theta\ |\eta_8\rangle - \sin\theta\ |\eta_0\rangle \\ |\eta'\rangle &= \sin\theta\ |\eta_8\rangle + \cos\theta\ |\eta_0\rangle \end{aligned} \tag{7.18}$$

where

$$\eta_0 = \frac{1}{\sqrt{3}}\ (u\bar{u} + d\bar{d} + s\bar{s}), \quad \eta_8 = \frac{1}{\sqrt{6}}\ (u\bar{u} + d\bar{d} - 2s\bar{s}). \tag{7.19}$$

One obtains values for the η and η' masses:

$$\begin{aligned} m^2_{\eta',\eta}\ &= (m^2_{\mathrm{K}} + \tilde{m}^2_{\eta_0}/2) \\ &\quad \pm\frac{1}{2}\sqrt{(2m^2_{\mathrm{K}} - 2m^2_\pi - \frac{1}{3}\tilde{m}^2_{\eta_0})^2 + \frac{8}{9}\tilde{m}^4_{\eta_0}}. \end{aligned} \tag{7.20}$$

The physical mass of the η and the octet mass $m_{\eta_8} = \sqrt{\frac{4}{3}m^2_{\mathrm{K}} - \frac{1}{3}m^2_\pi}$ are numerically close, within a few percent. However, to build a theory of the η on the octet approximation risks losing essential physics associated with the singlet component. Turning off the gluonic term, one finds the expressions $m_{\eta'} \sim \sqrt{2m^2_{\mathrm{K}} - m^2_\pi}$ and $m_\eta \sim m_\pi$. That is, without extra input from glue, in the OZI limit, the η would be approximately an isosinglet light-quark state ($\frac{1}{\sqrt{2}}|\bar{u}u + \bar{d}d\rangle$) degenerate with the pion and the η' would be a strange-quark state $|\bar{s}s\rangle$ – mirroring the isoscalar vector ω and ϕ mesons.

Taking the value $\tilde{m}^2_{\eta_0} = 0.73\ \mathrm{GeV}^2$ in the leading-order mass formula, Eq. (7.20), gives agreement with the physical masses at the 10% level. This value is obtained by summing over the two eigenvalues in Eq. (7.20): $m^2_\eta + m^2_{\eta'} = 2m^2_K + \tilde{m}^2_{\eta_0}$ and substituting the physical values of m_η, $m_{\eta'}$ and m_K. The corresponding $\eta - \eta'$ mixing angle $\theta \simeq -18^\circ$ is within the range -17° to -20° obtained from a study of

various decay processes in Gilman and Kauffman (1987) and Ball *et al.* (1996).[1] The key point of Eqs. (7.16)-(7.20) is that mixing and gluon dynamics play a crucial role in both the η and η' masses and that treating the η as an octet pure would-be Goldstone boson risks losing essential physics.

The flavour-singlet generalization of the Goldberger-Treiman was derived independently by Shore and Veneziano (1990, 1992) and Hatsuda (1990). In the chiral limit the flavour-singlet Goldberger-Treiman relation reads

$$2Mg_A^{(0)} = \sqrt{\chi'(0)}\; g_{\phi_0 NN}. \tag{7.21}$$

Here $\chi'(0)$ is the first derivative of the topological susceptibility and $g_{\phi_0 NN}$ denotes the one particle irreducible coupling to the nucleon of the flavour-singlet Goldstone boson which would exist in a gedanken world where OZI is exact in the singlet axial U(1) channel. The ϕ_0 is a theoretical object and not a physical state in the spectrum. The important features of Eq. (7.21) are first that $g_A^{(0)}$ factorizes into the product of the target dependent coupling $g_{\phi_0 NN}$ and the target independent gluonic term $\sqrt{\chi'(0)}$. The coupling $g_{\phi_0 NN}$ is renormalization scale invariant and the scale dependence of $g_A^{(0)}$ associated with the renormalization group factor $E(\alpha_s)$ is carried by the gluonic term $\sqrt{\chi'(0)}$. Motivated by this observation, Narison *et al.* (1995) conjectured that any OZI violation in $g_A^{(0)}|_{\rm inv}$ might be carried by the target independent factor $\sqrt{\chi'(0)}$ and suggested experiments to test this hypothesis by studying semi-inclusive polarized deep inelastic scattering in the target fragmentation region (which allows one to vary the de facto hadron target – e.g. a proton or Δ resonance) [Shore and Veneziano (1998)]. The flavour-singlet Goldberger-Treiman relation can also be expressed in terms of the physical η'–nucleon coupling constant $g_{\eta' NN}$. Working in the chiral limit it becomes

$$Mg_A^{(0)} = \sqrt{\frac{3}{2}} F_0 \Big(g_{\eta' NN} - g_{QNN} \Big) \tag{7.22}$$

where is an OZI violating coupling which measures the one particle irreducible coupling of the topological charge density $Q = \frac{\alpha_s}{4\pi} G\tilde{G}$ to the nucleon. Here F_0 ($\sim$ 0.1 GeV) renormalizes the flavour-singlet decay constant. The η'-nucleon coupling constant $g_{\eta' NN}$ and F_0 are renormalization scale independent so that the scale dependence of $g_A^{(0)}$ is carried just by g_{QNN} in this equation. The coupling constant g_{QNN} is, in part, related [Veneziano (1989); Shore and Veneziano (1992)] to the polarized gluon term $-3\frac{\alpha_s}{2\pi}\Delta g$ in the parton model decomposition of $g_A^{(0)}$. The OZI prediction $g_A^{(0)} \simeq 0.6$ would follow if polarized strange quarks and gluons were not important in the nucleon's internal spin structure. *If* we attribute the difference between $g_A^{(0)}|_{\rm pDIS}$ and the OZI value 0.6 to the gluonic correction $-\sqrt{\frac{3}{2}} F_0 g_{QNN}$ in Eq. (7.22), *then* we find $g_{QNN} \sim 2.45$ and $g_{\eta' NN} \sim 4.9$ with $F_0 \sim 0.1$ GeV. Note

[1] Closer agreement with the physical masses can be obtained by introducing the singlet decay constant $F_0 \neq F_\pi$ and including higher-order mass terms in the chiral expansion [Leutwyler (1998); Feldman (2000)].

that the two versions of the singlet Goldberger-Treiman relation in Eqs. (7.21) and (7.22) are quoted modulo any possible subtraction constant corrections in the corresponding dispersion relation. Experimentally, the value of $g_{\eta' NN}$ is not well determined with values quoted in the range $3.4 < g_{\eta' NN} < 7.3$ [Cheng (1996)].

Independent of the detailed QCD dynamics one can construct low-energy effective chiral Lagrangians which include the effect of the anomaly and axial U(1) symmetry, and use these Lagrangians to study low-energy processes involving the η and η'.

OZI violation associated with the gluonic topological charge density may also be important to a host of η and η' interactions in hadronic physics. We refer to Bass (2002b) for an overview of the phenomenology. Experiments underway at COSY-Jülich are measuring the isospin dependence of η and η' production close to threshold in proton-nucleon collisions [Moskal (2004)]. These experiments are looking for signatures of possible OZI violation in the η' nucleon interaction. Anomalous glue may play a key role in the structure of the light mass (about 1400-1600 MeV) exotic mesons with quantum numbers $J^{PC} = 1^{-+}$ that have been observed in experiments at BNL and CERN. These states might be dynamically generated resonances in $\eta\pi$ and $\eta'\pi$ rescattering [Bass and Marco (2002); Szczepaniak *et al.* (2003)] mediated by the OZI violating coupling of the η'. Planned experiments at the GSI in Darmstadt will measure the η mass in nuclei [Hayano *et al.* (1999)] and thus probe aspects of axial U(1) dynamics in the nuclear medium.

7.3 The low-energy effective Lagrangian

The physics of axial U(1) degrees of freedom is described by the U(1)-extended low-energy effective Lagrangian [Di Vecchia and Veneziano (1980); Witten (1980); Rozenzweig *et al.* (1980); Nath and Arnowitt (1981)]. In its simplest form this reads

$$\mathcal{L}_{\rm m} = \frac{F_\pi^2}{4}{\rm Tr}(\partial^\mu U \partial_\mu U^\dagger) + \frac{F_\pi^2}{4}{\rm Tr}\mathcal{M}\left(U + U^\dagger\right) + \frac{1}{2}iQ{\rm Tr}\left[\log U - \log U^\dagger\right] + \frac{3}{\tilde{m}_{\eta_0}^2 F_0^2}Q^2. \tag{7.23}$$

Here U is the unitary meson matrix

$$U = \exp\left(i\frac{\phi}{F_\pi} + i\sqrt{\frac{2}{3}}\frac{\eta_0}{F_0}\right) \tag{7.24}$$

where

$$\phi = \sum \pi_a \lambda_a = \sqrt{2}\begin{pmatrix} \frac{1}{\sqrt{2}}\pi^0 + \frac{1}{\sqrt{6}}\eta_8 & \pi^+ & K^+ \\ \pi^- & -\frac{1}{\sqrt{2}}\pi^0 + \frac{1}{\sqrt{6}}\eta_8 & K^0 \\ K^- & \bar{K}^0 & -\frac{2}{\sqrt{6}}\eta_8 \end{pmatrix} \tag{7.25}$$

denotes the octet of would-be Goldstone bosons associated with spontaneous chiral $SU(3)_L \otimes SU(3)_R$ breaking and η_0 is the singlet boson. $\mathcal{M} = \mathrm{diag}[m_\pi^2, m_\pi^2, (2m_K^2 - m_\pi^2)]$ is the meson mass matrix. The pion decay constant $F_\pi = 92.4$MeV. F_0 renormalizes the flavour-singlet decay constant – see Eq. (7.29) below – with $F_0 \sim F_\pi \sim 100$ MeV [Gilman and Kauffman (1987)].

The flavour-singlet potential involving Q is introduced to generate the gluonic contribution to the η and η' masses and to reproduce the anomaly in the divergence of the gauge-invariantly renormalized flavour-singlet axial-vector current. The gluonic term $Q = \frac{\alpha_s}{4\pi} G_{\mu\nu}\tilde{G}^{\mu\nu}$ is treated as a background field with no kinetic term. It may be eliminated through its equation of motion to generate a gluonic mass term for the singlet boson, *viz.*

$$\frac{1}{2} iQ \mathrm{Tr}\left[\log U - \log U^\dagger\right] + \frac{3}{\tilde{m}_{\eta_0}^2 F_0^2} Q^2 \;\mapsto\; -\frac{1}{2}\tilde{m}_{\eta_0}^2 \eta_0^2. \tag{7.26}$$

The most general low-energy effective Lagrangian involves a $U_A(1)$ invariant polynomial in Q^2. Higher-order terms in Q^2 become important when we consider scattering processes involving more than one η' [Di Vecchia *et al.* (1981)]. In general, couplings involving Q give OZI violation in physical observables.

When we expand out the Lagrangian (7.23) the first term contains the kinetic energy term for the pseudoscalar mesons; the second term contains the meson mass terms before coupling to gluonic degrees of freedom. After Q is eliminated from the effective Lagrangian via (7.26), we expand $\mathcal{L}_\mathrm{m}$ to $\mathcal{O}(p^2)$ in momentum keeping finite quark masses and obtain

$$\begin{aligned}
\mathcal{L}_\mathrm{m} = \quad & \sum_k \frac{1}{2}\partial^\mu \pi_k \partial_\mu \pi_k + \frac{1}{2}\partial_\mu \eta_0 \partial^\mu \eta_0 \left(\frac{F_\pi}{F_0}\right)^2 - \frac{1}{2}\tilde{m}_{\eta_0}^2 \eta_0^2 \\
& - \frac{1}{2} m_\pi^2 \left(2\pi^+\pi^- + \pi_0^2\right) - m_K^2 \left(K^+K^- + K^0\bar{K}^0\right) - \frac{1}{2}\left(\frac{4}{3}m_K^2 - \frac{1}{3}m_\pi^2\right)\eta_8^2 \\
& - \frac{1}{2}\left(\frac{2}{3}m_K^2 + \frac{1}{3}m_\pi^2\right)\left(\frac{F_\pi}{F_0}\right)^2 \eta_0^2 + \frac{4}{3\sqrt{2}}\left(m_K^2 - m_\pi^2\right)\left(\frac{F_\pi}{F_0}\right)\eta_8\eta_0 + \ldots
\end{aligned} \tag{7.27}$$

where π_a with $a = 1, \ldots, 8$ refers to the octet Goldstone boson fields. The masses of the physical η and η' mesons are found by diagonalising the (η_8, η_0) mass matrix which follows from Eq. (7.27). If we work in the approximation $m_u = m_d$ and set $F_0 = F_\pi$, then we obtain the $\eta - \eta'$ mass matrix in Eq. (7.16).

The $U_A(1)$ transformation for the effective Lagrangian (7.23) is defined by $U \to \exp(2i\beta)\, U$; Q is treated as $U_A(1)$ invariant. The flavour-singlet axial-vector current

$$J_{\mu 5} = \sqrt{6} F_\mathrm{singlet} \partial_\mu \eta_0 \tag{7.28}$$

with

$$F_\mathrm{singlet} = F_\pi^2 / F_0 \tag{7.29}$$

satisfies the anomalous divergence equation $\partial^\mu J_{\mu 5} = N_f Q +$ mass terms. The flavour-singlet decay constant is renormalized relative to F_π by gluonic intermediate states ($q\bar{q} \to gg \to q\bar{q}$).

The value of F_0 is usually determined from the decay rate for $\eta' \to 2\gamma$. In QCD one finds the relation [Shore and Veneziano (1992); Shore and White (2000)]

$$\frac{2\alpha}{\pi} = \sqrt{\frac{3}{2}} F_0 \Big(g_{\eta'\gamma\gamma} - g_{Q\gamma\gamma} \Big) \tag{7.30}$$

(in the chiral limit) which is derived by coupling the effective Lagrangian (7.23) to photons. The observed decay rate [Particle Data Group (2004)] is consistent [Gilman and Kauffman (1987)] with the OZI prediction for $g_{\eta'\gamma\gamma}$ *if* F_0 and $g_{Q\gamma\gamma}$ take their OZI values: $F_0 \simeq F_\pi$ and $g_{Q\gamma\gamma} = 0$. Motivated by this observation it is common to take $F_0 \simeq F_\pi$.

It is worthwhile to comment on the behaviour of $\mathcal{L}_{\rm m}$ when we take N_c, the number of colours, to infinity. In QCD the axial anomaly decouples as $1/N_c$ when we take $N_c \to \infty$. This is reflected in the equation for the η_0 mass squared if we take $a \propto 1/N_c$ [Witten (1979); Veneziano (1979)]. Phenomenologically, the large mass of the η' ($m_{\eta'} \sim 1$GeV) means that OZI and large N_c are not always good approximations in the $U_A(1)$ channel.

7.4 OZI violation and the η'–nucleon interaction

The low-energy effective Lagrangian (7.23) is readily extended to include η–nucleon and η'–nucleon coupling. Working to $O(p)$ in the meson momentum the chiral Lagrangian for meson-baryon coupling is

$$\begin{aligned}
\mathcal{L}_{\rm mB} = {} & {\rm Tr}\ \overline{B}(i\gamma_\mu D^\mu - M_0)B \\
& + F\ {\rm Tr}\Big(\overline{B}\gamma_\mu\gamma_5[a^\mu, B]_-\Big) + D\ {\rm Tr}\Big(\overline{B}\gamma_\mu\gamma_5\{a^\mu, B\}_+\Big) \\
& + \frac{i}{3}K\ {\rm Tr}\Big(\overline{B}\gamma_\mu\gamma_5 B\Big){\rm Tr}\Big(U^\dagger\partial^\mu U\Big) \\
& - \frac{\mathcal{G}_{QNN}}{2M_0}\partial^\mu Q {\rm Tr}\Big(\overline{B}\gamma_\mu\gamma_5 B\Big) + \frac{\mathcal{C}}{F_0^4}Q^2 {\rm Tr}\Big(\overline{B}B\Big)
\end{aligned} \tag{7.31}$$

Here

$$B = \begin{pmatrix} \frac{1}{\sqrt{2}}\Sigma^0 + \frac{1}{\sqrt{6}}\Lambda & \Sigma^+ & p \\ \Sigma^- & -\frac{1}{\sqrt{2}}\Sigma^0 + \frac{1}{\sqrt{6}}\Lambda & n \\ \Xi^- & \Xi^0 & -\frac{2}{\sqrt{6}}\Lambda \end{pmatrix} \tag{7.32}$$

denotes the baryon octet and M_0 denotes the baryon mass in the chiral limit. In Eq. (7.31)

$$D_\mu = \partial_\mu - iv_\mu \tag{7.33}$$

is the chiral covariant derivative

$$v_\mu = -\frac{i}{2}\left(\xi^\dagger\partial_\mu\xi + \xi\partial_\mu\xi^\dagger\right) \tag{7.34}$$

with $\xi = U^{\frac{1}{2}}$ and

$$a_\mu = -\frac{i}{2}\left(\xi^\dagger\partial_\mu\xi - \xi\partial_\mu\xi^\dagger\right) = -\frac{1}{2F_\pi}\partial_\mu\phi - \frac{1}{2F_0}\sqrt{\frac{2}{3}}\partial_\mu\eta_0 + ... \tag{7.35}$$

is the axial-vector current operator.

The SU(3) couplings are $F = 0.459 \pm 0.008$ and $D = 0.798 \pm 0.008$ [Close and Roberts (1993)]. The Pauli-principle forbids any flavour-singlet $J^P = \frac{1}{2}^+$ ground-state baryon degenerate with the baryon octet B. In general, one may expect OZI violation wherever a coupling involving the Q-field occurs. In Eq. (7.31) we have defined $\mathcal{G}_{QNN}$ and $\mathcal{C}$ so that they both have mass dimension -3.

Following Eq. (7.26), we eliminate Q from the total Lagrangian $\mathcal{L} = \mathcal{L}_{\rm m} + \mathcal{L}_{\rm mB}$ through its equation of motion. The Q dependent terms in the effective Lagrangian become:

$$\begin{aligned}\mathcal{L}_Q = \frac{1}{12}\tilde{m}^2_{\eta_0}\Bigg[&-6\eta_0^2 \;-\; \frac{\sqrt{6}}{M_0}\,\mathcal{G}_{QNN}\,F_0\,\partial^\mu\eta_0\,\mathrm{Tr}\Big(\bar{B}\gamma_\mu\gamma_5 B\Big) \\ &+ \mathcal{G}^2_{QNN}\,F_0^2\,\Big(\mathrm{Tr}\bar{B}\gamma_5 B\Big)^2 \;+\; 2\,\mathcal{C}\,\frac{\tilde{m}^2_{\eta_0}}{F_0^2}\,\eta_0^2\,\mathrm{Tr}\Big(\bar{B}B\Big) \\ &- \frac{\sqrt{6}}{3M_0F_0}\,\mathcal{G}_{QNN}\,\mathcal{C}\tilde{m}^2_{\eta_0}\eta_0\,\partial^\mu\mathrm{Tr}\Big(\bar{B}\gamma_\mu\gamma_5 B\Big)\,\mathrm{Tr}\Big(\bar{B}B\Big) + ...\Bigg]\end{aligned} \tag{7.36}$$

This equation describes the gluonic contributions to the η-nucleon and η'-nucleon interactions. The first term describes the gluonic correction to the mass of the singlet boson. The second term is a gluonic (OZI violating) contribution to the η'–nucleon coupling constant, which is read off from the coefficient of $\partial^\mu\eta_0\mathrm{Tr}\bar{B}B$ in the effective Lagrangian *after* we have eliminated Q. One finds

$$g_{\eta_0 NN} = \sqrt{\frac{2}{3}}\frac{m}{F_0}\left(2D + 2K + \mathcal{G}_{QNN}F_0^2\frac{\tilde{m}^2_{\eta_0}}{2m}\right). \tag{7.37}$$

The remaining terms in Eq. (7.36) describe contact terms in the η'–nucleon interaction. It is interesting to look for other observables which are sensitive to $\mathcal{G}_{QNN}$. OZI violation in the η'–nucleon system is a probe of the role of gluons in dynamical chiral symmetry breaking in low-energy QCD.

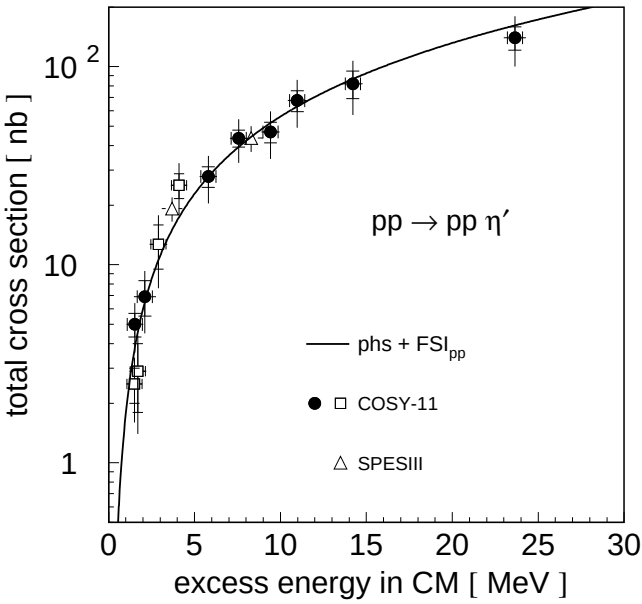

Fig. 7.1 The COSY and SATURNE data on $pp \to pp\eta'$. Figure from Moskal *et al.* (2000a).

7.5 Proton-proton collisions

The T-matrix for η' production in proton-proton collisions, $p_1(\vec{p}) + p_2(-\vec{p}) \to p + p + \eta'$, at threshold in the centre of mass frame is

$$\mathrm{T}_{\mathrm{th}}^{\mathrm{cm}}(pp \to pp\eta') = \mathcal{A}\Big[i(\vec{\sigma}_1 - \vec{\sigma}_2) + \vec{\sigma}_1 \mathrm{x} \vec{\sigma}_2\Big].\vec{p} \tag{7.38}$$

where $\mathcal{A}$ is the (complex) threshold amplitude for η' production. Measurements of the total cross-section for $pp \to pp\eta'$ have been published by COSY-11 [Moskal *et al.* (1998, 2000a)] and SATURNE [Hibou *et al.* (1998)] between 1.5 and 24 MeV above threshold – see Fig. 7.1.

The energy dependence of the data are well described by phase space plus proton-proton final state interaction (neglecting any η'-p FSI). Using the model of Bernard *et al.* (1999) treating the pp final state interaction in effective range approximation one finds a good fit to the measured total cross-section data with

$$|\mathcal{A}| = 0.21 \text{ fm}^4. \tag{7.39}$$

From Eq. (7.36) one finds a gluon-induced contact interaction in the $pp \to pp\eta'$ reaction close to threshold [Bass (1999c, 2000)]:

$$\mathcal{L}_{\mathrm{contact}} = -\frac{i}{F_0^2}\, g_{QNN}\, \tilde{m}_{\eta_0}^2\, \mathcal{C}\, \eta_0 \left(\bar{p}\gamma_5 p\right) \left(\bar{p}p\right) \tag{7.40}$$

where $g_{QNN} = \sqrt{\frac{1}{6}}\mathcal{G}_{QNN}F_0\tilde{m}^2_{\eta_0}$ The physical interpretation of the contact term (7.40) is a "short distance" ($\sim$ 0.2 fm) interaction where glue is excited in the interaction region of the proton-proton collision and then evolves to become an η' in the final state. This gluonic contribution to the cross-section for $pp \to pp\eta'$ is extra to the contributions associated with meson exchange models [Hibou *et al.* (1998); Fäldt and Wilkin (1997a); Fäldt *et al.* (2002)]. There is no reason, a priori, to expect it to be small.

What is the phenomenology of this gluonic interaction?

Since glue is flavour-blind the contact interaction (7.40) has the same size in both the $pp \to pp\eta'$ and $pn \to pn\eta'$ reactions. CELSIUS [Calen *et al.* (1988)] have measured the ratio $R_\eta = \sigma(pn \to pn\eta)/\sigma(pp \to pp\eta)$ for quasifree η production from a deuteron target up to 100 MeV above threshold. The data is shown in Fig. 7.2. One sees that R_η is approximately energy-independent with a value ~ 6.5 over the measured energy range. The observed ratio, different from one, signifies a strong isovector exchange contribution to the η production mechanism [Calen *et al.* (1988)]. This experiment is being repeated for η' production by COSY-11. The more important that the gluon-induced process is in the $pp \to pp\eta'$ reaction the more one would expect $R_{\eta'} = \sigma(pn \to pn\eta')/\sigma(pp \to pp\eta')$ to approach unity near threshold after we correct for the final state interaction between the two outgoing nucleons. (After we turn on the quark masses, the small $\eta - \eta'$ mixing angle $\theta \simeq -18$ degrees means that the gluonic effect (7.40) should be considerably bigger in η' production than η production.) η' phenomenology is characterised by large OZI violations. It is natural to expect large gluonic effects in the $pp \to pp\eta'$ process. The data will be very interesting.

7.6 Light mass "exotic" resonances

Recent experiments at BNL [Thompson *et al.* (1997); Adams *et al.* (1998); Chung *et al.* (1999); Ivanov *et al.* (2001)] and CERN [Abele *et al.* (1998)] have revealed evidence for QCD "exotic" meson states with quantum numbers $J^{PC} = 1^{-+}$. These mesons are particularly interesting because the quantum numbers $J^{PC} = 1^{-+}$ are inconsistent with a simple quark-antiquark bound state suggesting a possible "valence" gluonic component – for example through coupling to the operator $[\bar{q}\gamma_\mu qG^{\mu\nu}]$. Two such exotics, denoted π_1, have been observed through $\pi^- p \to \pi_1 p$ at BNL: with masses 1400 MeV (in decays to $\eta\pi$) and 1600 MeV (in decays to $\eta'\pi$ and $\rho\pi$). The $\pi_1(1400)$ state has also been observed in $\bar{p}N$ processes by the Crystal Barrel Collaboration at CERN [Abele *et al.* (1998)]. These states are considerably lighter than the predictions (about 1900 MeV) of quenched lattice QCD [Lacock *et al.* (1996, 1997); Bernard *et al.* (1997a,b)] and QCD inspired models [Isgur *et al.* (1985); Close and Page (1995); Barnes *et al.* (1995)] for the lowest mass $q\bar{q}g$ state with quantum numbers $J^{PC} = 1^{-+}$. While chiral corrections may bring the

lattice predictions down by about 100 MeV [Thomas and Szczepaniak (2002)] these results suggest that, perhaps, the "exotic" states observed by the experimentalists might involve significant meson-meson bound state contributions.

The decays of the light mass exotics to η or η' mesons plus a pion may hint at a possible connection to axial U(1) dynamics. This idea has recently been investigated [Bass and Marco (2002)] in a model of final state interaction in $\eta\pi$ and $\eta'\pi$ scattering using coupled channels and the Bethe-Salpeter equation following the approach in Oller and Oset (1997) and Oller *et al.* (1999). In this calculation the meson-meson scattering potentials were derived from the mesonic chiral Lagrangian working to $O(p^2)$ in the meson momenta. Fourth order terms in the meson fields are induced by the first two terms in Eq. (7.23) and also by the OZI violating interaction $\lambda\ Q^2\ \mathrm{Tr}\ \partial_\mu U \partial^\mu U^\dagger$ [Di Vecchia *et al.* (1981)]. A simple estimate for

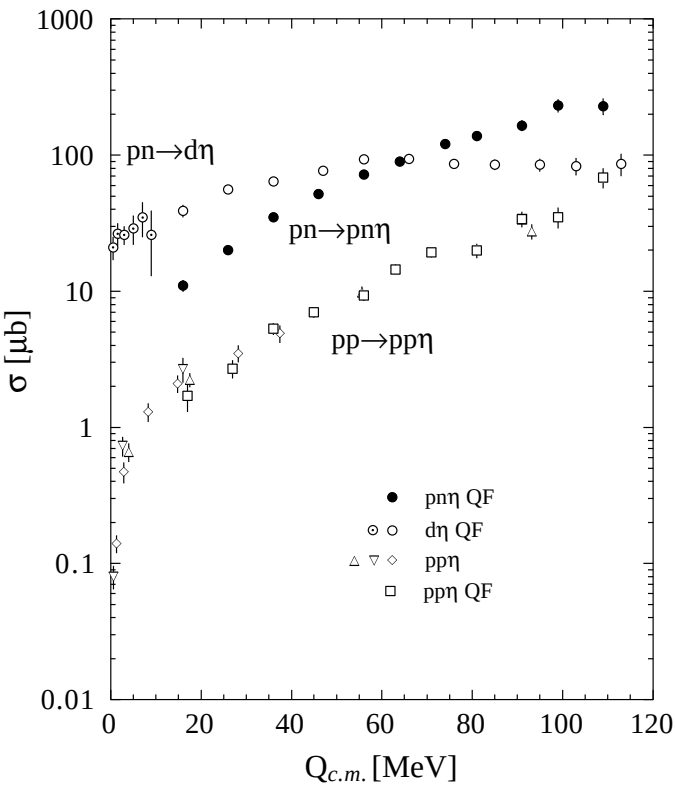

Fig. 7.2 CELSIUS data on the $pp \to pp\eta$ and $pn \to pn\eta$ reactions close to threshold [Calen *et al.* (1988)].

λ can be obtained from the decay $\eta' \to \eta\pi\pi$ yielding two possible solutions with different signs. These two different solutions yield two different dynamically generated resonance structures when substituted into the Bethe-Salpeter equation. The positive-sign solution for λ was found to dynamically generate a scalar resonance with mass $\sim$ 1300 MeV and width $\sim$ 200 MeV (and no p-wave resonance). This scalar resonance is a possible candidate for the $a_0(1450)$. The negative-sign solution for λ produced a p-wave resonance with exotic quantum numbers $J^{PC} = 1^{-+}$, mass $\sim$ 1400 MeV and width $\sim$ 300 MeV – close to the observed exotics – and no s-wave resonance. (The width of the $\pi_1(1400)$ state measured in decays to $\eta\pi$ is 385 ± 40 MeV; the width of the $\pi_1(1600)$ measured in decays to $\eta'\pi$ is 340 ± 64 MeV.) These calculations clearly illustrate the possibility to describe light-mass exotics as hadronic resonances in the $\eta'\pi$ and $\eta\pi$ systems. The topological charge density mediates the coupling of the light-mass exotic state to the $\eta\pi$ and $\eta'\pi$ channels in the model [Bass and Marco (2002)].

7.7 η bound states in nuclei

Measurements of the pion, kaon and eta meson masses and their interactions in finite nuclei provide new constraints on our understanding of dynamical symmetry breaking in low energy QCD [Kienle and Yamazaki (2004)]. New experiments at the GSI are employing the recoilless $(d,\ ^3He)$ reaction to study the possible formation of η meson bound states inside the nucleus [Hayano *et al.* (1999)], following on from the successful studies of pionic atoms in these reactions [Suzuki *et al.* (2004)]. The idea is to measure the excitation-energy spectrum and then, if a clear bound state is observed, to extract the in-medium effective mass, m^*_η, of the η in nuclei through performing a fit to this spectrum with the η-nucleus optical potential.

Meson masses in nuclei are determined from the scalar induced contribution to the meson propagator evaluated at zero three-momentum, $\vec{k} = 0$, in the nuclear medium. Let $k = (E, \vec{k})$ and m denote the four-momentum and mass of the meson in free space. Then, one solves the equation

$$k^2 - m^2 = \mathtt{Re}\ \Pi(E, \vec{k}, \rho) \tag{7.41}$$

for $\vec{k} = 0$ where Π is the in-medium s-wave meson self-energy. Contributions to the in medium mass come from coupling to the scalar σ field in the nucleus in mean-field approximation, nucleon-hole and resonance-hole excitations in the medium. The s-wave self-energy can be written as [Ericson and Weise (1988)]

$$\Pi(E, \vec{k}, \rho)\Big|_{\{\vec{k}=0\}} = -4\pi\rho\left(\frac{b}{1 + b\langle\frac{1}{r}\rangle}\right). \tag{7.42}$$

Here ρ is the nuclear density, $b = a(1 + \frac{m}{M})$ where a is the meson-nucleon scattering length, M is the nucleon mass and $\langle\frac{1}{r}\rangle$ is the inverse correlation length, $\langle\frac{1}{r}\rangle \simeq m_\pi$ for nuclear matter density (m_π is the pion mass). Attraction corresponds to positive

values of a. The denominator in Eq. (7.42) is the Ericson-Ericson-Lorentz-Lorenz double scattering correction.

It is reasonable to expect that m_η^* is sensitive to the flavour-singlet component in the η, and hence to non-perturbative glue [Bass (2002b); Shore (1998a)] associated with axial U(1) dynamics. An important source of the in-medium mass modification comes from light-quarks coupling to the scalar σ mean-field in the nucleus. Increasing the flavour-singlet component in the η at the expense of the octet component gives more attraction, more binding and a larger value of the η-nucleon scattering length, $a_{\eta N}$. This result may explain why values of $a_{\eta N}$ extracted from phenomenological fits to experimental data where the $\eta - \eta'$ mixing angle is unconstrained give larger values than those predicted in theoretical models where the η is treated as a pure octet state.

What can QCD tell us about the behaviour of the gluonic mass contribution in the nuclear medium? To investigate what happens to $\tilde{m}^2_{\eta_0}$ in the medium we first couple the σ (correlated two-pion) mean-field in nuclei to the topological charge density Q. The interactions of the η and η' with other mesons and with nucleons can be studied by coupling the Lagrangian Eq. (7.23) to other particles. For example, as noted in Section 7.6, the OZI violating interaction $\lambda Q^2 \partial_\mu \pi_a \partial^\mu \pi_a$ is needed to generate the leading (tree-level) contribution to the decay $\eta' \to \eta\pi\pi$ [Di Vecchia *et al.* (1981)]. When iterated in the Bethe-Salpeter equation for meson-meson rescattering this interaction yields a dynamically generated exotic state with quantum numbers $J^{PC} = 1^{-+}$ and mass about 1400 MeV [Bass and Marco (2002)]. This suggests a dynamical interpretation of the lightest-mass 1^{-+} exotic observed at BNL and CERN.

Motivated by this two-pion coupling to Q^2, we couple the topological charge density to the σ (two-pion) mean-field in the nucleus by adding the Lagrangian term

$$\mathcal{L}_{\sigma Q} = Q^2 \; g_\sigma^Q \sigma \tag{7.43}$$

where g_σ^Q denotes coupling to the σ mean field – that is, we consider an in-medium renormalization of the coefficient of Q^2 in the effective chiral Lagrangian. Following the treatment in Eq. (7.26) we eliminate Q through its equation of motion. The gluonic mass term for the singlet boson then becomes

$$\tilde{m}^2_{\eta_0} \mapsto \tilde{m}^{*2}_{\eta_0} = \tilde{m}^2_{\eta_0} \; \frac{1+2x}{(1+x)^2} \; < \tilde{m}^2_{\eta_0} \tag{7.44}$$

where

$$x = \frac{1}{3} g_\sigma^Q \sigma \; \tilde{m}^2_{\eta_0} F_0^2. \tag{7.45}$$

That is, *the gluonic mass term decreases in-medium* independent of the sign of g_σ^Q and the medium acts to partially neutralise axial U(1) symmetry breaking by gluonic effects.

This scenario has possible support from recent lattice calculations [Bissey *et al.* (2005)] which suggest that non-trivial gluon topology configurations are sup-

pressed inside hadrons. Further recent work at high chemical potential ($\mu >$ 500 MeV) suggests that possible confinement and instanton contributions to $\tilde{m}^2_{\eta_0}$ are suppressed with increasing density in this domain [Schafer (2003)].

The above discussion is intended to motivate the *existence* of medium modifications to $\tilde{m}^2_{\eta_0}$ in QCD. However, a rigorous calculation of m^*_η from QCD is beyond present theoretical technology. Hence, one has to look to QCD motivated models and phenomenology for guidance about the numerical size of the effect. The physics described in Eqs. (7.16)-(7.20) tells us that the simple octet approximation may not suffice.

We now discuss the size of flavour-singlet effects in m^*_η, $m^*_{\eta'}$ (the η' mass in-medium) and the scattering lengths $a_{\eta N}$ and $a_{\eta' N}$. First we consider the values of $a_{\eta N}$ and $a_{\eta' N}$ extracted from phenomenological fits to experimental data. There are several model predictions for the η mass in nuclear matter, starting from different assumptions. We collect and compare these approaches and predictions with particular emphasis on the contribution of $\eta - \eta'$ mixing.

Phenomenological determinations of $a_{\eta N}$ and $a_{\eta' N}$: Green and Wycech (1999) and (2005) have performed phenomenological K-matrix fits to a variety of near-threshold processes ($\pi N \to \pi N$, $\pi N \to \eta N$, $\gamma N \to \pi N$ and $\gamma N \to \eta N$) to extract a value for the η-nucleon scattering. In these fits the $S_{11}(1535)$ is introduced as an explicit degree of freedom – that is, it is treated like a 3-quark state – and the $\eta - \eta'$ mixing angle is taken as a free parameter. The real part of $a_{\eta N}$ extracted from these fits is 0.91(6) fm for the on-shell scattering amplitude.

From measurements of η production in proton-proton collisions close to threshold, COSY-11 have extracted a scattering length $a_{\eta N} \simeq 0.7 + i0.4$fm from the final state interaction (FSI) based on the effective range approximation [Moskal *et al.* (2004)]. For the η', COSY-11 have deduced a conservative upper bound on the η'-nucleon scattering length $|\mathtt{Re} a_{\eta' N}| < 0.8$fm [Moskal *et al.* (2000a)] with a prefered a value between 0 and 0.1 fm [Moskal *et al.* (2000b)] obtained by comparing the FSI in π^0 and η' production in proton-proton collisions close to threshold.

Chiral Models: Chiral models involve performing a coupled channels analysis of η production after multiple rescattering in the nucleus which is calculated using the Lippmann-Schwinger [Waas and Weise (1997)] or Bethe-Salpeter [Inoue and Oset (2002); Garcia-Oset *et al.* (2002)] equations with potentials taken from the SU(3) chiral Lagrangian for low-energy QCD. In these chiral model calculations the η is taken as pure octet state ($\eta = \eta_8$) with no mixing and the singlet sector turned off. These calculations yield a small mass shift in nuclear matter

$$m^*_\eta / m_\eta \simeq 1 - 0.05\rho/\rho_0 \tag{7.46}$$

The values of the η-nucleon scattering length extracted from these chiral model calculations are 0.2 + i 0.26 fm [Waas and Weise (1997)] and 0.26 + i 0.24 fm [Inoue and Oset (2002); Garcia-Oset *et al.* (2002)] with slightly different treatment of the intermediate state mesons.

Table 7.1 Physical masses fitted in free space, the bag masses in medium at normal nuclear-matter density, $\rho_0 = 0.15$ fm^{-3}, and corresponding meson-nucleon scattering lengths [Bass and Thomas (2006)].

	m (MeV)	m^* (MeV)	Rea (fm)
η_8	547.75	500.0	0.43
η (-10^o)	547.75	474.7	0.64
η (-20^o)	547.75	449.3	0.85
η_0	958	878.6	0.99
η' (-10^o)	958	899.2	0.74
η' (-20^o)	958	921.3	0.47

The Quark Meson Coupling Model (QMC) [Tsushima *et al.* (1998); Tsushima (2000); Bass and Thomas (2006)]. Here one uses the large η mass (which in QCD is induced by mixing and the gluonic mass term) to motivate taking an MIT Bag description for the η wavefunction, and then coupling the light (up and down) quark and antiquark fields in the η and η' to the scalar σ field in the nucleus working in mean-field approximation. The strange-quark component of the wavefunction does not couple to the σ field and $\eta - \eta'$ mixing is readily built into the model. The results for the masses for the η and η' mesons in nuclear matter are summarized in Table 7.1.

The values of Rea_η are obtained from substituting the in-medium and free masses into Eq. (7.42) with the Ericson-Ericson denominator turned-off, and using the free mass $m = m_\eta$ in the expression for b. The effect of exchanging m for m^* in b is a 5% increase in the quoted scattering length. The QMC model makes no claim about the imaginary part of the scattering length. The key observation is that $\eta - \eta'$ mixing leads to a factor of two increase in the mass-shift and in the scattering length obtained in the model.[2]

The density dependence of the mass-shifts in the QMC model is discussed in Tsushima *et al.* (1998). Neglecting the Ericson-Ericson term, the mass-shift is approximately linear. For densities ρ between 0.5 and 1 times ρ_0 (nuclear matter density) we find

$$m^*_\eta / m_\eta \simeq 1 - 0.17\rho/\rho_0 \tag{7.47}$$

for the physical mixing angle $-20°$. The scattering lengths extracted from this analysis are density independent to within a few percent over the same range of densities.

η-η' mixing increases the flavour-singlet and light-quark components in the η. The greater the flavour-singlet component in the η, the greater the η binding energy

[2]Because the QMC model has been explored mainly at the mean-field level, it is not clear that one should include the Ericson-Ericson term in extracting the corresponding η nucleon scattering length. Substituting the scattering lengths given in Table 7.1 into Eq. (7.42) (and neglecting the imaginary part) yields resummed values $a_{eff} = a/(1 + b\langle 1/r\rangle)$ equal to 0.44 fm for the η with the physical mixing angle $\theta = -20$ degrees, with corresponding reduction in the binding energy.

in nuclei through increased attraction and the smaller the value of m_η^*. Through Eq. (7.42), this corresponds to an increased η-nucleon scattering length $a_{\eta N}$, greater than the value one would expect if the η were a pure octet state. Measurements of η bound-states in nuclei are therefore a probe of singlet axial U(1) dynamics in the η.

This page intentionally left blank

Chapter 8

QCD INSPIRED MODELS OF THE PROTON SPIN PROBLEM

In semi-classical quark models Δq is interpreted as the amount of spin carried by quarks and antiquarks of flavour q, there is no $E(\alpha_s)$ factor and $\Sigma = g_A^{(0)}$. Relativistic quark-pion coupling models which contain no explicit strange quark or gluon degrees of freedom predict $g_A^{(0)} = g_A^{(8)}$. Whilst these models do not explain the small value of $g_A^{(0)}|_{\rm pDIS}$ they do give a good account of the flavour non-singlet axial charges $g_A^{(3)}$ and $g_A^{(8)}$.

Here, we first explain this result and then outline the different possible explanations that people have considered to explain the supression of $g_A^{(0)}|_{\rm pDIS}$ and the finite, negative value of Δs extracted from polarized deep inelastic scattering.

8.1 Constituent quarks and $g_A^{(k)}$

First, consider the static quark model. The simple SU(6) proton wavefunction

$$|p\uparrow\rangle = \frac{1}{\sqrt{2}}|u\uparrow(ud)_{S=0}\rangle + \frac{1}{\sqrt{18}}|u\uparrow(ud)_{S=1}\rangle - \frac{1}{3}|u\downarrow(ud)_{S=1}\rangle \qquad (8.1)$$
$$-\frac{1}{3}|d\uparrow(uu)_{S=1}\rangle + \frac{\sqrt{2}}{3}|d\downarrow(uu)_{S=1}\rangle$$

yields $g_A^{(3)} = \frac{5}{3}$ and $g_A^{(8)} = g_A^{(0)} = 1$.

In relativistic quark models one has to take into account the four-component Dirac spinor $\psi = \binom{f}{i\sigma.\hat{r}g}$. The lower component of the Dirac spinor is p-wave with intrinsic spin primarily pointing in the opposite direction to spin of the nucleon. Relativistic effects renormalize the NRQM axial charges by a factor $(f^2 - \frac{1}{3}g^2)$ with a net transfer of angular momentum from intrinsic spin to orbital angular momentum. In the MIT Bag $(f^2 - \frac{1}{3}g^2) = 0.65$ reducing $g_A^{(3)}$ from $\frac{5}{3}$ to 1.09. Centre of mass motion then increases the axial charges by about 20% bringing $g_A^{(3)}$ close to its physical value 1.27.

To see how this comes about consider the simplest version of Bag model of confinement. Here we consider a massless Dirac fermion moving freely inside a spherical volume of radius R, outside of which there is a scalar potential of strength

m. When we take the limit $m \to \infty$ the quarks are confined to the spherical volume. This is summarized through the Dirac equation with a central, scalar field $W(r)$

$$H\psi(r) = i\frac{\partial\psi}{\partial t} = \left\{\vec{\alpha}.\vec{\mathrm{p}} + \beta[m + W(r)]\right\}\psi(r) = E\psi(r) \tag{8.2}$$

with

$$\begin{aligned} W(r) &= -m, \qquad r \le R \\ &= \quad 0, \qquad r > R \end{aligned} \tag{8.3}$$

and

$$\psi(r) = \psi(\vec{\mathrm{r}}, t) = \psi(\vec{\mathrm{r}})e^{-iEt} \tag{8.4}$$

The Dirac matrices are take as

$$\beta = \gamma^0 = \begin{pmatrix} 1 & 0 \\ 0 & -1 \end{pmatrix} \quad , \quad \vec{\gamma} = \gamma^0\vec{\alpha} = \begin{pmatrix} 0 & \vec{\sigma} \\ -\vec{\sigma} & 0 \end{pmatrix} \tag{8.5}$$

One requires continuity of the wavefunction at the boundary $r = R$ and takes the limit $m \to \infty$. Solving the Dirac equation then yields the solution for the ground state $s_{\frac{1}{2}}$ level:

$$\psi^{\mu}_{ns_{1/2}} \equiv \psi^{\mu}_{n\kappa=-1} = \frac{N_{n,-1}}{(4\pi)^{\frac{1}{2}}} \begin{pmatrix} j_0(\frac{\omega r}{R}) \\ i\vec{\sigma}.\hat{r}\ j_1(\frac{\omega r}{R}) \end{pmatrix} \chi^{\mu}_{1/2} \tag{8.6}$$

subject to the boundary condition

$$j_0(ER) = j_1(ER) \tag{8.7}$$

for confined massless quarks. The normalization constant is

$$N^2_{n,-1} = \frac{\omega^3_{n,-1}}{2R^3(\omega_{n,-1} - 1)\sin^2(\omega_{n,-1})} \tag{8.8}$$

and $\chi^{\mu}_{1/2}$ a Pauli spinor. If we parametrize the energy levels as

$$E_{n\kappa} = \frac{\omega_{n\kappa}}{R} \tag{8.9}$$

where n is the principal quantum number, we find $\omega_{1-1} = 2.04$, $\omega_{2-1} = 5.40$, ...

The nucleon matrix element of the axial-vector current is then evaluated:

$$\begin{aligned} \int d^3x \sum_i \langle ps|\overline{q}_i\vec{\gamma}\gamma_5 q_i|ps\rangle &= \int_{\mathrm{bag}} d^3x\psi^{\dagger}_i(x)\gamma_0\vec{\gamma}\gamma_5\psi(x) \\ &= N^2\int_0^R dx x^2\left\{j_0^2(\frac{\omega x}{R}) - \frac{1}{3}j_1^2(\frac{\omega x}{R})\right\} \\ &= 1 - \frac{1}{3}(\frac{2\omega - 3}{\omega - 1}) = 0.65 \end{aligned} \tag{8.10}$$

when we substitute the Bag wavefunction (8.6). This factor 0.65 is the crucial difference from non-relativistic constituent quark models.

The pion cloud of the nucleon also renormalizes the nucleon's axial charges by shifting intrinsic spin into orbital angular momentum. Consider the Cloudy Bag Model (CBM). Here, the Fock expansion of the nucleon in terms of a bare MIT nucleon $|\mathrm{N}\rangle$ and baryon-pion $|\mathrm{N}\pi\rangle$ $|\Delta\pi\rangle$ Fock states converges rapidly. We may safely truncate the Fock expansion at the one pion level. The CBM axial charges are [Schreiber and Thomas (1988)]:

$$\begin{aligned} g_A^{(3)} &= \frac{5}{3}\mathcal{N}\left(1 - \frac{8}{9}P_{N\pi} - \frac{4}{9}P_{\Delta\pi} + \frac{8}{15}P_{N\Delta\pi}\right) \\ g_A^{(0)} &= \quad \mathcal{N}\left(1 - \frac{4}{3}P_{N\pi} + \frac{2}{3}P_{\Delta\pi}\right). \end{aligned} \tag{8.11}$$

Here, $\mathcal{N}$ takes into account the relativistic factor $N^2 \int_0^R drr^2(f^2 - \frac{1}{3}g^2)$ and centre of mass motion in the Bag. The coefficients $P_{N\pi} = 0.2$ and $P_{\Delta\pi} = 0.1$ denote the probabilities to find the physical nucleon in the $|N\pi\rangle$ and $|\Delta\pi\rangle$ Fock states respectively and $P_{N\Delta\pi} = 0.3$ is the interference term. The bracketed pion cloud renormalization factors in Eq. (8.11) are 0.94 for $g_A^{(3)}$ and 0.8 for $g_A^{(0)}$. Through the Goldberger-Treiman relation, the small pion cloud renormalization of $g_A^{(3)}$ translates into a small pion cloud renormalization of $g_{\pi NN}$, which is necessary to treat the pion cloud in low order perturbation theory [Thomas (1984)]. With a 20% centre of mass correction, the CBM predicts $g_A^{(3)} \simeq 1.25$ and $g_A^{(0)} = g_A^{(8)} \simeq 0.6$. Similar numbers [Steininger and Weise (1993)] are obtained in the Nambu-Jona-Lasinio model.

Including kaon loops into the model generates a small $\Delta s \simeq -0.003$ [Koepf *et al.* (1992)] in the Cloudy Bag Model and -0.006 [Steininger and Weise (1993)] in the Nambu-Jona-Lasinio model. These values are an order of magnitude smaller than the value of Δs extracted from inclusive polarized deep inelastic scattering experiments, *viz.* $\Delta s \sim -0.08$.

In QCD the axial anomaly induces various gluonic contributions to $g_A^{(0)}$. Since gluons are flavour singlet, it follows that, modulo flavour SU(3) breaking, explicit gluonic contributions to Δq will cancel in the isotriplet and SU(3) octet axial charges $g_A^{(3)}$ and $g_A^{(8)}$.

8.2 Possible explanations of the proton spin problem

We now collect and compare the various proposed explanations of the proton spin problem (the small value of $g_A^{(0)}$ extracted from polarized deep inelastic scattering) in roughly the order that they enter the derivation of the g_1 spin sum-rule:

(1) *A "subtraction at infinity" in the dispersion relation for* g_1 perhaps generated in the transition from current to constituent quarks and involving gluon topology and the mechanism of dynamical axial U(1) symmetry breaking. For example, when one puts a valence quark as a spin source in the QCD θ vacuum with non-trivial chiral structure instanton tunneling processes have the potential to

delocalise the spin so that the "quark spin content" of the proton becomes a property of the proton rather than the sum over the individual localised parton spin contributions measured in polarized deep inelastic scattering. In the language of Regge phenomenology the subtraction at infinity is associated with a fixed pole in the real part of the spin dependent part of the forward Compton amplitude.

In this scenario the strange quark polarization Δs extracted from inclusive polarized deep inelastic scattering and neutrino proton elastic scattering would be different. A precision measurement of νp elastic scattering would be very useful.

Note that fixed poles play an essential role in the Adler and Schwinger term sum-rules - one should be on the look out!

It is interesting to look for analogues in condensed matter physics. Consider Helium-3 and Helium-4 atoms. These have the same chemical structure and their properties at low temperatures are determined just by their spins – that is, the spin of the extra neutron in the nucleus of the Helium-4 atom. The proton spin problem addresses the question: Where does this spin come from at the quark level ? In low temperature physics Helium-4 becomes a superfluid at 2K whereas Helium-3 remains as a normal liquid at these temperatures and becomes superfluid only at 2.6 mK with a much richer phase diagram. In the A-phase which forms at 21 bars pressure the spins of the Cooper pairs align and a polarized condensate is formed [Anderson and Brinkman (1975)]. Our notion of a constituent quark in low energy QCD is an emergent quasi-particle excitation self-consistently interacting with the condensates generated through dynamical chiral and axial U(1) symmetry breaking. The singlet component of the total condensate in the proton can be spin polarized relative to the vacuum outside the proton. In this case the total singlet axial-charge, as calculated in constituent quark models, would be the sum of the partonic (finite momentum) and condensate (zero momentum) contributions. The proton spin problem may be teaching us about dynamical symmetry breaking in the transition from current to constituent quarks.

(2) *SU(3) flavour breaking in the analysis of hyperon beta decays.* Phenomenologically, SU(3) flavour symmetry seems to be well respected in the measured beta decays, including the recent KTeV and NA-48 measurements of the Ξ^0 decay [Alavi-Harati *et al.* (2001); Batley *et al.* (2007)]. Leader and Stamenov (2003) have recently argued that even the most extreme SU(3) breaking scenarios consistent with hyperon decays will still lead to a negative value of the strange quark axial charge Δs extracted from polarized deep inelastic data. Possible SU(3) breaking in the large N_c limit of QCD has been investigated by Flores-Mendiek *et al.* (2001).

One source of SU(3) breaking that we have so far observed is in the polarized sea generated through photon-gluon fusion where the strange-quark mass

term is important – see Eq. (6.33) and Fig. 6.2. The effect of including SU(3) breaking in the parton model for $\Delta q_{\rm partons}$ within various factorization schemes has been investigated in Glück *et al.* (2001).

(3) *Topological charge screening and target independence of the "spin effect" generated by a small value of* $\chi'(0)$ in the flavour-singlet Goldberger-Treiman relation. This scenario could be tested through semi-inclusive measurements where a pion or D meson is detected in the target fragmentation region, perhaps using a polarized *ep* collider with Roman pot detectors [Shore and Veneziano (1998)]. These experiments could, in principle, be used to vary the target and measure g_1 for e.g. Δ^{++} and Δ^{-} targets along the lines of the programme that has been carried through in unpolarized scattering [Holtmann *et al.* (1994)].

(4) *Non-perturbative evolution associated with the renormalization group factor* $E(\alpha_s)$ *between deep inelastic scales and the low-energy scale where quark models might, perhaps, describe the twist 2 parton distributions* [Jaffe (1987)]. One feature of this scenario is that (in the four flavour theory) the polarized charm and strange quark contributions evolve at the same rate with changing Q^2 since $\Delta s - \Delta c$ is flavour non-singlet (and therefore independent of the QCD axial anomaly) [Bass and Thomas (1993a)]. Heavy-quark renormalization group arguments suggest that Δc is small [Bass *et al.* (2002); Kaplan and Manohar (1988)] up to $1/m_c$ corrections.

The perturbative QCD expansion of $E(\alpha_s)$ is

$$E(\alpha_s) = \left[1 - \frac{24f}{33-2f}\frac{\alpha_s}{4\pi} + \frac{1}{2}\left(\frac{\alpha_s}{4\pi}\right)^2 \frac{f}{33-2f}\left(\frac{16f}{3} - 472 + 72\frac{102-\frac{14f}{3}}{33-2f}\right) + ...\right] \tag{8.12}$$

where f is the number of flavours. To $\mathcal{O}(\alpha_s^2)$ the perturbative expansion (8.12) remains close to one – even for large values of α_s. If we take $\alpha_s \sim 0.6$ as typical of the infra-red then

$$E(\alpha_s) \simeq 1 - 0.13 - 0.03 = 0.84. \tag{8.13}$$

Here -0.13 and -0.03 are the $\mathcal{O}(\alpha_s)$ and $\mathcal{O}(\alpha_s^2)$ corrections respectively. Perturbative QCD evolution is insufficient to reduce the flavour-singlet axial-charge from its naive value 0.6 to the value ~ 0.3 extracted from polarized deep inelastic scattering.

(5) *Large gluon polarization* $\Delta g \sim 1$ *at the scale* $\mu \sim 1 GeV$ could restore consistency between the measured $g_A^{(0)}$ and quark model predictions if the quark model predictions are associated with $\Delta q_{\rm partons}$ (the low k_t contribution to $g_A^{(0)}$) in Eq. (6.39). Δg is being measured through a variety of gluon induced partonic production processes including charm production and using high p_t hadron pairs as surrogate jets in polarized deep inelastic scattering, and high p_t pion production and jet studies in polarized proton collisions at RHIC – see Chapter 12 below. Attempts to extract Δg from QCD motivated fits to the Q^2 dependence

of g_1 data have yielded values between about -0.3 and 2 at $Q^2 \sim 1$ GeV^2, with values $|\Delta g| \sim 0.3$ favoured by recent fits to the most accurate recent data – see Chapter 10.

How big should we expect Δg to be? Since $\alpha_s \Delta g \sim$ `constant` as $Q^2 \to \infty$ it follows that the gluon polarization Δg must become large at some asymptotic scale. What about at the scales typical of experiments and quark models? Working in the framework of light-cone models one finds contributions from "intrinsic" and "extrinsic" gluons. Extrinsic contributions arise from gluon bremsstrahlung $q_V \to q_V g$ of a valence quark and have a relatively hard virtuality. Intrinsic gluons are associated with the physics of the nucleon wavefunction (for example, gluons emitted by one valence quark and absorbed by another quark) and have a relatively soft spectrum [Bass *et al.* (1999)]. Light-cone models including QCD colour coherence at small Bjorken x and perturbative QCD counting rules at large x [Brodsky and Schmidt (1990); Brodsky *et al.* (1995)] suggest values of $\Delta g \sim 0.6$ at low scales ~ 1 GeV^2 – sufficient to account for about one third of the "missing spin" or measured value of $g_A^{(0)}$.
Bag model calculations give values $\Delta g \sim -0.4$ (note the negative sign) when one includes gluon exchange contributions and no "self field" contribution where the gluon is emitted and absorbed by the same quark [Jaffe (1996)] and $\Delta g \sim 0.24$ (positive sign) when the "self field" contribution is included [Barone *et al.* (1998)].

(6) *Large negatively polarized strangeness in the quark sea (with small k_t).* This scenario can be tested through semi-inclusive measurements of polarized deep inelastic scattering provided that radiative corrections, fragmentation functions and the experimental acceptance are under control.

Of course, the final answer may prove to be a cocktail solution of these possible explanations or include some new dynamics that has not yet been thought of.

In testing models of quark sea and gluon polarization it is important to understand the transverse momentum and Bjorken x dependence of the different sea-quark dynamics. For example, sea quark contributions to deep inelastic structure functions are induced by perturbative photon-gluon fusion [Efremov and Teryaev (1988); Altarelli and Ross (1988); Carlitz *et al.* (1988)], pion and kaon cloud physics [Melnitchouk and Malheiro (1999); Koepf *et al.* (1992); Cao and Signal (2003); Bissey *et al.* (2006)], instantons [Forte and Shuryak (1991); Schafer and Zetocha (2004); Nishikawa (2004); Dolgov *et al.* (1999)], ... In general, different mechanisms produce sea-quarks with different x and k_t dependence.

Lattice calculations are also making progress in unravelling the spin structure of the proton [Mathur *et al.* (2000); Negele *et al.* (2004); Edwards *et al.* (2006); Hägler *et al.* (2007)]. Interesting new results [Negele *et al.* (2004)] suggest a value of $g_A^{(0)}$ about 0.7 in a heavy-pion world where the pion mass $m_\pi \sim 700 - 900$ MeV. Physically, in the heavy-pion world (away from the chiral limit) the quarks become less relativistic and it is reasonable to expect the nucleon spin to arise from the

valence quark spins. Sea quark effects are expected to become more important as the quarks become lighter and sea production mechanisms become important. It will be interesting to investigate the behaviour of $g_A^{(0)}$ in future lattice calculations as these calculations approach the chiral limit. For the isovector axial charge $g_A^{(3)}$ considerable progress has been made. The lattice calculations at $m_\pi^2 \sim 0.15$ GeV^2 plus chiral extrapolation are in good agreement with the physical value – see Fig. 8.1.

In an alternative approach to understanding low energy QCD Witten (1983a,b) noticed that in the limit that the number of colours N_c is taken to infinity ($N_c \to \infty$ with $\alpha_s N_c$ held fixed) QCD behaves like a system of bosons and the baryons emerge as topological solitions called Skyrmions in the meson fields. In this model the spin of the large N_c "proton" is a topological quantum number. The "nucleon's" axial charges turn out to be sensitive to which meson fields are included in the model and the relative contribution of a quark source and pure mesons – we refer to the lectures of Aitchison (1988) for a more detailed discussion of the Skyrmion approach. Brodsky *et al.* (1988) found that $g_A^{(0)}$ vanishes in a particular version of the Skyrmion model with just pseudoscalar mesons. Non-vanishing values of $g_A^{(0)}$ are found using more general Skyrmion Lagrangians [Ryzak (1989); Cohen and Banerjee (1989)], including with additional vector mesons [Johnson *et al.* (1990)].

Going beyond the first moment, the light-cone correlation functions permit quark model calculations of deep inelastic structure functions. First, one interprets the light-cone operator matrix element $\langle p,s|[\overline{q}(z_-)\gamma_+ q(0)]|p,s\rangle$ as the amplitude to take a quark out from (or insert an anti-quark into) the target proton at position 0 and re-insert the quark (take out the anti-quark) at a position z_- along the light cone. This matrix element is then calculated in one's favourite quark model. The renormalisation scale for the matrix element is taken at some low input scale $\mu^2 \sim 0.2 - 0.5$ GeV^2 where the quark model might be a good approximation to nature. The model structure functions are calculated at the input model scale and then evolved using DGLAP evolution up to the scale of the deep inelastic experiments, where they are compared to data. Typical predictions for the proton and neutron spin structure functions are shown in Fig. 8.2.

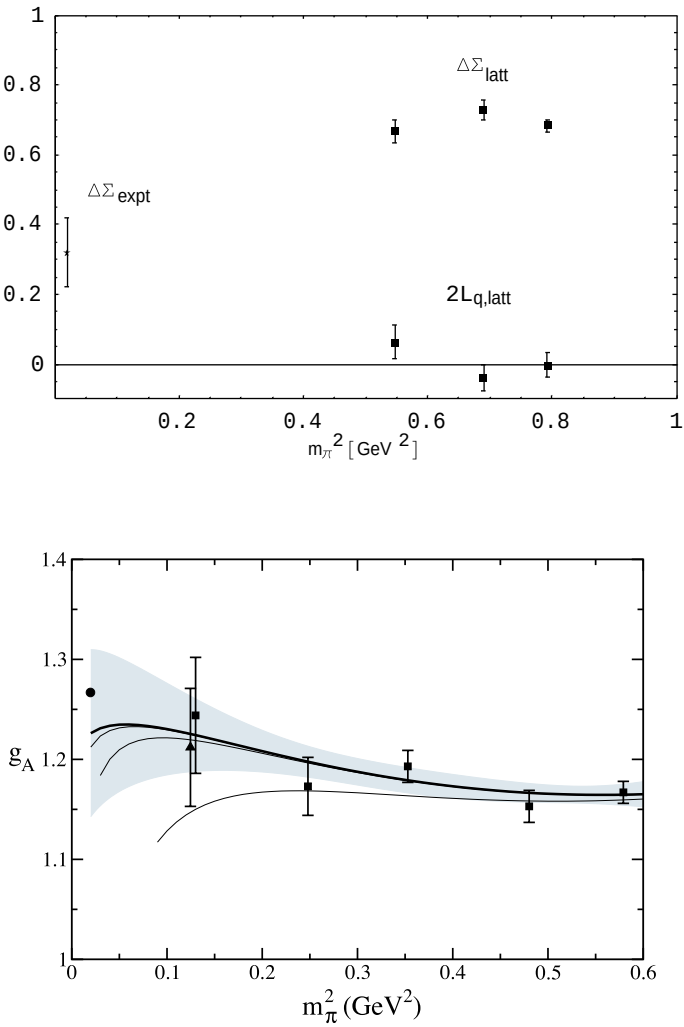

Fig. 8.1 Recent lattice results for the fraction of the proton spin arising from the quark spin $\Delta\Sigma$ and quark orbital angular momentum L_q. [Negele *et al.* (2004)] and $g_A^{(3)}$ [Edwards *et al.* (2006)]

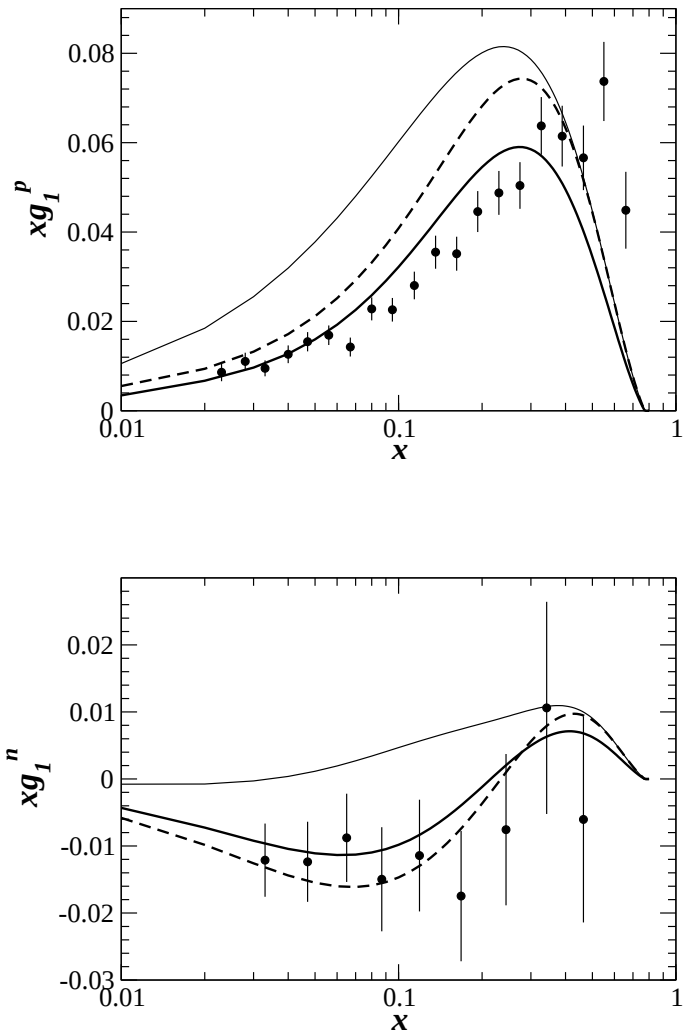

Fig. 8.2 Model predictions for the spin dependent structure functions xg_1^p and xg_1^n at $Q^2 = 2.5$ GeV^2 together with data from HERMES, from Bissey *et al.* (2006).

This page intentionally left blank

Chapter 9

THE SPIN-FLAVOUR STRUCTURE OF THE PROTON

9.1 The valence region and large x

The large x region (x close to one) is very interesting and particularly sensitive to the valence structure of the nucleon. Valence quarks dominate deep inelastic structure functions for large and intermediate x (greater than about 0.2). Experiments at Jefferson Lab are making the first precision measurements of the proton's spin structure at large x – see Figs. 9.1 and 9.2.

QCD motivated predictions for the large x region exist based on perturbative QCD counting rules and quarks models of the proton's structure based on SU(6) [flavour SU(3) $\otimes$ spin SU(2)] and scalar diquark dominance. We give a brief explanation of these approaches.

(1) Perturbative QCD counting rules predict that the parton distributions should behave as a power series expansion in $(1-x)$ when $x \to 1$ [Brodsky *et al.* (1995); Farrar and Jackson (1975)]. The fundamental principle behind these counting rules results is that for the leading struck quark to carry helicity polarized in the same direction as the proton the spectator pair should carry spin zero, whence they are bound through longitudinal gluon exchange. For the struck quark to be polarized opposite to the direction of the proton the spectator pair should be in a spin one state, and in this case one has also to consider the effect of transverse gluon exchange. Calculation shows that this is supressed by a factor of $(1-x)^2$. Further, the valence Fock states with the minimum number of constituents give the leading contribution to structure functions when one quark carries nearly all of the light-cone momentum; just on phase-space grounds alone, Fock states with a higher number of partons must give structure functions which fall off faster at $x \to 1$. We use $q^{\uparrow}(x)$ and $q^{\downarrow}(x)$ to denote the parton distributions polarized parallel and antiparallel to the polarized proton. One finds [Brodsky *et al.* (1995)]

$$q^{\uparrow\downarrow}(x) \to (1-x)^{2n-1+2\Delta S_z}, \quad (x \to 1) \tag{9.1}$$

Here n is the number of spectators and ΔS_z is the difference between the polarization of the struck quark and the polarization of the target nucleon.

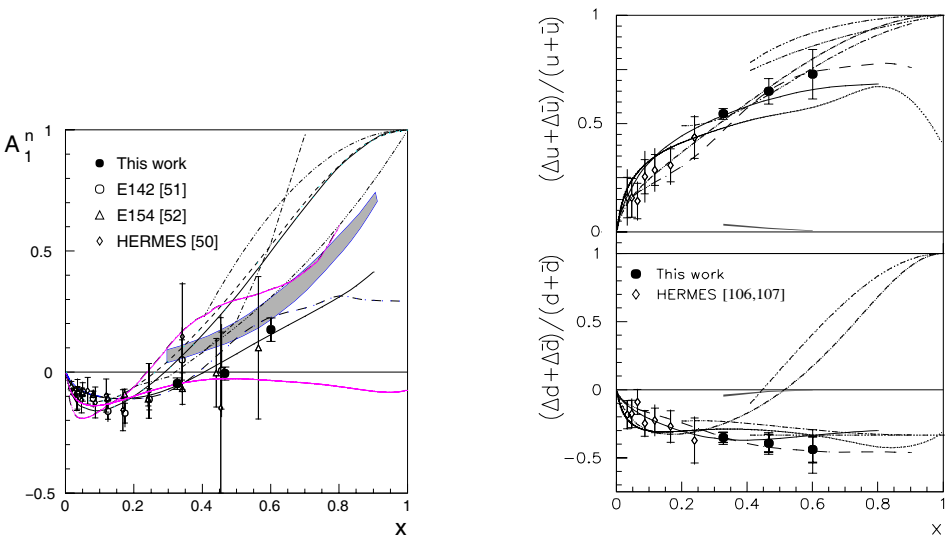

Fig. 9.1 Left: Recent data on $\mathcal{A}_1^n$ from the E99-117 experiment [Zheng *et al.* (2004a,b)]. Right: extracted polarization asymmetries for $u+\bar{u}$ and $d+\bar{d}$. For more details and references on the various model predictions, see Zheng *et al.* (2004a,b).

When $x \to 1$ the QCD counting rules predict that the structure functions should be dominated by valence quarks polarized parallel to the spin of the nucleon. The ratio of polarized to unpolarized structure functions should go to one when $x \to 1$. For the helicity parallel valence quark distribution one predicts

$$q^{\uparrow}(x) \sim (1-x)^3, \qquad (x \to 1) \tag{9.2}$$

whereas for the helicity anti-parallel distribution one obtains

$$q^{\downarrow}(x) \sim (1-x)^5, \qquad (x \to 1). \tag{9.3}$$

Sea distributions are suppressed and the leading term starts as $(1-x)^5$.

(2) Scalar diquark dominance is based on the observation that, within the context of the SU(6) wavefunction of the proton

$$|p\uparrow\rangle = \frac{1}{\sqrt{2}}|u\uparrow(ud)_{S=0}\rangle + \frac{1}{\sqrt{18}}|u\uparrow(ud)_{S=1}\rangle - \frac{1}{3}|u\downarrow(ud)_{S=1}\rangle$$

$$-\frac{1}{3}|d\uparrow(uu)_{S=1}\rangle + \frac{\sqrt{2}}{3}|d\downarrow(uu)_{S=1}\rangle, \tag{9.4}$$

one gluon exchange tends to make the mass of the scalar diquark pair lighter than the vector spin-one diquark combination. One-gluon exchange offers an

Table 9.1 QCD motivated model predictions for the large x limit of deep inelastic spin asymmetries and parton distributions.

Model	$\Delta u/u$	$\Delta d/d$	$\mathcal{A}_1^p$	$\mathcal{A}_1^n$	d/u
SU(6)	$\frac{2}{3}$	$-\frac{1}{3}$	$\frac{5}{9}$	0	$\frac{1}{2}$
Broken SU(6), scalar diquark	1	$-\frac{1}{3}$	1	1	0
QCD Counting Rules	1	1	1	1	$\frac{1}{5}$

explanation of the nucleon-Δ mass splitting and has the practical consequence that in model calculations of deep inelastic structure functions the scalar diquark term $\frac{1}{\sqrt{2}}|u\uparrow(ud)_{S=0}\rangle$ in Eq. (9.4) dominates the physics at large Bjorken x [Close and Thomas (1988)].

In the large x region (x close to one) where sea quarks and gluons can be neglected the neutron and proton spin asymmetries are given by

$$\mathcal{A}_1^n = \frac{\Delta u + 4\Delta d}{u + 4d},$$
$$\mathcal{A}_1^p = \frac{4\Delta u + \Delta d}{4u + d}. \tag{9.5}$$

in leading order QCD. Rearranging these expressions one obtains formulae for the separate up and down quark distributions in the proton:

$$\frac{\Delta u}{u} = \frac{4}{15}\mathcal{A}_1^p(4 + \frac{d}{u}) - \frac{1}{15}\mathcal{A}_1^n(1 + 4\frac{d}{u})$$
$$\frac{\Delta d}{d} = \frac{4}{15}\mathcal{A}_1^n(4 + \frac{u}{d}) - \frac{1}{15}\mathcal{A}_1^p(1 + 4\frac{u}{d}). \tag{9.6}$$

The predictions of perturbative QCD counting rules and scalar diquark dominance models for the large x limit of these asymmetries are given in Table 9.1. On the basis of both perturbative QCD *and* SU(6), one expects the ratio of polarized to unpolarized structure functions, $\mathcal{A}_{1n}$, should approach 1 as $x \to 1$ [Melnitchouk and Thomas (1996); Isgur (1999)].

Interesting measurements of the large x region are available from the Hall A and Hall B Collaborations at the Jefferson Laboratory. The Hall A Collaboration measurement of the neutron asymmetry $\mathcal{A}_1^n$ [Zheng *et al.* (2004a)] is shown in Fig. 9.1. These data show a clear trend for $\mathcal{A}_1^n$ to become positive at large x. The crossover point where $\mathcal{A}_1^n$ changes sign is particularly interesting because the value of x where this occurs in the neutron asymmetry is the result of a competition between the SU(6) valence structure [Close and Thomas (1988)] and chiral corrections [Schreiber and Thomas (1988); Steffens *et al.* (1995)]. Figure 9.2 also shows the extracted valence polarization asymmetries. The data are consistent with constituent quark models with scalar diquark dominance which predict $\Delta d/d \to -1/3$ at large x, while perturbative QCD counting rules predictions (which neglect quark orbital angular momentum) give $\Delta d/d \to 1$ and tend to deviate from the data, unless the convergence to 1 sets in very late. The Hall B measurements of the proton

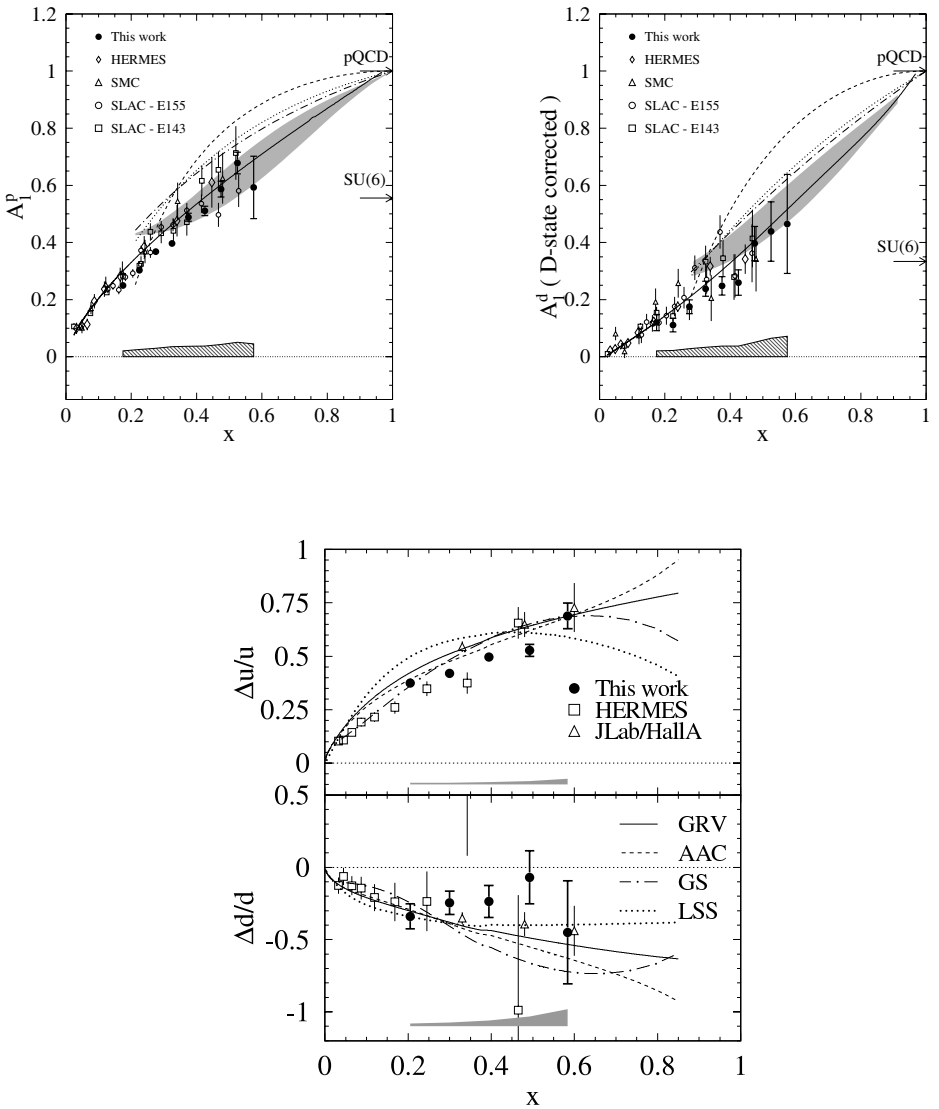

Fig. 9.2 JLab measurements from Hall B for the asymmetries $\mathcal{A}_1^p$ (above left) and $\mathcal{A}_1^d$ (above right). The quark polarizations $\Delta u/u$ and $\Delta d/d$ extracted from the data are shown below [Dharmawardane *et al.* (2006)]. Included are all data above $W = 1.77$ GeV and $Q^2 = 1$ GeV^2 and the results of various fits.

and deuteron large x asymmetries together with the extracted values of $\Delta u/u$ and $\Delta d/d$ are shown in Fig. 9.2 [Dharmawardane *et al.* (2006)]. The extracted values

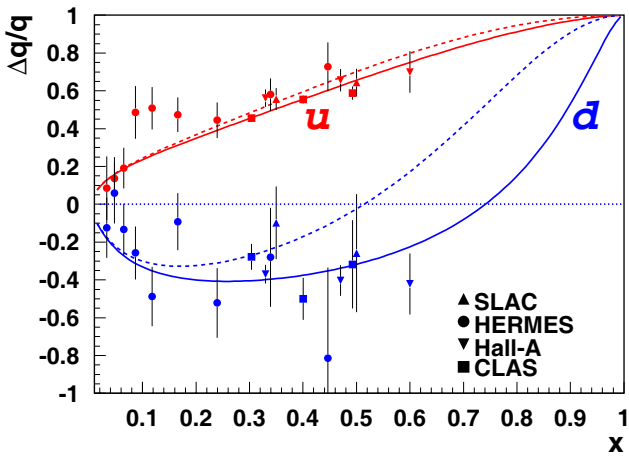

Fig. 9.3 Predictions for polarized quark distributions at large x with the inclusion of non-zero orbital angular momentum (solid curves) from Avakian *et al.* (2007).

of $\Delta d/d$ appear to deviate from the Hall A measurements in the larger x region, $x \sim 0.6$, and are less inconsistent with helicity counting rules predictions at large x.

Brodsky and collaborators [Avakian *et al.* (2007)] have recently argued that when one also includes valence Fock states with non-zero orbital angular momentum, one finds a large logarithm correction to the negative helicity quark distributions in addition to its power behaviour, scaling as

$$\sim (1-x)^5 \log^2(1-x) \tag{9.7}$$

The effect of including this contribution is illustrated in Fig. 9.3, and is consistent with the JLab measurements. An interesting prediction is that $\Delta d/d$ should cross zero at a value $x \sim 0.75$. A precision measurement of $\mathcal{A}_{1n}$ up to $x \sim 0.8$ will be possible following the 12 GeV upgrade of CEBAF and will provide valuable input to resolving these issues [Meziani (2002)].

9.2 The isovector part of g_1

Constituent quark model predictions for g_1 are observed to work very well in the isovector channel. First, as highlighted in Chapter 4, the Bjorken sum rule which relates the first moment of the isovector part of g_1, $(g_1^p - g_1^n)$, to the isovector axial charge $g_A^{(3)}$ has been confirmed in polarized deep inelastic scattering experiments at the level of 10% [Windmolders (1999)]. Second, looking beyond the first moment, one finds the following intriguing observation about the shape of $(g_1^p - g_1^n)$. Figure 9.4 shows $2x(g_1^p - g_1^n)$ (SLAC data) together with the isovector structure function

$(F_2^p - F_2^n)$ (NMC data from Arneodo *et al.* (1994)). In the QCD parton model one finds the leading order formulae[1]

$$2x(g_1^p - g_1^n) = \frac{1}{3}x\left[(u+\overline{u})^{\uparrow} - (u+\overline{u})^{\downarrow} - (d+\overline{d})^{\uparrow} + (d+\overline{d})^{\downarrow}\right] \tag{9.8}$$

and

$$(F_2^p - F_2^n) = \frac{1}{3}x\left[(u+\overline{u})^{\uparrow} + (u+\overline{u})^{\downarrow} - (d+\overline{d})^{\uparrow} - (d+\overline{d})^{\downarrow}\right]. \tag{9.9}$$

The ratio $R_{(3)} = 2x(g_1^p - g_1^n)/(F_2^p - F_2^n)$ is also plotted in Fig. 9.4. It measures the ratio of polarized to unpolarized isovector quark distributions.

The data reveal a large isovector contribution in g_1 and the ratio $R_{(3)}$ is observed to be approximately constant (at the value $\sim 5/3$ predicted by SU(6) constituent quark models) for x between 0.03 and 0.2, and goes towards one when $x \to 1$ (consistent with the prediction of both QCD counting rules and scalar diquark dominance models). The small x part of this data is very interesting. The area under $(F_2^p - F_2^n)/2x$ is determined by the Gottfried integral [Gottfried (1967); Arneodo *et al.* (1994)]

$$\begin{aligned} I_G &= \int_0^1 dx \left(\frac{F_2^p - F_2^n}{x}\right) \\ &= \frac{1}{3}\int_0^1 dx \left(u_V(x) - d_V(x)\right) + \frac{2}{3}\int_0^1 dx \left(\overline{u}(x) - \overline{d}(x)\right) \end{aligned} \tag{9.10}$$

which measures SU(2) flavour asymmetry in the sea, and is about 25% suppressed relative to the simple SU(6) prediction (by the pion cloud [Thomas (1983)], Pauli blocking [Field and Feynman (1977)], ...). The area under $(g_1^p - g_1^n)$ is fixed by the Bjorken sum rule (and is also about 25% suppressed relative to the SU(6) prediction – the suppression here being driven by relativistic effects in the nucleon and by perturbative QCD corrections to the Bjorken sum-rule). Given that perturbative QCD counting rules or scalar diquark models work and assuming that the ratio $R_{(3)}$ takes the constituent quark prediction at the canonical value of $x \sim \frac{1}{3}$, one finds [Bass (1999)] that the observed shape of $g_1^p - g_1^n$ is almost required to reproduce the area under the Bjorken sum rule (which is determined by the physical value of $g_A^{(3)}$ — a non-perturbative constraint)! The isovector part of g_1 has a valence-like small-x behaviour $g_1^{(p-n)} \sim x^{-0.5}$ in the presently measured kinematics. The constant ratio in the low to medium x range contrasts with the naive Regge prediction using a_1 exchange (and no hard-pomeron a_1 cut) that the ratio $R_{(3)}$ should fall and be roughly proportional to x as $x \to 0$. It would be very interesting to have precision

[1] In a full description one should also include the perturbative QCD Wilson coefficients for the non-singlet spin difference and spin averaged cross-sections. However, the effect of these coefficients makes a non-negligible contribution to the deep inelastic structure functions only at $x < 0.05$ and is small in the kinematics where there is high Q^2 spin data. There is no gluonic or singlet pomeron contributions to the isovector structure functions $(g_1^p - g_1^n)$ and $(F_2^p - F_2^n)$.

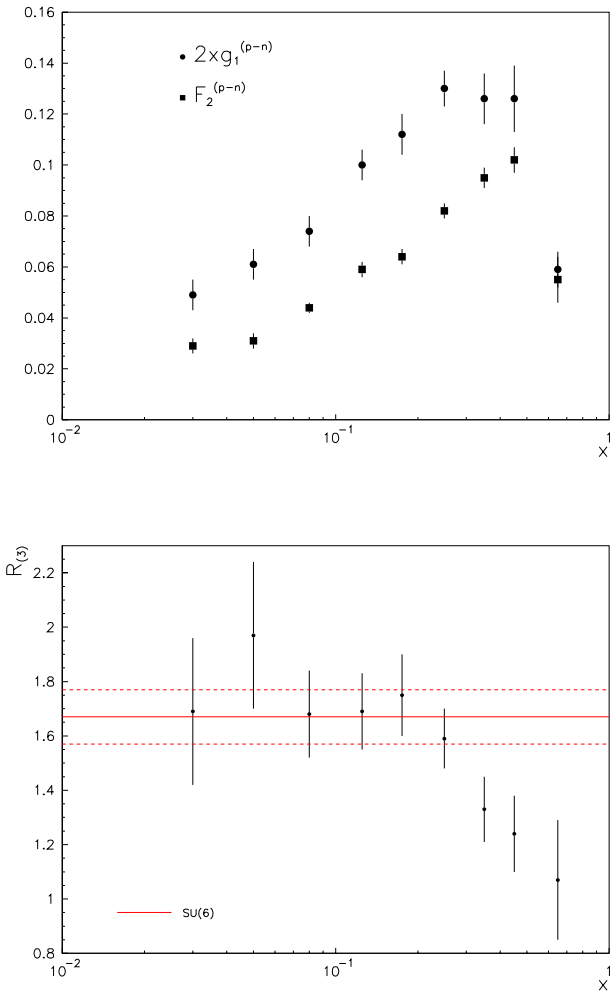

Fig. 9.4 Above: the isovector structure functions $2xg_1^{(p-n)}$ (SLAC data) and $F_2^{(p-n)}$ (NMC). Below: the ratio $R_{(3)} = 2xg_1^{(p-n)}/F_2^{(p-n)}$ from Bass (1999).

measurements of g_1 at high energy and low Q^2 from a future polarized ep collider to test the various scenarios how small x dynamics might evolve through the transition region and the application of spin dependent Regge theory.

This page intentionally left blank

Chapter 10

QCD FITS TO g_1 DATA

In deep inelastic scattering experiments the different x data points on g_1 are each measured at different values of Q^2, *viz.* $x_{\rm expt.}(Q^2)$. One has to evolve these experimental data points to the same value of Q^2 in order to test the Bjorken and Ellis-Jaffe sum-rules.

Next-to-leading order (NLO) QCD-motivated fits taking into account the scaling violations associated with perturbative QCD are used to evolve all the data points to the same Q^2 using DGLAP evolution. The results of these fits are then extrapolated to $x \sim 0$ to test spin sum-rules. The strategy is then to parameterize the parton distributions at some initial scale $Q^2 = Q_0^2$, and to determine the parameters by evolving the parton densities to (usually, larger) Q^2 and by comparing to experimental data for $g_1(x, Q^2)$. Thus the polarized gluon distribution $\Delta g(x, Q^2)$ can in principle be obtained from a QCD fit to the world data on the g_1 spin structure function.

The scale λ^2 dependence of the parton distributions is given by the DGLAP equations discussed in Chapter 3. The flavour singlet parton distributions evolve as

$$\begin{aligned}
\frac{d}{dt}\Delta\Sigma(x,t) &= \frac{\alpha_s(t)}{2\pi}\left[\int_x^1 \frac{dy}{y}\Delta P_{qq}(\frac{x}{y})\Delta\Sigma(y,t) + \ 2f\int_x^1 \frac{dy}{y}\Delta P_{qg}(\frac{x}{y})\Delta g(y,t)\right] \\
\frac{d}{dt}\Delta g(x,t) &= \frac{\alpha_s(t)}{2\pi}\left[\int_x^1 \frac{dy}{y}\Delta P_{gq}(\frac{x}{y})\Delta\Sigma(y,t) + \quad \int_x^1 \frac{dy}{y}\Delta P_{gg}(\frac{x}{y})\Delta g(y,t)\ \right]
\end{aligned} \tag{10.1}$$

where $\Delta\Sigma(x,t) = \sum_q \Delta q(x,t)$ and $t = \ln\lambda^2$ and the non-singlet term evolves as

$$\frac{d}{dt}\Delta q_3(x,t) = \frac{\alpha_s(t)}{2\pi}\int_x^1 \frac{dy}{y}\Delta P_{qq}(\frac{x}{y})\Delta q_3(y,t) \tag{10.2}$$

The DGLAP splitting functions P_{ij} have the nice physical interpretation of being the probability of finding a parton i in a parton j at a scale λ^2 [Altarelli and Parisi (1977)].

The spin dependent splitting functions ΔP_{ij} in Eqs. (10.1) and (10.2) have been calculated at leading-order by Altarelli and Parisi (1977) and at next-to-leading order by Zijlstra and van Neerven (1994), Mertig and van Neervan (1996)

and Vogelsang (1996). The leading order expressions are

$$\Delta P_{qq} = C_2(R)\left[\frac{1+z^2}{(1-z)_+} + \frac{3}{2}\delta(z-1)\right]$$
$$\Delta P_{qg} = \frac{1}{2}\left[z^2 - (1-z)^2\right] = \frac{1}{2}\left[2z-1\right]$$
$$\Delta P_{gq} = C_2(R)\frac{1-(1-z)^2}{z}$$
$$\Delta P_{gg} = C_2(G)\left[(1+z)^4\left(\frac{1}{z} + \frac{1}{(1-z)_+}\right) - \frac{(1-z)^3}{z} + \left(\frac{11}{6} - \frac{2}{3}\frac{T(R)}{C_2(G)}\right)\delta(1-z)\right] \tag{10.3}$$

Note that each of these spin-dependent splitting-functions are regular and go to a constant as $z \to 0$. Here, the constants (QCD group factors) are defined as follows. Let $t_a = \frac{1}{2}\lambda_a$ where λ_a are the Gell-Mann matrices satisfying the SU(3) algebra $[t^a, t^b] = if_{abc}t^c$. Then

$$\text{Tr } t_a t_b = T(R)\delta_{ab} = \frac{1}{2}\delta_{ab}$$
$$\sum_a^8 \sum_k^N t^a_{ik} t^a_{kj} = C_2(R)\delta_{ij} = \frac{4}{3}\delta_{ij}$$
$$\sum_{c,d}^8 f_{acd} f_{bcd} = C_2(G)\delta_{ab} = 3\delta_{ab} \tag{10.4}$$

The leading-order splitting functions ΔP_{qq} and ΔP_{qg} satisfy the equations

$$\int_0^1 dz\ \Delta P_{qq}(z) = \int_0^1 dz\ \Delta P_{qg}(z) = 0 \tag{10.5}$$

corresponding to chirality conservation.

Similar to the analysis that is carried out on unpolarized data, global NLO perturbative QCD analyses have been performed on the polarized structure function data sets. The aim is to extract the polarized quark and gluon parton distributions. These QCD fits are performed within a given factorization scheme, e.g. the "AB", chiral invariant (CI) or JET and $\overline{\text{MS}}$ schemes.

Let us briefly review these different factorization schemes.

Different factorization schemes correspond to different procedures for separating the phase space for photon-gluon fusion into "hard" and "soft" contributions in the convolution formula Eq. (3.33). In the QCD parton model analysis of photon gluon fusion that we discussed in Section 6.5 using the cut-off on the transverse momentum squared, the polarized gluon contribution to the first moment of g_1 is associated with two-quark jet events carrying $k_t^2 \sim Q^2$. The gluon coefficient function is given by $C_{\text{PM}}^{(g)} = g_1^{(\gamma^* g)}|_{\text{hard}}$ where $g_1^{(\gamma^* g)}|_{\text{hard}}$ is taken from Eq. (6.32) with $Q^2 \geq \lambda^2$ and $\lambda^2 \gg P^2, m^2$. This transverse-momentum cut-off scheme is sometimes called the "chiral invariant" (CI) [Cheng (1996)] or JET [Leader *et al.* (1998)] scheme.

Different schemes can be defined relative to this k_t cut-off scheme by the transformation

$$C^{(g)}\left(x,\frac{Q^2}{\lambda^2},\alpha_s(\lambda^2)\right) \;\rightarrow\; C^{(g)}\left(x,\frac{Q^2}{\lambda^2},\alpha_s(\lambda^2)\right) - \tilde{C}^{(g)}_{\rm scheme}\left(x,\alpha_s(\lambda^2)\right). \qquad (10.6)$$

Here $\tilde{C}^{(g)}_{\rm scheme}$ shall be $\frac{\alpha_s}{\pi}$ times a polynomial in x. The parton distributions transform as

$$\begin{aligned}\Delta\Sigma(x,\lambda^2)_{\rm scheme} &= \Delta\Sigma(x,\lambda^2)_{\rm PM}\\ &\quad + f\int_x^1 \frac{dz}{z}\Delta g(\frac{x}{z},\lambda^2)_{\rm PM}\tilde{C}^{(g)}_{\rm scheme}(z,\alpha_s(\lambda^2))\\ \Delta g(x,\lambda^2)_{\rm scheme} &= \Delta g(x,\lambda^2)_{\rm PM}\end{aligned} \qquad (10.7)$$

so that the physical structure function g_1 is left invariant under the change of scheme. The virtuality and invariant-mass cut-off versions of the parton model that we discussed in Chapter 6 correspond to different choices of scheme.[1]

The $\overline{\rm MS}$ and AB (Adler-Bardeen) schemes are defined as follows. In the $\overline{\rm MS}$ scheme the gluonic hard scattering coefficient is calculated using the operator product expansion with $\overline{\rm MS}$ renormalisation ['t Hooft and Veltman (1972)]. One finds [Cheng (1996); Bass (1992a)]:

$$C^{(g)}_{\overline{\rm MS}} = C^{(g)}_{\rm PM} \;+\; \frac{\alpha_s}{\pi}(1-x). \qquad (10.8)$$

In this scheme $\int_0^1 dx\; C^{(g)}_{\overline{\rm MS}} = 0$ so that $\int_0^1 dx\;\Delta g(x,\lambda^2)$ decouples from $\int_0^1 dx g_1$. This result corresponds to the fact that there is no gauge-invariant twist-two, spin-one, gluonic operator with $J^P = 1^+$ to appear in the operator product expansion for the first moment of g_1. In the $\overline{\rm MS}$ scheme the contribution of $\int_0^1 dx\;\Delta g$ to the first moment of g_1 is included into $\int_0^1 dx\;\Sigma_{\overline{\rm MS}}(x,\lambda^2)$. The AB scheme [Ball *et al.* (1996)] is defined by the formal operation of adding the x-independent term $-\frac{\alpha_s}{2\pi}$ to the $\overline{\rm MS}$ gluonic coefficient, *viz.*

$$C^{(g)}_{\rm AB}(x) = C^{(g)}_{\overline{\rm MS}} \;-\; \frac{\alpha_s}{2\pi}. \qquad (10.9)$$

In the $\overline{\rm MS}$ scheme the polarized gluon distribution does not contribute explictly to the first moment of g_1. In the AB and JET schemes on the other hand the polarized gluon (axial anomaly contribution) $\alpha_s\Delta g$ does contribute explicitly to the first moment since $\int_0^1 dx\; C^{(g)} = -\frac{\alpha_s}{2\pi}$.

The first attempts to extract information about gluon polarization in the polarized nucleon used next-to-leading order (NLO) QCD motivated fits to inclusive g_1 data.

[1] Note that the invariance of g_1 under a change of scheme can be violated by topological effects in the scenario where axial U(1) symmetry is spontaneously broken by instantons. There, quark instanton interactions produce a $\delta(x)$ term in g_1 which is not present in the explicit symmetry breaking scenario. See Chapter 6.

Typically, the input parametrisations are written as

$$\Delta F_k = \eta_k \frac{x^{\alpha_k}\,(1-x)^{\beta_k}\,(1+\gamma_k x)}{\int_0^1 x^{\alpha_k}\,(1-x)^{\beta_k}\,(1+\gamma_k x)dx}\,, \tag{10.10}$$

where ΔF_k represents each of the singlet, isovector and octet polarized quark distributions $\Delta\Sigma$, Δq_3, Δq_8 and the polarized gluon distribution Δg; η_k is the first moment of ΔF_k. The moments, η_k, of the non-singlet distributions Δq_3 and Δq_8 are fixed by the values extracted from neutron and hyperon β-decays, *viz.* F+D and 3F-D respectively assuming SU(3) flavour symmetry. The positivity of the distributions ($|\Delta q_i(x)| \leq q_i(x)$) is also enforced. Typical polarized distributions extracted from the fits are shown in Fig. 10.1. Given the uncertainties in the fits associated in part with the ansatz chosen for the shape of the spin-dependent quark and gluon distributions at a given input scale, values of Δg were extracted from the pre-COMPASS and pre-RHIC data ranging between about zero and +2. The main source of error in the QCD fits comes from lack of knowledge about g_1 in the small x region and (theoretical) the functional form chosen for the quark and gluon distributions in the fits.

New fits are now being produced taking into account all the available data including new data from polarized semi-inclusive deep inelastic scattering and the $pp \to \pi^0 X$ process in polarized proton-proton collisions at RHIC.

For a most recent fit to all inclusive g_1 data with $Q^2 > 1$ GeV^2 using the MS scheme COMPASS evolved the data to a common value $Q^2 = 3$ GeV^2 and obtained

$$g_A^{(0)}|_{\rm pDIS} = 0.35 \pm 0.03({\rm stat.}) \pm 0.05({\rm syst.}) \tag{10.11}$$

for the COMPASS data alone and

$$g_A^{(0)}|_{\rm pDIS} = 0.30 \pm 0.01({\rm stat.}) \pm 0.02({\rm evol.}) \tag{10.12}$$

for the world data. The COMPASS result corresponds to

$$g_A^{(0)}|_{\rm pDIS,Q^2\to\infty} = 0.33 \pm 0.03({\rm stat.}) \pm 0.05({\rm syst.}) \tag{10.13}$$

and polarized strangeness

$$\Delta s_{Q^2\to\infty} = \frac{1}{3}(g_A^{(0)}|_{\rm pDIS,Q^2\to\infty} - g_A^{(8)}) = -0.08 \pm 0.01({\rm stat.}) \pm 0.02({\rm syst.}) \tag{10.14}$$

Two good solutions for $\Delta g(x, Q^2)$ were found: one with a positive first moment Δg and one with a negative first moment – see Fig. 10.2. For both fits the absolute value was $|\Delta g| \simeq 0.2 - 0.3$ for $Q_0^2 = 3$ GeV^2 and the uncertainty from the fit was ~ 0.1. Contributions to the error arising from uncertainties in the factorization and renormalization scales as well as the influence of the particular parametrisation chosen for the distribution functions, were not considered. It is also interesting to note that the polarized strangeness distribution, $\Delta s(x) = \frac{1}{3}(\Delta\Sigma - \Delta q_8)(x)$, extracted from these fits (assuming no subtraction at infinity in the g_1 dispersion relation) is almost completely polarized at the large x threshold where it turns on.

The polarized gluon distribution extracted from this procedure is determined just through scaling violations in $g_1^{p,n}$. Present polarized deep inelastic data comes only from fixed target experiments which have a limited lever arm in Q^2, limiting the accuracy of the fitting procedure. This contrasts with unpolarized deep inelastic scattering where HERA and fixed-target data combined offer a large range in x and Q^2. Here the QCD fits rely largely on the rather small difference in Q^2 between the SLAC and HERMES data on one side and the SMC and COMPASS data on the other, spanning centre of mass energies from 8 GeV to 20 GeV. Future polarized ep collider data would expand the range of small x measurements and the lever arm in Q^2.

To go further more direct measurements involving glue sensitive observables are needed to really extract the magnitude of Δg and the shape of $\Delta g(x, Q^2)$ including any possible nodes in the distribution function. Also, the first moments depend on integrations from $x = 0$ to 1. Perhaps there is an additional component at very small x?

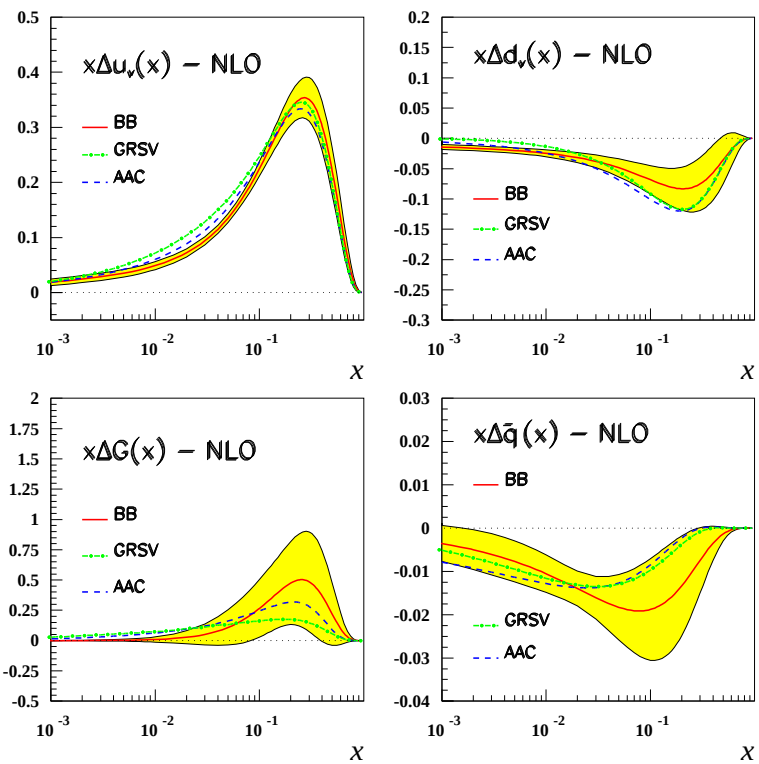

Fig. 10.1 Polarized parton distribution functions from NLO pQCD ($\overline{\text{MS}}$) fits at $Q^2 = 4\text{GeV}^2$ using SU(3) flavour assumptions [Stoesslein (2002)].

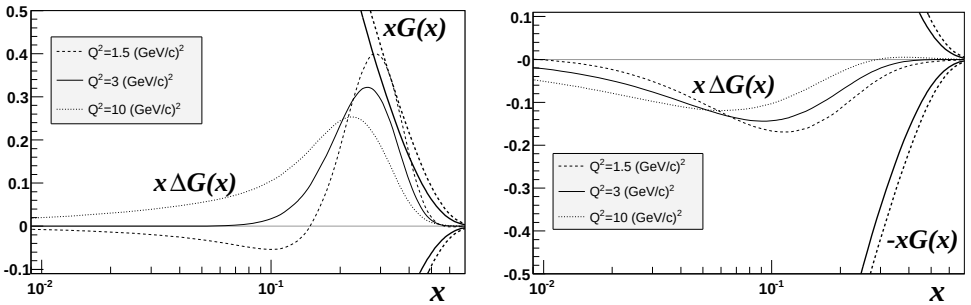

Fig. 10.2 The polarized gluon distribution $x\Delta g(x)$ corresponding to the fits with $\Delta g > 0$ (left) and $\Delta g < 0$ (right) in the COMPASS fits [Alexakhin *et al.* (2007a)].

10.1 Regge theory and perturbative evolution at small x

The application of perturbative QCD and evolution at small Bjorken x is an interesting topic. Regge phenomenology predicts that the structure functions should behave as $x^{-\alpha}$ where α is the leading Regge intercept. Perturbative DGLAP evolution acts to move the area under the structure function towards smaller x. Hence the question: Are the effective Regge intercepts which describe deep inelastic sctructure functions are Q^2 dependent or not?

Regge and small x physics has been vigorously studied in the context of HERA and is important for predicting the LHC total cross-section. There are various models and approaches which depend on whether the hard pomeron observed at HERA should be treated as a distinct exchange [Donnachie and Landshoff (1998)]. Predictions for the LHC total cross-section range from about 90 mb up to about 150 mb with the larger values associated with a distinct hard-pomeron [Godbole *et al.* (2006); Landshoff (2005)]. Can we use present information from polarized processes to help constrain models of Regge and small x dynamics and is there evidence in polarized data for distinct hard exchanges? [Bass (2007a)]

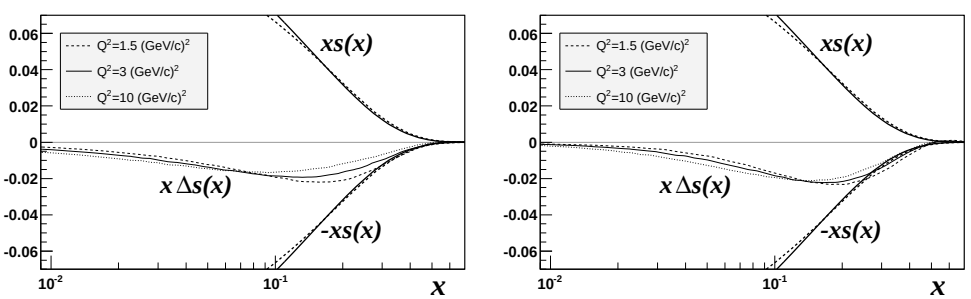

Fig. 10.3 The polarized strange quark distribution $x\Delta s(x)$ corresponding to the COMPASS NLO QCD fits with $\Delta g > 0$ (left) and $\Delta g < 0$ (right) [Alexakhin *et al.* (2007a)].

Models of small x physics generally fall into two clases. First consider unpolarized scattering. The first approach [Martin *et al.* (2000); Pumplin *et al.* (2002)] involves a soft-pomeron and perturbative QCD evolution (DGLAP, $\alpha_s^n \ln^m \frac{1}{x}$ ... resummation) which drives the increase in the effective intercept α, $F_2 \sim x^{-\alpha}$, from the soft-pomeron value 0.08 to the value ~ 0.4 extracted from HERA data [Adloff *et al.* (1997); Breitweg *et al.* (1997)]. In a second approach Cudell *et al.* (1999) – see also Donnachie and Landshoff (2002) – have argued that the Regge intercepts should be independent of Q^2 and that the HERA data is described by a distinct hard-pomeron exchange in addition to the soft-pomeron. The hard pomeron should also appear in low Q^2 photoproduction data and in proton-proton collisions. There are two conflicting measurements of the total cross-section at the Tevatron [Amos *et al.* (1989); Abe *et al.* (1994)]. The larger CDF measurement favours a separate hard pomeron contribution.

Is there a place in polarized data where similar physics issues occur? There are interesting clues in the data. The rise in $g_1^{p-n} \sim x^{-0.5}$ poses a challenge for Regge predictions and perturbative QCD. Recalling Chapter 2, the Regge prediction for g_1^{p-n} at small x is

$$g_1^{p-n} \sim \sum_i f_i \left(\frac{1}{x}\right)^{\alpha_i}. \tag{10.15}$$

Here the α_i denote the Regge intercepts for isovector a_1 Regge exchange and the a_1-pomeron cuts [Heimann (1973)]. The coefficients f_i are to be determined from experiment. If one makes the usual assumption that the a_1 Regge trajectories are straight lines parallel to the (ρ, ω) trajectories then one finds $\alpha_{a_1} \simeq -0.4$ for the leading trajectory, within the phenomenological range $-0.5 \leq \alpha_{a_1} \leq 0$ discussed in Ellis and Karliner (1988). Taking the masses of the $a_1(1260)$ and $a_3(2070)$ states together with the $a_1(1640)$ and $a_3(2310)$ states from the Particle Data Group (2004) yields two parallel a_1 trajectories with slope $\sim 0.75\text{GeV}^{-2}$ and a leading trajectory with slightly lower intercept: $\alpha_{a_1} \simeq -0.18$. For this value of α_{a_1} the effective intercepts corresponding to the a_1 soft-pomeron cut and the a_1 hard-pomeron cut are $\simeq -0.1$ and $\simeq +0.22$ respectively *if* one takes the soft and hard pomerons as two distinct exchanges. Values of α_{a_1} close to zero could be achieved with curved Regge trajectories; the recent model of Brisudova *et al.* (2000) predicts $\alpha_{a_1} = -0.03 \pm 0.07$. For this value the intercepts of the a_1 soft-pomeron cut and the a_1 hard-pomeron cut become $\sim +0.05$ and $\sim +0.37$. The a_1 and a_1 soft-pomeron cut alone are unable to account for the data.[2]

Does the observed rise in $g_1^{(p-n)}$ follow from a_1 exchange plus perturbative QCD evolution or is there a distinct hard exchange? – that is, a polarized analogue

[2]It should be noted that, in the measured x range, the effective isovector exponent 0.5 could be softened through multiplication by a $(1-x)^n$ factor – for example associated with perturbative QCD counting rules at large x (x close to one). For example, the exponent $x^{-0.5}$ could be modified to about $x^{-0.25}$ through multiplication by a factor $(1-x)^6$. However, this is not sufficient to reconcile the measured rising structure function with the naive Regge prediction involving soft a_1 exchange.

of the one *or* two pomerons question! The difference between the effective intercept describing g_1^{p-n} at deep inelastic values of Q^2 and the prediction based on soft a_1 exchange is a factor of up to 2-3 bigger than the difference in the effective intercept needed to describe F_2 in the unpolarized HERA data and the soft-pomeron prediction.

In the conventional approach the a_1 term (or a_1 soft-pomeron cut) should describe the high-energy part of g_1 close to photoproduction and provide the input for perturbative QCD evolution at deep inelastic values of Q^2 above the transition region. One then applies perturbative QCD (DGLAP or DGLAP plus double logarithm $\ln^2 \frac{1}{x}$ ... resummation) and out should come the rising structure function seen in the data. For g_1^{p-n} with DGLAP evolution this approach has the challenging feature that the input and output (at soft and hard scales) are governed by non-perturbative constraints with perturbative QCD evolution in the middle unless the a_1 Regge input has information about $g_A^{(3)}$ built into it. (Furthermore, perturbative $\alpha_s^{l+1} \ln^{2l} x$ resummation calculations predict a sharp rise [Badelek and Kwiecinski (1998); Ziaja (2003); Ermolaev *et al.* (2005)] $\sim x^{-\gamma}$ with $\gamma \sim 0.9$ in the absolute value of the isosinglet spin structure function g_1^d which is not observed in the present data. The measured structure function is consistent with zero for x between the lowest value 0.004 and 0.05 (Fig. 2.9 and [Alexakhin *et al.* (2007a)]), and the integral $\int_{x_{\min}}^1 dx g_1^d$ is observed to converge within the errors for $x_{\min} \sim 0.05$ (Fig. 4.2 and Airapetian *et al.* (2007)).) The alternative scenario is a separate hard-exchange contribution (perhaps an a_1 hard-pomeron cut) in addition to the soft a_1.

Some guidance may come from looking at the QCD evolution equations in moment space. We first consider the perturbative DGLAP approach since this is presently the prime tool used to analyse polarized deep inelastic data.

Let $\Delta q_3(x,t) = (\Delta u - \Delta d)(x,t)$ denote the isovector spin-dependent parton distribution with $t = \ln \frac{Q^2}{\Lambda^2}$; $\int_0^1 dx \Delta q_3(x,t) = g_A^{(3)}$. The DGLAP equation for $\Delta q_3(x,t)$ is

$$\frac{d}{dt}\Delta q_3(x,t) = \frac{\alpha_s(t)}{2\pi} \int_x^1 \frac{dy}{y} \Delta P\left(\frac{x}{y}\right) \Delta q_3(y,t) \tag{10.16}$$

where

$$\Delta P(z) = C_2(R)\left[\frac{1+z^2}{(1-z)_+} + \frac{3}{2}\delta(z-1)\right] \tag{10.17}$$

is the leading-order spin-dependent splitting function; $C_2(R) = \frac{4}{3}$ and $\Delta P(z)$ goes to a constant as $z \to 0$. The area under $\Delta q_3(x,t)$ is conserved because of the Bjorken sum-rule. DGLAP evolution acts to shift the weight of the distribution and g_1^{p-n} to smaller x with increasing Q^2, meaning that a convergent input will be unstable to DGLAP evolution at a given value of small x [Altarelli *et al.* (1997)] and prompting the question at what values of Q^2 and small x should spin-dependent Regge predictions work in this approach, if any?

The evolution equation (10.16) becomes "singular" in the $x \to 0$ limit if Δq_3 behaves as a constant for $x \to 0$:

$$\text{convolution} \sim \int_x^1 \frac{dy}{y}\Big\{ ... \Big\}. \tag{10.18}$$

This compares with the singlet channel in unpolarized scattering where the splitting matrix has a $1/z$ singularity as z goes to zero for evolution into gluons. If the unpolarized gluon distribution were to have a leading $1/y$ pole then the contribution

$$\Delta P\left(\frac{x}{y}\right) g(y) \sim \frac{y}{x}.\frac{1}{y} \tag{10.19}$$

would yield the same structure in the evolution equation.

Take the Mellin transform $\int_0^1 dz z^{N-1} \Delta P(z)$:

$$P(N, \alpha_s(Q^2)) = \int_0^1 dz z^{N-1} \Delta P(z) = C_2(R)\left[-\frac{1}{2} + \frac{1}{N(N+1)} - 2\sum_{j=2}^{N}\frac{1}{j}\right]. \tag{10.20}$$

The zeroth moment of the DGLAP splitting function has a pole at $N = 0$ at leading order (LO) plus higher-order poles at NLO [Glück *et al.* (1996)]. *If* we require that the scattering amplitude is analytic in Q^2 [Eden *et al.* (2002)], then Regge singularities are independent of Q^2 and new singularities should not suddenly appear as Q^2 increases. This result has practical consequences for singularities in the Mellin transform of the DGLAP splitting function: the $N = 0$ poles become an artifact of the perturbative expansion. That is, they should vanish in a full (non-perturbative) resummation [Cudell *et al.* (1999); Donnachie and Landshoff (2002)] otherwise one will generate an unphysical fixed pole $\alpha = 0$ contribution in the isovector part of g_1 as soon as one reaches large enough Q^2 to apply DGLAP evolution. To see this, consider the Mellin transform of the spin dependent parton distribution

$$u(N, Q^2) = \int_0^1 dx x^{N-1} \Delta q_3(x, Q^2/\Lambda^2) \tag{10.21}$$

and its DGLAP equation

$$\frac{\partial}{\partial t} u(N, Q^2) = P(N, \alpha_s(Q^2)) u(N, Q^2). \tag{10.22}$$

If the twist-two term $u(N, Q^2)$ has no pole at $N = 0$ at Q^2 values close to photoproduction, then the solution to the DGLAP equation

$$u(N, Q^2) = \exp\left[\ C\ \log\frac{\log(Q^2/\Lambda^2)}{\log(Q_0^2/\Lambda^2)}\ P(N)\ \right] u(N, Q_0^2) \tag{10.23}$$

automatically generates an essential singularity in $u(N, Q^2)$ at $N = 0$ as soon as Q^2 becomes large enough for the application of perturbative QCD; $C = 6/(33 - 2f)$ where f is the number of active flavours. This is not allowed if we assume that $u(N, Q^2)$ is analytic at $N = 0$ for some finite range of Q^2. It cannot suddenly acquire a fixed singularity at $N = 0$ when it is analytically continued in Q^2. To

help understand $P(N)$, Donnachie and Landshoff (2003) consider the example of the analogous expansion of the function $\psi(N,\alpha_s) = \sqrt{N^2+\alpha_s} - N = \frac{\alpha_s}{2N} - \frac{\alpha_s^2}{8N^3} + ...$ Although each term in the expansion is singular at $N=0$, the function ψ is not: the expansion is valid only for $|N| > \alpha_s$. (Related issues in unpolarized scattering are discussed in Altarelli *et al.* (2006) where a new small x splitting function has been proposed with no $1/N$ pole in the Mellin transform.)

The first moment of $\Delta P(z)$ vanishes, $P(1,\alpha_s) = 0$, corresponding to the conserved axial-charge $g_A^{(3)}$. The positive odd moments of the DGLAP splitting function correspond to the anomalous dimensions of axial-tensor operators in the light-cone operator product expansion for deep inelastic scattering. There are no operators corresponding to the poles at $N=0$ or $N=-1$.

Going beyond DGLAP evolution, Blümlein and Vogt (1996) have considered the resummation of $\alpha_s^{l+1} \ln^{2l} x$ terms in the evolution kernels of non-singlet contributions to g_1. An all orders resummation of these terms in perturbation theory leads only to corrections of 1% for g_1^{p-n} relative to NLO calculations in the kinematics accessible to present experiments. The most singular contributions in the perturbation expansion behave like a power series in $N(\alpha_s/N^2)^k$ when we take the Mellin transform and work with the moments. The perturbative expansion assumes that $\alpha_s < 3\pi N^2/8$. Like for the DGLAP procedure discussed above, each term in the perturbative expansion is singular for $N=0$ in moment space. One again encounters the issue of whether the isovector g_1^{p-n} structure function is analytic at $N=0$ for finite Q^2.

Motivated by this discussion we consider a hard exchange "input" to perturbative evolution. For a fixed power behaviour $u(x,t) \sim f(Q^2)x^{-\epsilon}$ the Mellin transform is $u(N,Q^2) \sim \frac{f(Q^2)}{N-\epsilon}$. Substituting this into the DGLAP equation and equating the coefficient of the pole gives an equation for the coefficent of the Regge exponent:

$$\frac{\partial}{\partial t} f(Q^2) = P(N=\epsilon, \alpha_s(Q^2))\ f(Q^2). \tag{10.24}$$

If there is a hard exchange with fixed intercept away from the pole at $\epsilon = 0$, e.g. $\epsilon = 0.5$ or perhaps ~ 0.2 for the a_1 hard-pomeron cut (plus $(1-x)^n$ counting rules factors still at work in the measured x range), then a combined Regge-DGLAP approach should be a good approximation – just as a distinct hard pomeron would resolve challenging issues in the interpretation of the unpolarized structure function. Further, if the intercept is Q^2 independent the issue of reconciling the Regge input to perturbative QCD evolution and the Bjorken sum rule constraint would be resolved. The hard exchange could be looked for in low Q^2 data – see below.

In the isosinglet sector it is harder to draw firm conclusions. g_1^{p+n} is small and consistent with zero in the measured small x data from COMPASS – see Fig. 2.9. The Regge prediction involves a contribution $\sim \{2\ln\frac{1}{x} - 1\}$ from two non-perturbative gluon exchange [Bass and Landshoff (1994); Close and Roberts (1994)] plus contributions from the f_1 trajectory and f_1-pomeron cuts. It is un-

known whether the gluon exchange contribution Reggeizes or whether it is a fixed pole. In the singlet channel the Mellin transforms of the DGLAP splitting functions are

$$\begin{aligned}
\int_0^1 dz z^{N-1}\Delta P_{qq}(z) &= C_2(R)\left[-\frac{1}{2}+\frac{1}{N(N+1)}-2\sum_{j=2}^{N}\frac{1}{j}\right]\\
\int_0^1 dz z^{N-1}2f\Delta P_{qg}(z) &= 4T(R)C_2(R)\frac{N+2}{N(N+1)}\\
\int_0^1 dz z^{N-1}\Delta P_{gq}(z) &= 2T(R)\frac{N-1}{N(N+1)}\\
\int_0^1 dz z^{N-1}\Delta P_{gg}(z) &= C_2(G)\left[\frac{11}{6}-\frac{2}{3}\frac{T(R)}{C_2(G)}+\frac{2}{N}-\frac{4}{N+1}-2\sum_{j=1}^{N-1}\frac{1}{j}\right]
\end{aligned} \tag{10.25}$$

Each term develops a $1/N$ pole as $N \to \infty$. If the two non-perturbative gluon exchange contribution is a fixed pole then the analytic continuation argument that we used for g_1^{p-n} will not invalidate the application of DGLAP evolution for the flavour singlet component. Brodsky *et al.* (1995) have argued that colour coherence forces $\Delta g(x)/g(x) \propto x$ when $x \to 0$. In this scenario we might also expect a polarized version of the hard pomeron with intercept $\sim +0.4$ which would correspond to a rising term (in absolute value) like $x^{-0.4}$ as $x \to 0$. Perhaps the coefficients of these terms are separately suppressed or perhaps they cancel in the measured kinematics?

To summarize, *if* we assume analyticity in Q^2 then the isovector spin structure function g_1^{p-n} favours a hard exchange contribution at small x with a Q^2 independent Regge intercept. This exchange should also contribute to and could be looked for in high-energy polarized photoproduction and in the transition region between $Q^2 = 0$ and deep inelastic values of Q^2 – *viz.* $Q^2 < 1\text{GeV}^2$. High-energy polarized photoproduction and the transition region could be investigated through accurate measurements of low Q^2 asymmetries using a polarized electron-proton collider [Bass and De Roeck (2001)] or perhaps with COMPASS using a proton target. A hard exchange contribution might also show up in the spin-dependent part of the proton-proton total cross-section. In polarized proton-proton collisions one would be looking for a leading behaviour $\Delta\sigma \sim s^{-0.5}$ to $\sim s^{-0.8}$ instead of the simple a_1 prediction $\sim s^{-1.4}$ and non-perturbative gluon-exchange contribution $\sim (\ln s/\mu^2)/s$ with $\mu \sim 0.5 - 1$ GeV a typical hadronic scale [Bass and Landshoff (1994); Close and Roberts (1994)]. Will these processes exhibit evidence of a hard exchange with Regge intercept $\alpha \sim +0.5$ or just the exchanges predicted by soft Regge theory? These spin measurements, together with the total cross-section at the LHC, would help constrain our understanding of hard and soft exchanges in high energy collisions. Knowledge of spin-dependent Regge behaviour would fur-

ther help to constrain the high-energy part of the Gerasimov-Drell-Hearn sum-rule as well as the high-energy extrapolations of g_1^{p-n} at intermediate Q^2 that go into the JLab programme to extract information about higher-twist matrix elements in the nucleon.

Chapter 11

POLARIZED QUARK DISTRIBUTIONS

Having found that the value of $g_A^{(0)}$ extracted from polarized deep inelastic scattering is about half the prediction $\sim 60\%$ of both relativistic quark models and the value of $g_A^{(8)}$ extracted from hyperon beta-decays, we would next like to understand whether the spin suppression is a property of the valence quarks or the sea and glue in the proton.

For x greater than ~ 0.2 the structure functions are essentially saturated by valence quark contributions. Ignoring contributions from polarized glue the partonic light-quark (u and d) contribution is

$$\Delta u + \Delta d \sim \frac{1}{3}(2g_A^{(0)}|_{\rm pDIS} + g_A^{(8)}) \tag{11.1}$$

where the octet axial-charge is

$$g_A^{(8)} = \Big(\Delta u + \Delta d - 2\Delta s\Big)_{\rm partons} \tag{11.2}$$

and the singlet axial-charge is

$$g_A^{(0)}|_{\rm pDIS} = \Big(\Delta u + \Delta d + \Delta s\Big)_{\rm partons} - 3\frac{\alpha_s}{2\pi}\Delta g \tag{11.3}$$

Given the weighting factor in the expansion for g_1, the first moment of the isosinglet term and the extracted valence distribution is dominated by the flavour-singlet piece.

There are several possible mechanisms for producing sea quarks in the nucleon: photon-gluon fusion, the meson cloud of the nucleon, instantons, ... In general the different dynamics will produce polarized sea with different x and transverse momentum dependence. Is this sea polarized and, if yes, does the strange sea polarization line up against the spin of the proton to suppress the measured value of $g_A^{(0)}$ relative to the value of $g_A^{(8)}$? Alternatively, is the valence spin contribution suppressed through spin delocalisation and a shift of (valence quark) spin into topological $x = 0$ polarization?

There are several probes of valence and sea polarization in the nucleon: semi-inclusive measurements of polarized deep inelastic scattering, W-boson production in polarized proton-proton collisions at RHIC, and possible future neutrino factories or deep inelastic measurements using W-boson exchange at a future polarized ep collider.

11.1 Semi-inclusive polarized deep inelastic scattering

Semi-inclusive measurements of fast pions and kaons in the current fragmentation region with final state particle identification can be used to reconstruct the individual up, down and strange quark contributions to the proton's spin [Close (1978); Frankfurt *et al.* (1989); Close and Milner (1991)]. In contrast to inclusive polarized deep inelastic scattering where the g_1 structure function is deduced by detecting only the scattered lepton, the detected particles in the semi-inclusive experiments are high-energy (greater than 20% of the energy of the incident photon) charged pions and kaons in coincidence with the scattered lepton. For large energy fraction $z = E_h/E_\gamma \to 1$ the most probable occurence is that the detected $\pi^\pm$ and $K^\pm$ contain the struck quark or antiquark in their valence Fock state. They therefore act as a tag of the flavour of the struck quark [Close (1978)].

In leading order (LO) QCD the double-spin asymmetry for the production of hadrons h in semi-inclusive polarized γ^* polarized proton collisons is:

$$\mathcal{A}_{1p}^h(x,Q^2) \simeq \frac{\sum_{q,h} e_q^2 \Delta q(x,Q^2) \int_{z_{\min}}^1 dz\ D_q^h(z,Q^2)}{\sum_{q,h} e_q^2 q(x,Q^2) \int_{z_{\min}}^1 dz\ D_q^h(z,Q^2)} \tag{11.4}$$

where $z_{\min} \sim 0.2$. Here

$$D_q^h(z,Q^2) = \int dk_t^2 D_q^h(z,k_t^2,Q^2) \tag{11.5}$$

is the fragmentation function which describes the probability for the struck quark or antiquark to produce a hadron h $(= \pi^\pm, K^\pm)$ carrying energy fraction $z = E_h/E_\gamma$ in the target rest frame; $\Delta q(x,Q^2)$ is the quark (or antiquark) polarized parton distribution and e_q is the quark charge. Note the integration over the transverse momentum k_t of the final-state hadrons [Close and Milner (1991)]. (In practice this integration over k_t is determined by the acceptance of the experiment.) Since pions and kaons have spin zero, the fragmentation functions are the same for both polarized and unpolarized leptoproduction. NLO corrections to Eq. (11.4) are discussed in de Florian *et al.* (1998); de Florian and Sassot (2000).

This programme for polarized deep inelastic scattering was pioneered by the SMC [Adeva *et al.* (1998c)] and HERMES [Ackerstaff *et al.* (1999)]. More recent measurements from HERMES are reported in Airapetian *et al.* (2004, 2005a) and COMPASS measurements in Alekseev *et al.* (2007).

Two different methods are used: the "difference" and Monte-Carlo based "purity" analyses. We next review the difference and purity methods and the results.

In general the fragmentation functions $D_i^h(z,Q^2)$ depend on both the quark flavor and the hadron type. In particular for a given hadron $D_i^h \neq D_j^h$. This effect can be understood in terms of the parton model: if the struck quark is a valence quark for a particular hadron, it is more likely to fragment into that hadron (e.g. $D_u^{\pi^+} > D_d^{\pi^+}$). Flavour sensitivity is manifest as sensitivity to anti-quarks (e.g. $D_{\bar{d}}^{\pi^+} > D_d^{\pi^+}$).

Let $D_1(z)$ denote the favoured fragmentation

$$D_1(z) \equiv D_u^{\pi^+}(z) = D_{\bar{d}}^{\pi^-}(z) = D_{\bar{d}}^{\pi^+}(z) = D_{\bar{u}}^{\pi^-}(z) \tag{11.6}$$

and $D_2(z)$ denote the unfavoured fragmentation function

$$D_2(z) \equiv D_{\bar{d}}^{\pi^+}(z) = D_u^{\pi^-}(z) = D_{\bar{u}}^{\pi^+}(z) = D_{\bar{d}}^{\pi^-}(z). \tag{11.7}$$

We write the strange quark fragmentation function as

$$D_3(z) \equiv D_s^{\pi^+}(z) = D_{\bar{s}}^{\pi^-}(z) = D_{\bar{s}}^{\pi^+}(z) = D_{\bar{s}}^{\pi^-}(z) \tag{11.8}$$

Dependence on the fragmentation functions cancels in some combinations of asymmetries. We let $N_{\uparrow\Downarrow}^{\pi^+}(x,z)$ denote the number of π^+ produced in a bin characterised by Bjorken x (> 0.2) and z, where the virtual photon helicity is $\uparrow$ and the target proton helicity is $\Downarrow$. The spin averaged pion production rates are independent of the anomaly. It follows that:

$$\begin{aligned}
N_{\uparrow\Downarrow}^{\pi^+} &\sim [\frac{4}{9}u^{\uparrow}(x) + \frac{1}{9}\bar{d}^{\uparrow}(x)]D_1(z) + [\frac{4}{9}\bar{u}^{\uparrow}(x) + \frac{1}{9}d^{\uparrow}(x)]D_2(z) + \frac{1}{9}[s^{\uparrow}(x) + \bar{s}^{\uparrow}]D_3(z) \\
N_{\uparrow\Uparrow}^{\pi^-} &\sim [\frac{4}{9}u^{\uparrow}(x) + \frac{1}{9}\bar{d}^{\uparrow}(x)]D_2(z) + [\frac{4}{9}\bar{u}^{\uparrow}(x) + \frac{1}{9}d^{\uparrow}(x)]D_1(z) + \frac{1}{9}[s^{\uparrow}(x) + \bar{s}^{\uparrow}]D_3(z) \\
N_{\uparrow\Uparrow}^{\pi^+} &\sim [\frac{4}{9}u^{\downarrow}(x) + \frac{1}{9}\bar{d}^{\downarrow}(x)]D_1(z) + [\frac{4}{9}\bar{u}^{\downarrow}(x) + \frac{1}{9}d^{\downarrow}(x)]D_2(z) + \frac{1}{9}[s^{\downarrow}(x) + \bar{s}^{\downarrow}]D_3(z) \\
N_{\uparrow\Uparrow}^{\pi^-} &\sim [\frac{4}{9}u^{\downarrow}(x) + \frac{1}{9}\bar{d}^{\downarrow}(x)]D_2(z) + [\frac{4}{9}\bar{u}^{\downarrow}(x) + \frac{1}{9}d^{\downarrow}(x)]D_1(z) + \frac{1}{9}[s^{\downarrow}(x) + \bar{s}^{\downarrow}]D_3(z)
\end{aligned} \tag{11.9}$$

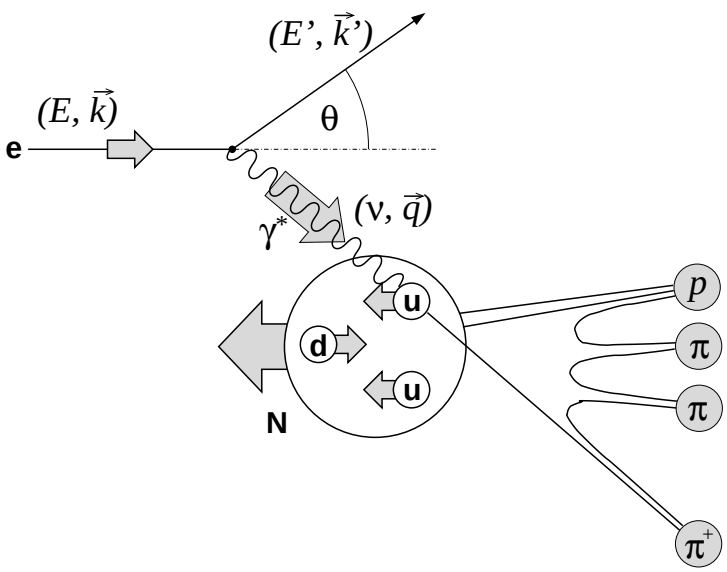

Fig. 11.1 Kinematics of semi-inclusive deep inelastic scattering.

whence

$$N^{\pi^+-\pi^-}_{\uparrow\Downarrow-\uparrow\Uparrow} \sim \left[\frac{4}{9}(u^\uparrow - u^\downarrow)(x) - \frac{1}{9}(d^\uparrow - d^\downarrow)(x)\right](D_1 - D_2)(z)$$

$$N^{\pi^+-\pi^-}_{\uparrow\Downarrow+\uparrow\Uparrow} \sim \left[\frac{4}{9}(u^\uparrow + u^\downarrow)(x) - \frac{1}{9}(d^\uparrow + d^\downarrow)(x)\right](D_1 - D_2)(z)$$

In leading order QCD the fragmentation functions cancel in the difference asymmetry which is determined from the difference of cross sections of positive and negative hadrons h^+ and h^-:

$$\mathcal{A}^{h^+-h^-} = \frac{(\sigma^{h+}_{\uparrow\downarrow} - \sigma^{h-}_{\uparrow\downarrow}) - (\sigma^{h+}_{\uparrow\uparrow} - \sigma^{h-}_{\uparrow\uparrow})}{(\sigma^{h+}_{\uparrow\downarrow} - \sigma^{h-}_{\uparrow\downarrow}) + (\sigma^{h+}_{\uparrow\uparrow} - \sigma^{h-}_{\uparrow\uparrow})}. \tag{11.10}$$

Here arrows indicate the relative direction of the beam and target polarizations. The difference asymmetries for the deuteron target give direct access to the polarized valence distributions

$$\mathcal{A}^{h^+-h^-}_d \equiv \mathcal{A}^{\pi^+-\pi^-}_d = \mathcal{A}^{K^+-K^-}_d = \frac{\Delta u_v + \Delta d_v}{u_v + d_v} \tag{11.11}$$

where $\Delta q_v \equiv \Delta q - \Delta\bar{q}$ and

$$\mathcal{A}^{\pi^+-\pi^-}_p = \frac{4\Delta u_v - \Delta d_v}{4u_v - d_v} \tag{11.12}$$

for a proton target. This difference method is being used by COMPASS for a deuteron target. Since kaons contribute to the asymmetry (11.11) just like pions one avoids statistical losses due to hadron identification.

In practice the leading order polarized valence distribution $\Delta u_v + \Delta d_v$ is obtained by multiplying $\mathcal{A}^{h^+-h^-}$ by the corresponding leading-order unpolarized valence distribution taking into account the deuteron D-state probability discussed in Eq. (2.30) and the fact that the unpolarized parton distributions are extracted from F_2 and the finite value of $R(x) = \sigma_L/\sigma_T$, *viz.*

$$\Delta u_v + \Delta d_v = \frac{u_v + d_v}{(1 + R(x, Q^2))(1 - 1.5\omega_D)}\mathcal{A}^{h^+-h^-}. \tag{11.13}$$

Since sea distributions are negligible for $x > 0.3$ it follows that the large x region is essentially valence quark saturated:

$$\Delta u_v + \Delta d_v \sim \frac{36}{5}\frac{g_1^d(x, Q^2)}{(1 - 1.5\omega_D)} \tag{11.14}$$

for these kinematics. This relation has been used for the largest x region to minimise experimental uncertainites. The COMPASS data together with the first moment integral for the valence quark spin is shown in Fig. 11.2. The result extracted from the data is

$$\Gamma_v(0.006 < x < 0.7)\Big|_{\mathrm{Q}^2=10\,\mathrm{GeV}^2} = 0.40 \pm 0.07(\mathrm{stat.}) \pm 0.05(\mathrm{syst.}), \tag{11.15}$$

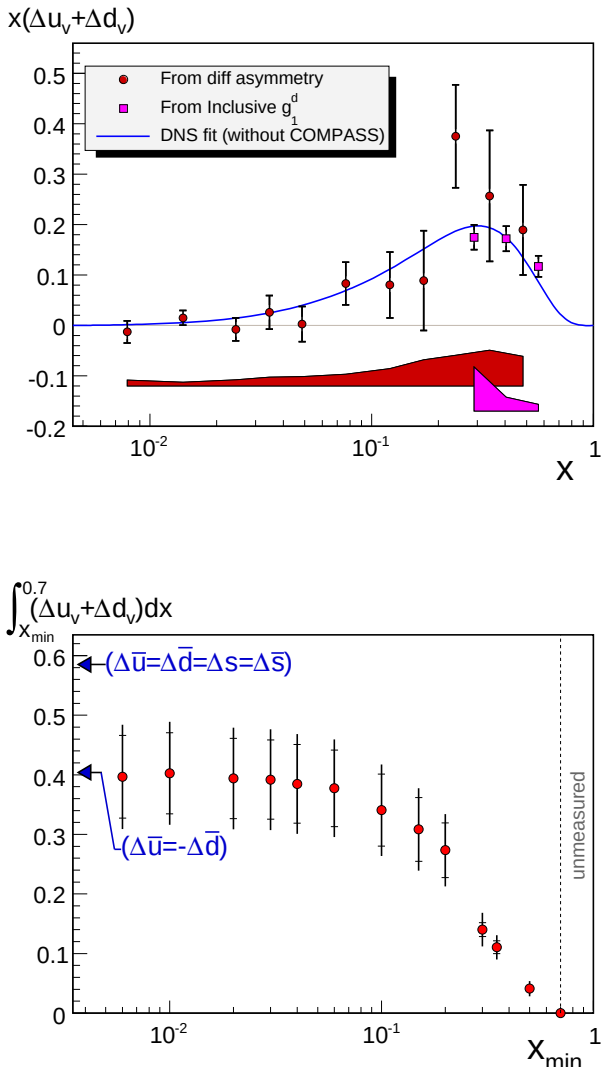

Fig. 11.2 The polarized valence quark distribution $x(\Delta u_v{+}\Delta d_v)$ evolved to $Q^2 = 10\,\mathrm{GeV}^2$ from Alekseev *et al.* (2007) and (below) the first moment of $\Delta u_v(x){+}\Delta d_v(x)$ evaluated as a function of the lower x limit of integration.

Note that the integral is practically saturated at small x within the errors, just like the isosinglet g_1 integral shown in Fig. 4.2 for $x < 0.05$. The valence quark spin contribution appears suppressed compared to the quark model prediction ~ 0.6.

It is interesting to compare the number in Eq. (11.14) with the value of $g_A^{(0)}|_{\mathrm{pDIS}} \sim 0.35 \pm 0.03 \pm 0.05$. If we assume no subtraction at infinity in the g_1

Table 11.1 Estimates of the first moments $\Delta u_v + \Delta d_v$ and $\Delta\bar{u} + \Delta\bar{d}$ from the SMC [Adeva *et al.* (1998c)], HERMES [Airapetian *et al.* (2004)], COMPASS [Alekseev *et al.* (2007)].

	x-range	Q^2 (GeV^2)	$\Delta u_v + \Delta d_v$	$\Delta\bar{u} + \Delta\bar{d}$
SMC 98	0.003–0.7	10	$0.26 \pm 0.21 \pm 0.11$	$0.02 \pm 0.08 \pm 0.06$
HERMES 05	0.023–0.6	2.5	$0.43 \pm 0.07 \pm 0.06$	$-0.06 \pm 0.04 \pm 0.03$
COMPASS	0.006–0.7	10	$0.40 \pm 0.07 \pm 0.05$	$0.0 \pm 0.04 \pm 0.03$

spin dispersion relation, then the deep inelastic value $\Delta s \sim -0.08 \pm 0.02$ disfavours a symmetric polarized sea ($\Delta\bar{u} = \Delta\bar{d} = \Delta s = \Delta\bar{s}$) and favours a strong asymmetry for the first moments of light sea quarks $\Delta\bar{u} = -\Delta\bar{d}$. The comparison with first moments obtained with results of SMC and HERMES is summarized in Table 11.1. Clearly, more direct measurements of Δs would be very interesting to help resolve this issue. A first step in this direction has been taken by HERMES.

In a different approach to semi-inclusive deep inelastic scattering HERMES have combined semi-inclusive data from proton and deuteron targets with a "purity" extraction method which uses Monte-Carlo methods to simulate the fragmentation processes. Assuming isospin symmetry of the quark distributions and fragmentation functions a system of linear equations can be constructed:

$$\begin{pmatrix} \mathcal{A}^p_{\pi^+} \\ \mathcal{A}^p_{\pi^-} \\ \mathcal{A}^n_{K^+} \\ \mathcal{A}^n_{K^+} \\ \vdots \end{pmatrix} = f[q_i(x), D_i^h] \begin{pmatrix} \Delta u \\ \Delta d \\ \Delta s \\ \Delta\bar{u} \\ \vdots \end{pmatrix} \tag{11.16}$$

These equations are solved for the Δq_i taking the unpolarized quark distributions from previous parametrizations and the fragmentation functions from either the LUND Monte-Carlo or fits to (unpolarized) pion and kaon production data.

Figure 11.3 shows the results on the flavor separation from HERMES [Airapetian *et al.* (2004)], which were obtained using a leading-order (naive parton model) analysis. The polarization of the up and down quarks are positive and negative respectively, while the sea polarization data are consistent with zero and not inconsistent with the negative sea polarization suggested by inclusive deep inelastic data within the measured x range [Glück *et al.* (2001); Blümlein and Böttcher (2002)]. However, there is also no evidence from this semi-inclusive analysis for a large negative strange quark polarization. For the region $0.023 < x < 0.3$ the extracted Δs integrates to the value $+0.03 \pm 0.03 \pm 0.01$ which contrasts with the negative value for the polarized strangeness $\sim -0.08 \pm 0.02$ extracted from inclusive measurements of g_1.

In a new analysis HERMES combine the inclusive deuteron asymmetry and semi-inclusive kaon asymmetries to make a new extraction of Δs. The analysis used just isospin invariance and the charge conjugation properties of the fragmentation functions. Preliminary results from Jackson (2006) are shown in Fig. 11.4 and

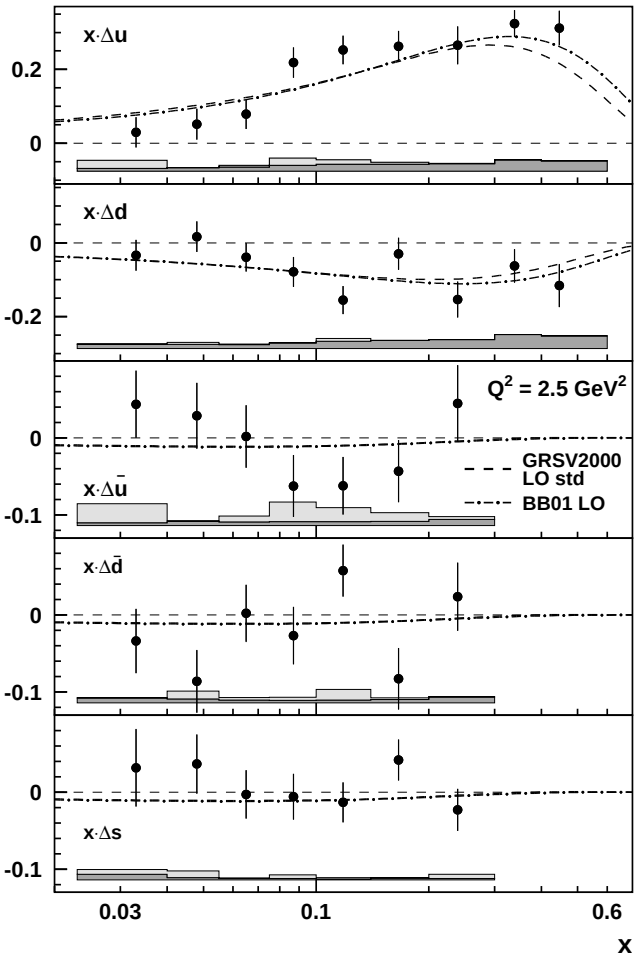

Fig. 11.3 Recent HERMES results for the quark and antiquark polarizations extracted from semi-inclusive deep inelastic scattering [Airapetian *et al.* (2004)].

the extracted Δs is again consistent with zero. (Within the measured region one finds a strangeness polarization contribution $0.006 \pm 0.029(\text{stat.}) \pm 0.007(\text{sys.})$.) The present semi-inclusive data hint at a scenario where the missing spin is a problem for the valence quarks and that the sea, including the strange sea, carries little polarization. It will be interesting to see whether this effect persists in forthcoming semi-inclusive data from COMPASS. The HERMES data also favour an isospin symmetric sea $\Delta\bar{u} - \Delta\bar{d}$, but with large uncertainties.

An important issue for semi-inclusive measurements is the angular coverage of the detector [Bass (2003a)]. The non-valence spin-flavour structure of the proton extracted from semi-inclusive measurements of polarized deep inelastic scattering

Table 11.2 First moment integrals extracted from HERMES data [Airapetian *et al.* (2004)].

$\int_{0.023}^{0.6} dx \Delta q_i(x)$	HERMES results ($Q^2 = 2.5$ GeV^2)
Δu	$0.601 \pm 0.039 \pm 0.049$
$\Delta \bar{u}$	$-0.002 \pm 0.036 \pm 0.023$
Δd	$-0.226 \pm 0.039 \pm 0.050$
$\Delta \bar{d}$	$-0.054 \pm 0.033 \pm 0.011$
Δs	$0.028 \pm 0.033 \pm 0.009$
Δu_v	$0.603 \pm 0.071 \pm 0.040$
Δd_v	$-0.172 \pm 0.068 \pm 0.045$
$\Delta \Sigma$	$0.347 \pm 0.024 \pm 0.066$
Δq_3	$0.880 \pm 0.045 \pm 0.107$
Δq_8	$0.262 \pm 0.078 \pm 0.045$

may depend strongly on the transverse momentum (and angular) acceptance of the detected final-state hadrons which are used to determine the individual polarized sea distributions. The present semi-inclusive experiments detect final-state hadrons produced only at small angles from the incident lepton beam (about 150 mrad angular coverage) The perturbative QCD "polarized gluon interpretation" [Efremov and Teryaev (1988); Altarelli and Ross (1988)] of the inclusive measurement of $g_A^{(0)}|_{\rm pDIS}$ involves physics at the maximum transverse momentum [Carlitz *et al.* (1988); Bass (2003a)] and large angles – see Fig. 6.2. Observe the small value for the light-quark sea polarization at low transverse momentum and the positive

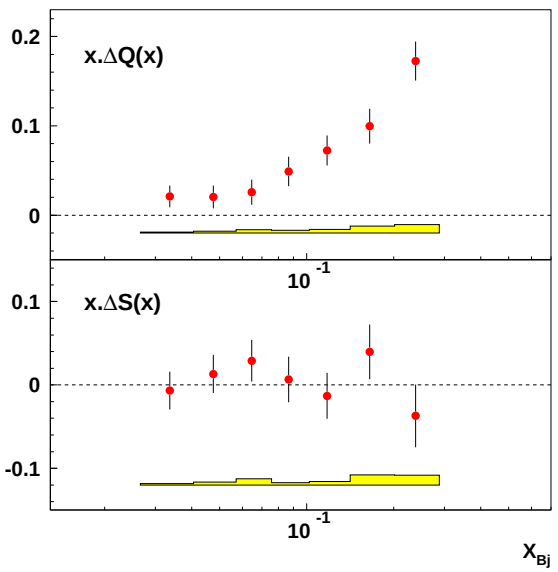

Fig. 11.4 Strange and non-strange quark helicity distributions at $\langle Q^2 \rangle = 2.5\,\mathrm{GeV}^2$ from a recent HERMES analysis [Jackson (2006)]. Here $\Delta Q(x) = (\Delta u + \Delta \bar{u} + \Delta d + \Delta \bar{d})(x)$.

value for the integrated strange sea polarization at low k_t^2: $k_t < 1.5$ GeV at the HERMES $Q^2 = 2.5$ GeV^2. When we relax the transverse momentum cut-off, increasing the acceptance of the experiment, the measured strange sea polarization changes sign and becomes negative (the result implied by fully inclusive deep inelastic measurements). For HERMES the average transverse momentum of the detected final-state fast hadrons is less than about 0.5 GeV whereas for SMC the k_t of the detected fast pions was less than about 1 GeV. Hence, there is a question whether the leading-order sea quark polarizations extracted from semi-inclusive experiments with limited angular resolution fully include the effect of the axial anomaly or not.

Recent theoretical studies motivated by this data also include possible effects associated with spin dependent fragmentation functions [Kretzer *et al.* (2001)], possible higher twist effects in semi-inclusive deep inelastic scattering, and possible improvements in the Monte Carlo [Kotzinian (2003)]. A recent global analysis of fragmentation functions is given in de Florian *et al.* (2007a,b).

11.2 Weak boson production

The W boson production programme at RHIC will provide flavour-separated measurements of up and down quarks and antiquarks [Bunce *et al.* (2000)]. At RHIC the polarization of the $u, \overline{u}, d$ and $\overline{d}$ quarks in the proton will be measured directly and precisely using W boson production in $u\overline{d} \to W^+$ and $d\overline{u} \to W^-$. The charged weak boson is produced through a pure left-handed V-A coupling and the chirality of the quark and anti-quark in the reaction is fixed.

The leading-order production of W bosons, $u\bar{d} \to W^+$, is illustrated in Fig. 11.5. The longitudinally polarized proton at the top of each diagram collides with an unpolarized proton, producing a W^+. At RHIC the polarized protons will be in bunches, alternately right- (+) and left- (−) handed. The parity-violating asymmetry is the difference of left-handed and right-handed production of W bosons, divided by the sum and normalized by the beam polarization:

$$\mathcal{A}_L^W = \frac{1}{P} \times \frac{N_-(W) - N_+(W)}{N_-(W) + N_+(W)} \quad . \tag{11.17}$$

A parity violating asymmetry for W^+ production in pp collisions can be expressed as

$$\mathcal{A}(W^+) = \frac{\Delta u(x_1)\overline{d}(x_2) - \Delta\overline{d}(x_1)u(x_2)}{u(x_1)\overline{d}(x_2) + \overline{d}(x_1)u(x_2)}. \tag{11.18}$$

where we set the Cabbibo angle to zero in a first approximation. For W^- production u and d quarks should be exchanged. The expression converges to $\Delta u(x)/u(x)$ and $-\Delta\overline{d}(x)/\overline{d}(x)$ in the limits $x_1 \gg x_2$ and $x_2 \gg x_1$ respectively. The momentum fractions are calculated as $x_1 = \frac{M_W}{\sqrt{s}} e^{y_W}$ and $x_2 = \frac{M_W}{\sqrt{s}} e^{-y_W}$, with y_W the rapidity of the W. The experimental difficulty is that the W boson is observed through its leptonic decay $W \to l\nu$ and only the charged lepton is observed. The resulting

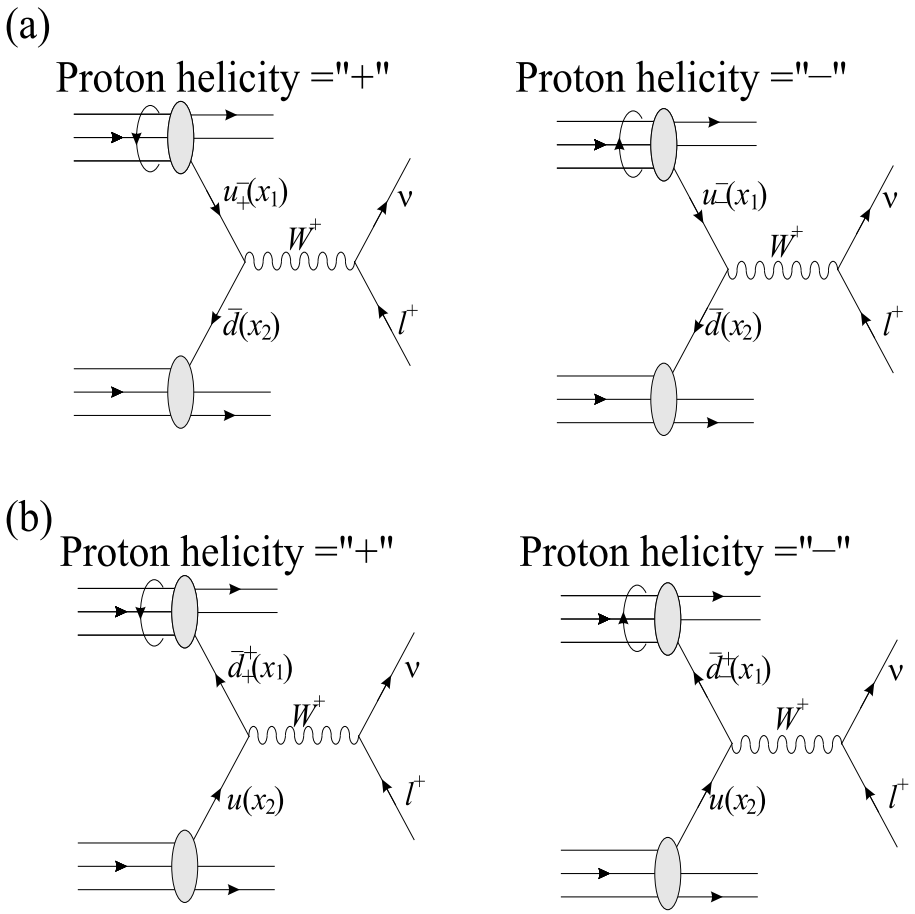

Fig. 11.5 Production of a W^+ in a $\vec{p}p$ collision, at lowest order. (a) Δu is probed in the polarized proton. (b) $\Delta\bar{d}$ is probed.

measurement precision is shown in Fig. 11.6 for the assumed integrated luminosity of 800 pb^{-1} at $\sqrt{s} = 500$ GeV. A 500-GeV commissioning run took place in June 2006, and the high-energy program is expected to start in earnest in 2009.

11.3 Inclusive spin-dependent structure functions

It has also been pointed out that neutrino factories and deep inelastic scattering through electroweak $W^{\pm}$ boson exchange measurements at a future ep collider would be ideal tools for polarized quark flavour decomposition studies. These would allow one to collect large data samples of charged current events, in the kinematic region (x, Q^2) of present fixed target data and beyond [Anselmino *et al.* (1994); Forte

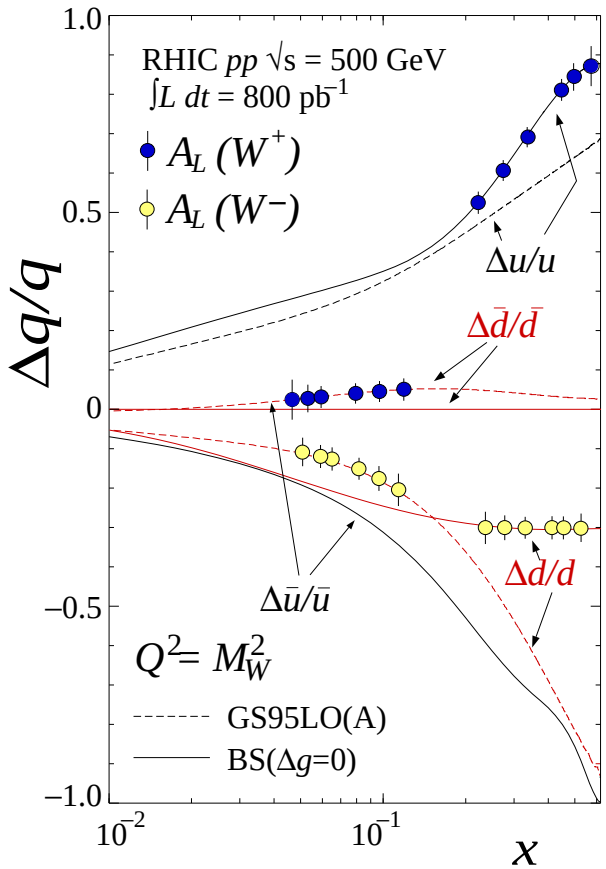

Fig. 11.6 Expected sensitivity for the flavor decomposition of quark and anti-quark polarizations using the PHENIX detector at RHIC [Bunce *et al.* (2000)] .

et al. (2001); Deshpande *et al.* (2005)]. A complete separation of all four flavours and anti-flavours would become possible, including $\Delta s(x, Q^2)$.

Going beyond electromagnetic interactions, there are extra structure functions which occur in deep inelastic scattering involving parity violating $W^{\pm}$ and Z^0 exchanges. When parity violation is allowed extra parity-odd Lorentz structures enter the hadron tensor $W_{\mu\nu}$ – each with an accompanying extra structure function. Since CP symmetry is conserved in these processes it follows that these extra structure functions F_3 for spin-independent scattering, and g_3, g_4 and g_5 for spin-dependent scattering measure charge-parity odd combinations of parton distributions. The

hadronic tensor can be written in full generality as

$$\begin{aligned} W_{\mu\nu}(p,q,s) &= \frac{1}{4\pi}\int d^4z\, \mathrm{e}^{iq\cdot z}\langle p,s|\,[J_\mu(z),J_\nu(0)]\,|p,s\rangle \\ &= -g_{\mu\nu}F_1(x,Q^2)+\frac{p_\mu p_\nu}{p\,q}F_2(x,Q^2)-i\varepsilon_{\mu\nu\rho\sigma}\frac{q^\rho p^\sigma}{2\,p.q}F_3(x,Q^2) \\ &+ i\varepsilon_{\mu\nu\rho\sigma}q^\rho\left[\frac{s^\sigma}{p.q}\,g_1(x,Q^2)\,+\frac{s^\sigma(p.q)-p^\sigma(s.q)}{(p.q)^2}\,g_2(x,Q^2)\right] \\ &+ \left[\frac{p_\mu s_\nu+s_\mu p_\nu}{2p.q}-\frac{s.q}{(p.q)^2}p_\mu p_\nu\right]\,g_3(x,Q^2) \\ &+ \frac{s.q}{(p.q)^2}p_\mu p_\nu\,g_4(x,Q^2)\;-\;\frac{s.q}{p.q}g_{\mu\nu}\,g_5(x,Q^2)\,. \end{aligned} \tag{11.19}$$

Note that parity-violating interactions mediated by electroweak boson exchange are required for F_3, g_3, g_4, g_5 to contribute. These extra structure functions are sensitive to charge parity odd distributions

For longitudinal polarization the contributions of the g_2 and g_3 spin structure functions g_2 to the cross-section are suppressed by powers of M^2/Q^2. At leading order

$$g_4(x,Q^2)=2xg_5(x,Q^2) \tag{11.20}$$

so that, at leading twist, there are only two independent polarized structure functions, *viz.* g_1 (parity conserving) and g_5 (parity violating). The leading-order formulae for g_1 and g_5 are obtained by calculating the hadronic tensor for $W^\pm$ scattering off a free quark. Above the charm threshold one has

$$\begin{aligned} g_1^{W^+}(x,Q^2) &= \Delta\bar{u}(x,Q^2)+\Delta d(x,Q^2)+\Delta\bar{c}(x,Q^2)+\Delta s(x,Q^2) \\ g_1^{W^-}(x,Q^2) &= \Delta u(x,Q^2)+\Delta\bar{d}(x,Q^2)+\Delta c(x,Q^2)+\Delta\bar{s}(x,Q^2) \\ g_5^{W^+}(x,Q^2) &= \Delta\bar{u}(x,Q^2)-\Delta d(x,Q^2)+\Delta\bar{c}(x,Q^2)-\Delta s(x,Q^2) \\ g_5^{W^-}(x,Q^2) &= -\Delta u(x,Q^2)+\Delta\bar{d}(x,Q^2)-\Delta c(x,Q^2)+\Delta\bar{s}(x,Q^2). \end{aligned} \tag{11.21}$$

Chapter 12

POLARIZED GLUE $\Delta g(x, Q^2)$

There is a vigorous and ambitious global programme to measure Δg. Interesting channels include gluon mediated processes in semi-inclusive polarized deep inelastic scattering (COMPASS) and hard QCD processes in high energy polarized proton-proton collisions at RHIC.

We would like to know how big the gluon spin contribution is to the total spin of the proton. The discovery of Altarelli and Ross (1988) and Efremov and Teryaev (1988) that polarized glue makes a scaling contribution to the first moment of g_1, $\alpha_s \Delta g \sim$ `constant`, means that gluon polarization is, a priori, not necessarily small and must become large at very high momentum scales. The perturbative QCD anomaly mechanism means that gluon polarization can, in part, screen the quark spin content that we extract from polarized deep inelastic scattering. How big is this effect?

Early NLO QCD motivated fits to the inclusive g_1 data were suggestive that, perhaps, the net polarized glue might be positive but more direct measurements involving glue sensitive observables are needed to really extract the magnitude of Δg and the shape of $\Delta g(x, Q^2)$ including any possible nodes in the distribution function. Hence, the dedicated programme of measurements at COMPASS and RHIC.

The first experimental attempt to look at gluon polarization was made by the FNAL E581/704 Collaboration which measured the double-spin asymmetry $\mathcal{A}_{LL}$ for inclusive multi-γ and $\pi^0\pi^0$ production with a 200 GeV polarized proton beam and a polarized proton target suggesting that $\Delta g/g$ is not so large in the region of $0.05 < x < 0.35$ [Adams *et al.* (1994)].

12.1 Polarized lepto-production

COMPASS has been conceived to measure Δg via the study of the photon-gluon fusion process, as shown in Fig. 12.1. The cross section of this process is directly related to the gluon density at the Born level. The experimental technique consists of the reconstruction of charmed mesons in the final state. COMPASS also use the

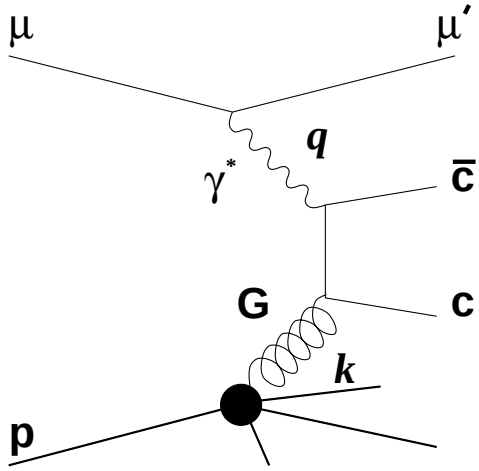

Fig. 12.1 c $\overline{\text{c}}$ production in polarized photon gluon fusion is being used to measure gluon polarization in the polarized proton.

same process with high p_t particles instead of charm to access Δg. This leads to samples with larger statistics, but these have larger background contributions, from QCD Compton processes and fragmentation that one has to control.

The main idea behind the high p_t particles measurement is the following. Ideally one would like to look at the two-hard-jet cross-section to identify (polarized) photon-gluon fusion events. However, this is impractical for fixed target experiments at moderate centre-of-mass energies. The strategy instead [Bravar *et al.* (1998)] is to use high p_t charged hadron pairs (e.g. pions) as surrogate jets to tag the polarized photon-gluon fusion process and to extract information about gluon polarization. The hope and expectation is that because of the large invariant mass of the charged hadron pairs, the underlying QCD subprocesses can still be described using perturbative QCD even if the virtuality of the incident photon is small or zero.

HERMES was the first to attempt to measure Δg using high p_t charged particles, as proposed for COMPASS above, and nearly real photons $\langle Q^2 \rangle = 0.06$ GeV^2. The measurement is at the limit of where a perturbative treatment of the data can be expected to be valid, but the result is interesting: $\Delta g/g = 0.41 \pm 0.18 \pm 0.03$ at an average $< x_g >= 0.17$ [Airapetian *et al.* (2000)]. The momentum of the hadron was required to be above 4.5 GeV with a transverse component above 0.5 GeV. The minimum value of the invariant mass of the two hadrons, in the case of two pions, was 1.0 GeV^2. A nonzero asymmetry was observed if the pairs with $p_t^{h_1} > 1.5$ GeV

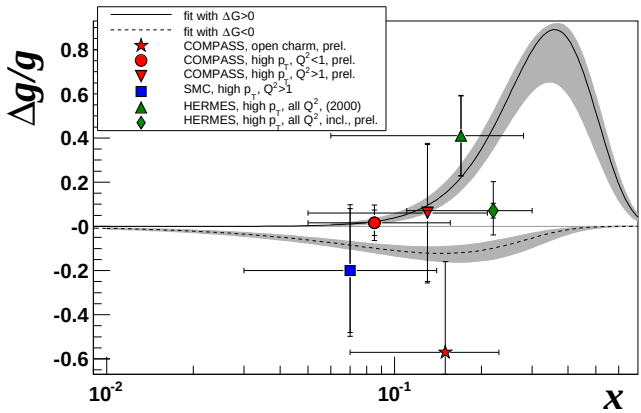

Fig. 12.2 Measurements of gluon polarization from COMPASS, HERMES and SMC together with the COMPASS fits (Chapter 10) for $\Delta g(x)/g(x)$ at $Q^2 = 3$ GeV^2 corresponding to $\Delta g > 0$ and $\Delta g < 0$ [Mallot (2006)].

and $p_t^{h_2} > 1.0$ GeV were selected. If $p_t^{h_1} > 1.5$ GeV is not enforced the asymmetry was consistent with zero. The SMC Collaboration performed a similar analysis for their own data keeping $Q^2 > 1$GeV^2. An average gluon polarization was extracted $\Delta g/g = -0.20 \pm 0.28 \pm 0.10$ at an average gluon momentum $x_g = 0.07$ [Adeva *et al.* (2004)].

COMPASS have performed separate analyses for hadron pairs produced with $Q^2 > 1$ GeV^2 and $Q^2 < 1$ GeV^2. Here transverse momentum cuts on the p_t of the charged particles $p_{t,h1}^2 + p_{t,h2}^2 \geq 2.5$ GeV^2 were applied. The gluon polarization extracted from the high and low Q^2 analyses are both compatible with zero and probe the region around $x_g \sim 0.1$ [Ageev *et al.* (2006)]. These measurements together with the most recent results reported from COMPASS from charm production [Koblitz (2007)] are summarised in Fig. 12.2 and Table 12.1 for gluon momentum $x_g \sim 0.1$.

Table 12.1 Polarized gluon measurements from deep inelastic experiments.

Experiment	process	$\langle x_g \rangle$	$\langle \mu^2 \rangle$	$\Delta g/g$
HERMES	hadron pairs	0.17	~ 2	$0.41 \pm 0.18 \pm 0.03$
HERMES	inclusive hadrons	0.22	1.35	$0.071 \pm 0.034^{+0.105}_{-0.127}$
SMC	hadron pairs	0.07		$-0.20 \pm 0.28 \pm 0.10$
COMPASS	hadron pairs, $Q^2 < 1$	0.085	~ 3	$0.016 \pm 0.058 \pm 0.055$
COMPASS	hadron pairs, $Q^2 > 1$	0.13		$0.06 \pm 0.31 \pm 0.06$
COMPASS	open charm	0.15	13	$-0.57 \pm 0.41 \pm 0.17$ *(prelim.)*

12.2 RHIC data

The hunt for Δg is one of the main physics drives for polarized RHIC.

RHIC Spin is achieving polarized proton-proton collisions at 200 GeV centre of mass energy and $\sim 60\%$ polarization. First test runs at 22 GeV and 500 GeV centre of mass took place in June 2006. Experiments using the PHENIX and STAR detectors are investigating polarized glue in the proton. Measurements of $\Delta g/g$ are expected in the gluon x range $0.03 < x_g < 0.3$ and the key hard scattering processes are summarized in Table 12.2.

The accelerator performance thus far into the RHIC spin programme and the current PHENIX detector configuration have made the double-helicity asymmetry for production of neutral pions with large transverse momentum the best probe of the gluon polarization in PHENIX [Adare *et al.* (2007)]. The high p_t pion acts as a surrogate jet. NLO perturbative QCD corrections to this process have been calculated in de Florian (2003) and Jäger *et al.* (2003). Charged pion asymmetries will complement current measurements [Morreale (2007)]. Direct photons provide a theoretically cleaner probe of Δg and are directly sensitive to its sign but require higher luminosity running. The direct photon cross section has already been measured [Adler *et al.* (2005b)], with the first asymmetry measurement expected from the 2006 data and a definitive measurement at 200 GeV anticipated by 2009. Future detector upgrades will allow access to other probes sensitive to the gluon polarization, such as open charm and jets. In particular, a silicon vertex barrel detector is planned for 2009, and a forward calorimeter ($1 < |\eta| < 3$) is planned for 2011.

An important channel at STAR providing sensitivity to the gluon is jet production [Abelev *et al.* (2006); Surrow (2007)]. Charged pion asymmetries will provide complementary sensitivity to gluon polarization. The mid-rapidity cross section for neutral pions at STAR was recently released and is in good agreement with NLO perturbative QCD calculations. This represents an important stepping stone for future neutral pion and direct photon asymmetry measurements, probing Δg. Photon-jet correlations will provide information on the kinematics of the partonic scattering.

The successful application of NLO perturbative QCD to unpolarized RHIC data for $pp \to \pi^0 X$ at $\sqrt{s} = 62$ GeV and 200 GeV is shown in Fig. 12.3. Fac-

Table 12.2 Polarized partons from RHIC.

reaction	LO subprocesses	partons probed	x range
$pp \to \text{jets}X$	$q\overline{q}, qq, qg, gg \to \text{jet}X$	$\Delta q, \Delta g$	$x > 0.03$
$pp \to \pi X$	$q\overline{q}, qq, gg \to \pi X$	$\Delta q, \Delta g$	$x > 0.03$
$pp \to \gamma X$	$qg \to q\gamma$, $q\overline{q} \to g\gamma$	Δg	$x > 0.03$
$pp \to Q\overline{Q}X$	$gg \to Q\overline{Q}$, $q\overline{q} \to Q\overline{Q}$	Δg	$x > 0.01$
$pp \to W^{\pm}X$	$q\overline{q}' \to W^{\pm}$	$\Delta u, \Delta\overline{u}, \Delta d, \Delta\overline{d}$	$x > 0.06$

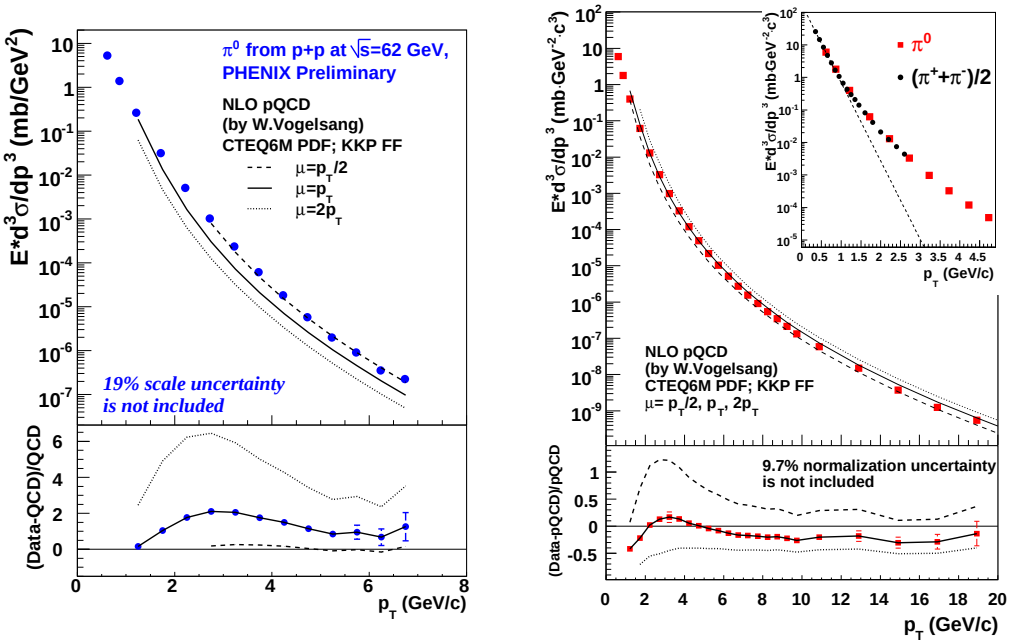

Fig. 12.3 PHENIX data for unpolarized $pp \to \pi^0 X$ in comparison with the predictions of NLO perturbative QCD calculations. Figures from Adare *et al.* (2007) for 200 GeV and for 62 GeV private communication, to appear in the proceedings of the International Nuclear Physics Conference, Tokyo, Japan, June 3-8, 2007 (author K. Aoki).

torization is seen to work, inspiring its application to polarized processes and the extraction of Δg.

The longitudinal spin asymmetries for $pp \to \pi^0 X$ (PHENIX) and $pp \to \texttt{jet}X$ (STAR) are shown in Figs. 12.4 and 12.5. together with the expectations of different NLO fits to the inclusive g_1 data. In Figs. 12.4 and 12.5 the curves "$\Delta g = 0$ input", "GRSV-std", "GRSV-max" (or "$\Delta g = g$ input") and "GRSV-min" (or "$\Delta g = -g$ input") correspond to a first moment of $\Delta g \sim 0.1$, 0.4, 1.9 and -1.8 respectively at $Q^2 \sim 1$ GeV^2 and "input" refers to the "input scale" $\mu^2 = 0.4$ GeV^2 in the analysis of Glück *et al.* (2001).

The COMPASS and RHIC Spin measurements suggest that polarized glue is, by itself, not sufficient to resolve the difference between the small value of $g_A^{(0)}|_{\rm pDIS}$ and the constituent quark model prediction, ~ 0.6. The COMPASS semi-inclusive data suggest that the gluon polarization is small *or* that it has a node in it around $x_g \sim 0.1$, whereas the NLO QCD fits to the inclusive g_1 data suggest modest gluon polarization. The PHENIX and STAR data are consistent with modest gluon polarization. A combined NLO analysis of all the data would be valuable and, so far,

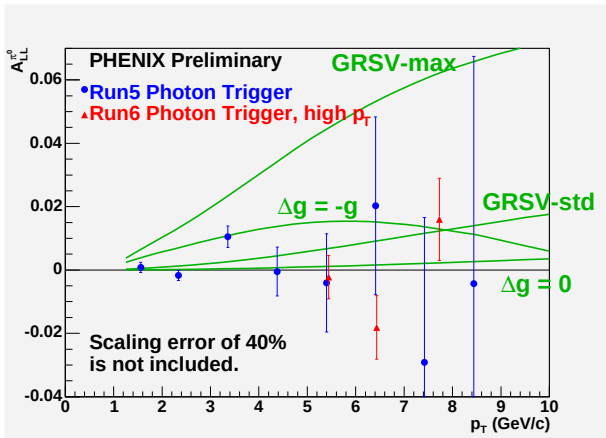

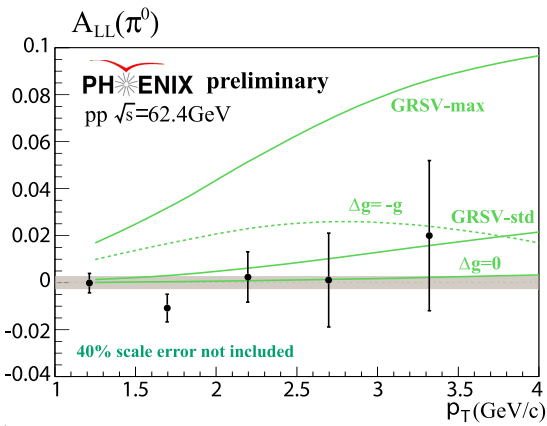

Fig. 12.4 Preliminary PHENIX results on $\mathcal{A}_{LL}^{\pi^0}$ together with the predictions from various QCD fits at $s^{\frac{1}{2}} = 200$ GeV (above) and 62.4 GeV (below). Figures from [Boyle (2007)] and [Aoki (2007)].

the COMPASS processes have been analysed only at leading order. Nevertheless, the tentative conclusion is that the gluon polarization may be small, $\ll 1$.

Future polarized ep colliders could add information in two ways: by extending the kinematic range for measurements of g_1 or by direct measurements of Δg. A precise measurement of Δg is crucial for a full understanding of the proton spin

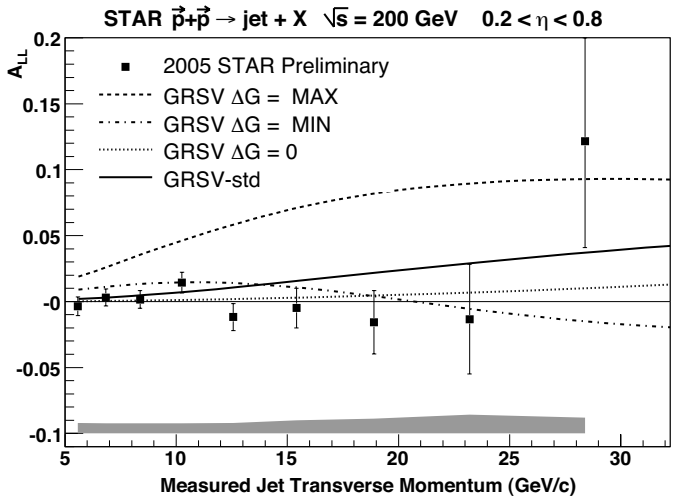

Fig. 12.5 Preliminary STAR data on the longitudinal double spin inclusive jet asymmetry A_{LL} [Surrow (2007)].

problem. HERA has shown that large centre of mass energy allows several processes to be used to extract the unpolarized gluon distribution. These include jet and high p_t hadron production, charm production both in deep inelastic scattering and photoproduction, and correlations between multiplicities of the current and target hemisphere of the events in the Breit frame. The most promising process for a direct extraction of Δg is di-jet production [De Roeck *et al.* (1999); Rädel and De Roeck (2002)]. The underlying idea is to isolate boson-gluon fusion events where the gluon distribution enters at the Born level.

This page intentionally left blank

Chapter 13

TRANSVERSITY

There are three species of twist-two quark distributions in QCD. These are the spin independent distributions $q(x)$ measured in the unpolarized structure functions F_1 and F_2, the spin dependent distributions $\Delta q(x)$ measured in g_1 and the transversity distributions $\delta q(x)$.

The transversity distributions describe the density of transversely polarized quarks inside a transversely polarized proton [Barone *et al.* (2002)]. Measuring transversity is an important experimental challenge in QCD spin physics. We briefly describe the physics of transversity and the programme to measure it.

The twist-two transversity distributions [Ralston and Soper (1979); Artru and Mekhfi (1990); Jaffe and Ji (1992)] can be interpreted in parton language as follows. Consider a nucleon moving with (infinite) momentum in the $\hat{e}_3$-direction, but polarized along one of the directions transverse to $\hat{e}_3$. Then $\delta q(x, Q^2)$ counts the quarks with flavour q, momentum fraction x and their spin parallel to the spin of a nucleon minus the number antiparallel. That is, in analogy with Eq. (2.21), $\delta q(x)$ measures the distribution of partons with transverse polarization in a transversely polarized nucleon, *viz.*

$$\delta q(x, Q^2) = q^{\uparrow}(x) - q^{\downarrow}(x). \tag{13.1}$$

In a helicity basis, transversity corresponds to the helicity-flip structure shown in Fig. 13.1 making transversity a probe of chiral symmetry breaking [Collins (1993b)]. The first moment of the transversity distribution is proportional to the nucleon's C-odd tensor charge, *viz.* $\delta q = \int_0^1 dx \delta q(x)$ with

$$\langle p, s| \; \bar{q} i \sigma_{\mu\nu} \gamma_5 q \; |p, s\rangle = (1/M)(s_\mu p_\nu - s_\nu p_\mu)\delta q. \tag{13.2}$$

Transversity is C-odd and chiral-odd.

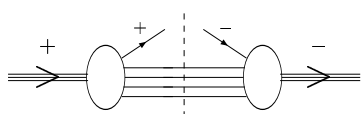

Fig. 13.1 Transversity in helicity basis.

If quarks moved non-relativistically in the nucleon δq and Δq would be identical since rotations and Euclidean boosts commute and a series of boosts and rotations can convert a longitudinally polarized nucleon into a transversely polarized nucleon at infinite momentum. The difference between the transversity and helicity distributions reflects the relativistic character of quark motion in the nucleon. In the MIT Bag Model this effect is manifest as follows. The lower component of the Dirac spinor enters the relativistic spin depolarization factor with the opposite sign to Δq because of the extra factor of γ_μ in the tensor charge [Jaffe and Ji (1992)]. That is, the relativistic depolarization factor

$$N^2 \int_0^R dr r^2 (f^2 - \frac{1}{3} g^2) = 1 - \frac{1}{3} \frac{2\omega - 3}{\omega - 1} = 0.65 \tag{13.3}$$

for Δq mentioned in Chapter 8 is replaced by

$$N^2 \int_0^R dr r^2 (f^2 + \frac{1}{3} g^2) = 1 - \frac{1}{6} \frac{2\omega - 3}{\omega - 1} = 0.83 \tag{13.4}$$

for δq where $\psi = \frac{N}{\sqrt{4\pi}} \begin{pmatrix} f \\ i\sigma.\hat{r} g \end{pmatrix}$ is the Dirac spinor and we take $\omega = 2.04$ for the proton with all quarks in the $(1s)$ state.

Little is presently known about the shape of the transversity distributions. However some general properties can be deduced from QCD arguments. The spin distributions $\Delta q(x)$ and $\delta q(x)$ have opposite charge conjugation properties: $\Delta q(x)$ is C-even whereas $\delta q(x)$ is C-odd. The spin dependent quark and gluon helicity distributions (Δq and Δg) mix under Q^2-evolution. In contrast, there is no analog of gluon transversity in the nucleon so δq evolves without mixing, like a non-singlet parton distribution function. Not coupling to glue or perturbative $\bar{q}q$ pairs, $\delta q(x)$ and the tensor charge promise to be more quark-model–like than the singlet axial-charge (though they are both scale dependent) and should be an interesting contrast [Jaffe (2001)]. Under QCD evolution the moments $\int_0^1 dx x^n \delta q(x, Q^2)$ decrease with increasing Q^2. In leading order QCD the transversity distributions are bounded above by Soffer's inequality [Soffer (1995)]

$$|\delta q(x, Q^2)| \leq \frac{1}{2} \Big[q(x, Q^2) + \Delta q(x, Q^2) \Big]. \tag{13.5}$$

Experimental study of transversity distributions at leading-twist requires observables which are the product of two objects with odd chirality – the transversity distribution and either a second transversity distribution or a chiral odd fragmentation function. In proton-proton collisions the transverse double spin asymmetry, $\mathcal{A}_{TT}$, is proportional to $\delta q \delta \bar{q}$ with even chirality. However the asymmetry is small requiring very large luminosity samples because of the large background from gluon induced processes in unpolarized scattering. The most promising process to measure this double spin asymmetry is perhaps Drell-Yan production.

Transverse single spin asymmetries $\mathcal{A}_N$ are also being studied with a view to extracting information about transversity distributions. Here the focus is on single

hadron production with a transversely polarized proton beam or target in pp and ep collisions. The key process is

$$A(p, \vec{s}_t) + B(p') \to C(l) + X \tag{13.6}$$

where C is typically a pion produced at large transverse momentum l_t.

Several mechanisms for producing these transverse single spin asymmetries have been discussed in the literature. The asymmetries $\mathcal{A}_N$ are powered suppressed in QCD. Leading l_t behaviour of the produced pion can occur from the Collins (1993b) and Sivers (1991) effects plus twist-3 mechanisms [Qiu and Sterman (1999)]. The Collins effect involves the chiral-odd twist-2 transversity distribution in combination with a chiral-odd fragmentation function for the high l_t pion in the final state. It gives a possible route to measuring transversity. The Sivers effect is associated with intrinsic quark transverse momentum in the initial state. The challenge is to disentangle these effects from experimental data.

Factorization for transverse single spin processes in proton-proton collisions has been derived by Qiu and Sterman (1999) in terms of the convolution of a twist-two parton distribution from the unpolarized hadron, a twist-three quark-gluon correlation function from the polarized hadron, and a short distance partonic hard part calculable in perturbative QCD. We refer to Anselmino *et al.* (2005) for a discussion of factorization for processes such as the Collins and Sivers effects involving unintegrated transverse momentum dependent parton and fragmentation functions.

We next outline the Collins and Sivers effects.

The Collins effect [Collins (1993b)] uses properties of fragmentation to probe transversity. The idea is that a pion produced in fragmentation will have some transverse momentum with respect to the momentum k of the transversely polarized fragmenting parent quark. One finds a correlation of the form $i\vec{s}_t \cdot (\vec{l}^{(\pi)} \times \vec{k}_t)$. The Collins fragmentation function associated with this correlation is chiral-odd and T-even. It combines with the chiral-odd transversity distribution to contribute to the transverse single spin asymmetry.

For the Sivers effect [Sivers (1991)] the k_t distribution of a quark in a transversely polarized hadron can generate an azimuthal asymmetry through the correlation $\vec{s}_t \cdot (\vec{p} \times \vec{k}_t)$. In this process final state interaction (FSI) of the active quark produces the asymmetry before it fragments into hadrons [Brodsky *et al.* (2002); Yuan (2003); Burkardt and Hwang (2004); Bachetta *et al.* (2004)]. This process involves a k_t unintegrated quark distribution function in the transversely polarized proton. The dependence on intrinsic quark transverse momentum means that this Sivers process is related to quark orbital angular momentum in the proton [Burkardt (2002)]. The Sivers distribution function is chiral-even and T-odd. The possible role of quark orbital angular momentum in understanding transverse single-spin asymmetries is also discussed in Boros *et al.* (1993). Brodsky and Gardner (2006) have highlighted the gluon Sivers function as a possible way to access gluon orbital angular momentum in the proton.

The Sivers process is associated with the gauge link in operator definitions of the parton distributions. The gauge link factor is trivial and equal to one for the usual k_t integrated parton distributions measured in inclusive polarized deep inelastic scattering. However, for k_t unintegrated distributions the gauge link survives in a transverse direction at light-cone component $\xi^- = \infty$. The gauge-link plays a vital role in the Sivers process [Burkardt (2005)]. Without it (e.g. in the pre-QCD "naive" parton model) time reversal invariance implies vanishing Sivers effect [Ji and Yuan (2002); Belitsky *et al.* (2003a)]. The Sivers distribution function has the interesting property that it has the opposite sign in deep inelastic scattering and Drell-Yan reactions [Collins (2002)]. It thus violates the universality of parton distribution functions.

The FermiLab experiment E704 found large transverse single-spin asymmetries $\mathcal{A}_N$ for π and Λ production in proton-antiproton collisions at centre of mass energy $\sqrt{s} = 20$ GeV [Adams *et al.* (1991a,b); Bravar *et al.* (1996)]. Large transverse single-spin asymmetries have also been observed in recent data from the STAR collaboration at RHIC in proton-proton collisions at centre of mass energy $\sqrt{s} = 200$GeV [Adams *et al.* (2004)] – see Figure 13.2 which also shows various theoretical predictions. Anselmino *et al.* (2005) take into account intrinsic parton motion in the distribution and fragmentation functions as well as in the elementary dynamics and argue that the Collins mechanism may be strongly suppressed at large Feynman x_F in this process. The Sivers effect is not suppressed and remains a can-

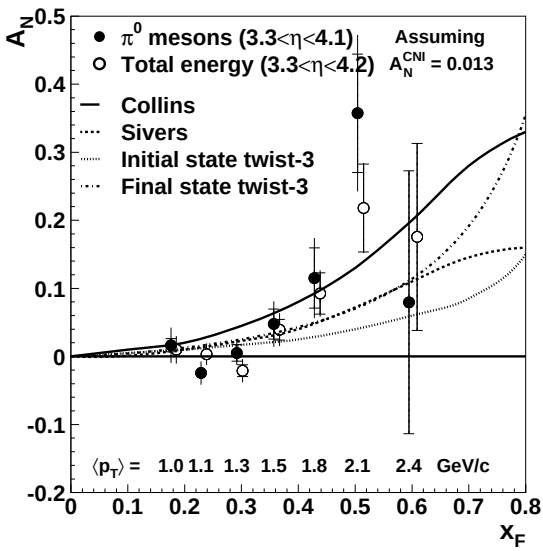

Fig. 13.2 Recent STAR results for the asymmetry $A_{\rm N}$ in $pp \to \pi^0 X$ in the forward Feynman-x_F region [Adams *et al.* (2004)].

didate to explain the data. Higher-twist contributions [Qiu and Sterman (1999)] from quark-gluon correlations may also be important. Recent PHENIX data on $p^{\uparrow}p \to \pi^0 X$ at midrapidity [Adler *et al.* (2005a)] has been interpreted to suggest a small gluon Sivers function [Anselmino *et al.* (2006)]. The BRAHMS collaboration has also measured significant non-zero asymmetries in forward charged pion production at 200 (as well as 62.4) GeV [Lee and Videbaek (2006)].

The HERMES experiment has taken measurements of charged pion production in ep scattering with transverse target polarization [Airapetian *et al.* (2005b)]. This data has been analysed for possible contributions from the Collins and Sivers effects. The azimuthal distribution of the final state pions with respect to the virtual photon axis is expected to carry information about transversity through the Collins effect and about intrinsic transverse momentum in the proton through the Sivers effect. In this analysis one first writes the transverse single-spin asymmetry $\mathcal{A}_N$ as the sum

$$\mathcal{A}_N(x,z) = \mathcal{A}_N^{\text{Collins}} + \mathcal{A}_N^{\text{Sivers}} + ... \tag{13.7}$$

where

$$\mathcal{A}_N^{\text{Collins}} \propto |\vec{s}_t| \sin(\phi + \phi_S) \frac{\sum_q e_q^2 \delta q(x) H_1^{\perp,q}(z)}{\sum_q e_q^2 q(x) D_q^{\pi}(z)} \tag{13.8}$$

and

$$\mathcal{A}_N^{\text{Sivers}} \propto |\vec{s}_t| \sin(\phi - \phi_S) \frac{\sum_q e_q^2 f_{1T}^{\perp,q} D_q^{\pi}(z)}{\sum_q e_q^2 q(x) D_q^{\pi}(z)} \tag{13.9}$$

denote the contributions from the Collins and Sivers effects. Here ϕ is the angle between the lepton direction and the $(\gamma^*\pi)$ plane and ϕ_S is the angle between the lepton direction and the transverse target spin; $H_1^{\perp q}$ is the Collins function for a quark of flavour q, $f_{1T}^{\perp,q}$ is the Sivers distribution function, and D_q^{π} is the regular spin independent fragmentation function. When one projects out the two terms with different azimuthal angular dependence the HERMES analysis suggests that both the Collins and Sivers effects are present in the data – see Fig. 13.3. Futhermore, the analysis suggests the puzzling result that the "favoured" (for $u \to \pi^+$) and "unfavoured" (for $d \to \pi^+$) Collins fragmentation functions may contribute with equal weight (and opposite sign) [Airapetian *et al.* (2005b)].

Recent COMPASS data for pion production from a transverse deuteron target taken at higher energy and higher Q^2 are shown in Fig. 13.4 [Ageev *et al.* (2007)]. These data are consistent with zero Collins and Sivers asymmetries for the isoscalar deuteron. (The figure shows the results for "leading hadron" production where all events involve at least one hadron with the fraction of available energy $z > 0.25$ and the hadron with the largest z was defined as "leading".) They are consistent with the HERMES measurement of non-zero Collins asymmetries on a transversely polarized proton target if the Collins asymmetry is dominated by its isovector component, like the situation for $g_1^{(p-n)}$ with longitudinal polarization. The smallness

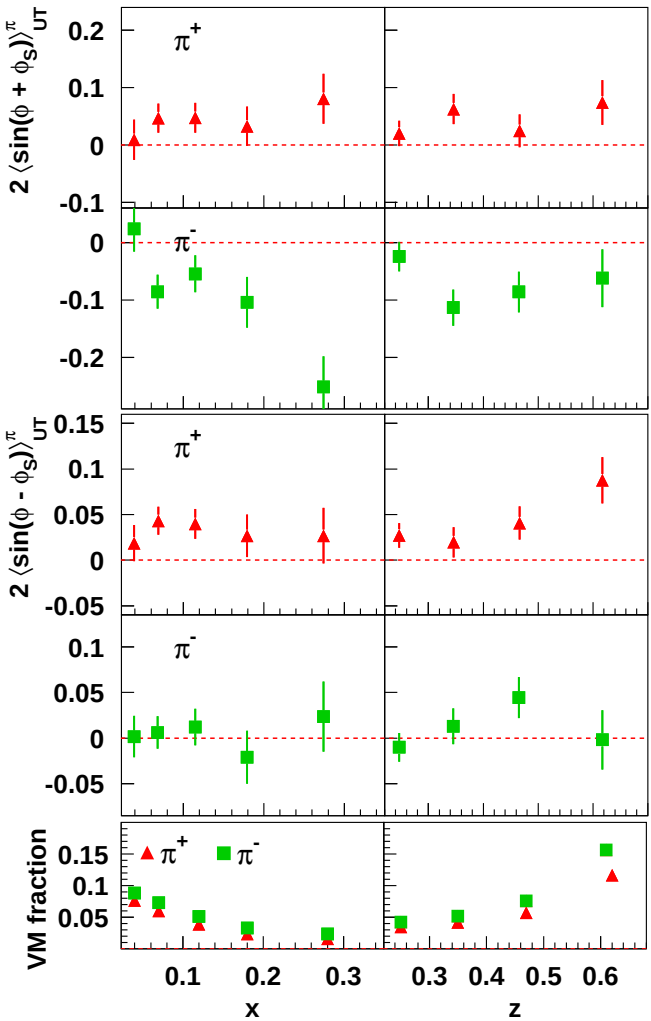

Fig. 13.3 HERMES measurements of the virtual-photon Collins and Sivers moments for charged pion production from a proton target as a function of x and z, multiplied by two to have the possible range ± 1 [Airapetian *et al.* (2005b)].

of the COMPASS Sivers asymmetry for positive and negative hadron production from the deuteron has been interpreted as evidence for the absence of large gluon orbital angular momentum in the nucleon [Brodsky and Gardner (2006)], which is consistent with the interpretation of a small gluonic Sivers contribution [Anselmino *et al.* (2006)] to the PHENIX measurements of $pp^{\uparrow} \to \pi^0 X$.

Other processes and experiments will help to clarrify the importance of the Collins and Sivers processes. Additional studies of the Collins effect have been proposed in e^+e^- collisions using the high statistics data samples of BABAR and

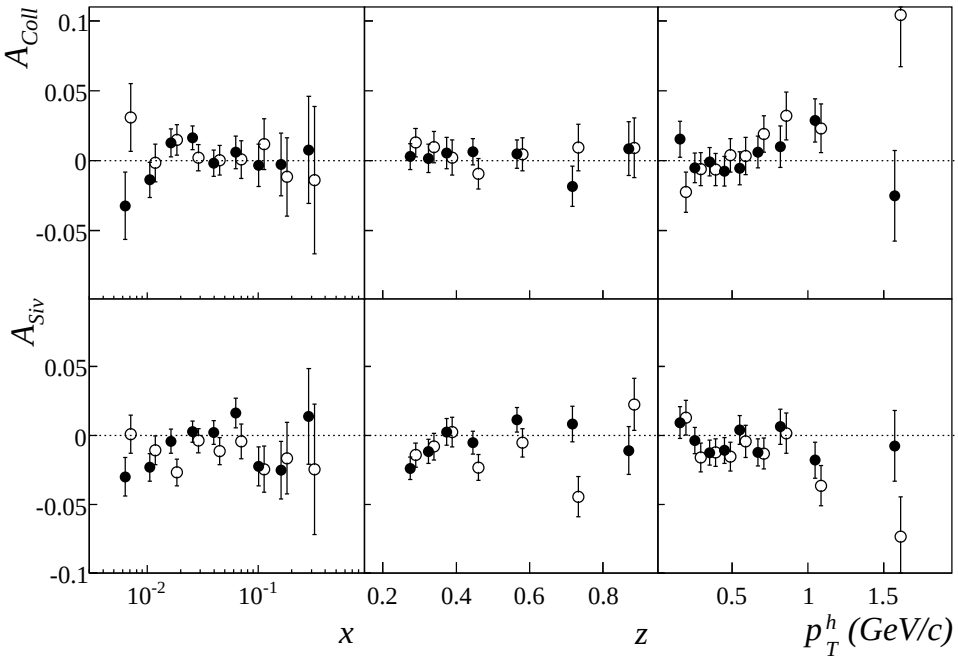

Fig. 13.4 Collins asymmetry (top) and Sivers asymmetry (bottom) against x, z and p_t^h for positive (full circles) and negative leading hadrons (open circles) from the COMPASS 2003–2004 data taken with a deuteron target. Error bars are statistical only. In all the plots the open circles are slightly shifted horizontally with respect to the measured value [Ageev *et al.* (2007)].

BELLE. The aim is to measure two relevant fragmentation functions: the Collins function $H_1^\perp$ and the interference fragmentation functions $\delta\hat{q}^{h_1,h_2}$. For the first, one measures the fragmentation of a transversely polarized quark into a charged pion and the azimuthal distribution of the final state pion with respect to the initial quark momentum (jet-axis). For the second, one measures the fragmentation of transversely polarized quarks into pairs of hadrons in a state which is the superposition of two different partial wave amplitudes, e.g. π^+,π^- pairs in the ρ and σ invariant mass region [Collins *et al.* (1994); Jaffe *et al.* (1998)]. The high luminosity and particle identification capabilities of detectors at B-factories makes these measurements possible. First data from BELLE are reported in Seidl *et al.* (2006) and support a finite Collins asymmetry.

The Sivers distribution function might be measurable through the transverse single spin asymmetry $\mathcal{A}_N$ for D meson production generated in $p^\uparrow p$ scattering [Anselmino *et al.* (2004)]. Here the underlying elementary processes guarantee the absence of any polarization in the final partonic state so that there is no contamination from Collins like terms. Large dominance of the process $gg \to c\bar{c}$ process at low and intermediate x_F offers a unique opportunity to measure the gluonic Sivers

distribution function. The gluonic Sivers function could also be extracted from back-to-back correlations in the azimuthal angle of jets in collisions of unpolarized and transversely polarized proton beams at RHIC [Boer and Vogelsang (2004)]. A first measurement of this observable has been made by the STAR collaboration [Abelev *et al.* (2007)].

Measurements with transversely polarized targets have a bright future and are already yielding surprises. The results promise to be interesting and to teach us about transversity and about the role of transverse and orbital angular momentum in the structure of the proton and fragmentation processes.

Chapter 14

DEEPLY VIRTUAL COMPTON SCATTERING AND EXCLUSIVE PROCESSES

So far we have concentrated on intrinsic spin in the proton. The orbital angular momentum structure of the proton is also of considerable interest and much effort has gone into devising ways to measure it. The strategy involves the use of hard exclusive reactions and the formalism of generalized parton distributions (GPDs) which describes deeply virtual Compton scattering (DVCS) and meson production (DVMP). Possible hints of quark orbital angular momentum are also suggested by recent form-factor measurements at Jefferson Laboratory [Jones *et al.* (2000); Gayou *et al.* (2002)] – see Fig. 14.1. The ratio of the spin-flip Pauli form-factor to the Dirac form-factor is observed to have a $1/\sqrt{Q^2}$ behaviour in the measured region in contrast with the $1/Q^2$ behaviour predicted by QCD Counting Rules (helicity conservation neglecting angular momentum), *viz.* $F_1 \sim 1/Q^4$ and $F_2 \sim 1/Q^6$ [Brodsky and Lepage (1980)]. However, this data can also be fit with the formula

$$\frac{F_2(Q^2)}{F_1(Q^2)} = \frac{\mu_A}{1 + (Q^2/c)\ln^b(1 + Q^2/a)} \tag{14.1}$$

(with $\mu_A = 1.79$, $a = 4m_\pi^2 = 0.073$ GeV^2, $b = -0.5922$, $c = 0.9599$ GeV^2) prompting the question at which Q^2 the Counting Rules prediction is supposed to work and at which Q^2 higher twist effects can be neglected [Brodsky (2002a)]. At this point it is interesting to recall that the simple Counting Rules prediction fails to describe the large x behaviour of $\Delta d/d$ in the presently measured JLab kinematics – Chapter 9.

A $1/Q$ behaviour for $F_2(Q^2)/F_1(Q^2)$ is found in a light-front Cloudy Bag calculation [Miller and Frank (2002); Miller (2002)] and in quark models with orbital angular momentum [Ralston and Jain (2004); Ralston *et al.* (2002)]. A new perturbative QCD calculation which takes into account orbital angular momentum [Belitsky *et al.* (2003b)] gives

$$F_2/F_1 \sim (\log^2 Q^2/\Lambda^2)/Q^2 \tag{14.2}$$

and also fits the Jefferson Lab data well. This logarithmic correction is consistent with contribution from finite orbital angular momentum Fock states quoted in Eq. (9.7). The planned 12 GeV upgrade at Jefferson Laboratory will enable us to

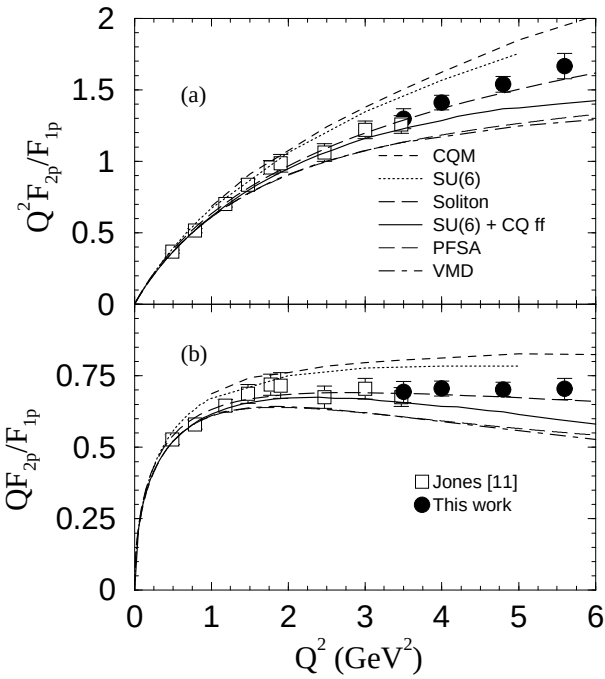

Fig. 14.1 Jefferson Lab data on the the ratio of the proton's Pauli to Dirac form-factors [Gayou *et al.* (2002)].

measure these nucleon form-factors at higher Q^2 and the inclusive spin asymmetries at values of Bjorken x closer to one, and thus probe deeper into the kinematic regions where QCD Counting Rules should apply. This data promises to be very interesting!

Deeply virtual Compton scattering (DVCS) provides a possible experimental tool to access the quark total angular momentum, J_q, in the proton through the physics of generalized parton distributions (GPDs) [Ji (1997a,b)]. The form-factors which appear in the forward limit ($t \to 0$) of the second moment of the spin-independent generalized quark parton distribution in the (leading-twist) spin-independent part of the DVCS amplitude project out the quark total angular momentum defined through the proton matrix element of the QCD angular-momentum tensor. We explain this physics below.

DVCS studies have to be careful to chose the kinematics not to be saturated by a large Bethe-Heitler (BH) background where the emitted real photon is radiated from the electron rather than the proton – see Fig. 14.2. The HERMES and Jefferson Laboratory experiments measure in the kinematics where they expect to be dominated by the DVCS-BH interference term and observe the $\sin\phi$ azimuthal angle and helicity dependence expected for this contribution – see Fig. 14.3. First measurements of the single spin asymmetry have been reported in Airapetian *et al.* (2001) and Stepanyan *et al.* (2001), which have the characteristics expected from

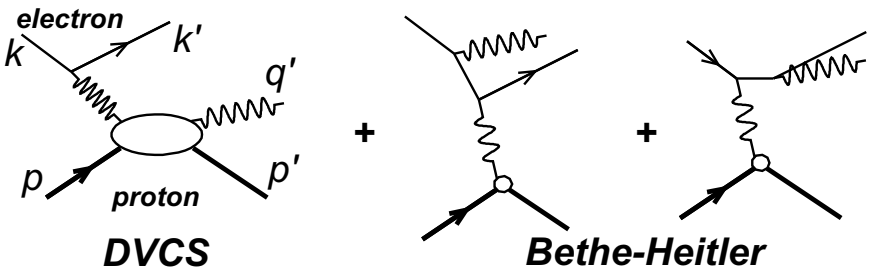

Fig. 14.2 The DVCS and Bethe-Heitler processes.

the DVCS-BH interference. DVCS has also been observed by the H1 [Adloff *et al.* (2001); Aktas *et al.* (2005)] and ZEUS [Chekanov *et al.* (2003b)] experiments at HERA at $x \sim 10^{-3}$ and close to the forward direction.

For exclusive processes such as DVCS or hard meson production the generalized parton distributions involve non-forward proton matrix elements [Goeke *et al.* (2001); Ji (1998); Diehl (2003); Radyushkin (1997); Vanderhaeghen *et al.* (1998)]. The important kinematic variables are the virtuality of the hard photon Q^2, the momenta $p - \Delta/2$ of the incident proton and $p + \Delta/2$ of the outgoing proton, the invariant four-momentum transferred to the target $t = \Delta^2$, the average nucleon momentum P, the generalized Bjorken variable $k^+ = xP^+$ and the light-cone momentum transferred to the target proton $\xi = -\Delta^+/2p^+$. The generalized parton distributions are defined as the light-cone Fourier transform of the point-split matrix element

$$\begin{aligned}
&\frac{P_+}{2\pi}\int dy^- e^{-ixP^+y^-}\,\langle p'|\bar\psi_\alpha(y)\psi_\beta(0)|p\rangle_{y^+=y_\perp=0}\\
&=\frac{1}{4}\gamma^-_{\alpha\beta}\Big[H(x,\xi,\Delta^2)\bar u(p')\gamma^+u(p)\\
&\qquad\qquad +E(x,\xi,\Delta^2)\bar u(p')\sigma^{+\mu}\frac{\Delta_\mu}{2M}u(p)\Big]\\
&\quad+\frac{1}{4}(\gamma_5\gamma^-)_{\alpha\beta}\Big[\tilde H(x,\xi,\Delta^2)\bar u(p')\gamma^+\gamma_5u(p)\\
&\qquad\qquad +\tilde E(x,\xi,\Delta^2)\bar u(p')\gamma_5\frac{\Delta^+}{2M}u(p)\Big].
\end{aligned}\tag{14.3}$$

(Here we work in the light-cone gauge $A_+ = 0$ so that the path-ordered gauge-link becomes trivial and equal to one to maintain gauge invariance through-out.)

The physical interpretation of the generalized parton distributions (before

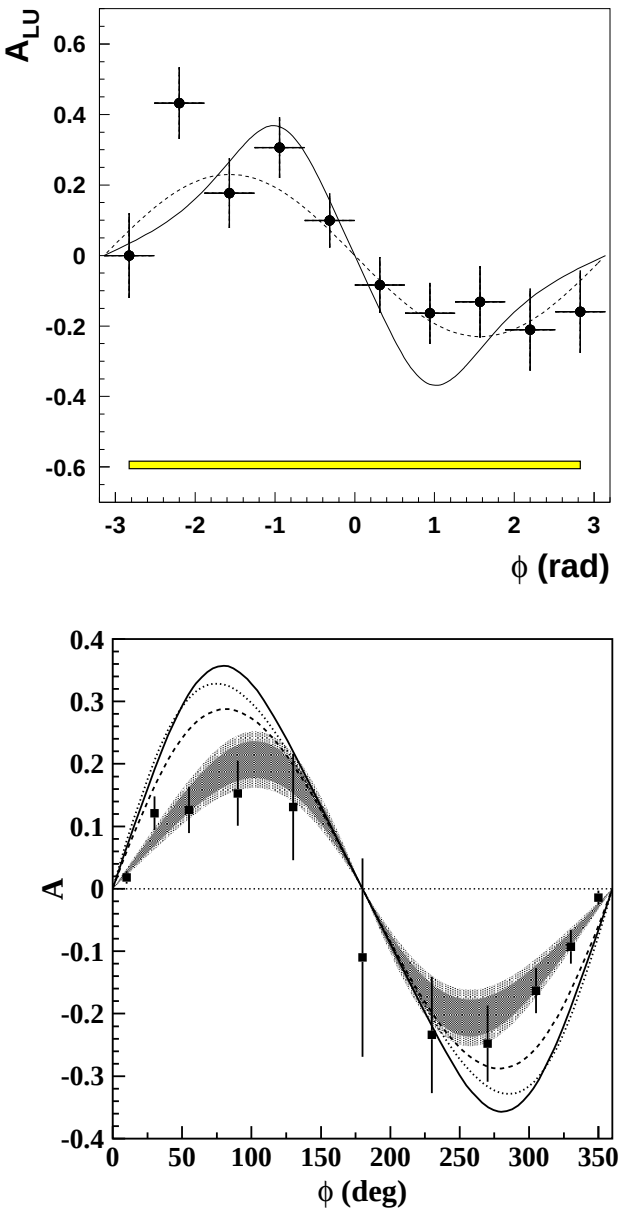

Fig. 14.3 Recent data from HERMES (above) and the CLAS experiment at Jefferson Laboratory (below) in the realm of DVCS Bethe-Heitler interference. The $\sin\phi$ azimuthal dependence of the single spin asymmetry is clearly visible in the data [Airapetian *et al.* (2001); Stepanyan *et al.* (2001)].

worrying about possible renormalization effects and higher order corrections) is the following. Expanding out the quark field operators in Eq. (14.3) in terms of light-cone quantized creation and annihilation operators one finds that for $x > \xi$ ($x < \xi$) the GPD is the amplitude to take a quark (anti-quark) of momentum $k - \Delta/2$ out of the proton and reinsert a quark (anti-quark) of momentum $k + \Delta/2$ into the proton some distance along the light-cone to reform the recoiling proton. In this region the GPD is a simple generalization of the usual parton distributions studied in inclusive and semi-inclusive scattering. In the remaining region $-\xi < x < \xi$ the GPD involves taking out (or inserting) a $q\bar{q}$ pair with momentum $k - \Delta/2$ and $-k - \Delta/2$ (or $k + \Delta/2$ and $-k + \Delta/2$) respectively. Note that the GPDs are interpreted as probability amplitudes rather than densities.

In the forward limit the GPDs H and $\tilde{H}$ are related to the forward parton distributions studied in (polarized) deep inelastic scattering:

$$\begin{aligned} H(x,\xi,\Delta^2)|_{\xi=\Delta^2=0} &= q(x) \\ \tilde{H}(x,\xi,\Delta^2)|_{\xi=\Delta^2=0} &= \Delta q(x) \end{aligned} \tag{14.4}$$

whereas the GPDs E and $\tilde{E}$ have no such analogue. In the fully renormalized theory the spin dependent distributions $\tilde{H}$ and $\tilde{E}$ will be sensitive to the physics of the axial anomaly and, in this case, it is not easy to separate off an "anomalous component" because the non-forward matrix elements of the gluonic Chern-Simons current are non-gauge-invariant even in the light-cone gauge $A_+ = 0$. Integrating over x the first moments of the GPDs are related to the nucleon form-factors:

$$\begin{aligned} \int_{-1}^{+1} dx H(x,\xi,\Delta^2) &= F_1(\Delta^2) \\ \int_{-1}^{+1} dx E(x,\xi,\Delta^2) &= F_2(\Delta^2) \\ \int_{-1}^{+1} dx \tilde{H}(x,\xi,\Delta^2) &= G_A(\Delta^2) \\ \int_{-1}^{+1} dx \tilde{E}(x,\xi,\Delta^2) &= G_P(\Delta^2). \end{aligned} \tag{14.5}$$

Here F_1 and F_2 are the Dirac and Pauli form-factors of the nucleon, and G_A and G_P are the axial and induced-pseudoscalar form-factors respectively. (The dependence on ξ drops out after integration over x.)

The GPD formalism allows one, in principle, to extract information about quark angular momentum from hard exclusive reactions [Ji (1997a)]. The current associated with Lorentz transformations is

$$M_{\mu\nu\lambda} = z_\nu T_{\mu\lambda} - z_\lambda T_{\mu\nu} \tag{14.6}$$

where $T_{\mu\nu}$ is the QCD energy-momentum tensor. Thus, the total angular momentum operator is related to the energy-momentum tensor through the equation

$$J^z_{q,g} = \langle p', \frac{1}{2}| \int d^3z \ (\vec{z} \times \vec{T}_{q,g})^z \ |p, \frac{1}{2}\rangle. \tag{14.7}$$

The form-factors corresponding to the energy-momentum tensor can be projected out by taking the second moment with respect to x) of the GPD. One finds Ji's sum-rule for the total quark angular momentum

$$J_q = \frac{1}{2}\int_{-1}^{+1} dx x\Big[H(x,\xi,\Delta^2=0) + E(x,\xi,\Delta^2=0)\Big]. \tag{14.8}$$

The gluon "total angular momentum" could then be obtained through the equation

$$\sum_q J_q + J_g = \frac{1}{2}. \tag{14.9}$$

In principle, it could also be extracted from precision measurements of the Q^2 dependence of hard exclusive processes like DVCS and meson production at next-to-leading-order accuracy where the quark GPD's mix with glue under QCD evolution.

To obtain information about the "orbital angular momentum" L_q we need to subtract the value of the "intrinsic spin" measured in polarized deep inelastic scattering (or a future precision measurement of νp elastic scattering) from the total quark angular momentum J_q. This means that L_q is scheme dependent with different schemes corresponding to different physics content depending on how the scheme handles information about the axial anomaly, large k_t physics and any possible "subtraction at infinity" in the dispersion relation for g_1. The quark total angular momentum J_q is anomaly free in QCD so that QCD axial anomaly effects occur with equal magnitude and opposite sign in L_q and S_q [Bass (2002a); Shore and White (2000)]. The "quark orbital angular momentum" L_q is measured by the proton matrix element of $[\bar{q}(\vec{z}\times\vec{D})_3 q](0)$, *viz.*

$$\begin{aligned}
\vec{J}_q &= \int d^3x\ \vec{x}\times\vec{T}_q \\
&= \int d^3x\ \left[\psi^\dagger\frac{\vec{\Sigma}}{2}\psi + \psi^\dagger\vec{x}\times(-i\vec{D})\psi\right], \\
\vec{J}_g &= \int d^3x\ \vec{x}\times(\vec{E}\times\vec{B})
\end{aligned} \tag{14.10}$$

The gauge covariant derivative means that L_q becomes sensitive to gluonic degrees of freedom in addition to the axial anomaly, — for a recent discussion see Jaffe (2001). A first attempt to extract the valence contributions to the energy-momentum form-factors entering Ji's sum rule is reported in Diehl *et al.* (2004).

A recent lattice calculation [Hägler *et al.* (2007)] gives

$$\begin{aligned}
J_u &= 0.22 \pm 0.02 \\
J_d &= 0.00 \pm 0.02
\end{aligned} \tag{14.11}$$

corresponding to $m_\pi \sim 350$ MeV with $L_u \sim -L_d \sim 20-30\%$ of the proton's spin $\frac{1}{2}$. These values of the total angular momentum contributions are close to the asymptotic values predicted by QCD evolution. The connection between the

quark and gluon total angular momentum contributions J^q and J^g and the QCD energy-momentum tensor allows us to write down their QCD evolution equations:

$$\frac{\partial}{\partial \ln \mu^2} \begin{pmatrix} J_q(\mu) \\ J_g(\mu) \end{pmatrix} = \frac{\alpha_s(\mu)}{2\pi} \frac{1}{9} \begin{pmatrix} -16 & 3f \\ 16 & -3f \end{pmatrix} \begin{pmatrix} J_q(\mu) \\ J_g(\mu) \end{pmatrix} \tag{14.12}$$

As $\mu \to \infty$ the total angular momentum contributions tend to

$$\begin{aligned} J_q(\infty) &= \frac{1}{2} \frac{3f}{16+3f} \\ J_g(\infty) &= \frac{1}{2} \frac{16}{16+3f} \end{aligned} \tag{14.13}$$

like the quark and gluon momentum contributions in Eq. (2.28).

The study of GPDs is being pioneered in experiments at HERMES, Jefferson Laboratory and COMPASS. Proposals and ideas exist for dedicated studies using a 12 GeV CEBAF machine, a possible future polarized *ep* collider (EIC) in connection with RHIC or JLab, and a high luminosity polarized proton-antiproton collider at GSI. To extract information about quark total angular momentum one needs high luminosity, plus measurements over a range of kinematics Q^2, x and Δ (bearing in mind the need to make reliable extrapolations into unmeasured kinematics). There is a challenging programme to disentangle the GPDs from the formalism and to undo the convolution integrals which relate the GPDs to measured cross-sections. Recent data from the Hall A Collaboration at JLab suggests the twist-2 dominance of DVCS even at the relatively low Q^2 of 1.5 - 2.3 GeV^2 [Munoz Camacho *et al.* (2006)]. Varying the photon or meson in the final state will give access to different spin-flavour combinations of GPDs even with unpolarized beams and targets. Besides yielding possible information about the spin structure of the proton, measurements of hard exclusive processes will, in general, help to constrain our understanding of the structure of the proton.

This page intentionally left blank

Chapter 15

POLARIZED PHOTON STRUCTURE FUNCTIONS

Deep inelastic scattering from photon targets reveals many novel effects in QCD. The unpolarized photon structure function has been well studied both theoretically and experimentally. The polarized photon spin structure function is an ideal (theoretical) laboratory to study the QCD dynamics associated with the axial anomaly.

The photon structure functions are observed experimentally in $e^+\ e^- \rightarrow$ hadrons where for example a hard photon (large Q^2) probes the quark structure of a soft photon ($P^2 \sim 0$). For any virtuality P^2 of the target photon the measured structure functions receive a contribution both from contact photon-photon fusion and also a hadronic piece, which is commonly associated with vector meson dominance (VMD) of the soft target photon. The hadronic term scales with Q^2 whilst the contact term behaves as $\ln Q^2$ as we let Q^2 tend to ∞. This result was discovered by Witten (1977) for the unpolarized structure function F_2^γ and extended to the polarized case in Manohar (1989) and Sasaki (1980). The $\ln Q^2$ scaling behaviour mimics the leading-order box diagram prediction but the coefficient of the logarithm receives a finite renormalization in QCD. From the viewpoint of the renormalization group the essential detail discovered by Witten is that the coefficient functions of the photonic and singlet hadronic operators will mix under QCD evolution. The hadronic matrix elements are of leading order in α whilst the photon operator matrix elements are $O(1)$. Since the hadronic coefficient functions are $O(1)$ and the photon coefficient functions start at $O(\alpha)$ the photon structure functions receive leading order contributions in α from both the hadronic and photonic channels.

In polarized scattering the first moment of g_1^γ is especially interesting. First, consider a real photon target (and assume no fixed pole correction). The first moment of g_1^γ vanishes

$$\int_0^1 dx\ g_1^\gamma(x, Q^2) = 0 \tag{15.1}$$

for a real photon target independent of the virtuality Q^2 of the photon that it is probed with [Bass (1992); Bass *et al.* (1998)]. This result is non-perturbative. To understand it, consider the real photon as the beam and the virtual photon as the

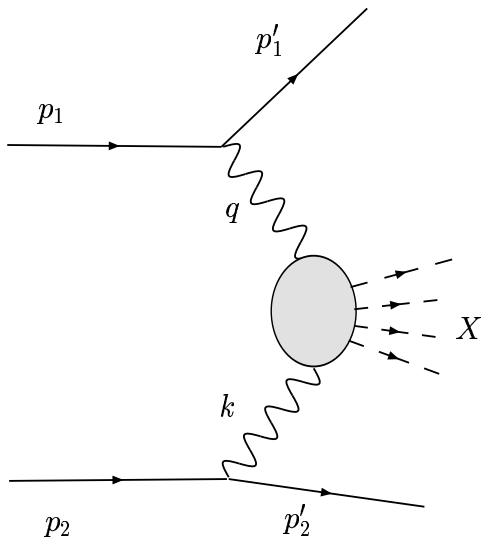

Fig. 15.1 Kinematics for the two-photon DIS process $e^+e^- \to e^+e^-X$. The photon structure functions are observed experimentally in $e^+\,e^- \to$ hadrons where for example a hard photon (large Q^2) probes the quark structure of a soft photon ($P^2 = -k^2 \sim 0$).

target. Next apply the Gerasimov-Drell-Hearn sum rule. The anomalous magnetic moment of a photon vanishes to all orders because of Furry's theorem whence one obtains the sum-rule. The sum rule (15.1) holds to all orders in perturbation theory and at every twist [Bass *et al.* (1998)].

The interplay of QCD and QED dynamics here can be seen through the axial anomaly equation

$$\partial^\mu J_{\mu 5} = 2m\overline{q}i\gamma_5 q + \frac{\alpha_s}{4\pi}G_{\mu\nu}\tilde{G}^{\mu\nu} + N_c\frac{\alpha}{2\pi}F_{\mu\nu}\tilde{F}^{\mu\nu} \tag{15.2}$$

(including the QED anomaly). The gauge-invariantly renormalized axial-vector current can then be written as the sum of the partially conserved current plus QCD and abelian QED Chern-Simons currents

$$J_{\mu 5} = J_{\mu 5}^{\rm con} + K_\mu + N_c k_\mu \tag{15.3}$$

where k_μ is the anomalous Chern Simons current in QED.

The vanishing first moment of $\int_0^1 dx g_1^\gamma$ is the sum of a contact term $-\frac{\alpha}{\pi}N_c\sum_q e_q^4$ measured by the QED Chern Simons current and a hadronic term associated with the two QCD currents in Eq. (15.3). The contact term is associated with high k_t leptons and two quark jet events (and no beam jet) in the final state.

For the gluonic contribution associated with polarized glue in the hadronic component of the polarized photon, the two quark jet cross section is associated with an extra soft "beam jet".

For a virtual photon target one expects the first moment to exhibit similar behaviour to that suggested by the tree box graph amplitude – that is, for $P^2 \gg m^2$ the first moment tends to equal just the QED anomalous contribution and the hadron term vanishes. However, here the mass scale m^2 is expected to be set by the ρ meson mass corresponding to a typical hadronic scale and vector meson dominance of the soft photon instead of the light-quark mass or the pion mass [Shore and Veneziano (1993a,b)]. Measurements of g_1^γ might be possible with a polarized $e\gamma$ collider [De Roeck (2001)] or high luminosity B factory [Shore (2005)]. The virtual photon target could be investigated through the study of resolved photon contributions to polarized deep inelastic scattering from a nucleon target [Stratmann (1998)]. Target mass effects in the polarized virtual photon structure function are discussed in Baba *et al.* (2003).

We now explain these results.

15.1 A sum-rule for g_1^γ

Consider polarized $\gamma\gamma$ scattering where σ_A and σ_P denote the two cross-sections for the absorption of a transversely polarized photon with spin anti-parallel σ_A and parallel σ_P to the spin of the target photon. We let q_μ and p_μ denote the momentum of the "incident" and "target" photons and define $Q^2 = -q^2$, $P^2 = -p^2$ and $\nu = p.q$. The spin dependent part of the total $\gamma\gamma$ cross-section is given by

$$(\sigma_A - \sigma_P) = \frac{8\pi^2\alpha}{\mathcal{F}} g_1^\gamma(Q^2, \nu, P^2). \tag{15.4}$$

Here g_1^γ is the target photon's spin dependent structure function and $\mathcal{F}$ is the flux factor for the incident photon. The structure function $g_1^\gamma(Q^2, \nu, P^2)$ is symmetric under the exchange of the incident and target photons ($p \leftrightarrow q$). There is no g_2 contribution to $(\sigma_A - \sigma_P)$ [Ahmed and Ross (1975); Manohar (1989)].

Now consider a real photon beam: $Q^2 = 0$. The Gerasimov-Drell-Hearn sum-rule for spin dependent photoproduction tells us that the integral $\int_0^\infty \frac{d\nu}{\nu}(\sigma_A - \sigma_P)$ is proportional to α times the square of the (photon) target's anomalous magnetic moment – see Eq. (4.45) and Chapter 4.5. For a real incident photon the flux factor $\mathcal{F} = \nu$. Furry's theorem tells us that the photon has zero anomalous magnetic moment (both in QED and in QED coupled to QCD). It follows that

$$\int_0^\infty \frac{d\nu}{\nu}(\sigma_A - \sigma_P) = 8\pi^2\alpha \int_{\nu_{th}}^\infty \frac{d\nu}{\nu}\frac{g_1^\gamma}{\nu} = 0, \qquad (P^2 = Q^2 = 0). \tag{15.5}$$

Here ν_{th} is the threshold energy: $\nu_{th} = 2m_e^2$ in QED and $\nu_{th} = \frac{1}{2}m_\pi^2$ in QCD. Eq. (15.5) is a non-perturbative result. It holds to all orders in perturbation theory.

We now generalise this result to the case where one of the two photons becomes virtual: $Q^2 > 0$. Furry's theorem implies that the anomalous magnetic moment of a photon vanishes independently of whether the photon is real or virtual. Since g_1^γ and ν are each symmetric under the exchange of $(p \leftrightarrow q)$, we can treat the virtual photon as the target and the real photon as the beam, and then apply the Drell-Hearn-Gerasimov sum-rule to find

$$I^\gamma(Q^2) \equiv \int_{\nu_{th}}^{\infty} \frac{d\nu}{\nu} \frac{g_1^\gamma(\nu, Q^2)}{\nu} = 0 \tag{15.6}$$

independent of Q^2 provided that $P^2 = 0$. Changing the integration variable from ν to Bjorken $x = \frac{Q^2}{2\nu}$, we can rewrite Eq. (15.6) as

$$I^\gamma(Q^2) = \frac{2}{Q^2} \int_0^{x_{max}} dx g_1^\gamma(x, Q^2) = 0 \qquad \forall Q^2. \tag{15.7}$$

The threshold factors in Eqs. (15.6) and (15.7) are $\nu_{th} = (Q^2 + 4m^2)/2$ and $x_{max} = Q^2/(Q^2 + 4m^2)$ in QED, and $\nu_{th} = (Q^2 + m_\pi^2)/2$ and $x_{max} = Q^2/(Q^2 + m_\pi^2)$ in QCD. Since the first moment of g_1^γ vanishes, the mean value theorem implies that g_1^γ must change sign at least once at a value $x = x^*(Q^2)$. The function $I^\gamma(Q^2)$ interpolates between $Q^2 = 0$ and polarized deep inelastic scattering. The corresponding integral for a nucleon target is given in Eq. (4.50) and was introduced previously by Anselmino *et al.* (1989).

15.2 Twist expansion for g_1^γ when $Q^2 \to \infty$

When $Q^2 \to \infty$, the light-cone operator product expansion relates the first moment of the structure function g_1^γ to the scale-invariant axial charges of the target photon [Ahmed and Ross (1975); Manohar (1989); Bass (1992)] plus an expansion of higher-twist matrix elements:

$$\begin{aligned}
&\int_0^1 dx g_1^\gamma(x, Q^2) \\
&\quad = \left(\frac{1}{12}a^{(3)} + \frac{1}{36}a^{(8)}\right)\Big\{1 + \sum_{\ell \geq 1} c_{\mathrm{NS}\ell}\, \bar{g}^{2\ell}(Q)\Big\} + \frac{1}{9}a^{(0)}|_{\mathrm{inv}}\Big\{1 + \sum_{\ell \geq 1} c_{\mathrm{S}\ell}\, \bar{g}^{2\ell}(Q)\Big\} \\
&\qquad + \sum_{j=1}^{\infty}\left(\frac{P^2}{Q^2}\right)^j \{\text{twist } (2+2j) \text{ operator matrix elements}\} \\
&\qquad + \sum_{j=1}^{\infty}\left(\frac{m^2}{Q^2}\right)^j \sum_{k=0}^{\infty}\left(\frac{P^2}{Q^2}\right)^k \{\text{twist } (2+2k) \text{ operator matrix elements}\}.
\end{aligned} \tag{15.8}$$

where m is the quark mass.

15.2.1 *Leading twist 2*

For photon states $|\gamma(p,\lambda)\rangle$ with momentum p_μ and polarisation λ

$$ia^{(k)}\epsilon_{\mu\nu\alpha\beta}p^\nu\epsilon^\alpha(\lambda)\epsilon^{*\beta}(\lambda) = \langle\gamma(p,\lambda)|J^{(k)}_{\mu 5}|\gamma(p,\lambda)\rangle \tag{15.9}$$

where $k = (3, 8, 0)$ and the subscript c denotes the connected matrix element. The non-singlet isovector and SU(3) octet currents are

$$\begin{aligned} J^{(3)}_{\mu 5} &= \left(\bar{u}\gamma_\mu\gamma_5 u - \bar{d}\gamma_\mu\gamma_5 d\right) \\ J^{(8)}_{\mu 5} &= \left(\bar{u}\gamma_\mu\gamma_5 u + \bar{d}\gamma_\mu\gamma_5 d - 2\bar{s}\gamma_\mu\gamma_5 s\right) \end{aligned} \tag{15.10}$$

and

$$J^{(0)}_{\mu 5} = E(g)\ \left(\bar{u}\gamma_\mu\gamma_5 u + \bar{d}\gamma_\mu\gamma_5 d + \bar{s}\gamma_\mu\gamma_5 s\right)_{GI} \tag{15.11}$$

is the scale invariant and gauge-invariantly renormalized singlet axial-vector operator. The renormalisation group factor $E(\alpha_s)$ compensates for the non-zero anomalous dimension of the singlet axial-vector current $J^{(0)}_{\mu 5}/E(\alpha_s)$. The flavour non-singlet $c_{\mathrm{NS}\ell}$ and singlet $c_{\mathrm{S}\ell}$ coefficients are calculable in ℓ-loop perturbation theory [Larin *et al.* (1997)]. There are no twist two, spin one, gauge-invariant photon or gluon operators which can contribute to the first moment of g_1^γ.

One can derive a rigorous sum-rule for the leading twist (=2) contribution to the first moment of g_1^γ in polarized deep inelastic scattering where one of the photons is deeply virtual ($Q^2 \to \infty$) and the other photon is either real [Bass (1992)] or carries small but finite virtuality [Narison *et al.* (1993); Shore and Veneziano (1993b)]. Electromagnetic gauge-invariance implies [Bass (1992)] that the axial charges of a real photon vanish provided that there is no exactly massless Goldstone boson coupled to $J^{(k)}_{\mu 5}$, which is certainly true in nature with massive quarks. For real photons we find

$$\int_0^1 dx g_1^\gamma|_{\{\text{twist }2\}}(x,Q^2) = 0, \qquad (P^2 = 0,\ Q^2 \to \infty). \tag{15.12}$$

This deep inelastic sum-rule holds at every order in perturbation theory – starting with the box graph for photon - photon fusion. Comparing Eqs. (15.11) and (15.7) we find that the vanishing of the leading twist contribution to $\int_0^1 dx g_1^\gamma$ is a special case of the Drell-Hearn-Gerasimov sum-rule when the beam and target photons are interchanged.

The general form for the matrix element of the axial vector current $J^i_{\mu 5}$ between on-shell photon states is given by covariance and parity. Allowing for Bose crossing symmetry we have

$$\langle\gamma(l,\lambda_2)|J^{(k)}_{\mu 5}|\gamma(p,\lambda_1)\rangle = R^k_{\mu\alpha\beta}(p,-l)\epsilon^\alpha(\lambda_1)\epsilon^{*\beta}(\lambda_2) \tag{15.13}$$

where

$$\begin{aligned} R^k_{\mu\alpha\beta}(p,-l) = \Bigg[&\epsilon_{\mu\nu\alpha\beta}(p^\nu + l^\nu)A^k(s^2) + \epsilon_{\mu\alpha\nu\delta}p^\nu l^\delta\left(B^k_1(s^2)p_\beta + B^k_2(s^2)l_\beta\right) \\ &+ \epsilon_{\mu\beta\nu\delta}p^\nu l^\delta\left(B^k_1(s^2)l_\alpha + B^k_2(s^2)p_\alpha\right)\Bigg] \end{aligned} \tag{15.14}$$

with $s^\mu = (p-l)^\mu$ [Adler (1970)]. The A^k, B_1^k and B_2^k are scalar form factors of the variable s^2 (for real photons: $p^2 = l^2 = 0$). The forward matrix element, which is relevant to deep inelastic scattering, is given by

$$ia^{(k)} = 2A^k(s^2 = 0) \tag{15.15}$$

with $\lambda_1 = \lambda_2 = \lambda$. Here, we have tacitly assumed that there are no massless bosons coupled to $J_{\mu 5}^k$. This is true in nature. The would-be Goldstone bosons π^0 and η, which couple to $J_{\mu 5}^{(3)}$ and $J_{\mu 5}^{(8)}$ respectively have a finite mass due to the chiral symmetry breaking quark mass term in the QCD Lagrangian. There is no massless singlet Goldstone boson.

Electromagnetic gauge invariance (current conservation) at the photon vertices, *viz.*

$$p^\alpha R_{\mu\alpha\beta}^k = l^\beta R_{\mu\alpha\beta}^k = 0, \tag{15.16}$$

leads to the identities

$$A^k(s^2) = \frac{s^2}{2} B_1^k(s^2) + p^2 B_2^k(s^2)$$

$$A^k(s^2) = \frac{s^2}{2} B_1^k(s^2) + l^2 B_2^k(s^2) \tag{15.17}$$

respectively. Since $R_{\mu\alpha\beta}^k$ contains no massless poles we can drop the B_2^k term in Eqs. (15.16). Clearly, $A^k(s^2 = 0) = 0$ for each of $k = 3, 8, 0$. Hence, electromagnetic current conservation and the absence of any massless bosons coupled to $J_{\mu 5}^{(k)}$ imply the exact (scale independent) sum-rule

$$a^{(k)} = 0 \tag{15.18}$$

for the real photon.

The vanishing first moment of the twist-2 part of $\int_0^1 dx g_1^\gamma$ is the sum of a contact term $-\frac{\alpha}{\pi}\sum_q e_q^2$ measured by the QED Chern Simons current and a hadronic term associated with the two QCD currents in Eq. (15.3). The contact term is associated with high k_t leptons and two quark jet events (and no beam jet) in the final state. For the gluonic contribution associated with polarized glue in the hadronic component of the polarized photon, the two quark jet cross section is associated with an extra soft "beam jet". The contact anomalous interaction contribution is identically cancelled by the hadronic term associated with the operators $2m_q \overline{q} i\gamma_5 \frac{\lambda_k}{2} q$ and $\frac{\alpha_s}{4\pi} G.\tilde{G}$. If we define

$$\chi^q(s^2)\epsilon_{\mu\nu\alpha\beta} p^\mu l^\nu \epsilon^\alpha(\lambda_1)\epsilon^{*\beta}(\lambda_2) = \langle \gamma(l,\lambda_2)|2m\overline{q}i\gamma_5 q|\gamma(p,\lambda_1)\rangle$$

$$f\chi^g(s^2)\epsilon_{\mu\nu\alpha\beta} p^\mu l^\nu \epsilon^\alpha(\lambda_1)\epsilon^{*\beta}(\lambda_2) = \langle \gamma(l,\lambda_2)|f\frac{\alpha_s}{4\pi} G.\tilde{G}|\gamma(p,\lambda_1)\rangle \tag{15.19}$$

with $p^2 = l^2 = 0$ and the number of flavours $f = 3$, then $\chi^q(0)$ and $\chi^g(0)$ satisfy the sum-rules

$$(\chi^u - \chi^d)(0) = \frac{2\alpha}{\pi}(e_u^2 - e_d^2)N_c$$

$$(\chi^u + \chi^d - 2\chi^s)(0) = \frac{2\alpha}{\pi}(e_u^2 + e_d^2 - 2e_s^2)N_c$$

$$(\chi^u + \chi^d + \chi^s + f\chi^g)(0) = \frac{2\alpha}{\pi}(e_u^2 + e_d^2 + e_s^2)N_c \tag{15.20}$$

This result (without the singlet gluon term) was first noted by Adler (1970) before the advent of QCD.

15.2.2 *Higher twists*

We now consider the higher-twist terms.

The higher twist terms receive contributions from both the "handbag" and "cat-ears" diagrams. To classify these terms we note that there are five scales in the physical problem: Q^2, P^2, ν, the quark mass m and a QCD scale Λ associated with non-perturbative bound-state dynamics. We integrate over the scale ν when we evaluate the first moment of g_1^γ.

To understand the higher-twist terms in Eq. (15.8) it is helpful to first consider the QED contributions to g_1^γ. There are higher-twist terms proportional to non-zero powers of P^2/Q^2 and m^2/Q^2. The terms proportional to P^2/Q^2 vanish for a real photon target ($P^2 = 0$). The higher-twist terms proportional to m^2/Q^2 start with the leading twist (=2) operator matrix element. Quark mass terms make a non-leading contribution to the Dirac trace over γ_μ matrices when we evaluate g_1^γ to any given order in α. They yield a unity matrix contribution to the trace so that the leading term in the Dirac trace is the twist two operator matrix element. Since the photon's axial charges $a^{(k)}$ vanish when $P^2 = 0$ it follows that the higher-twist contributions to Eq. (15.8) vanish for a real photon target in QED.

In QCD we also have to consider the possible effects of Λ and whether we can have any higher-twist terms proportional to Λ^2/Q^2 – extra to the higher-twist terms listed in Eq. (15.8). If we could calculate g_1^γ exactly in QCD, we would find an expression which is symmetric under $(p \leftrightarrow q)$. This symmetry imposes strong constraints on the possible Λ dependence of g_1^γ. If we impose the physically sensible condition of not allowing Λ^2 to scale the kinematic variables, then we find that any higher-twist contribution involving Λ^2 comes from rescaling the quark mass in one or more terms in the complete QCD expression for g_1^γ, *viz.* $m^2 \to (m^2+\Lambda^2)$. That is, if there are higher-twist terms in g_1^γ proportional to Λ^2/Q^2, then they induce a constituent-quark mass-term in the higher-twist expansion. These higher-twist terms vanish at $P^2 = 0$ because the photon's axial charges vanish on-shell.

15.3 $g_1^\gamma(x, Q^2)$ in QCD: The leading order Witten analysis

In perturbative QCD the box graph contribution to the spin structure function of a polarized photon $g_1^\gamma(x, Q^2)$ is readily obtained from Eq. (6.31) by replacing the factor $\frac{\alpha_s}{2\pi}$ by $\frac{\alpha}{\pi}$. Separating the total phase space into "hard" ($k_t^2 \geq \lambda^2$) and "soft"

$(k_t^2 < \lambda^2)$ contributions, one finds

$$g_1^\gamma|_{\rm hard} =$$
$$-\frac{\alpha}{\pi}N_c\sum_q e_q^4\frac{\sqrt{1-\frac{4(m^2+\lambda^2)}{s}}}{1-\frac{4x^2P^2}{Q^2}}\Bigg[(2x-1)\left(1-\frac{2xP^2}{Q^2}\right)$$
$$\times\Bigg\{1-\frac{1}{\sqrt{1-\frac{4(m^2+\lambda^2)}{s}}\sqrt{1-\frac{4x^2P^2}{Q^2}}}\ln\Bigg(\frac{1+\sqrt{1-\frac{4x^2P^2}{Q^2}}\sqrt{1-\frac{4(m^2+\lambda^2)}{s}}}{1-\sqrt{1-\frac{4x^2P^2}{Q^2}}\sqrt{1-\frac{4(m^2+\lambda^2)}{s}}}\Bigg)\Bigg\}$$
$$+\left(x-1+\frac{xP^2}{Q^2}\right)\frac{\left(2m^2(1-\frac{4x^2P^2}{Q^2})-P^2x(2x-1)(1-\frac{2xP^2}{Q^2})\right)}{(m^2+\lambda^2)(1-\frac{4x^2P^2}{Q^2})-P^2x(x-1+\frac{xP^2}{Q^2})}\Bigg] \tag{15.21}$$

When $Q^2 \to \infty$ the expression for $g_1^\gamma|_{\rm hard}$ simplifies to the leading twist (=2) contribution:

$$g_1^\gamma|_{\rm hard} = \frac{\alpha}{\pi}N_c\sum_q e_q^4\Bigg[(2x-1)\Bigg\{\ln\frac{1-x}{x}-1+\ln\frac{Q^2}{x(1-x)P^2+(m^2+\lambda^2)}\Bigg\}$$
$$+(1-x)\frac{2m^2-P^2x(2x-1)}{m^2+\lambda^2-P^2x(x-1)}\Bigg] \tag{15.22}$$

In the deep inelastic limit $(Q^2 \gg \lambda^2 \gg P^2, m^2)$ we can write

$$g_1^\gamma|_{\rm hard} = \frac{\alpha}{\pi}N_c\sum_q e_q^4\left[(2x-1)\left\{\ln\frac{1-x}{x}-1+\ln\frac{Q^2}{\lambda^2)}\right\}\right] \tag{15.23}$$

For three flavours (u, d and s) $N_c\sum_q e_q^4 = \frac{2}{3}$. As we found in Chapter 6, there is an unambiguous contribution to the first moment of $g_1^\gamma(x,Q^2)$ which comes from a purely pointlike part of the box at $k_t^2 \sim Q^2$. The higher $(n \geq 2)$ moments of $g_1^\gamma(x,Q^2)$ are dominated by the logarithm term, *viz.*

$$G_n = \int_0^1 dx x^{n-1} g_1^\gamma(x,Q^2) \sim \frac{\alpha}{\pi}\frac{2}{3}(\gamma_{gg}^q)_n \ln\frac{Q^2}{\mu^2} \tag{15.24}$$

where $(\gamma_{gg}^q)_n = \int_0^1 dx x^{n-1}(2x-1)$.

Going beyond the simple box diagram, the total inclusive cross-section for γ $\gamma \to$ hadrons may be written as the absorptive part of the forward γ γ scattering amplitude [Ahmed and Ross (1975)]

$$T_{\mu\nu\alpha\beta} = \frac{1}{2}\int dx\ dy\ dz e^{iq.x}e^{ip.(y-z)}\langle{\rm vac}|T[J_\mu(x)J_\nu(0)J_\alpha(y)J_\beta(z)]|{\rm vac}\rangle \tag{15.25}$$

where $J_\alpha(y)$ and $J_\beta(z)$ are understood to couple to the soft photons. The forward matrix element in Eq. (15.24) is a function of six distances x, y, z, $x-y$, $x-z$,

$y-z$. It is only when all of these distances are small simultaneously that we can apply perturbative QCD (which includes the lowest order box calculation). For a real photon target, we contract Eq. (15.24) with the target photon's polarisation vector $\epsilon^{\alpha}(\lambda)$ and consider

$$W_{\mu\nu} = \frac{1}{2\pi}\mathrm{Im}\int dx\ e^{iq.x}\langle\gamma(p,\lambda)|T[J_{\mu}(x)J_{\nu}(0)]|\gamma(p,\lambda)\rangle \tag{15.26}$$

Since $Q^2 \to \infty$ in deep inelastic scattering we can use the phase oscillation argument in Section 3.2 for the exponential to show that $W_{\mu\nu}$ receives a contribution only when $x^2 \to 0$. We can apply the operator product expansion to $J_{\mu}(x)$ and $J_{\nu}(0)$. In all, there are eight independent structure functions for the spin-one photon [Budnev *et al.* (1975)]. The antisymmetric part of $W_{\mu\nu}$ is described (up to a Lorentz factor) by the polarized deep inelastic structure function $g_1^{\gamma}(x,Q^2)$, where the n^{th} moment of $g_1^{\gamma}(x,Q^2)$ is defined by

$$\begin{aligned} iS\ \epsilon^{\mu\lambda\alpha\beta}\epsilon_{\alpha}\epsilon^{*}_{\beta}p_{\lambda}p^{\mu_1}...p^{\mu_{n-1}}\int_0^1 dx\ x^{n-1}g_1^{\gamma}(x,Q^2) \\ = \frac{1}{2}\sum_{\theta}C_{\theta,n}(Q^2)\langle\gamma(p)|O_{\theta,n}^{\mu\mu_1..\mu_{n-1}}|\gamma(p)\rangle \end{aligned} \tag{15.27}$$

Here S denotes symmetrisation over μ, μ_1,..., μ_{n-1} and $\epsilon_{0123} = +1$. The relevant twist two operators $O_{\theta,n}$ are the hadronic operators $O_{H,n}^{\mu\mu_1..\mu_{n-1}}$, *viz.*

$$\begin{aligned} O_{q,n}^{a\mu\mu_1..\mu_{n-1}} &= i^{n-1}S\ \overline{q}\gamma^{\mu}\gamma_5 D^{\mu_1}...D^{\mu_{n-1}}\frac{\lambda^a}{2}q, \quad \mathrm{a} = 0,1,...,8 \\ O_{g,n}^{\mu\mu_1..\mu_{n-1}} &= \frac{1}{2}i^{n-2}S\ \mathrm{Tr}[G^{\mu\alpha}D^{\mu_1}...D^{\mu_{n-2}}\tilde{G}_{\alpha}^{\mu_{n-1}}] \end{aligned} \tag{15.28}$$

and also the photon operators

$$O_{\gamma,n}^{\mu\mu_1..\mu_{n-1}} = \frac{1}{2}i^{n-2}S\ F^{\mu\alpha}\partial^{\mu_1}...\partial^{\mu_{n-2}}\tilde{F}_{\alpha}^{\mu_{n-1}} \tag{15.29}$$

The $O_{H,n}$ are the same operators which appear in deep inelastic scattering from hadronic targets; $G_{\mu\nu}$ and $F_{\mu\nu}$ are the gluon and photon field tensors respectively with $\tilde{G}_{\mu\nu}$ and $\tilde{F}_{\mu\nu}$ the corresponding dual tensors, *viz.* $\tilde{G}_{\mu\nu} = \frac{1}{2}\epsilon_{\mu\nu\alpha\beta}G^{\alpha\beta}$ and $\tilde{F}_{\mu\nu} = \frac{1}{2}\epsilon_{\mu\nu\alpha\beta}F^{\alpha\beta}$.

As it was first pointed out by Witten (1977), the coefficient functions of the photonic and singlet hadronic operators will mix under the renormalisation group. The hadronic matrix elements are of leading order α_{QED} (henceforth written α) whilst the photon operator matrix elements are $O(1)$. Since the hadronic coefficient functions are $O(1)$ and the photon coefficient functions start at $O(\alpha)$. Eq. (15.26) receives leading order (in α) contributions both from the hadronic and photonic channels.

At leading order in α the renormalisation group equation reads

$$\left\{\frac{d}{d\ln\mu^2} - \gamma(g)\right\}C(\frac{Q^2}{\mu^2},g,\alpha) = \left\{\frac{\partial}{\partial\ln\mu^2} + \beta\frac{\partial}{\partial g} - \gamma\right\}C(\frac{Q^2}{\mu^2},g,\alpha) = 0 \tag{15.30}$$

Here, $C(\frac{Q^2}{\mu^2}, g, \alpha)$ is a column vector which runs over both the singlet and non-singlet hadronic coefficients, as well as the coefficients for the new photonic operators. (There is no $\beta_{QED}\frac{\partial}{\partial e}$ term written here in the total scale derivative; it does not occur at leading order in α.) The renormalization group equation has the solution

$$\begin{aligned}\begin{pmatrix} C_H \\ C_\gamma \end{pmatrix}(\frac{Q^2}{\mu^2}, g, \alpha) &= T\exp\int_{\overline{g}}^{g}\frac{dt}{\beta(t)}\begin{bmatrix}\gamma_H & 0\\ k & 1\end{bmatrix}(t)\begin{pmatrix} C_H \\ C_\gamma \end{pmatrix}\left(1, \overline{g}\left(\frac{Q^2}{\mu^2}\right), \alpha\right)\\ &= \begin{bmatrix}M & 0\\ X & 1\end{bmatrix}\left(\frac{Q^2}{\mu^2}, g, \alpha\right)\begin{pmatrix} C_H \\ C_\gamma \end{pmatrix}\left(1, \overline{g}\left(\frac{Q^2}{\mu^2}\right), \alpha\right)\end{aligned} \tag{15.31}$$

Here, γ_H and k are the purely hadronic and photon-hadron mixing anomalous dimensions respectively. The hadronic part γ_H forms a 4x4 block diagonal matrix comprising the singlet anomalous dimensions in the upper left 2x2 entries and the non-singlet anomalous dimensions diagonally in the lower right 2x2 entries. The mixing term k is a 1x4 row vector and is proportional to γ^q_{gg} in Eq. (3.60), *viz.* $k = -e^2\frac{f}{T(R)}N_c\gamma^q_{gg}[\frac{2}{9}, 0, \frac{1}{6}, \frac{1}{18}] + O(e^2g^2)$. It is the same calculation as for γ^q_{gg} - only with the group factors for QED instead of QCD. The constants f and N_c are number of quark flavours (=3) and colours (=3), and $T(R) = \frac{1}{2}f$. The numbers in the row vector in k are the coefficients of the SU(3) flavour decomposition of $\sum \mathrm{e}_\mathrm{q}^2$.

In the solution to the renormalization group equation, Eq. (15.30), M is the familiar hadronic evolution coefficient

$$M\left(\frac{Q^2}{\mu^2}, g, \alpha\right) = T\exp\int_{\overline{g}}^{g} dt\frac{\gamma_H(t)}{\beta(t)} \tag{15.32}$$

The mixing term is

$$X\left(\frac{Q^2}{\mu^2}, g, \alpha\right) = \int_{\overline{g}}^{g} dt\frac{k}{\beta(t)}T\exp\int_{\overline{g}}^{t} ds\frac{\gamma_H(s)}{\beta(s)} \tag{15.33}$$

These two coefficient functions are readily evaluated by expanding γ_H in terms of its eigenvalues λ_k and the corresponding projection matrices P_k (viz. $\gamma_H = \sum \lambda_k P_k$) [Gross and Wilczek (1974); Witten (1977)]. Since $P_iP_j = \delta_{ij}P_j$ this trick simplifies the matrix multiplication considerably. We find

$$X\left(\frac{Q^2}{\mu^2}, g, \alpha\right) = \frac{k}{2\beta_0\overline{g}^2}\sum_k \frac{P_k}{(1+\frac{\lambda_k}{2\beta_0})} \quad + \text{ non} - \text{leading terms} \tag{15.34}$$

The mixing term X has been calculated by Witten (1977) to leading order in α_s (and to next to leading order by Bardeen and Buras (1979)) for the unpolarized case. The anomalous dimensions for polarized deep inelastic scattering are known

only to leading order in α_s. After including the effect of (leading order) renormalization group, the moments of $g_1^\gamma(x,Q^2)$ are given by

$$
\begin{aligned}
&2iS\ \epsilon^{\mu\lambda\alpha\beta}\epsilon_\alpha\epsilon^*_\beta p_\lambda p^{\mu_1}..p^{\mu_{n-1}}\int_0^1 dx\ x^{n-1}g_1^\gamma(x,Q^2)\\
&\quad=\sum_{O_H} M\left(\frac{Q^2}{\mu^2},g,\alpha\right)C_{H,n}\left(1,\overline{g}\left(\frac{Q^2}{\mu^2}\right),\alpha\right)\langle\gamma|O_{H,n}^{\mu\mu_1..\mu_{n-1}}(\mu^2)|\gamma\rangle\\
&\qquad+\sum_{O_\gamma}\left(X\left(\frac{Q^2}{\mu^2},g,\alpha\right)C_{H,n}\left(1,\overline{g}\left(\frac{Q^2}{\mu^2}\right),\alpha\right)\right.\\
&\qquad\left.+C_{\gamma,n}\left(1,\overline{g}\left(\frac{Q^2}{\mu^2}\right),\alpha\right)\right)\langle\gamma|O_{\gamma,n}^{\mu\mu_1..\mu_{n-1}}(\mu^2)|\gamma\rangle
\end{aligned}
\tag{15.35}
$$

Here, $\langle\gamma|O_{\gamma,n}|\gamma\rangle=1$ to leading order in α. After diagonalising γ_H, we construct the row vector X and contract it with the hadronic coefficients $C_{H,n}$. For the spin dependent case (with three flavours) we obtain

$$
\begin{aligned}
&X\big(\frac{Q^2}{\mu^2},g,\alpha\big)C_{H,n}(1,\overline{g},\alpha)=\\
&\frac{\alpha}{\pi}\frac{2}{3}(\gamma_{gg}^q)_n\ln\frac{Q^2}{\mu^2}\left[\frac{2}{3}(1+\frac{(\gamma_{gg}^g)_n}{2\beta_0})\frac{1}{\delta_n}+\frac{5}{12}\frac{1}{1+\frac{(\gamma_{qg}^q)_n}{2\beta_0}}\right]\\
&+\text{non-leading terms}
\end{aligned}
\tag{15.36}
$$

The coefficient

$$
\delta_n=1+\frac{(\gamma_{qq}^q)_n+(\gamma_{gg}^g)_n}{2\beta_0}+\frac{(\gamma_{qq}^q)_n(\gamma_{gg}^g)_n-(\gamma_{gg}^q)_n(\gamma_{qq}^g)_n}{4\beta_0^2}
\tag{15.37}
$$

For $n\geq 2$ the $\ln Q^2$ factor, which we observed in Eq. (15.23) for the perturbative box diagram calculation reappears in the mixing term. However, by comparison with Eq. (15.23), there is a finite QCD renormalization of the coefficient of the logarithm. This logarithm term dominates the other (scaling) terms in the expression for $g_1^\gamma(x,Q^2)$. The $C_\gamma\langle\gamma|O_\gamma|\gamma\rangle$ and $C_H\langle\gamma|O_H|\gamma\rangle$ terms scale up to the purely photonic and hadronic evolution respectively, which is due to the QED (QCD) anomalous dimensions.

This page intentionally left blank

Chapter 16

CONCLUSIONS AND OPEN QUESTIONS: HOW DOES THE PROTON SPIN?

The exciting challenge to understand the *Spin Structure of the Proton* has produced many unexpected surprises in experimental data and inspired much theoretical activity and new insight into QCD dynamics and the interplay between spin and chiral/axial U(1) symmetry breaking in QCD. There is a vigorous global programme in experimental spin physics spanning (semi-)inclusive polarized deep inelastic scattering, photoproduction experiments, exclusive measurements over a broad kinematical region, polarized proton-proton collisions, fragmentation studies in e^+e^- collisions and νp elastic scattering.

Polarized deep inelastic scattering has taught us that the proton's flavour singlet axial-charge is about 0.3, or half the value predicted by relativistic quark models and the value of $g_A^{(8)}$ extracted from hyperon beta-decays. In this book we surveyed the present (and near future) experimental situation and the new theoretical understanding that spin experiments have inspired. New experiments (planned and underway) will surely produce more surprises and exciting new challenges for theorists as we continue our quest to understand the internal structure of the proton and QCD confinement related dynamics.

We conclude with a summary of key issues and open problems in QCD spin physics where the next generation of present and future experiments should yield vital information:

- What happens to "spin" in the transition from current to constituent quarks through dynamical axial U(1) symmetry breaking?
- Is the "missing spin" a physics issue for the valence quarks and/or the sea/glue?
- How large is the gluon spin polarization in the proton? Present measurements of gluon polarization suggest that this gluon spin contribution is too small to resolve the difference through the Efremov-Teryaev-Altarelli-Ross term. It may still play an important role in building up the total spin of the proton.
- Are there fixed pole corrections to spin sum rules for polarized photon nucleon scattering? If yes, which ones?
- Is gluon topology important in the spin structure of the proton?
- How large is the polarized strangeness in the proton? NLO analyses of inclusive

g_1 data without a subtraction constant suggest a value ~ -0.08 whereas there is no evidence for polarized strangeness in the HERMES semi-inclusive data.

- Is the valence quark spin contribution suppressed as suggested by leading order analyses of semi-inclusive data from SMC, HERMES and COMPASS? The chiral properties of the QCD θ-vacuum are quite different to the vacuum in QED. When we place a valence quark in the vacuum it can act as a source for polarizing the vacuum so that the spin of the quark becomes in-part delocalized and the spin of the proton becomes a property of the proton rather than the sum over localized quark and gluon contributions. The "missing spin" then becomes associated with the θ-vacuum and is manifest as a subtraction constant in the g_1 spin dispersion relation or $x = 0$.
- How (if at all) do the effective intercepts for small x physics change in the transition region between polarized photoproduction and polarized deep inelastic scattering? This issue is connected to the analyticity of the g_1 structure function as a function of Q^2.
- In which kinematics, if at all, does the magnitude of the isosinglet component of g_1 at small x exceed the magnitude of the isovector component?
- How does $\Delta d/d$ behave at x very close to one?
- Does perturbative QCD factorization work for spin dependent processes? – *viz.* will the polarized quark and gluon distributions extracted from the next generation of experiments prove to be process independent?
- Is the small value of $g_A^{(0)}$ extracted from polarized deep inelastic scattering "target independent", e.g. through topological charge screening?
- Can we find and observe processes in the η' nucleon interaction which are also sensitive to dynamics which underlies the singlet axial charge?
- How large is quark (and gluon) "orbital angular momentum" in the proton?
- Transversity measurements are sensitive to k_t dependent effects in the proton and fragmentation processes. The difference between the C-odd transversity distribution $\delta q(x)$ and the C-even spin distribution $\Delta q(x)$, *viz.* $(\delta q - \Delta q)(x)$, probes relativistic dynamics in the proton. Precision measurements at large Bjorken x where just the valence quarks contribute would allow a direct comparison and teach us about relativistic effects in the confinement region.

Acknowledgments

My understanding of the issues discussed here has benefited from collaboration, conversations and correspondence with many colleagues. It is a pleasure to thank C. Aidala, M. Brisudova, S.J. Brodsky, R.J. Crewther, A. De Roeck, A. Deshpande, B.L. Ioffe, P.V. Landshoff, N.N. Nikolaev, I. Schmidt, F.M. Steffens and A.W. Thomas for collaboration and sharing their insight on the spin structure of the proton. In addition I have benefited particularly from discussions with M. Anselmino, B. Badelek, N. Bianchi, V.N. Gribov, R.L. Jaffe, P. Kienle, A. Ko-

rzenev, W. Melnitchouk, P. Moskal, G. Rädel, H. Santos, G.M. Shore, J. Soffer, P. van Baal, W. Vogelsang and R. Windmolders. I also thank A. Bravar, R. Fatemi, K. Helbing, N. d' Hose, A. Magnon, Z.-E. Meziani, S. Pate, U. Stoesslein and E. Voutier for helpful communications about experimental data during the writing of this book.

Parts of this book were completed during pleasant research visits to CERN and to Clare Hall, Cambridge. This work was supported in part by the Austrian Science Fund (FWF grant P17778-N08).

This page intentionally left blank

BIBLIOGRAPHY

H.D. Abarbanel, F.E. Low, I.J. Muzinich, S. Nussinov and J.H. Schwarz (1967), *Phys. Rev.* **160** 1329.

H.D. Abarbanel and M.L. Goldberger (1968), *Phys. Rev.* **165** 1594

P. Abbon *et al.* (2007) (COMPASS Collaboration), `hep-ex/0703049`.

F. Abe *et al.* (1994) (CDF Collaboration) *Phys. Rev.* **D50** 5550.

K. Abe *et al.* (1997) (E-154 Collaboration), *Phys. Rev. Lett.* **79** 26.

A. Abele *et al.* (1998) (Crystal Barrel Collaboration), *Phys. Lett.* **B423** 246.

B.I. Abelev *et al.* (2006) (STAR Collaboration), *Phys. Rev. Lett.* **97** 252001.

B.I. Abelev *et al.* (2007) (STAR Collaboration), `arXiv:0705.4629 [hep-ex]`

A. Acha *et al.* (2007) (HAPPEX Collaboration), *Phys. Rev. Lett.* **98** 032301.

K. Ackerstaff *et al.* (1997) (HERMES Collaboration), *Phys. Lett.* **B404** 383.

K. Ackerstaff *et al.* (1999) (HERMES Collaboration), *Phys. Lett.* **B464** 123.

D.L. Adams *et al.* (1991a) (FNAL E704 Collaboration), *Phys. Lett.* **B261**, 201.

D.L. Adams *et al.* (1991b) (FNAL E704 Collaboration) *Phys. Lett.* **B264** 462.

D.L. Adams *et al.* (1994) (FNAL E581/704 Collaboration) *Phys. Lett.* **B336** 269.

G.S. Adams *et al.* (1998) (E852 Collaboration), *Phys. Rev. Lett.* **81** 5760.

J. Adams *et al.* (2004) (STAR Collaboration) *Phys. Rev. Lett.* **92** 171801.

A. Adare *et al.* (2007) (PHENIX Collaboration), arXiv:0704.3599 [hep-ex]

B. Adeva *et al.* (1998a) (SMC Collaboration), *Phys. Rev.* **D58** 112001.

B. Adeva *et al.* (1998b) (SMC Collaboration), *Phys. Rev.* **D58** 112002.

B. Adeva *et al.* (1998c) (SMC Collaboration), *Phys. Lett.* **B420** 180.

B. Adeva *et al.* (1999) (SMC Collaboration), *Phys. Rev.* **D60** 072004.

B. Adeva *et al.* (2004) (SMC Collaboration), *Phys. Rev.* **D70** 012002.

S.L. Adler (1966), *Phys. Rev.* **143** 1144.

S.L. Adler (1969), *Phys. Rev.* **177** 2426.

S.L. Adler (1970), in *Brandeis Lectures on Elementary Particles and Quantum Field Theory*, edited by S. Deser, M. Grisaru and H. Pendleton (MIT Press, 1970).

S.L. Adler and R.F. Dashen (1968), *Current Algebras and Applications to Particle Physics* (W.A. Benjamin, New York).

S.L. Adler and D.G. Boulware (1969), *Phys. Rev.* **184** 1740.

S.S. Adler *et al.* (2004), (PHENIX Collaboration) *Phys. Rev. Lett.* **93** 202002.

S.S. Adler *et al.* (2005a), (PHENIX Collaboration) *Phys. Rev. Lett.* **95** 202001.

S.S. Adler *et al.* (2005b) (PHENIX Collaboration), *Phys. Rev.* **D71** 071102 (R).

C. Adloff *et al.* (1997) (H1 Collaboration) *Nucl. Phys.* **B497** 3.

C. Adloff *et al.* (2001) (H1 Collaboration), *Phys. Lett.* **B517** (2001) 47.

E.S. Ageev *et al.* (2005) (COMPASS Collaboration), *Phys. Lett.* **B612** 154.

E.S. Ageev *et al.* (2006) (COMPASS Collaboration) *Phys. Lett.* **B633** 25.
E.S. Ageev *et al.* (2007), (COMPASS Collaboration) *Nucl. Phys.* **B765** (2007) 31.
M.A. Ahmed and G.G. Ross (1975), *Phys. Lett.* **B59** 369.
L.A. Ahrens *et al.* (1987) (E734 Collaboration), *Phys. Rev.* **D35** 785.
J. Ahrens *et al.* (2000) (GDH Collaboration), *Phys. Rev. Lett.* **84** 5950.
J. Ahrens *et al.* (2001) (GDH Collaboration), *Phys. Rev. Lett.* **87** 022003.
J. Ahrens *et al.* (2002) (GDH Colaboration), *Phys. Rev. Lett.* **88** 232002.
A. Airapetian *et al.* (1998) (HERMES Collaboration), *Phys. Lett.* **B442** 484.
A. Airapetian *et al.* (2000) (HERMES Collaboration), *Phys. Rev. Lett.* **84** 2584.
A. Airapetian *et al.* (2001) (HERMES Collaboration), *Phys. Rev. Lett.* **87** 182001.
A. Airapetian *et al.* (2004) (HERMES Collaboration), *Phys. Rev. Lett.* **92** 012005.
A. Airapetian *et al.* (2005a) (HERMES Collaboration), *Phys. Rev.* **D71** 012003.
A. Airapetian *et al.* (2005b) (HERMES Collaboration), *Phys. Rev. Lett.* **94** 012002.
A. Airapetian *et al.* (2007) (HERMES Collaboration), *Phys. Rev.* **D75** 012007.
I.J.R. Aitchison Oxford preprint OX 24/88 "The Skyrme Model of the Nucleon".
A. Aktas *et al.* (2005) (H1 Collaboration), *Eur. Phys. J* **C44** 1.
A. Alavi-Harati *et al.* (2001) (KTeV Collaboration), *Phys. Rev. Lett.* **87** 132001.
W. Alberico, S.M. Bilenky and C. Maieron (2002), *Phys. Rep.* **358** 227.
M. Alekseev *et al.* (2007) (COMPASS Collaboration), `arXiv:0707.4077 [hep-ex]`
V. Yu. Alexakhin *et al.* (2007a) (COMPASS Collaboration), *Phys. Lett.* **B647** 8.
V. Yu. Alexakhin *et al.* (2007b) (COMPASS Collaboration), *Phys. Lett.* **B647** 330.
M.J. Alguard *et al.* (1976), *Phys. Rev. Lett.* **37** 1261.
M.J. Alguard *et al.* (1978), *Phys. Rev. Lett.* **41** 70.
G. Altarelli, N. Cabibbo and L. Maiani (1972), *Phys. Lett.* **B40** 415.
G. Altarelli and G. Parisi (1977), *Nucl. Phys.* **B126** 298.
G. Altarelli and G.G. Ross (1988), *Phys. Lett.* **B212** 391.
G. Altarelli, R.D. Ball, S. Forte and G. Ridolfi (1997), *Nucl. Phys.* **B496** 337.
G. Altarelli, R.D. Ball and S. Forte (2006), *Nucl. Phys.* **B742** 1.
M. Amarian *et al.* (2004), (Jefferson Lab E94-010 Collaboration) *Phys. Rev. Lett.* **92** 022301.
N. Amos *et al.* (1989) (E710 Collaboration) *Phys. Rev. Lett.* **63** 2784.
P. W. Anderson and W. F. Brinkman (1975), Theory of Anistropic Superfluidity in He^3, in *The Helium Liquids: Proc. 15th Scottish Universities Summer School in Physics 1974*, eds. J. G. M. Armitage and I. E. Farquhar (Academic Press, New York).
K.A. Aniol *et al.* (2004) (HAPPEX Collaboration), *Phys. Rev.* **C69** 065501.
K.A. Aniol *et al.* (2006) (HAPPEX Collaboration), *Phys. Lett.* **B635** 275.
M. Anselmino, B.L. Ioffe and E. Leader (1989), *Yad. Fiz.* **49** 214.
M. Anselmino, P. Gambino and J. Kalinowski (1994), *Z Physik* **C64** 267.
M. Anselmino, A. Efremov and E. Leader (1995), *Phys. Rep.* **261** 1.
M. Anselmino, M. Boglione, U. D' Alesio, E. Leader and F. Murgia (2004), *Phys. Rev.* **D70** 074025.
M. Anselmino, M. Boglione, U. D' Alesio, E. Leader and F. Murgia (2005), *Phys. Rev.* **D71** 014002.
M. Anselmino, U. D' Alesio, S. Mellis and F. Murgia (2006), *Phys. Rev.* **D74** 094011.
P.L. Anthony *et al.* (1999) (E-155 Collaboration), *Phys. Lett.* **B463** 339.
P.L. Anthony *et al.* (2000) (E-155 Collaboration), *Phys. Lett.* **B493** 19.
P.L. Anthony *et al.* (2003) (E-155 Collaboration), *Phys. Lett.* **B553** 18.
K. Aoki (2007), arXiv:0704.1369 [hep-ex]
D.S. Armstrong *et al.* (2005) (G0 Collaboration), *Phys. Rev. Lett.* **95** 092001.
M. Arneodo *et al.* (1994) (NMC Collaboration), *Phys. Rev.* **D50** R1.

X. Artru and M. Mekhfi (1990), *Z. Phys.* **C45** 669.
J. Ashman *et al.* (1988) (EMC Collaboration), *Phys. Lett.* **B206** 364.
J. Ashman *et al.* (1989) (EMC Collaboration), *Nucl. Phys.* **B328** 1.
H. Avakian, S.J. Brodsky, A. Deur and F. Yuan (2007), `arXiV:0705.1553 [hep-ph]`
H. Baba, K. Sasaki and T. Uematsu (2003), *Phys. Rev.* **D68** 054025.
A. Bachetta, A. Schafer and J.J. Yang (2004), *Phys. Lett.* **B578** 109.
B. Badelek and J. Kwiecinski (1998), *Phys. Lett.* **B418** 229.
P. Ball, J.M. Frere and M. Tytgat (1996), *Phys. Lett.* **B365** 367.
R.D. Ball, S. Forte and G. Ridolfi (1996), *Phys. Lett.* **B378** 255.
W.A. Bardeen and A.J. Buras (1979), *Phys. Rev.* **D20** 166.
T. Barnes, F.E. Close and E.S. Swanson (1995), *Phys. Rev.* **D52** 5242.
V. Barone, T. Calarco and A. Drago (1998), *Phys. Lett.* **B431** 405.
V. Barone, A. Drago and P.G. Ratcliffe (2002), *Phys. Rept.* **359** 1.
S.D. Bass (1992), *Int. J. Mod. Phys.* **A7** 6039.
S.D. Bass (1992a), *Z Physik* **C55** 653.
S.D. Bass (1997), *Mod. Phys. Lett.* **A12** 1051.
S.D. Bass (1998), *Mod. Phys. Lett.* **A13** 791.
S.D. Bass (1999), *Eur. Phys. J.* **A5** 17.
S. D. Bass (1999c), *Phys. Lett.* **B463** 286.
S. D. Bass (2000), `hep-ph/0006348`.
S.D. Bass (2002a), *Phys. Rev.* **D65** 074025.
S.D. Bass (2002b), *Phys. Scripta* **T99** 96.
S.D. Bass (2003a), *Phys. Rev.* **D67** 097502.
S.D. Bass (2003b), *Acta Phys. Pol. B* **34** 5893.
S.D. Bass (2004), *Phys. Lett.* **B590** 115.
S.D. Bass (2005), *Rev. Mod. Phys.* **77** 1257.
S.D. Bass (2007), *Mod. Phys. Lett.* **A22** 1005.
S.D. Bass, B.L. Ioffe, N.N. Nikolaev and A.W. Thomas (1991), *J. Moscow Phys. Soc.* **1** 317.
S.D. Bass and A.W. Thomas (1993a), *Phys. Lett.* **B293** 457.
S.D. Bass and A.W. Thomas (1993b), *J. Phys.* **G19** 925.
S.D. Bass and P.V. Landshoff (1994), *Phys. Lett.* **B336** 537.
S.D. Bass, S.J. Brodsky and I. Schmidt (1998b), *Phys. Lett.* **B437** 417.
S.D. Bass and M. Brisudova (1999a), *Eur. Phys. J.* **A4** 251.
S.D. Bass, S.J. Brodsky and I. Schmidt (1999b), *Phys. Rev.* **D60** 034010.
S.D. Bass and A. De Roeck (2001), *Eur. Phys. J.* **C18** 531.
S.D. Bass and E. Marco (2002), *Phys. Rev.* **D65** 057503.
S.D. Bass and A. De Roeck (2002c), *Nucl. Phys. B (Proc. Suppl.)* **105** 1.
S.D. Bass, R.J. Crewther, F.M. Steffens and A.W. Thomas (2002d), *Phys. Rev.* **D66** 031901(R).
S.D. Bass, R.J. Crewther, F.M. Steffens and A.W. Thomas (2003), *Phys. Rev.* **D68** 096005.
S.D. Bass, R.J. Crewther, F.M. Steffens and A.W. Thomas (2006), *Phys. Lett.* **B634** 249.
S.D. Bass and A.W. Thomas (2006), *Phys. Lett.* **B634** 368.
S.D. Bass and C.A. Aidala (2006), *Int. J. Mod. Phys.* **A21** 4407.
J.R. Batley *et al.* (2007) (NA 48/1 Collaboration), *Phys. Lett.* **B645** 36.
G. Baum *et al.* (1983) (The E-130 Collaboration), *Phys. Rev. Lett.* **51** 1135.
G. Baum *et al.* (1996) (The COMPASS Collaboration), Proposal CERN/SPSLC 96-14.
A. Belitsky, X. Ji and F. Juan (2003a), *Phys. Rev. Lett.* **91** 092003.
A. Belitsky, X. Ji and F. Juan (2003b), *Nucl. Phys.* **B656** 165.
J.S. Bell and R. Jackiw (1969), *Nouvo Cim.* **A60** 47.

C. Bernard *et al.* (1997a) (MILC Collaboration), *Phys. Rev.* **D56** 7039.
C. Bernard *et al.* (1997b) (MILC Collaboration), *Nucl. Phys. B (Proc. Suppl.)* **53** 228.
V. Bernard, N. Kaiser and U-G. Meissner (1999), *Eur. Phys. J* **A4** 259.
V. Bernard, T.R. Hemmert and U.-G. Meissner (2003), *Phys. Rev.* **D67** 076008.
S. Bethke (2002), `hep-ph/0211012`.
N. Bianchi and E. Thomas (1999), *Phys. Lett.* **B450** 439.
F. Bissey *et al.* (2005), *Nucl. Phys. B (Proc. Suppl.)* **141** 22.
F. Bissey, F-G. Cao and A.I. Signal (2006), *Phys. Rev.* **D73** 094008.
J.D. Bjorken (1966), *Phys. Rev.* **148** 1467.
J.D. Bjorken (1970), *Phys. Rev.* **D1** 1376.
J.D. Bjorken and S.D. Drell (1965), *Relativistic Quantum Fields*, Mc Graw Hill
J. Blümlein and A. Vogt (1996), *Phys. Lett.* **B370** 149.
J. Blümlein and H. Böttcher (2002), *Nucl. Phys.* **B636** 225.
G.T. Bodwin and J. Qiu (1990), *Phys. Rev.* **D41** 2755.
D. Boer and W. Vogelsang (2004), *Phys. Rev.* **D69** 094025.
C. Boros, Zuo-tang Liang and Ta-chung Meng (1993), *Phys. Rev. Lett.* **70** 1751.
K. Boyle (2007), `hep-ex/0701048`
A. Bravar *et al.* (1996) (FNAL E704 Collaboration), *Phys. Rev. Lett.* **77** 2626.
A. Bravar, D. von Harrach and A. Kotzinian (1998), *Phys. Lett.* **B421** 349.
J. Breitweg *et al.* (1997) (ZEUS Collaboration), Phys. Lett. **B407** 432.
M.M Brisudova, L. Burakovsky and T. Goldman (2000), *Phys. Rev.* **D61** 054013.
D.J. Broadhurst, J.F. Gunion and R.L. Jaffe (1973), *Ann. Phys.* **81** 88.
S.J. Brodsky (2002), `hep-ph/0208158`.
S.J. Brodsky and J.R. Primack (1969), *Ann. Phys.* **52** 315.
S.J. Brodsky, F.E. Close and J.F. Gunion (1972), *Phys. Rev.* **D5** 1384.
S.J. Brodsky and G.P. Lepage (1980), *Phys. Rev.* **D22** 2157.
S.J. Brodsky, J. Ellis and M. Karliner (1988), *Phys. Lett.* **B206** 309.
S.J. Brodsky and I. Schmidt (1990), *Phys. Lett.* **B234** 144.
S.J. Brodsky, M. Burkardt and I. Schmidt (1995), *Nucl. Phys.* **B441** 197.
S.J. Brodsky and I. Schmidt (1995), *Phys. Lett.* **B351** 344.
S.J. Brodsky, D.S. Hwang and I. Schmidt (2002), *Phys. Lett.* **B530** 99.
S.J. Brodsky and S. Gardner (2006), *Phys. Lett.* **B643** 22.
D. Bruss, T. Gasenzer and O. Nachtmann (1998), *Phys. Lett.* **A239** 81.
D. Bruss, T. Gasenzer and O. Nachtmann (1999), *Eur. Phys. J direct* **D1** 2.
V.M. Budnev *et al.* (1975), *Phys. Rept.* **15** 181.
S. Bültmann *et al.* (2003) (pp2pp Collaboration), *Phys. Lett.* **B579** 245.
S. Bültmann *et al.* (2007) (pp2pp Collaboration), *Phys. Lett.* **B647** 98
G. Bunce, N. Saito, J. Soffer and W. Vogelsang (2000), *Ann. Rev. Nucl. Part. Sci.* **50** 525.
M. Burkardt (2002), *Phys. Rev.* **D66** 114005.
M. Burkardt (2005), *Nucl. Phys. B (Proc. Suppl.)* **141** 86.
M. Burkardt and D.S. Hwang (2004), *Phys. Rev.* **D69** 074032.
V.D. Burkert and B.L. Ioffe (1994), *JETP* **78** 619.
H. Burkhardt and W.N. Cottingham (1970), *Ann. Phys. (N.Y.)* **56** 453.
H. Calen *et al.* (1988) (CELSIUS Collaboration), *Phys. Rev.* **C58** 2667.
C.G. Callan, R.F. Dashen, and D.J. Gross (1976), *Phys. Lett.* **B63** 334.
B.A. Campbell, J. Ellis and R.A. Flores (1989), *Phys. Lett.* **B225** 419.
F.-G. Cao and A.I. Signal (2003), *Phys. Rev.* **D68** 074002.
R.D. Carlitz, J.C. Collins and A. Mueller (1988), *Phys. Lett.* **B214** 229.
S. Chekanov *et al.* (2003a) (ZEUS Collaboration), *Phys. Rev.* **D67** 012007.
S. Chekanov *et al.* (2003b) (ZEUS Collaboration), *Phys. Lett.* **D573** 46.

T.P. Cheng and L-F. Li (1989), *Phys. Rev. Lett.* **62** 1441.
H-Y. Cheng (1996), *Int. J. Mod. Phys.* **A11** 5109.
K.G. Chetyrkin and J.H. Kühn (1993), *Z. Phys.* **C60** 497.
S.U. Chung *et al.* (1999) (E852 Collaboration), *Phys. Rev.* **D60** 092001.
C. Ciofi degli Atti *et al.* (1993), *Phys. Rev.* **C48** 968.
F.E. Close (1978), *An Introduction to Quarks and Partons* (Academic, New York).
F.E. Close and A.W. Thomas (1988), *Phys. Lett.* **B212** 227.
F.E. Close and R. Milner (1991), *Phys. Rev.* **D44** 3691.
F.E. Close and R.G. Roberts (1993), *Phys. Lett.* **B316** 165.
F.E. Close and R.G. Roberts (1994), *Phys. Lett.* **B336** 257.
F.E. Close and P.R. Page (1995), *Nucl. Phys.* **B443** 233.
T.D. Cohen and M.K. Banerjee (1989), *Phys. Lett.* **B230** 129.
J.C. Collins (2002), *Phys. Lett.* **B536** 43.
J.C. Collins (1993a), *Nucl. Phys.* **B394** 169.
J.C. Collins (1993b), *Nucl. Phys.* **B396** 161.
J.C. Collins, F. Wilczek and A. Zee (1978), *Phys. Rev.* **D18** 242.
J.C. Collins, S.F. Heppelmann and G.A. Ladinsky (1994), *Nucl. Phys.* **B420** 565.
J.L. Cortes, B. Pire and J.P. Ralston (1992), *Z. Physik* **C55** 409.
R. Courant and D. Hilbert (1953), *Methods of Mathematical Physics* volume 1, (Interscience 1953) 103.
R.J. Crewther (1979), Effects of Topological Charge in Gauge Theories, in Facts and Prospects of Gauge Theories, Schladming, Austria, February 1978, ed. P. Urban, *Acta Phys. Austriaca Suppl.* **19** 47.
C. Cronström and J. Mickelsson (1983), *J. Math. Phys.* **24** 2528.
J.R. Cudell, A. Donnachie and P.V. Landshoff (1999), *Phys. Lett.* **B448** 281.
D. de Florian (2003), *Phys. Rev.* **D67** 054004.
D. de Florian, O.A. Sampayo and R. Sassot (1998), *Phys. Rev.* **D57** 5803.
D. de Florian and R. Sassot (2000), *Phys. Rev.* **D62** 094025.
D. de Florian, G.A. Navarro and R. Sassot (2005), *Phys. Rev.* **D71** 094018.
D. de Florian, R. Sassot and M. Stratmann (2007a), *Phys. Rev.* **D75** 114010.
D. de Florian, R. Sassot and M. Stratmann (2007b), `arXiv:0707.1506`
A. Deshpande, R. Milner, R. Venugopalan and W. Vogelsang (2005), *Ann. Rev. Nucl. Part. Sci.* **55** 165.
K.V. Dharmawardane *et al.* (2006) (JLab Hall B Collaboration), *Phys. Lett.* **B641** 11.
A. De Roeck, A. Deshpande, V.W. Hughes, J. Lichtenstadt and G. Rädel (1999), *Eur. Phys. J.* **C6** 121.
A. De Roeck (2001), `hep-ph/0101075`.
D.M. Dennison (1927), *Proc. R. Soc.* **A115** 483.
A. Deur *et al.* (2004), *Phys. Rev. Lett.* **93** 212001.
D.A. Dicus and R. Vega (2001), *Phys. Lett.* **B501** 44.
M. Diehl (2003), *Phys. Rept.* **388** 41.
M. Diehl, T. Feldmann, R. Jakob and P. Kroll (2004), *Eur. Phys. J.* **C39** 1.
P. Di Vecchia and G. Veneziano (1980), *Nucl. Phys.* **B171** 253.
P. Di Vecchia, F. Nicodemi, R. Pettorino and G. Veneziano (1981), *Nucl. Phys.* **B181** 318.
D. Dolgov *et al.* (1999), *Nucl. Phys. B (Proc. Suppl.)* **73** 300.
A. Donnachie and P.V. Landshoff (1988), *Nucl. Phys.* **B311** 509.
A. Donnachie and P.V. Landshoff (1988), *Phys. Lett.* **B437** 408.
A. Donnachie and P.V. Landshoff (2002), *Phys. Lett.* **B533** 277.
A. Donnachie and P.V. Landshoff (2003), *Acta Phys. Pol. B* **34** 2989.
D. Drechsel, B. Pasquini and M. Vanderhaeghen (2003), *Phys. Rept.* **378** 99.

D. Drechsel and L. Tiator (2004), *Ann. Rev. Nucl. Part. Sci.* **54** 69.
S.D. Drell and A.C. Hearn (1966), *Phys. Rev. Lett.* **16** 908.
H. Dutz *et al.* (2003) (GDH Collaboration), *Phys. Rev. Lett.* **91** 192001.
H. Dutz *et al.* (2005) (GDH Collabortation), *Phys. Rev. Lett.* **94** 162001.
R.J. Eden, P.V. Landshoff, D.I. Olive and J.C. Polkinghorne, (2002), *The Analytic S-Matrix*, Cambridge University Press.
R.G. Edwards *et al.* (2006) (LHPC Collaboration), *Phys. Rev. Lett.* **96** 052001.
A.V. Efremov and O. Teryaev (1988), JINR Report E2-88-287, and in Proceedings of the International Hadron Symposium, Bechyně 1988, eds. J. Fischer et al. (Czechoslovakian Academy of Science, Prague, 1989) p. 302. .
J. Ellis and R.L. Jaffe (1974), *Phys. Rev.* **D9** 1444; (E) **D10** 1669.
J. Ellis and M. Karliner (1988), *Phys. Lett.* **B213** 73.
T.E.O. Ericson and W. Weise, *Pions and Nuclei* (Oxford UP, 1988).
B.I. Ermolaev, M. Greco and S.I. Troyan (2005), *Phys. Lett.* **B622** 93.
I. Estermann and O. Stern (1933), *Z Physik* **85** 17.
G. Fäldt and C. Wilkin (1997a), *Z Physik* **A357** 241.
G. Fäldt, T. Johansson and C. Wilkin (2002), *Physica Scripta* **T99** 146.
G.R. Farrar and D.R. Jackson (1975), *Phys. Rev. Lett.* **35** 1416.
R. Fatemi *et al.* (2003) (Jefferson Lab CLAS Collaboration), *Phys. Rev. Lett.* **91** 222002.
T. Feldmann (2000), *Int. J. Mod. Phys.* **A15** 159.
R.D. Field and R.P. Feynman (1977), *Phys. Rev.* **D15** 2590.
B.W. Fillipone and X. Ji (2001), *Adv. Nucl. Phys.* **26** 1.
R. Flores-Mendiek, E. Jenkins and A.V. Manohar (2001), *Phys. Rev.* **D58** 094028.
S. Forte and E.V. Shuryak (1991), *Nucl. Phys.* **B357** 153.
S. Forte, M.L. Mangano and G. Ridolfi (2001), *Nucl. Phys.* **B602** 585.
E.N. Fortson and L.L. Lewis (1984), *Phys. Rep.* **113** 289.
L.L. Frankfurt *et al.* (1989), *Phys. Lett.* **B230** 141.
C. Garcia-Recio, T. Inoue, J. Nieves and E. Oset (2002), *Phys. Lett.* **B550** 47.
G. Garvey, W.C. Louis and D.H. White (1993), *Phys. Rev.* **C48** 761.
O. Gayou *et al.* (2002) (Jefferson Lab Hall A Collaboration), *Phys. Rev. Lett.* **88** 092301.
T. Gehrmann and W.J. Stirling (1996), *Phys. Rev.* **D53** 6100.
M. Gell-Mann and M.L. Goldberger (1964), *Phys. Rev.* **96** 1433.
S.B. Gerasimov (1965), *Yad. Fiz.* **2** 598.
F.J. Gilman and R. Kauffman (1987), *Phys. Rev.* **D36** 2761; (E) **D37** (1988) 3348.
M. Glück, E. Reya, M. Stratmann and W. Vogelsang (1996), *Phys. Rev.* **D53** 4775.
M. Glück, E. Reya, M. Stratmann and W. Vogelsang (2001), *Phys. Rev.* **D63** 094005.
R.M. Godbole *et al.* (2006), Pramana **66** 657, `hep-ph/0604214`.
K. Goeke, M.V. Polyakov and M. Vanderhaeghen (2001), *Prog. Part. Nucl. Phys.* **47** 401.
Y. Goto *et al.* (2000) (Asymmetry Analysis Collaboration), *Phys. Rev.* **D62** 034017.
K. Gottfried (1967), *Phys. Rev. Lett.* **18** 1174.
A.M. Green and S. Wycech (1999), *Phys. Rev.* **C60** 035208.
A.M. Green and S. Wycech (2005), *Phys. Rev.* **C71** 014001.
D.P. Grosnick *et al.* (1997), *Phys. Rev.* **D55** 1159.
D.J. Gross and F. Wilczek (1974), *Phys. Rev.* **D9** 980.
D.J. Gross, S.B. Treiman and F. Wilczek (1979), *Phys. Rev.* **D19** 2188.
P. Hägler *et al.* (2007), `arXiv:0705.4295`.
R. Hasty *et al.* (2000) (SAMPLE Collaboration), *Science* **290** 2117.
T. Hatsuda (1990), *Nucl. Phys.* **B329** 376.
R.S. Hayano, S. Hirenzaki and A. Gillitzer (1999), *Eur. Phys. J.* **A6** 99.
R.L. Heimann, A.J.G. Hey and J.E. Mandula (1972), *Phys. Rev.* **D6** 3506.

R.L. Heimann (1973), *Nucl. Phys.* **B64** 429.
K. Helbing (2002), *Nucl. Phys. B (Proc. Suppl.)* **105** 113.
F. Hibou *et al.* (1998) (SATURNE Collaboration), *Phys. Lett.* **B438** 41.
M. Hirai *et al.* (2004) (Asymmetry Analysis Collaboration), *Phys. Rev.* **D69** 054021.
M. Hirai, S. Kumano and N. Saito (2006a) (Asymmetry Analysis Collaboration), *Phys. Rev.* **D74** 014015.
M. Hirai, S. Kumano and N. Saito (2006b) (Asymmetry Analysis Collaboration), `hep-ph/0612037`
H. Holtmann, G. Levman, N.N. Nikolaev, A. Szczurek and J. Speth (1994), *Phys. Lett.* **B338** 363.
G. 't Hooft and M.J.G. Veltman (1972), *Nucl. Phys.* **B44** 189.
G. 't Hooft (1976a), *Phys. Rev. Lett.* **37** 8.
G. 't Hooft (1976b), *Phys. Rev.* **D14** 3432.
G. 't Hooft (1986), *Phys. Rep.* **142** 357.
E. Iancu, A. Leonidov and L. McLerran (2002), `hep-ph/0202270`.
T. Inoue and E. Oset (2002), *Nucl. Phys.* **A710** 354.
B.L. Ioffe (1979), *Sov. J. Nucl. Phys.* **29** 827.
B.L. Ioffe, V.A. Khoze and L.N. Lipatov (1984), *Hard processes, Vol.1* (North Holland, Amsterdam)
N. Isgur, R. Kokoski and J. Paton (1985), *Phys. Rev. Lett.* **54** 869.
N. Isgur (1999), *Phys. Rev.* **D59** 034013.
T.M. Ito *et al.* (2004) (SAMPLE Collaboration), *Phys. Rev. Lett.* **92** 102003.
C. Itzykson and J-B. Zuber (1980), *Quantum Field Theory* (Mc Graw Hill, Singapore), Section 13-5-2.
E.I. Ivanov *et al.* (2001) (E852 Collaboration), *Phys. Rev. Lett.* **86** 3977.
R. Jackiw and K. Johnson (1969), *Phys. Rev.* **182** 1459.
R. Jackiw and C. Rebbi (1976), *Phys. Rev. Lett.* **37** 172.
H. Jackson (2006) (HERMES Collaboration), `hep-ex/0601006`.
B. Jäger, A. Schafer, M. Stratmann and W. Vogelsang (2003), *Phys. Rev.* **D67** 054005.
B. Jäger, M. Stratmann, S. Kretzer and W. Vogelsang (2004), *Phys. Rev. Lett.* **92** 121803.
R.L. Jaffe (1987), *Phys. Lett.* **B193** 101.
R.L. Jaffe (1990), *Comm. Nucl. Part. Phys.* **19** 239.
R.L. Jaffe (1996), *Phys. Lett.* **B365** 359.
R.L. Jaffe (2001), `hep-ph/0102281`.
R.L. Jaffe and C.H. Llewellyn Smith (1973), *Phys. Rev.* **D7** 2506.
R.L. Jaffe and A. Manohar (1990), *Nucl. Phys.* **B337** 509.
R.L. Jaffe and X. Ji (1992), *Nucl. Phys.* **B375** 527.
R.L. Jaffe, X. Jin and J. Tang (1998), *Phys. Rev. Lett.* **80** 1166.
X. Ji (1997a), *Phys. Rev. Lett.* **78** 610.
X. Ji (1997b), *Phys. Rev.* **D55** 7114.
X. Ji (1998), *J. Phys.* **G24** 1181.
X. Ji and F. Yuan (2002), *Phys. Lett.* **B543** 66.
R. Johnson, N.W. Park, J. Schechter, V. Soni and H. Weigel (1990), *Phys. Rev.* **D42** 2998.
M.K. Jones *et al.* (2000) (Jefferson Lab Hall A Collaboration), *Phys. Rev. Lett.* **84** 1398.
D.B. Kaplan and A.V. Manohar (1988), *Nucl. Phys.* **B310** 527.
I.B. Khriplovich (1991), *Parity Non-conservation in Atomic Phenomena* (Gordon and Breach, Philadelphia).
P. Kienle and T. Yamazaki (2004), *Prog. Part. Nucl. Phys.* **52** 85.
S. Koblitz (2007), arXiv:0707.0175 [hep-ex]
J. Kodaira (1980), *Nucl. Phys.* **B165** 129.

W. Koepf, E.M. Henley and S.J. Pollock (1992), *Phys. Lett.* **B288** 11.
J. Kogut and L. Susskind (1974), *Phys. Rev.* **D11** 3594.
A. Kotzinian (2003), *Phys. Lett.* **B552** 172.
S. Kretzer, E. Leader and E. Christova (2001), *Eur. Phys. J.* **C22** 269.
J. Kuti, Erice lectures (1995), *in* Proc. Erice School *The spin structure of the nucleon*, eds. B. Frois, V. Hughes and N. de Groot (World Scientific, 1997).
V.A. Kuzmin, V.A. Rubakov and M.E. Shaposhnikov (1985), *Phys. Lett.* **B155** 36.
J. Kwiecinski and B. Ziaja (1999), *Phys. Rev.* **D60** 054004.
P. Lacock *et al.* (1996) (UKQCD), *Phys. Rev.* **D54** 6997.
P. Lacock *et al.* (1997) (UKQCD), *Phys. Lett.* **B401** 308.
M. Lacombe *et al.* (1981), *Phys. Lett.* **B101**, 139.
B. Lampe and E. Reya (2000), *Phys. Rep.* **332** 1.
P.V. Landshoff and J.C. Polkinghorne (1972), *Phys. Rev.* **D5** 2056.
P.V. Landshoff and O. Nachtmann (1987), *Z Physik* **C35** 405.
P.V. Landshoff (1994), Zuoz lecture, `hep-ph/9410250`.
P.V. Landshoff (2005), `hep-ph/0509240`.
S.A. Larin, T. van Ritbergen and J.A.M. Vermaseren (1997), *Phys. Lett.* **B404** 153.
E. Leader, A.V. Sidorov and D.B. Stamenov (1998), *Phys. Lett.* **B445** 232.
E. Leader, A.V. Sidorov and D.B. Stamenov (2002), *Eur. Phys. J.* **C23** 479.
E. Leader and D.B. Stamenov (2003), *Phys. Rev.* **D67** 037503.
J.H. Lee and F. Videbaek (2006), *Proc. of the 17th International Spin Physics Symposium (SPIN2006), Kyoto, Japan* AIP conference proceedings 915, 533.
H. Leutwyler (1998), *Nucl. Phys. B (Proc. Suppl.)* **64** 223.
C.H. Llewellyn Smith, Oxford preprint: OX 89/88: "Quark Correlation Functions and Deep Inelastic Scattering".
F. Low (1954), *Phys. Rev.* **96** 1428.
F. E. Maas *et al.* (2004) (A4 Collaboration), *Phys. Rev. Lett.* **93** 022002.
F. E. Maas *et al.* (2005) (A4 Collaboration), *Phys. Rev. Lett.* **94** 152001.
G.K. Mallot (2006), `hep-ex/0612055`
L. Mankiewicz (1991), *Phys. Rev.* **D43** 64.
A.V. Manohar (1989), *Phys. Lett.* **B219** 357.
A.V. Manohar (1990), *Phys. Rev. Lett.* **65** 2511.
A.V. Manohar (1991), *Phys. Lett.* **B255** 579.
A.D. Martin, R.G. Roberts, W.J. Stirling and R.S. Thorne (2000), *Eur. Phys. J* **C18** 117.
A. Martin (2002), `hep-ph/0209068`.
N. Mathur, S.J. Dong, K.F. Liu, L. Mankiewicz and N.C. Mukhopadhay (2000), *Phys. Rev.* **D62** 114504.
W. Melnitchouk and A.W. Thomas (1996), *Acta Phys. Polon. B* **27** 1407.
W. Melnitchouk and M. Malheiro (1999), *Phys. Lett.* **B451** 224.
R. Mertig and W.L. van Neerven (1996), *Z Physik* **C70** 637.
Z.E. Meziani (2002), *Nucl. Phys. B (Proc. Suppl.)* **105** 105.
G.A. Miller and M.R. Frank (2002), *Phys. Rev.* **C65** 065205.
G.A. Miller (2002), *Phys. Rev.* **C66** 032201.
J. Missimer and L.M. Simons (1985), *Phys. Rep.* **118** 179.
A. Morreale (2007), arXiv:0707.1371 [hep-ex]
P. Moskal *et al.* (COSY-11 Collaboration) (1998), *Phys. Rev. Lett.* **80** 3202.
P. Moskal *et al.* (COSY-11 Collaboration) (2000a), *Phys. Lett.* **B474** 416.
P. Moskal *et al.* (COSY-11 Collaboration) (2000b), *Phys. Lett.* **B482** 356.
P. Moskal *et al.* (COSY-11 Collaboration) (2004), *Phys. Rev.* **C69** 025203.
P. Moskal (2004), `hep-ph/0408162`.

B. Mueller *et al.* (1997) (SAMPLE Collaboration), *Phys. Rev. Lett.* **78** 3824.
C. Munoz Camacho *et al.* (2006) (JLab Hall A Collaboration), *Phys. Rev. Lett.* **97** 262002.
T. Muta (1998), *Foundations of Quantum Chromodynamics* (2nd edition, World Scientific, Singapore).
S. Narison, G.M. Shore, and G. Veneziano (1993), *Nucl. Phys.* **B391** 69.
S. Narison, G.M. Shore, and G. Veneziano (1995), *Nucl. Phys.* **B433** 209.
P. Nath and R. Arnowitt (1981), *Phys. Rev.* **D23** 473.
J.W. Negele *et al.* (2004) *Nucl. Phys. B (Proc. Suppl.)* **128** 170.
T. Nishikawa (2004), *Phys. Lett.* **B597** 173.
J. A. Oller and E. Oset (1997), *Nucl. Phys.* **A620** 438; (E) **A652** 407.
J. A. Oller, E. Oset and J. R. Pelaez (1999), *Phys. Rev.* **D59** 074001; (E) **D60** 099906.
Particle Data Group (2004), S. Eidelman *et al.*, *Phys.Lett.* **B592** 1.
S. Pate (2007), `arXiV:0704.1115 [hep-ex]`
G. Piller and W. Weise (2000), *Phys. Rep.* **330** 1.
J. Pumplin *et al.* (2002) (CTEQ Collaboration), JHEP **0207** 012.
J. Qiu and G. Sterman (1999), *Phys. Rev.* **D59** 014004.
H. Quinn (2004), `SLAC preprint: SLAC-PUB-10698`.
A. Radyushkin (1997), *Phys. Rev.* **D56** 5524.
G. Rädel and A. De Roeck (2002), *Nucl. Phys. B (Proc. Suppl.)* **105** 90.
J.P. Ralston and D.E. Soper (1979), *Nucl. Phys.* **B152** 109.
J.P. Ralston, P.V. Buniy and P. Jain (2002), `hep-ph/0206063`.
J.P. Ralston and P. Jain (2004), *Phys. Rev.* **D69** 053008.
R.G. Roberts (1990), *The structure of the proton* (Cambridge University Press).
C. Rosenzweig, J. Schechter and C.G. Trahern (1980), *Phys. Rev.* **D21** 3388.
V.A. Rubakov and M.E. Shaposhnikov (1996), *Usp. Fiz. Nauk.* **166** 493, `hep-ph/9603208`.
Z. Ryzak (1989), *Phys. Lett.* **B217** 325.
M. Sarsour (2006), hep-ex/0612065
K. Sasaki (1980), *Phys. Rev.* **D22** 2143.
T. Schafer (2003), *Phys. Rev.* **D67** 074502.
T. Schafer and V. Zetocha (2004), *Phys. Rev.* **D69** 094028.
A. Schreiber and A.W. Thomas (1988), *Phys. Lett.* **B215** 141.
R. Seidl *et al.* (2006) (Belle Collaboration) *Phys. Rev. Lett.* **96** 232002.
G.M. Shore (1998a), Zuoz lecture, `hep-ph/9812354`.
G.M. Shore (1998b), `hep-ph/9812355`.
G.M. Shore (2005), *Nucl. Phys.* **B712** 411.
G.M. Shore and G. Veneziano (1990), *Phys. Lett.* **B244** 75.
G.M. Shore and G. Veneziano (1992), *Nucl. Phys.* **B381** 23.
G.M. Shore and G. Veneziano (1993a), *Nucl. Phys.* **B391** 69.
G.M. Shore and G. Veneziano (1993b), *Mod. Phys. Lett.* **A8** 373.
G.M. Shore and G. Veneziano (1998), *Nucl. Phys.* **B516** 333.
G.M. Shore and B.E. White (2000), *Nucl. Phys.* **B581** 409.
D. Sivers (1991), *Phys. Rev.* **D43** 261.
J. Soffer (1995), *Phys. Rev. Lett.* **74** 1292.
J. Soffer and O. Teryaev (1993), *Phys. Rev. Lett.* **70** 3373.
J. Soffer and O. Teryaev (1997), *Phys. Rev.* **D56** 1549.
D.T. Spayde *et al.* (2004) (SAMPLE Collaboration), *Phys. Lett.* **B583** 79.
F.M. Steffens, H. Holtmann and A.W. Thomas (1995), *Phys. Lett.* **B358** 139.
K. Steininger and W. Weise (1993), Phys. Rev. D48 (1993) 1433.
S. Stepanyan *et al.* (2001) (CLAS Collaboration), *Phys. Rev. Lett.* **87** 182002.
U. Stoesslein (2002), *Acta Phys. Polon. B* **33** 2813.

M. Stratmann (1998), hep-ph/9810481.
B. Surrow (2007), arXiv:0705.3483 [hep-ex]
K. Suzuki *et al.* (2004), *Phys. Rev. Lett.* **92** 072302.
A.P. Szczepaniak, A.R. Dzierba and S. Teige (2003), *Phys. Rev. Lett.* **91** 092002.
R. Tayloe (2002), *Nucl. Phys. B (Proc. Suppl.)* **105** 62.
A.W. Thomas (1983), *Phys. Lett.* **B126** 97.
A.W. Thomas (1984), *Adv. Nucl. Phys.* **13** 1.
A.W. Thomas and A.P. Szczepaniak (2002), *Phys. Lett.* **526** 72.
A.W. Thomas (2002), *Nucl. Phys. B (Proc. Suppl.)* **105** 80.
A.W. Thomas and W. Weise (2001), *The Structure of the Nucleon*, Wiley-VCH
D.R. Thompson *et al.* (1997) (E852 Collaboration), *Phys. Rev. Lett.* **79** 1630.
S. Tomonaga (1997), *The Story of Spin*, (University of Chicago Press)
K. Tsushima, D.H. Lu, A.W. Thomas and K. Saito (1998), *Phys. Lett.* **B443** 26.
K. Tsushima (2000), *Nucl. Phys.* **A670** 198c.
M. Vanderhaeghen, P.A.M. Guichon and M. Guidal (1998), *Phys. Rev. Lett.* **80** 5064.
G. Veneziano (1979), *Nucl. Phys.* **B159** 213.
G. Veneziano (1989), *Mod. Phys. Lett.* **A4** 1605.
W. Vogelsang (1996), *Phys. Rev.* **D54** 2023.
T. Waas and W. Weise (1997), *Nucl. Phys.* **A625** 287.
S. Wandzura and F. Wilczek (1977), *Phys. Lett.* **B72** 195.
S. Weinberg (1975), *Phys. Rev.* **D11** 3583.
R. Windmolders (1999), *Nucl. Phys. B (Proc. Suppl.)* **79** 51.
R. Windmolders (2002), hep-ph/0211350
E. Witten (1976), *Nucl. Phys.* **B104** 445.
E. Witten (1977), *Nucl. Phys.* **B120** 189.
E. Witten (1979), *Nucl. Phys.* **B156** 269.
E. Witten (1980), *Annals Phys.* **128** 363.
E. Witten (1983a), *Nucl. Phys.* **B223** 422.
E. Witten (1983b), *Nucl. Phys.* **B223** 433.
R.D. Young, J. Roche, R.D. Carlini and A.W. Thomas (2006), *Phys. Rev. Lett.* **97** 102002.
F. Yuan (2003), *Phys. Lett.* **B575** 45.
X. Zheng *et al.* (2004a) (Jefferson Lab Hall A Collaboration), *Phys. Rev. Lett.* **92** 012004.
X. Zheng *et al.* (2004b) (Jefferson Lab Hall A Collaboration), *Phys. Rev.* **C70** 065207.
B. Ziaja (2003), *Acta Phys. Polon. B* **34** 3013.
E.B. Zijlstra and W.L. van Neervan (1994), *Nucl. Phys.* **B417** 61; (E) **B426** 245.

INDEX

absorption cross section 13–16, 64–65, 175
anomalous dimension 46–47, 52, 78, 82, 134, 177, 182–183
antiquark distribution 16, 44, 143, 147
asymptotic freedom 2, 17
axial anomaly 5, 52, 73–74, 78, 91, 170, 174
axial U(1) problem 6, 76, 79–80, 89
bag model 107–109, 158
beta function 46
Bjorken sum rule 53, 89, 121
Burkhardt-Cottingham sum rule 62, 71
charm 8, 149–151, 152
chiral Lagrangian 94–97, 102
coefficient function 36–38, 51
Collins asymmetry 157–163
counting rules 29, 117–121, 165
DGLAP equations 19, 47, 125, 132
Ellis-Jaffe moment 54
factorization scheme 41, 84, 126–127
figure of merit (spin experiments) 22
fixed poles 10, 69–72
generalized parton distributions 167
Gerasimov-Drell-Hearn sum rule 64, 72, 175
Goldberger-Treiman relations 5, 89–93
gluon distribution 17, 21, 43–45, 125, 149
gluon topology 76–80, 92
hadronic tensor 12, 32, 148
higher twist 63, 176
instantons 78–81, 92
large x 117–121
lattice calculations 60, 99, 102, 112–114, 170
leptonic tensor 12
light cone dominance 36–37
moments of structure functions 17, 38–40
neutrino interactions 58–62, 146
next-to-leading-order QCD corrections 52–53, 152
nuclear corrections 25
operator product expansion 36–39, 176
orbital angular momentum 5, 107, 114, 121, 159–164, 170
parton-parton interactions 48–50, 145, 152
parton distributions 16, 18–19, 39–45
photon-gluon fusion 82–87
polarized gluons 75, 128, 149
polarized structure functions 12–15, 23–29
pomeron 25–29, 130
quark parton model 15–19
Regge theory 26-29, 130
renormalisation group 45–47, 52, 181
running coupling of QCD 17–18
scaling 16
sea quarks 21, 112, 143
semi-inclusive deep inelastic scattering 138–145
Sivers asymmetry 159–164
small x 28–29, 131
splitting functions 47, 126, 133
strange quark distribution 5, 17, 55, 130, 143–144
twist 36–37
valence quarks 2, 21, 117, 141